Acta Universitatis Tamperensis 2273

SUVI TUOHINEN

Detection of the Early Radiotherapy-induced Cardiac Changes in Breast Cancer Patients

Impact of advanced echocardiography techniques

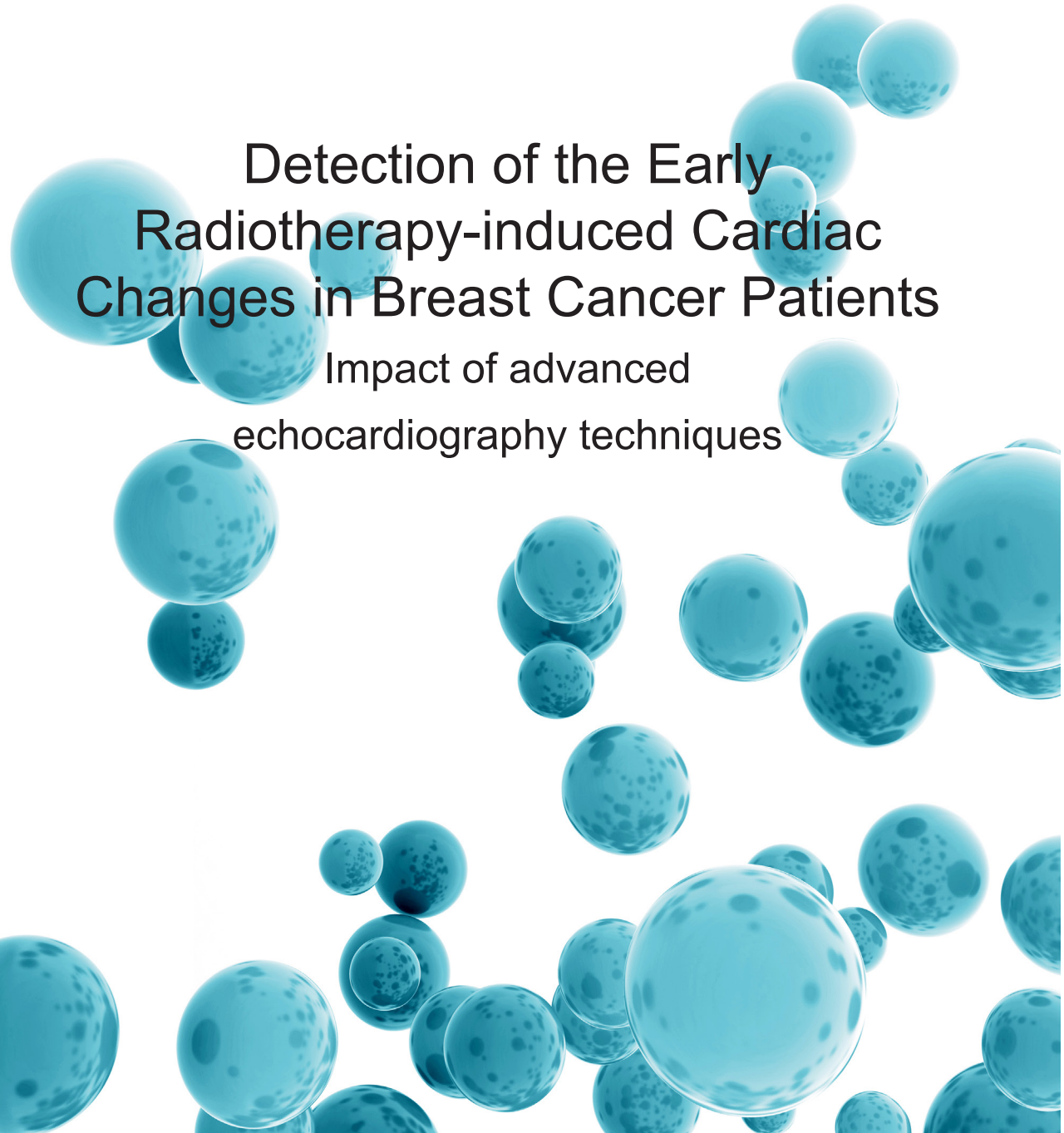

SUVI TUOHINEN

Detection of the Early Radiotherapy-induced Cardiac Changes in Breast Cancer Patients

Impact of advanced echocardiography techniques

ACADEMIC DISSERTATION
To be presented, with the permission of
the Faculty council of the Faculty of Medicine and Life Sciences
of the University of Tampere,
for public discussion in the auditorium F115 of the Arvo building,
Lääkärinkatu 1, Tampere,
on 19 May 2017, at 12 o'clock.

UNIVERSITY OF TAMPERE

SUVI TUOHINEN

Detection of the Early Radiotherapy-induced Cardiac Changes in Breast Cancer Patients

Impact of advanced echocardiography techniques

Acta Universitatis Tamperensis 2273
Tampere University Press
Tampere 2017

UNIVERSITY OF TAMPERE

ACADEMIC DISSERTATION
University of Tampere, Faculty of Medicine and Life Sciences
Tampere University Hospital, Heart Center
Finland

Supervised by
Docent Pekka Raatikainen
University of Oulu
Finland

Reviewed by
Docent Marja Hedman
University of Eastern Finland
Finland
Docent Tiina Ojala
University of Helsinki
Finland

The originality of this thesis has been checked using the Turnitin OriginalityCheck service in accordance with the quality management system of the University of Tampere.

Copyright ©2017 Tampere University Press and the author

Cover design by
Mikko Reinikka

Acta Universitatis Tamperensis 2273
ISBN 978-952-03-0417-1 (print)
ISSN-L 1455-1616
ISSN 1455-1616

Acta Electronica Universitatis Tamperensis 1774
ISBN 978-952-03-0418-8 (pdf)
ISSN 1456-954X
http://tampub.uta.fi

Suomen Yliopistopaino Oy – Juvenes Print
Tampere 2017

To my family

Contents

LIST OF ORIGINAL COMMUNICATIONS

This dissertation is based on the following four original publications, referred to in the text by their Roman numerals I-IV. Some additional unpublished data are also presented.

I Tuohinen SS, Skyttä T, Virtanen V, Luukkaala T, Kellokumpu-Lehtinen PL, Raatikainen P (2015): Early effects of adjuvant breast cancer radiotherapy on right ventricular systolic and diastolic function. Anticancer Res 35:2141-2147.

II Tuohinen SS, Skyttä T, Virtanen V, Virtanen M, Luukkaala T, Kellokumpu-Lehtinen PL, Raatikainen P (2016): Detection of radiotherapy-induced myocardial changes by ultrasound tissue characterisation in patients with breast cancer. Int J Cardiovasc Imaging 32:767-76.

III Tuohinen SS, Skyttä T, Huhtala H, Virtanen V, Virtanen M, Kellokumpu-Lehtinen PL, Raatikainen P (2017): Detection of early radiotherapy-induced changes in intrinsic myocardial contractility by ultrasound tissue characterization in patients with early-stage breast cancer. Echocardiography 34:191-198.

IV Tuohinen SS, Skyttä T, Poutanen T, Huhtala H, Virtanen V, Kellokumpu-Lehtinen PL, Raatikainen P (2017): Radiotherapy-induced global and regional differences in early-stage left-sided versus right-sided breast cancer patients: speckle tracking echocardiography study. Int J Cardiovasc Imaging 33:463-472.

The original publications are reprinted with the kind permission of the copyright holders.

ABBREVIATIONS (in alphabetic order)

ACE	Angiotensin converting enzyme inhibitor
AI	Aromatase inhibitor
ANS	Autonomic nervous system
ARBs	Angiontensin reseptor blockers
BMI	Body mass index
CABG	Coronary artery by-pass grafting
CAD	Coronary artery disease
cIBS	Calibrated integrated back scatter
CMR	Cardiac magnetic resonance imaging
CT	Computed tomography
CTGF	Connective tissue growth factor
CVIBS	Cyclic variation of the integrated backscatter
dB	Desibel
DIBH	Deep inspiratory breath hold
DNA	Deoxyribonucleic acid
Dt	Declaration time
ECG	Electrocardiogram
ECM	Extracellular matrix
FDG	Fluorodeoxyglucose
GCS	Global circumferential strain
GLS	Global longitudinal strain
Gy	Gray
HER2	Human epidermal reseptor 2
hsTnt	High sensitivity troponin T
IBS	Integrated backscatter
IMRT	Intensity modulated radiotherapy
IVA	Acceleration of the isovolumetric velocity
IVRT	Isovolumetric relaxation time
IVV	Isovolumetric velocity
LAD	Left anterior descending coronary artery
LET	Linear energy transfer
LGE	Late gadolinium enhancement
LV	Left ventricle
LVEF	Left ventricle ejection fraction
PDGF	Platelet-derived growth factor
proBNP	pro-B-type natriutetic peptide
Rho-ROCK	Rho and Rho-associated kinase
RIHD	Radiotherapy-induced heart disease
ROI	Region of interest
RT	Radiotherapy
RV	Right ventricle
SPECT	Single photon emission computed tomography

SR	Strain rate
STE	Speckle tracking echocardiography
TAPSE	Tricuspid annular plane systolic excursion
TAVI	Transcutaneous aortic valve implantation
TDI	Tissue Doppler imaging
TGFβ	Transforming growth factor beta
TGFβ1	Transforming growth factor beta 1
TKI	Tyrosine kinase inhibitors
TNF-α	Tumor necrosis factor alfa
WHO	World Health Organization
2D	Two-dimensional
3D	Three-dimensional

ABSTRACT

Background and aims: Radiotherapy (RT) has been routinely used as a part of cancer treatment since the 1950s. It can be administered as a curative or palliative treatment. Adverse effects in healthy tissue limit the use of RT. RT in the thorax induces cardiac side-effects, which have been associated with 2 to 6-fold increase in cardiac morbidity and mortality. However, cardiac radiation exposure has been significantly reduced with improvements in RT techniques, and the cardiac impact of the contemporary RT is unknown. Our aim was to evaluate whether conformal RT causes echocardiographically detectable changes in the early phase after RT for early-stage breast cancer patients, and to characterise the location and type of the changes.

Subjects and methods: Altogether, 80 patients with early-stage breast cancer were recruited in this single-center prospective study. All patients underwent thorough echocardiographic examination a week prior to the RT and within three days after the completion of RT. In addition, each study visit included an electrocardiogram (ECG), Holter monitoring, blood samples for analysis of cardiac biomarkers and the measurement of blood pressure.

Results: RT induced multiple structural and functional changes in the early phase after RT. The walls of the left ventricle (LV) thickened and their reflectivity increased. In addition, filling of the LV becaime impaired, and sensitive markers of LV systolic function declined. Furthermore, there were changes in the RV. RV systolic function declined and RV wall reflectivity increased after RT. The changes were associated with RT dose and localisation.

Conclusions: The results of our study demonstrated that RT for early-stage breast cancer induced multiple structural and functional echocardiographic changes in patients with early-stage breast cancer. The changes were more prevalent in patients who received RT for left-sided breast cancer and in patients who received higher cardiac radiation dose. These findings may have important clinical relevance since the subclinical early changes seem to predict future development of radiation-induced heart disease (RIHD). Some of the echocardiography measurements could be suitable for the screening of early RT-induced cardiac changes, and for the follow-up of the patients with high risk of RIHD such as tricuspid annular plane systolic excursion (TAPSE) and global longitudinal strain (GLS). On the other hand, the RT-induced early changes in cardiac tissue reflectivity [integrated backscatter (IBS)] provided new information regarding the possible mechanisms of RT-induced cardiac adverse effects.

TIIVISTELMÄ (Abstract in Finnish)

Tausta ja tavoitteet: Sädehoitoa on käytetty syöpähoidossa 1950-luvulta lähtien. Sitä voidaan antaa parantavana tai oireita lievittävänä hoitona. Terveen kudoksen haittavaikutukset ovat merkittävin sädehoitoa rajoittava tekijä. Rintakehälle annetun sädehoidon tiedetään lisäävän sydänsairauksia ja sydänkuolleisuutta 2-6 kertaiseksi sädehoitoa saamattomiin verrattuna vuosien viiveellä. Nykyisillä hoitomenetelmillä sydämen sädeannosta ollaan saatu merkittävästi pienennettyä, eikä täyttä varmuutta ole nykyhoitojen sydänvaikutusten ilmenemisajankohdasta, laajuudesta tai kliinisestä merkitysestä. Tutkimuksemme tarkoituksena oli selvittää rintasyövän sädehoidon aiheuttamia sydänvaikutuksia. Väitöskirjan osatöissä olemme keskittyneet varhaisessa vaiheessa mahdollisesti ilmenevien sydänvaikutusten tunnistamiseen, paikantamiseen sekä luonnehdintaan.

Potilasaineisto ja menetelmät: Tässä prospektiivisessa yhden keskuksen tutkimuksessa oli mukana 80 potilasta, joilla oli todettu varhaisen vaiheen rintasyöpä. Kaikille potilaille tehtiin kattava sydämen kaikututkimus keskimäärin viikkoa ennen sädehoidon aloitusta ja kolmen vuorokauden kuluessa sädehoidon päättymisestä. Kukin tutkimuskerta sisälsi lisäksi EKG:n, holterin sekä sydänlihaksen vauriota kuvaavien verikokeiden määrityksen ja verenpaineen mittauksen.

Tulokset: Rintasyöpäpotilaille annettu sädehoito aiheutti sekä rakenteellisia että toiminnallisia muutoksia sydämen ultraäänitutkimuksessa varhaisessa vaiheessa sädehoidon jälkeen. Vasemmassa kammiossa todettiin seinämien paksuuntumista, muutoksia herkissä supistumista kuvaavissa mittareissa sekä täyttymisen hidastumista. Oikean kammion supistuvuudessa todettiin heikentymistä. Kudosheijastavuus lisääntyi molemmissa kammiossa. Muutoksilla oli yhteys sekä sädehoidon määrään että paikkaan.

Yhteenveto: Tutkimuksessamme totesimme, että rintasyöpään annettu sädehoito aiheuttaa sydämen ultraäänitutkimuksessa todettavia sekä rakenteellisia että toiminnallisia muutoksia jo varhaisessa vaiheessa. Muutoksia oli enemmän vasemman puoleista sädehoitoa, ja toisaalta suurempaa sydämen keskisädeannosta saaneilla. Näillä muutoksilla on kliinistä merkitystä. Oireettomien varhaisvaiheen muutosten ajatellaan edeltävän myöhäisvaiheen kliinisesti merkittäviä sydänmuutoksia. Näin ollen varhaisvaiheen muutokset voivat kieliä potilaan lisääntyneestä myöhäisvaiheen riskistä – ja ehkä seurannan tarpeesta. Tutkimuksemme tuotti useita aiemmin todentamattomia muutoksia, joista osa soveltuu erinomaisesti kliiniseen käyttöön (TAPSE, GLS), osan tärkein merkitys on niiden tuoma uusi tieto sädehoidon kudosvaikutusten mekanismeista (IBS).

1 INTRODUCTION

The World Health Organization (WHO) has estimated that cancer is responsible for more deaths than stroke and cardiovascular diseases combined (1). In 2012 there were over 14 million new cancer cases worldwide, and it has been estimated that the annual rate of new cases will be over 20 million in 2025 (1). Breast cancer is the most common cancer in women. In 2012, there were 1.67 million new breast cancer cases globally (1). In Western Europe, the incidence of breast cancer was 94-96 per 100 000 patients (2, 3), and it has been estimated that one in eight women will be diagnosed with breast cancer in her lifetime (4, 5).

Radiotherapy (RT) is the most important non-surgical treatment for cancer. It has been estimated that more than half of the cancer patients require RT either to cure or to alleviate cancer-related symptoms (6). The cost of RT is low, and it accounts for only approximately 5% of the total cost of cancer treatment (7). On the other hand, its adverse effects on healthy tissue limit the use of RT. A small part of the RT is distributed or scattered to the nearby healthy tissue. RT in the chest can affect the heart (8). This may cause excess cardiac mortality and counterbalance the survival benefit of RT in cancer treatment. It has been estimated that cardiac manifestations are the most important non-malignant causes of excess mortality and are responsible for death in one-quarter to one-third of the patients receiving RT in the chest region (4, 9, 10).

RT for breast cancer roughly doubles the risk for radiotherapy-induced heart disease (RIHD) (11). Considering the high number of breast cancer patients and their generally good prognosis (2), RT treatment generates a large patient population that is at increased risk for RIHD. The short- and long-term side effects of cancer treatment have triggered vivid research activity and resulted in recommendations of screening, treatment and follow-up of these patients (8, 11-16). However, the current knowledge is largely based on obsolete treatment protocols, and the knowledge of the impact of modern conformal RT on the burden of clinically significant cardiac sequalae is limited (10). Improvements in RT techonology and refinements in the treatment protocols have reduced cardiac radiation exposure (10, 17). The long delay of years to decades in the development of RIHD makes it difficult to evaluate the cardiac benefits of these new protocols in patients receiving RT in the chest region (10). Our study aimed to resolve questions conserning the development of cardiac changes early after modern conformal RT in patients with early-stage breast cancer.

2 REVIEW OF THE LITERATURE

2.1. Breast cancer

2.1.1 Prevalence and characteristics of breast cancer

Breast cancer is the most frequent cancer among women. In the recent years, the incidence of breast cancer has been 94-96 per 100 000 patients in Western countries, and 29 per 100 000 patients in China (2, 3, 18). The incidence of the breast cancer is steadily rising (2, 18, 19). In Finland, over 5 000 new cases are diagnosed annually (3). The risk factors for breast cancer include age, genetic predisposition, ionising radiation, low parity and lack of breast feeding, prolonged hormonal replacement therapy (oestrogen and progesterone), smoking, alcohol consumption, obesity and metabolic syndrome (2, 19). The long-term prognosis of early-stage breast cancer is excellent. In Finland, the 5-year survival is 91%, and the 10-15-year survival is approximately 80-85% (3, 10). Despite this, breast cancer is the leading cause of female cancer mortality, accounting for 450 000 cancer deaths per year among women globally (2, 20).

Breast cancer can be characterised in several ways. In addition to size, the number and spreading of the tumour as well as the morphological and molecular profiles are also important. Morphologically breast cancer is classified into lobular, ductal or other subtype carcinomas, and into invasive or non-invasive carsinoma (*in situ*) (19). Oestrogen and progesterone receptor expression is evaluated by immunohistochemistry, while human epidermal reseptor 2 (HER2) status can also be identified using in situ hybridisation (2). In addition, mitotic activity is graded (19). Molecular subtyping can be used in combination with clinical characteristics to estimate the prognosis, and to guide the adjuvant treatment of breast cancer (20, 21).

2.1.2 Treatment of breast cancer

Surgery is the cornerstone of breast cancer therapy. Breast-conserving surgery was adopted in the 1980s, and it can be safely performed even in patients with adverse tumor characteristics, such as tumours larger than 5 cm, multifocal tumours (in the same segment), and triple-negative subtypes (2, 21-24). Approximately 60-80% of breast cancer patients in Western Europe are amenable for breast-conserving surgery (2). Patients with extensive ductal carcinoma in situ, with severe contraindications of RT or very young age (<35 years), should be considered for mastectomy. Patients with

inflammatory breast cancer or malignant spreading to the axillary lymph nodes should undergo axillary lymph node dissection (19, 25-27). Adjuvant therapy prior to surgical treatment (*i.e.*, neoadjuvant therapy) is recommended for patients with locally advanced or inoperable tumours as well as to those with inflammatory breast cancer in order to enhance surgical success (2, 21, 28, 29).

Adjuvant therapies include endocrine therapy, chemotherapy, HER2-targeted treatment and RT. Adjuvant endocrine therapy aims to eliminate oestrogen-derived growth stimulus in patients with oestrogen reseptor positive breast cancer, which is defined as >1% of the tumour cells expressing oestrogen reseptor (2, 19). Endocrine therapy is recommended for patients with stage I tumours posessing adverse features or patients with stages II or greater tumours (30). The menopausal status defines the treatment of choice (2). Aromatase inhibitors (AIs) block the final pathway of oestrogen synthesis, and they are used in postmenopausal patients (19). Younger patients are treated with antioestrogens (*e.g.* tamoxifen) or with ovarian suppression with or without AI (2). Chemotherapy is considered for patients who need more aggressive adjuvant therapy due to the increased risk of breast cancer relapse. Characteristis indicating increased risk for relapse include large tumour size, axillary node metastasis, younger age and certain breast cancer subtypes (21, 31). The contemporary chemotherapy regimes for breast cancer include taxanes and anthracyclines (21). Approximately one-fifth of the breast cancers are HER2-positive, and carry a worse prognosis (32-34). HER2-positive breast cancer patients benefit from HER2-targeted therapy, and it is currently routinely applied for these patients (19, 35, 36). RT is administered after breast-conserving surgery. It is also considered after mastectomy in patients with adverse tumour characteristics (2, 19). Post-operative RT after breast-conserving surgery reduces breast cancer mortality by sixth and halves recurrencies (37).

2.2 Radiotherapy

2.2.1 Radiotherapy in the treatment of cancer

William Conrad Roentgen discovered X-rays at the end of the 19th century, and the first attempts to use it in cancer treatment were made soon thereafter (38-41). The initial experiences with gastric carcinoma, skin cancer and malignant sarcoma were encouraging, as the size of the tumours declined (40). The first RT machines had low-energy output and low penetrance, and the therapy caused apparent adverse effects with severe skin burns and erosions in patients and in the personnel (41, 42). Lead shields

were employed to protect the healthy tissue, and single high-doses were replaced by multiple lower doses (fractions) in the 1920s (40-42). Orthovoltage machines were replaced by betatrons in the 1940s, and linear accelerators with higher energy output were introduced in the 1950s (41, 43). In the modern era, a pretreatment three-dimensional (3D) computed tomography (CT) scan is routinely used for treatment planning. The treatment is delivered from multiple directions with multileaf collimators to produce a 3D treatment field with maximal therapeutic effect and minimal healthy tissue burden (40, 44). Additional actions are employed to further minimise the adverse effects of the healthy tissue. Patient position, breathing phases and different treatment calculation protocols (intensity modulated radiotherapy, IMRT) are used for this purpose (45-47).

With a strictly fixed patient position, treatment can be administered in one single dose as in stereotactic radiosurgery (48, 49). Different types of radiation can be used to optimise the effect. For example, electrons are well suited for superficial lesions, since their low tissue penetrance assures minimal adverse effects in healthy tissue (45). A new treatment modality, boron neutron capture treatment, allows for a targeted radiation effect in the cancer tissue. The boron-atoms are transported to the cancer tissue by liposomes, monoclonal antibodies or polymers and then activated by neutron beams (50). RT can be given also locally (such as brachytherapy in the treatment of bronchial obstructing cancers), or with radioisotopes or immunoglobulins combined with radiating agents that have specific targets, such as radioactive iodine for thyroidea cancer or radioimmunotherapy for the treatment of lymphoma (41, 51-53).

In summary, within the last 100 years, RT has evolved into a sophisticated and versatile treatment tool and has earned its place as an essential part of cancer treatment alongside surgery and chemotherapy. Currently, about half of the cancer patients receive RT (40). In breast cancer patients, adjuvant RT after breast conserving surgery reduces long term relapses by 10-15% and mortality by 4-8% (2).

2.2.2 Radiotherapy-induced changes in healthy tissues

Radiation acts via ionisation. Ionisation is a very rapid process that occurs in 10^{-14} to 10^{-18} seconds (45, 54). Ionisation disrupts the cellular composition either directly or via formation of oxygen radicals (55). The ability of different radiation sources to cause ionisation differs. Energy sources with high linear energy transfer (LET), such as neutrons, have greater direct effects on deoxyribonucleic acid (DNA) strands, whereas

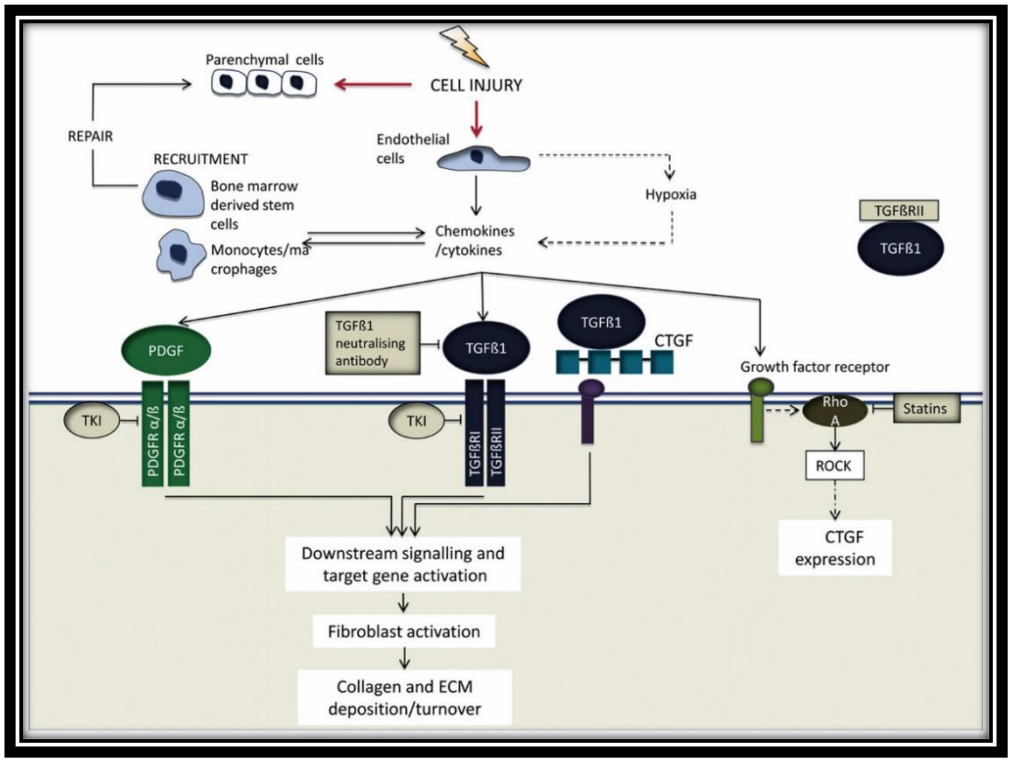

Figure 1. Simplified overview of the pathogenesis of radiation fibrosis. Radiation-induced cellular injury promotes secretion of profibrotic chemokines and cytokines by several mechanisms. The downstream fibrotic signaling can be activated by platelet-derived growth factor (PDGF), transforming growth factor beta 1 (TGFβ1) or by Rho and Rho-associated kinase (Rho-ROCK) pathway. Connective tissue growth factor (CTGF) is a central mediator in the downstream signaling pathway. Several therapeutic targets are presented in the picture. Tyrosine kinase inhibitors (TKI) have been tested to suppress the intracellular cascade, statins to inhibit Rho-ROCK pathway and monoclonal antibodies to block TGFβ1 signaling. ECM, extracellular matrix. Reprinted with permission from Elsevier ltd [Clinical Oncology] (Westbury C.B et al 2012), copyright (2012).

the effects of low LET sources (photons and electrons) are more dependent on an indirect mechanism (45). The energy of radiation absorbed by the tissue is measured by Gray-units (Gy), where each Gy is 1 Joule/kg of absorbed enegy (45). One Gy of high LET radiation produces 10^5 ionisations and 1 000 DNA-strands breaks (45).

The inflammatory process is initiated at the time of radiation exposure. Biological effects appear within minutes, and the first signs of the cellular changes can be oberserved in

histological samples within a few hours (10, 56, 57). Endothelial damage plays a central role in this process (55). Affected endothelium releases inflammatory chemokines and chemoattractants for leucocytes (*e.g.*, E- and P-selectin), and activated neutrophils release pro-inflammatory cytokines in turn (10, 55). Oxygen radicals are formed by ionising effects of radiation, but also by macrophages (10, 55). In tissue samples, swelling, extravasation, the accumulation of inflammatory cells and sings of thrombosis in capillaries can be observed (56). In the skin, this can manifest as redness and oedema (56). The second phase, also known as the 'latent phase', is characterised by endothelial damage of the capillaries (56). The capillaries are narrowed and thrombosed, and these changes lead to rarefaction of the capillaries and to reduced capillary/muscle ratio (56).

Clinically significant late changes in healthy tissues are caused by fibrosis. The rarefaction of the capillaries with subsequent perfusion defects is partially responsible for fibrosis, but apparently, fibrosis is also caused by a fibrotic cascade that is launched at the time of radiation (55, 56). The fibrotic cascade is a complex process with multiple mediators, and it is not fully understood. Oxidative stress is exacerbated by tissue hypoxia, and it propagates inflammation (10, 55). The transformation of fibroblast into collagen-secreting myofibroblasts seems to be central to the fibrotic process (57). The transformation is enhanced by pro-fibrotic cytokines, matricellular signals and epigenetic reprogramming (10). Pro-fibrotic cytokines, such as transforming growth factor-beta (TGF-β) and interleukins 13 and 4, are secreted by neutrophils (10). TGF-β induces the release of matricellular signals (*e.g.* CTGF), which promote fibroblast differentiation into myofibroblasts (10, 55, 57). Finally, there are studies suggesting that radiation induces epigenetic reprogramming via DNA methylation (10). Myofibroblasts with hypermethylated genes have decreased rates of apoptosis. In normal wound healing, myofibroblasts undergo apoptosis, which results in an acellular scar. Persisting myofibroblasts are considered to promote fibrosis (55). Once initiated, the fibrotic process seems to continue with increasing amounts of tissue changes over time (56).

2.3 Radiotherapy-induced heart disease

2.3.1 Prevalence and clinical characteristics of RIHD

Data regarding long-term cardiovascular events after radiation have been collected from survivors after therapeutic, accidental or malicious radiation exposure. Therapeutic radiation increases the incidence of adverse cardiac events (Table 1). Significant cardiac exposure occurs when chest RT is administered to patients with lymphoma, breast cancer (especially left-sided breast cancer), oesophageal cancer and, to a lesser extend, to patients with thymoma and lung cancer. The long-term follow-up of these patient groups show that each Gy of the mean heart dose increases the risk for RIHD by 4% and coronary events by 7.4% (58, 59). The survivors of the atomic bombs at Hiroshima and Nagasaki have been followed-up for more than 50 years. These data showed that each Gy of radiation exposure increased cardiovascular risk by 14%, and that the dose-response curve is linear, meaning that even low doses (0.5-2 Gy) increased the risk with no apparent safe treshold (60). In patients with Hodgkin's lymphoma, the incidence of RIHD is 10-30% in 10 years and up to 50% in 40 years after treatment (4, 8). Frandsen *et al* followed-up a large patient population that was treated with RT for oesophagus cancer, which involved high cardiac radiation doses. The excess cardiovascular mortality started to increase already 8 months after RT. The absolute increased risk for cardiac mortality in these patients was 3%, 5% and 9% at 5, 10 and 20 years after RT treatment, respectively (61). Breast cancer roughly doubles the risk for RIHD (11, 62), and harzard ratios for myocardial infarction have been estimated to be 2.66 after median follow-up time of 18 years after RT, for congestive heart failure, it is 1.85, and for valvular dysfunction, it is 3.17 (63).

Table 1. Summary of the early and late RT-induced cardiac changes

	Early changes (*days to months*)	Late changes (*years*)
Pericardium	Acute pericarditis *After high dose RT exposure* *Usually self-limited*	Chronic pericarditis Constriction
Coronary arteries	None	Coronary artery disease *May be silent* *Increases RIDH-related mortality*
Valves	None	Mitral and aortic valve *Regurgitation 10 years after RT* *Stenosis 20 years after RT*
Myocardium	Capillary rarefaction Changes in diastolic function Decline in GLS and local STE analysis	Diastolic heart failure Restrictive cardiomyopathy
Heart rhythm and conduction system	ECG changes in 13-45%	Autonomic nervous system changes Sick sinus syndrome Increased risk of pacemaker Different types of arythmia

RT, radiotherapy; RIHD, radiotherapy-induced heart disease; GLS, global longitudinal strain; STE, speckle tracking echocardiography; ECG, electrocardiogram.

2.3.1.1 RT-induced pericardial changes

Pericardial manifestations induced by RT are highly dose-dependent (10, 64). High-dose regimes increase the hazard ratio of pericardial complication by 2.8 to 8.3-fold (65). The early RT-induced pericarditis occurring during the treatment or within days to weeks after a very high dose of radiation is nowadays a rare complication (10). The symptoms of early RT-induced pericarditis in the modern era are mild and usually self-limited (8). Their presence, however, indicates that the risk for the development of late chronic perdicarditis or pericardial constriction is increased (4, 10, 66). With refinements in RT shielding and dosimetrics, the insidence of chronic symptomatic pericarditis has declined

from 20% to 2.5% since the 1970s (4, 10). The median onset of the symptoms of chronic RT-induced pericarditis is one year, ranging from three months to a decade (10). Pericardial thickening is a frequent finding after chest RT, and in nearly 20% of these patients, pericardial thickening becomes severe enough to cause constriction (8, 10, 67, 68). It has been estimated that in 9-31% of the patients with symptomatic constriction, the cause of the pericardial pathology is previous chest RT (69). A special form of constriction, effusive-constrictive pericarditis, characterised by fibrotic fusion of the visceral and parietal pericardial layers and as well as tense effusions in the free pericardial space, is often related to RT (4).

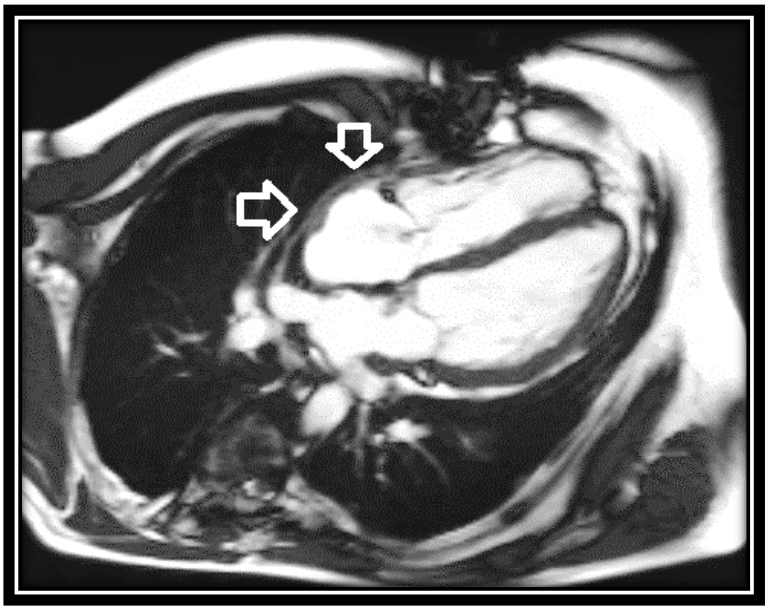

Figure 2. Radiotherapy-induced pericardial changes in a 47-year old man who was treated for mediastinal tumours with high-dose RT during childhood. He was thoroughly examined for exercise intolerance. A thickened pericardium (arrows) was observed in this CMR image. Constriction was confirmed by cardiac cathetrisation. Courtesy from Miia Holmström.

The treatment of acute RT-induced pericarditis complies with the general recommendations. Anti-inflammatory medication is used in symptomatic cases, and perdicardial drainage is used in case of tamponade with compromised haemodynamics (10, 69). Pericardial constriction is a complex entity that usually has simultaneous myocardial involvement. Pericardiectomy is the treatment of choice, but due to technical difficulties and other concomitant RT-induced cardiac lesions, perioperative mortality is reported to be as high as 21%, and 5 and 7-year survival is as low as 55% and 27%, respectively (10, 70).

2.3.1.2 RT-induced coronary changes

Coronary lesions secondary to RT are the major cause of increased RIHD-related cardiac mortality (4, 9). Even a relatively low mean heart radiation dose can cause coronary lesions. In the study by Darby *et al*, a mean heart dose of < 2 Gy, 2-4 Gy, 5-9 Gy and > 10 Gy imposed an excess risk for coronary artery disease (CAD) of 10%, 30%, 40% and 116%, respectively (59). RT leads to an increased incidence of CAD within 5 years post-treatment, and it continues to increase for at least 20 years (8, 59, 65). The lesions are in close proximity to RT fields and preferentially occur in the proximal parts of the left anterior descending coronary artery (LAD) in patients who have received breast cancer RT and in the left main coronary artery, the circumflex coronary artery or in the right coronary artery in patients who have received RT for lymphoma (8, 71).

Histologically the RT-induced coronary lesions are more fibrous than other atherosclerotic lesions (4, 68, 72). In addition, the lesions tend to be longer, more friable and more often ostially located (4, 10, 72). Simultaneous RT-induced changes in the autonomic nervous system seem to increase the incidence of silent CAD (8). Reduced exercise capacity, atypical symptoms and diagnostic difficulties due to absence of traditional risk factors may cause significant diagnostic delays (70). Therefore, screening for silent ischemia 5 to 10 years after RT has been suggested (8, 11, 70). The treatment for RT-induced CAD does not deviate from general guidelines. The complex anatomy of the lesions might pose a challenge for percutaneous interventions. There have been reports of increased rates of restenosis with earlier protocols, while reports of the treatment strategies currently employd, show no difference between irradiated and non-irradiated patients after stenting with the drug-eluting stent (73, 74). Surgical revascularisation can be complicated by concomitant fibrotic damage in the lungs, skin, mediastinum and pericardium (8, 75). In addition, the RT-induced vascular lesions in the mammarian arteries might reduce their usability as grafts, and aortic calsification might be a contraindication for surgery (10, 76). The operative mortality of coronary artery by-pass grafting (GABG) in post-RT patients is 7% (77). Long-term survival depends on radiation exposure. At 4 years, patients with previous breast cancer RT had a survival rate of 80%, close to general population, while patients with previous RT for Hodgkins lymphoma had 57% survival (76).

2.3.1.3 RT-induced valvular changes

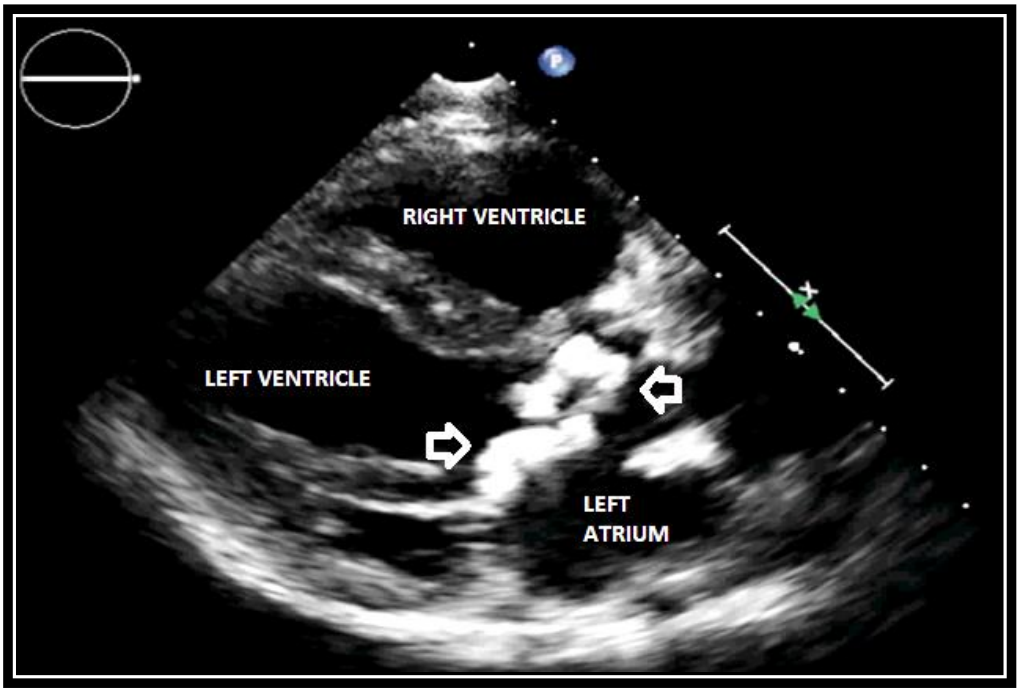

Figure 3. Radiotherapy-induced valvular changes. A lady with RT for left-sided breast cancer 31 years earlier had been followed-up for the heavily calsified stenosis in aortic and mitral valves (arrows). A preoperative coronary angiography revealed a significant proximal left circumflex coronary artery lesion. In surgery, aortic and mitral valves were replaced by biological artificial valves, and a coronary by-pass grafting (GABG) to the stenosed coronary artery was performed. In addition, a dual-chamber pacemaker was implanted prior the operation due to episodes of syncope and a complete atrio-ventricular block on ECG. Reprinted with permission from Duodecim ltd [Duodecim] (Tuohinen S. et al 2015), copyright (2015).

Valvular lesions after RT are common. Depending on the radiation dose, valvular dysfunction can be detected in 32% to 55% of patients with previous lymphoma within 6 to 20 years after RT (78-84). Clinically significant valvular disease is observed in 4-25% of the RT-treated patients 13 to 22 years after the treatmet, and the incidence seems to rise significantly 15 years after treatment (8, 84, 85). In patients who received lower cardiac doses, the absolute risk for significant valvular lesions is markedly lower, 1.4%

30 years after RT (83). Van der Pal and co-workers found a dose-assosiation with increased risk by 1.33 per 10 Gy, and Bijl *et al* found a time-association with 1.3-fold increase of risk for aortic regurgitation per each year after RT (84, 85). Fibrotic retraction of the valvular apparatus occurs within 10 years and thickening and calcifications of the valve appears 20 years after RT (4, 10, 86). Fibrosis and accumulation of calsification induce stenosis, but regurgitations are even more common (10, 85). The mitral and aortic valves are more commonly affected than the pulmonary and tricuspid valves, probably due to altered aortic elasticity and higher haemodynamic demands on the left side (4, 10, 85). The need for valvular surgery in Hodgkin's lymphoma patients was 9.16-fold higher than in general population (87). Six years post-RT, the hazard ratio was 3.5 to 8.6 after high-dose treatment for childhood cancers (65).

Mitral and tricuspid valve replacement might be better than valve repair in patients who have previously undergone chest RT. Crestellano *et al* reported a 32% incidence rate of valvular dysfunction at three years after mitral or tricuspid valve repair in patients with previous mediastinal RT. It was speculated that the fibrotic process was not halted by the surgery and that this was one of the reasons leading to repair failure (75). Due to increased surgical risk, transcutaneous aortic valve implantation (TAVI) could be a better artenative for patients with severe aortic stenosis with previous chest RT. TAVI has been successfully implanted in patients with history of chest RT. In the current Cardio-oncology position paper by European Society of Cardiology it was stated that TAVI might be a suitable option for this patient group (8, 88).

2.3.1.4 RT-induced myocardial changes

Clinically significant myocardial changes after RT usually manifest 5 years after the treatment (89). RT-related severe CAD or significant valuvular changes can induce changes in systolic function, but RT-induced cardiomyopathy in its classic form is caused by increased fibrosis in the myocardium (4). The rarefaction of the myocardial capillaries in the irradiated areas is an early phenomenon, and perfusion defects can already be detected at six months after RT (90). At the later follow-ups, the perfusion defects persist or increase (91-95). In addition to the capillary changes, diffuse, patchy interstitial fibrosis accumulates (58). These changes lead to thicker and stiffer tissue as well as diastolic dysfunction and restrictive cardiomyopathy in extreme cases. Chest RT increases the risk for heart failure upto 7-fold (4, 65). The medical treatment of the RT-induced cardiomyophathy complies with the general guidelines for heart failure. Specific drugs for the treatment of RT-induced inflammation or fibrosis are not yet available

(10). The survival of patients with RT-induced heart failure after heart transplantation has been reported to be lower than for patients with other ethiology in some studies, but not in all studies (96, 97). Even asymptomatic RT-induced myocardial changes can reduce cardiac tolerance for other stress factors (4). Poorer post-operative results after CABG or pericardiectomy in post-irradiated patients are partially due to RT-induced myocardial fibrosis (10, 76, 77).

2.3.1.5 RT-induced changes in heart rhythm and the conduction system

All kinds of bradycardia and tachycardia can occur after RT due to changes in the autonomic nervous system (ANS) and RT-induced fibrosis in the sinus node and conduction system (4, 8, 70, 82). As a result of the changes in the ANS, the heart rate increases and its variability gets blunted, heart rate recovery after excersise is abnormal and perception to CAD-associated pain is disminished (4, 8, 82, 98). ECG abnormalities have been reported in 50-75% of the Hodgkin lymphoma patients after mediastinal RT (82, 99, 100). Right bundle branch block is the most common RT-induced intraventricular conduction disturbance (4, 70, 82). Slama *et al* and Orzan *et al* have reported small series of patients who developed third-degree atrio-ventricular heart block 12-20 years after RT (67, 68). The need for pacemaker therapy is increased by 1.9-fold in patients previously treated with chest RT vs general population (87). Furthermore, patients who have previously undergone RT for Hodgkin's disease have a two-fold risk of needing post-operative pacemaker after cardiac surgery (4). Ventricular ectopic beats secondary to fibrotic changes have been reported in up to 50% of patients after chest RT (4). Additionally, prolongation of the QT-time and an increased incidence of sick sinus syndrome have been reported after chest RT (70).

2.3.1.6 RT-induced extracardiac changes in the chest

RT-induced changes in the lungs, arteries, skin and thyroid can induce symptoms that are similar to cardiac diseases, and even more importantly, they can complicate the interventions of RT-induced cardiac manifestations. Pulmonary and cutaneous changes display similar time-dependent development as cardiac manifestations. Breast cancer RT induces pneumonitis in 1-5% of the patients (101). Pneumonitis subsides within 1-3 months with oral corticosteroid treatment, but often precedes irreversible lung fibrosis (102). Cutanoeus changes are experienced by the majority of patients in the initial phase, and 10-27% develop grade I to II fibrosis later on (103, 104). RT seems to increase arterial lesions (105). Isolated carotid or subclavian artery stenosis, which is not

commonly seen in other patient populations, has been found in up to 40% of patients with previous RT for Hodgkin's lymphoma (70). The internal mammarian arteries may be friable or scarred, and cannot be used as coronary grafts in half of the post-irradiated patients (76). In cases where the RT fields reach the thyroidea gland, the risk of late hypothyreosis is significant (106). In addition, the risk of secondary malignancies is increased by 1.2-fold after breast cancer RT (107).

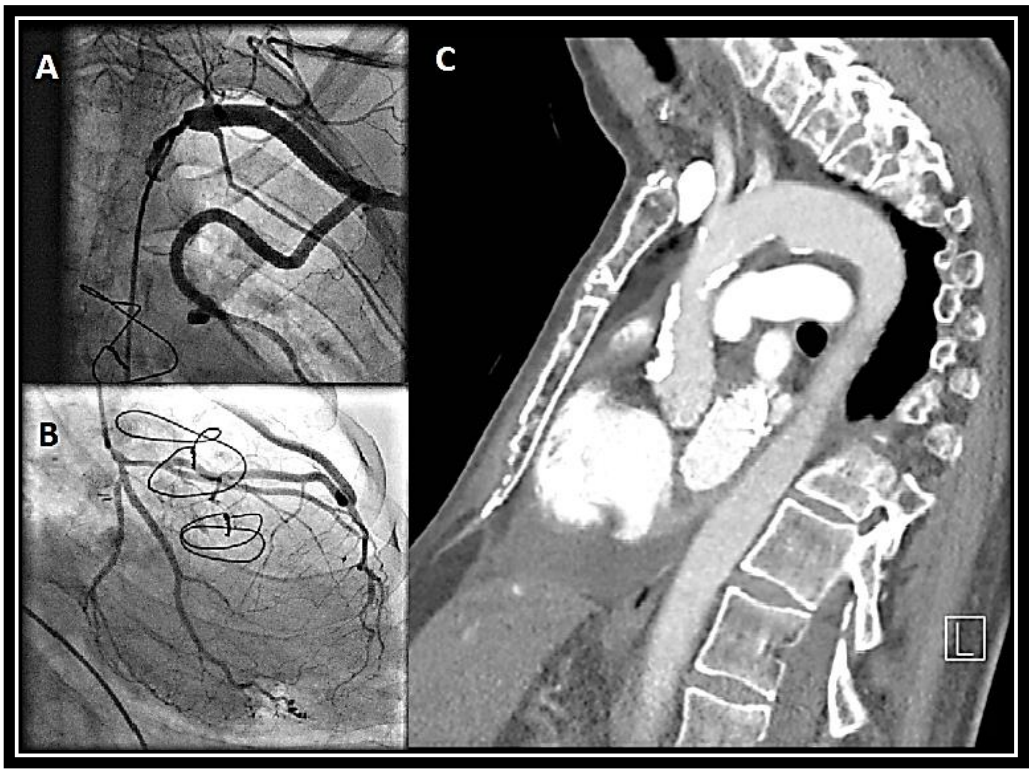

Figure 4. Radiotherapy-induced vascular changes in a man who underwent high-dose chest radiotherapy four decades earlier. On the left side, a severe subclavian stenosis is illustrated (A). This patient had undergone a CABG surgery five years previously, and he was re-examined for chest pain provoked by the use of his left arm. The use of the left arm induced steal from the coronaries via left mammarian graft. A stenting of the stenotic subclavian artery was perfomed. The native left coronary is shown in panel B. On the right side, the sclerotic aorta of this patient is illustrated (C). Courtesy from Juha Virolainen and Miia Holmström.

These extracardiac changes must be taken into account when treating patient with cardiac problems. Surgery can be complicated by mediastinal and skin fibrosis. Aortic calsification poses a risk for thrombotic emblisation and can restrict technical options during the operation. Changes in mammarian arteries can reduce their usability as grafts (4, 76, 108). Furthermore, pulmonary changes can increase operative risk. The risk for poor wound healing and post-operative infections is increased by skin fibrosis and reduced perfusion due to arterial changes (76).

2.3.1.7 Progression of the RT-induced cardiac changes

The progression of the RT-induced cardiac changes has been documented in several prospective studies as well as in cross-sectional surveys (4, 11, 57, 86, 109-111). Prosnitz *et al* showed that the initial myocardial perfusion defects persist and even increase in six-year follow-up study (91). The absolute excess risk of angina pectoris increases with longer follow-up time from 5.5 to 59.9 per 100 000 patient years from 10 to 20 years after RT (110). The incidence of CAD, heart failure and changes in the ANS also increases with longer follow-up times (63, 98, 112). Also, the incidence of valvular lesions rose by 56% in eight years in a prospective follow-up study by Cutter *et al* (83). Bijl and co-workers determined an odds ratio of 1.13 for aortic regurgitation per year after RT-treatment (85). The overall risk for cardiac events rises with longer observation times (65, 111), and the absolute risk for cardiac mortality increases from 5% to 54% from 5 to 20 years after RT (4, 17, 113, 114).

2.3.2 Factors predisposing to RIHD

The most important factors that affect RT effects in the heart are the volume of the heart that is exposed to radiation and the cardiac radiation dose (4, 8, 11, 63, 64, 84, 111). The overall risk for RIHD seems to be dose-dependent as each Gy imposes a 4-7.4% increase in risk with no apparent safe threshold (58-60).

Concurrent treatment and patient specific factors influence individual suspectibility to the adverse cardiac effects. The prior or simultaneous use of anthracyclines, trastutsumab or other cardiotoxic regimes increases the radiation toxicity in tissues and potentiates the adverse RT-induced effects (4, 8, 63). Furthermore, the oxygen level in the tissues plays an important role. Hypoxic tissues are radiation resistant, and hypoxic condition reduce cardiac damage (115, 116).

The conventional risk factors for cardiovascular disease impose an additive risk for patients receiving RT (10). High bloodpressure predisposes to left ventricle (LV) dysfunction, occult CAD or valvulary dysfuntion with an odd ratio of 3.0 (117). Additionally, Harris *et al* showed an increased risk of CAD in hypertensive patients who have previously received RT (112). High cholesterol, especially at the time of RT, increases the risk of atherosclerosis and valvular changes (56, 83, 94, 105, 118, 119). Furthermore, pre-existing diabetes increases the risk of major coronary events by 3.23-fold and obesity by 1.57-fold (59). Smoking predisposes to the development of coronary artery lesions, and it has a more than additive effect in combination with RT (59, 63, 120). All in all, traditional risk factors roughly double the relative risk of RIHD, and their aggressive management is of paramount importance to reduce excess cardiac risk produced by radiation (10).

Genetic factors influence patients' vulnerability to RT effects. A genetic defect in DNA repair, such as in ataxia-telangiectasia, Fanconi Anemia and Nijmegen syndrome, carries a high risk for severe RT adverse effects with lethal reactions observed following a dose as low as 3 Gy (42). Over 80% of the differences in RT-induced changes in tissues cannot be explained by known factors, and a genetic variation is thought to explain a part of this (6). Genetic factors leading to disturbance in fibrogenesis, oxidative stress and enthotelial function seem to affect patients' reaction to RT. In particular, TGF β1 T/T variant seems to increase the risk for RIHD by 1.79 (121). Currently, genetic tests are not available to characterise patients' genetic suspectibility for RIHD (6). Theoretically,

such knowledge could be used to modify individual RT-protocol in the future – taking into account the sensitivity of both cancer and healthy tissue to radiation (6).

2.3.3 Prevention and treatment of RIHD

Prevention of RIHD includes methods to reduce cardiac exposure to radiation and to optimise concomitant cancer treatment as well as other patient derived risk factors for RIHD. (10). However, spesific options to ameliorate RT-induced changes are limited. The treatment of cardiac diseases does not deviate from other patients, exept for the limitations and considerations mentioned in the chapters featuring the RT-induced cardiac changes (2.3.1.1 -2.3.1.5).

Prevention. The cardiac radiation exposure is the most important factor affecting adverse cardiac effects. Hence, actions to minimise cardiac dose are the most important means to reduce RT-induced cardiac damage. The radiation dose can be reduced by spesific treatment protocols. RT given in multiple fractions has different effects on the healthy tissue and on the cancer tissue (45). 3D treatment planning based on CT images is routinely used to maximise the effect of RT on the cancer tissues and to minimise healthy tissue burden. In IMRT, the treatment fields affecting both healthy and cancer tissue are delivered with reduced radiation doses. In contrast, fields affecting cancer tissue only will be treated with higher doses (45). Deep inspiratory breath hold (DIBH) or respiratory gating creates a greater distance between the heart and breast cancer tissue. In a study by Smyth *et al,* DIBH induced a mean cardiac dose reduction of 3.4 Gy, which corresponds to 13.6% reduction in RIHD risk (47).

The position of the patient during the RT treatment also plays a role. In breast cancer patients, a supine position reduces cardiac doses by 85% compared to prone position (46). In other studies, the supine position resuted in even greater LAD exposure because of the more anterior position of the heart (122). An elevated ortolateral arm reduces cardiac radiation doses in patients with left-sided breast cancer.

With the modern techniques, the current cardiac radiation doses for left-sided breast cancer are estimated to be 4.2 Gy, and tangential fields with DIBH deliveres a mean heart dose of 0.4-2.5 Gy. The average mean heart dose for patients with right-sided breast cancer was 3.3 Gy (123). The cardiac morbidity and mortality after breast cancer RT has decreased (17, 120). In addition, dose reductions in overall chest RT has resulted in decrease in absolute cardiac mortality from 13% to 5.8% since the 1970s (17). Despite

adopting these methods, cardiac exposure is unavoidable and other considerations for the prevention, detection, follow-up and treatment should be applied (57).

As mentioned in chapter 2.3.2, the conventional risk factors for cardiovascular diseases increase the risk for adverse effects secondary to RT. It has been proposed that they shold be actively addressed and aggressively treated prior to cancer treatment (11). This includes lifestyle counselling for obesity and sedentary habits, smoking refrainment, and adequate medication for high blood pressure, dyslipidemia and diabetes. It has been suggested that these patients should have a life-long screening of cholesterol and blood pressure levels (10).

Anticancer medication can have direct adverse cardiac effects and potentiate RT-induced damage. Anthracycline-based therapies along with chest RT is the best known combination that exhitis such an additive effect (8). Patients receiving such therapies could be considered for more thorough follow-ups. Patients with several cardiovascular risk factors or reduced LV function at the baseline might be considered for specific cardioprotection with angiotensin converting enzyme inhibitors (ACE) or angiontesin reseptor blockers (ARBs) and betablockers as well as for modifications of the chemotherapy treatment (8). Similar considerations should be made with other concurrent cancer treatments with special attention to compounds with known sensitising effects towards radiation.

Spesific treatment. Hyperbaric oxygen therapy and amifostine are used to mitigate the RT-induced adverse effects. Hyperbaric oxygen has been used to treat radiation necrosis and has a success rate of 94-100% in the jaws, 76% in cutaneous wounds, 82% in laryngeal radionecrosis, 86% in cystitis, and 63% of the gastrointestinal radionecrosis (124). The regrowth of the vessels stimulated by hyperbaric oxygen has been suggested as the mechanism behind the treatment effect (57). Amifostine, an antioxidant, is used to treat radiation-induced dryness of mouth, also known as xerostomia (10).

There is flourishing reseach in order to find different means to alter the radiation-induced cascades and tissue changes. The different agents tested target the mechanisms involved in radiation initiated processes – enchaced fibrotic activity, oxicative stress, and different mediators of the fibrotic cascade (55). RT-induced enteropathy and kidney damage have been treated with the inhibition of platelet aggregation by clopidogrel and acetylsalicyl acid (125-127). Clopidogrel reduced the initial enteropathy changes, but it did not reduce the late effects (125), whereas acetylsalicyl acid seemed to protect the

kidneys of mice in 12-month follow-up (127). Different antioxidants have been tested to reduce the effects of oxidative reactions. Aminofistine has been approved for the treatment of xerostomia (10). Combined therapy with pentoxifylline and vitamin E has been tested for the treatment of superficial fibrosis in breast cancer patients. The results are conflicting (128, 129). In addition, there have been promising experimental reports on several agents. Alpha-lipoic acid decreases the local levels of interleukin 1, interleukin 6, metalloproteinases and enteritis in mice (130). Melatonin reduces post-RT levels of interleukin 1, tumour necrosis factor alfa (TNF-α), TGF-β together with milder lung changes (131). Furthermore, high-dose selenium seems to effectively abate nephropathy changes in the rats after high-dose total body radiation (132).

The studies of statins and ACE/ARBs are perhaps the most interesting ones. Several acute and chronic radiation-induced pro-inflammatory and pro-fibrotic responses are reduced by pravastatin, lovastatin and atorvastatin in studies utilising explanted human tissues (133-136). Furthermore, in the rat model, pravastatin at physiologically relevant doses impoved radiation-induced enteropathy changes (133, 134). One rodent model has shown reduced levels of fibrosis-mediators and cardiac fibrosis following atorvastatin treatment (137).Treatment with ACE/ARBs seems to protect from RT-induced tissue changes. Captopril has been the most often used ACE to study radiation tissue effects, but ramipril, enalapril, losartan and fosinopril have also been utilized (138-141). In animal studies, these agents have ameliorated effects in the lungs (138, 139, 142-144), bowel (145), kidneys (146, 147), neurons and brain (141, 148), skin (149) and heart (150, 151). The effects have been dose-dependent (142, 143, 146), and the use of ACE/ARBs has been effective even when administered 1-2 weeks after RT (138, 147, 152). In histologic samples, reduced proliferation of fibroblasts (142), halted capillary damage (146, 151), abated fibrosis (150, 151) and decreased levels of collagen deposits (139, 143, 144, 146) compared to radiated controls without medical treatment, has been observed. Despite these studies demonstrating the potential benefits of ACE/ARBs, no randomised clinical trials in humans on the use of these agents in prevention of RIHD currently exist.

2.4 Detection of early cardiac changes after modern conformal RT

The clinically significant RT-induced lesions appear after several years of latency. Early subclinical changes precede the late sequel. The potential clinical signifigance of the early changes as a marker of increased risk for evolution toward RIHD has induced vast scientific activity in this field. The central findings of these studies are presented in the following chapters (2.4.1 – 2.4.5).

2.4.1 Echocardiography

2.4.1.1 Conventional echocardiography

Conventional echocardiography has been used for the detection of RT-induced changes in several cross-sectional retrospective studies as well as in prospective studies. Most of them have indicated that RT has an adverse effect on LV diastolic function. Several investigators have reported a significant decrease in LV dimensions in average 17 to 20 years after mediastinal RT for lymphoma (80, 82). Retrospective studies have shown lower septal e', higher E/e' ratio, lower E/A ratio or longer isovolumetric relaxation time (IVRT) and mitral inflow declaration time (dt), and greater levels of diastolic dysfunction 13 to 23 years after chest RT with correlation to greater radiation doses and longer follow-up times (76, 80, 81, 153-156). However, the findings in Christiansen's reports are undermined by the fact that the patients in the RT group were significantly older than the patients in the control group (80). In some prospective studies, similar diastolic findings have been discovered (156, 157), with a recovery in half of the patients during a 6-month follow-up (157), while in others, no significant changes could be identified within a 14-month follow-up nor 13-year retrospective studies (85, 158, 159).

2.4.1.2 Myocardial deformation imaging

RT-induced changes in myocardial strain have been studied both with tissue Doppler imaging and with speckle tracking echocardiography (STE) (154, 158). Early changes and late alterations have been identified. In prospective studies, a decline in global strain persisted six weeks to 14 months (158-160). Regional analysis has shown decline in strain corresponding to the anterior and apical radiation fields (158, 159, 161). A dose response has been found on a regional and global level (158, 160). In some reports, the deterioration of the strain values has been transient (161), but retrospective long-term studies show a global longitudinal strain (GLS) decline in patients exposed to RT

treatment years to decades earlier (153, 154, 162). The decline of the strain values was considered significant due to its ability to detect early changes in systolic function and due to its prognostic power (154).

2.4.2 Myocardial perfusion imaging

In modern perfusion studies with single photon emission computed tomography (SPECT), RT induced constant or reversible perfusion defects in 37-71% of the patients with left-sided breast cancer and in 17-44% in patients with right-sided breast cancer (92, 93, 95, 163-165). On the other hand, in a study by Chung *et al* in patients with low mean cardiac exposure, perfusion defects were not detected (166). The perfusion defects were located in the apical and anterior parts of the LV that corresponded to the RT fields in patients with left-sided breast cancer and in the antero-inferior fiels in patients with oesophageal cancer (92-95, 167). The most important factor influensing the perfusion defects was the volume of the heart in the radiation field (90, 91, 94, 167). In the study by Hardenbergh and co-workers, the magnitude of the defect was dose-dependent (92). Regional disturbancies in systolic contraction and chest pain episodes have been associated with perfusion defects in some studies (90, 165), though the findings have been silent in others (93, 163). In the study by Prosnitz *et al,* the initial defects persist in the same location in six-years follow-up in 80% of the patients, and additional new perfusion defects during the six-year follow-up period increased the percentage of affected patients from 50-60% to 52-71% (91).

2.4.3 Cardiac magnetic resonance imaging

Radiation-induced cardiac changes in cardiac magnetic resonance imaging (CMR) of patients with breast cancer or childhood Hodgkin's disease revealed a transient decline in LV ejection fraction (LVEF), but not late gadolinium enchancement (LGE) indicating focal fibrosis at two to eight years after RT (161, 168). In patients who underwent curative RT for esophageal cancer, the cardiac radiation doses were significantly higher. Two years after RT treatment, these patients showed LGE in 21% of the segments that received 60 Gy or more and in 15% of the segments that received 40 to 60 Gy dose. The LGE was mid-myocardial in most of the patients (169). CMR performed twenty years after RT for Hodgkin's disease revealed abnormalities in 70% of the patients (79). LGE with subendocardial and transmural distribution was observed in 26% of the patients. LVEF was reduced in 23% of the patients, and significant valvular changes were observed in 42% of the patients. Perfusion defects at rest were observed in 61% of the

patients, and perfusion defects during stress were observed in 68% of the patients. Finally, in a work reporting early RT-induced regional changes in myocardial metabolism showed LGE in two out of eight patients with increased metabolism (170).

2.4.4 Positron emission tomography

Studies with positron emission tomography (PET) show increased metabolism in radiated myocardial area three months after irradiation. In an animal trial involving 12 beagles, the radiated areas with increased metabolism showed perivascular fibrosis and vacuolisation of the mitochodria in histological samples compared to the non-irradiated areas without increased metabolism (171). In a work by Jingu *et al*, 20% of eosophageal cancer patients showed increased fluorodeoxyglucose (FDG) uptake in radiation-exposed areas three months after chemoradiotherapy, and LGE was detected by CMR in two patients out of eight in the areas of increased FDG uptake (170) .

2.4.5 Exercise testing

Post-irradiation exercise testing has been studied by Heidenreidh, Chen and Groarke (98, 117, 155). Occult ischaemia was detected by ECG in 11-23% of the patients after a 15-year follow-up (155), and in 46% after 19-year follow-up (117). In addition, RT-induced changes in ANS was associated with reduced excersice capacity, and in 30% of the patients, there was a low peak oxygen consumption level (82, 98). Excercise-induced ischaemia, changes in ANS and reduced exercise capacity were associated with increased mortality in 3-year follow-up (98, 155).

2.4.6 ECG

RT induces changes in ECG in 13-45% of the patients (172-174). The most common changes include ST-segment and T-wave alterations and poor R-wave progression (173-175), while Dogan and co-workers reported prolonged corrected QT-time without other accompanying changes after RT (156). The ECG changes seem to appear very early after RT and to increase in prevalence up to 6 months (173). Mean heart dose over 20 Gy, hypertension, RT for left-sided breast cancer and the use of tamoxifen increase the prevalence of these changes (172, 173). At one year, 27% of the initial changes persist and in 37% of breast cancer patients, a new fragmentation of the QRS-complex appears (172, 175, 176). Hypertension has been associated with irreversible changes during the first year of follow-up (172). Strender *et al* reported a decresed insidence of anterior T-

wave inversions from 61% at 6 months to 25% at 10 years and an increase of ST-abnormalities from 14% to 22% in patients with left-sided breast cancer, respectively, and concluded with a minor clinical signifigance of the initial ECG-changes (174).

2.4.7 Cardiac biomarkers

RT seems to induce a rise of both troponins and pro-B-type natriuretic peptide (proBNP/BNP) (159, 177-180). The rise of troponins is higher in patients with left-sided breast cancer compared with patients with right-sided breast cancer, and it is associated with RT doses and concomitant changes in echocardiography (159, 177). The rise in proBNP/BNP is also associated with the RT dose (178, 181). Furthermore, alterations of the myocardial metabolism have been detected in the areas prone to RT, and they have been associated with significant BNP rise (179). The rise of troponins and proBNP signals a cardiac impact and is associated with a poor prognosis over a wide variety of cardiac pathologies, in patients with non-cardiac diagnosis and even in community screening (182-189). Therefore, a rise in these biomarkers has been considered as a clinically significant when detected after RT.

2.5 Advanced echocardiography

2.5.1 Integrated backscatter

Myocardial acoustic properties can be characterised non-invasively by integrated backscatter (IBS) measurements. In the myocardium, the ultrasound beam is scattered by objects smaller than ultrasound wavelength (190). A part of the scattered signals is directed back to the ultrasound probe, which is referred as the backscattered signal (191). The IBS signal of the myocardium varies throughout the cardiac cycle. There are two types of measurements, the calibrated integrated backscatter (cIBS) and the cyclic variation of the integrated backscatter (CVIBS) (192). The cIBS value is measured at one time-point, usually at the end-diastole (191, 193-195), while the CVIBS presents the total variability of the signal intensity (196, 197). The cIBS is considered to measure myocardial texture properties, while CVIBS reflects the intrinsic myocardial contractility (198).

The first attempts to measure myocardial acoustic properties were made in the late 1970s (199). Prototype ultrasound machines measured objects immersed in liquid with complex multistep processing (199-202). Next, radiofrequency ultrasound signals were amplified and displayd on oscilloscopes, recorded on Polaroid films and then analysed (200, 202). Later in the 1980s processed M-mode acquisitions were used in IBS analysis (198, 203-205). Two-dimensional greyscale echocardiography replaced the previous methods in the 1990s (193, 195, 197, 201, 206-210). Currently, ordinary commercial echocardiography machines can be used instead of specific equipment, and digital raw data has replaced data stored in video signals (191, 192, 211-213).

The use of IBS has been limited to reseach only, propably due to severeal reasons. *First*, the method has been considered difficult and prone to artefacts (192, 199). Especially during the era when video signals were used, the non-linear effect of different gain settings was problematic, and the first attempts were sensitive to noise (192). In addition, the measurements are affected by specular reflections of the tissue border, bright reflections and myocardial fiber direction (192). Additionally, single myocardial measurements are affected by ultrasound power, and to be comparable with other measurements, it needs to be calibrated with acoustic stable objects. Such objects can be LV cavity, pericardium or a phantom (191, 192, 206, 207, 212-214). *Second*, a plethora of different kinds of measurements in the previous decades made the direct comparison of the results difficult. The earliest studies used millivolts (193, 199, 203, 207), while most

of the studies later utilised desibels (dB) (200-202). Tissue reflectivity has been described as a percentage (IB%, normalized IB or correction/attenuation coefficient of the IBS) compared to a reference object (193, 195, 199-201, 203, 207, 208, 214, 215). Others have used the mean value of the IBS signal (mIBS) or transmural gradient (216), while in the modern studies a reference value is subtracted from the measurement value to calculate the cIBS (191, 209-213). The dynamic nature of the IBS has been measured with different time-intervals, their relative percentage or as a total difference of the maximal and the minimal values (197, 198, 204-206, 214, 215, 217-223).

On the other hand, a cheap, widely available and non-invasive method for tissue characterisation is appealing. In a work by Sagar *et al*, IBS values were stable under different haemodynamic conditions, changes in puls, preload and afterload, which increase the reliability of these values (224). Furthermore, the validation in the recent years show that the intraobserver variability for cIBS varies from 0.4 dB to 2.2 dB, or 2.5 – 4.9 % (206, 215, 220). The interobserber variability for cIBS values has been 1.1 - 6.5 % (206, 213). The intraobserver variability values for CVIBS varies from 0.3 dB to 0.6 dB, or 3.6 – 5.4% (191, 197, 206, 215, 220, 223, 225). The interobserver variability of the CVIBS values is 0.6 to 1.1 dB or 3.8 – 8.0% (191, 197, 206, 220, 223, 225). These results give a more solid ground for assessment of the measured results and cofirm their comparability.

2.5.1.1 Calibrated integrated backscatter

The cIBS measurement is considered to reflect the myocardial properties. In the early era, studies of hearts with infarction or cardiomyopathy showed a correlation between myocardial scar tissue, especially collagen content, and a higher tissue reflectivity (200, 201, 203, 226). However, perioperative cardiac biopsies were taken from patients undergoing CABG in a work by Prior *et al*. These patients had a low percentage of fibrosis (0.7-4.0%), and there was no correlation between the histological sample and the cIBS measurements (211). Even though the different locations of the histological sample and the cIBS measurements undermine the results of this study, it seems that while evaluating the replacement fibrosis, the collagen content is the principal contributor to tissue reflectivity, whereas in myocardium with diffuse fibrosis or normal structure, other factors dominate (202, 211). This is also evident considering the reversibility of the cIBS measurements. In patients with acute myocardial infarction or allograft rejection, a transient increase of the tissue reflectivity was observed (194, 227). Additionally, an effective treatment for thyroid dysfunction, overweight or kidney

function has been shown to decrease tissue reflectivity (214, 228, 229). Furthermore, postmenopausal replacement therapy with oestrogen or raloxifen seems to reduce tissue reflectivity and to improve diastolic function (225). Since a scar tissue is unlikely to vary, other factors obviously affect the measurements of tissue reflectivity.

Myocardial water content, the size of the cells and fibre orientation as well as their 3D arrangement has been suggested to contribute to the myocardial reflectivity (211). A difference in myocardial reflectivity was detected between hypertrophied myocardium of patients with hypertension and that of patients with hypertrofic cardiomyopathy. Likewise, a difference was detected in the myocardium with normal thickness of the patients with hypertrofic cardiomyopathy and normal controls (207, 216). The difference in an otherwise similar phenotype suggests that the disarray of the fibre orientation in patients with hypertrophied cardiomyopathy might contribute to the increased cIBS value. Furthermore, increased tissue contents of copper and iron seemed to increase myocardial tissue reflectivity (195, 215). In Wilson's disease, intracellular copper accumulation induces multiorgan changes along with cardiomyopathy changes (215). Eighteen patients with Wilson's disease were evaluated by echocardiography in a study by Arat *et al.* Otherwise normal appearing hearts had increased values of cIBS compared to controls (215). Likewise, in a study by Lattanzi *et al.*, thalassemia patients with repeated transfusions and iatrogenic iron overload showed higher tissue reflectivity (195). Early subclinical changes have also been observed in patients with hypertension, diabetes, hypothyreosis, Kawasaki disease and Becher's muscular hypertrophy, though not all studies support these findings (206, 208, 209, 214, 216). Accumulation of water and different kinds of extracellular material have been suggested to modulate to the myocardial reflectivity in these patient groups without other overt cardiac changes. In addition, increased myocardial reflectivity has been associated with changes in diastology (210, 213).

Increased myocardial reflectivity seems to predict adverse changes in myocardial function later on. In patients with Becher's muscular hypertrophy, an increased cIBS value was an independent predictor of LV dysfunction in a two-year follow-up (206).

2.5.1.2 Cyclic variation of the integrated backscatter

Myocardial reflectivity changes during the cardiac cycle, and it is considered to reflect intrinsic myocardial contractility although the exact basis is unknown (205, 219). It seems to be a sensitive and early sign of changes in myocardial contractility that can predict

adverse events. In addition, changes in the CVIBS correlate with other early sensitive markers of myocardial dysfunction, such as global longitudinal, circumferential and radial strain in STE analysis (191). On the other hand, in patients with overt systolic dysfunction, there is a correlation between the CVIBS and regional systolic thickening and global shortening fraction and CVIBS seems to decline with age (204, 212).

In experimental myocardial ischaemia, changes in the magnitude and delay of the CVIBS appeared within ten minutes (218, 230). The blunted contractility of the CVIBS recovered after reperfusion within ten to twenty minutes, while wall motion abnormalities and wall thickening remained reduced for over two hours (198, 218). Therefore, the CVIBS seems to uncover the restoration of the myocardial function earlier than the conventional parameters. In chronic ischaemia, myocardial viability was assessed with FDG-PET and it was compared to the measurement of CVIBS in a work by Komuro *et al* (197). The CVIBS could detect myocardial viability with 92% sensitivity and 94% specificity. Furthermore, in a work by Zuber and co-workers, a dissociation between systolic wall thickening and CVIBS was found, which was considered to indicate myocardial hibernation (212). All in all, the CVIBS seems to promptly detect ischaemia-induced changes and recovery after reperfusion as well as myocardial viability and hibernation. However, compared with the dobutaminen stress test the CVIBS failed to predict contratile reserve (197), which might be due to its ability to pick up the segments with hibernation, too.

A depression in the CVIBS is the first sign of myocardial dysfunction in several conditions. In Wilson's disease, cardiad sarcoidosis, primary hyperaldosteronism and in progressive external ophthalmoplegia, blunted CVIBS is able to discriminate patients from controls in the absence of other changes in conventional echocardiograpy (204, 215, 219, 220). Effective treatment of hypertension, thyroidal dysfunction and postmenopausal status seems to reverse the changes in CVIBS (214, 221, 225). On the other hand, reduced CVIBS predicts cardiac allograft rejection, mortality from cardiac amyloidosis and LV remodeling in ischaemic and non-ischaemic situations (191, 205, 222, 223). In summary, the CVIBS reveals cardiac abnormalities early on, shows effective treatment responses and predicts adverse events.

2.5.2 Speckle tracking echocardiography

The era of strain measurements by echocardiography started in the 1990s with tissue Doppler imaging (TDI) (231). However, the method had inherent weaknesses due to poor signal-to-noise ratio, suboptimal reproducibility and angle dependency. Therefore, it has not been adopted to the clinical practice (192, 232). Later on, speckle tracking technology was created. STE is based on acoustically stable spots formed by myocardial fibres that are oriented in different directions (Fig. 2.5.2). Blocks of speckles can be followed frame by frame in STE soft-ware off-line analysis to determine the myocardial deformation (192, 231, 232). A change from the baseline value, also referred to as Lagrangian strain, is expressed as a percentage. Shortening is presented as a negative value, and lengthening or thickening is presented as a positive value (231-233). Myocardial strain can be measured in two-dimensional (2D) imaging in three directions, in longitudinal, in circumferential and in radial directions (231). The speed of the change, also known as strain rate (SR), is expressed as 1/s (232, 233). In addition, LV rotational movements can be measured.

The strain values can be derived locally, regionally or globally. Local changes can be used in clinical diagnostics in some extend. In ischemic heart diseases local changes in the affected coronary territory can be detected, but this needs to be more profoundly verified (234, 235). In hypertrophic cardiomyopathy, longitudinal strain is often decreased in the area of hypertrophy, most often in the septum and in patients with amyloidosis typical apical sparing is observed (231, 236, 237). In constrictive pericarditis, lateral depression can be observed, whereas typical decline after anthracycline treatment is located apically and anteriorly (12, 238). Of the global values, GLS seems to be the most robust measurement.

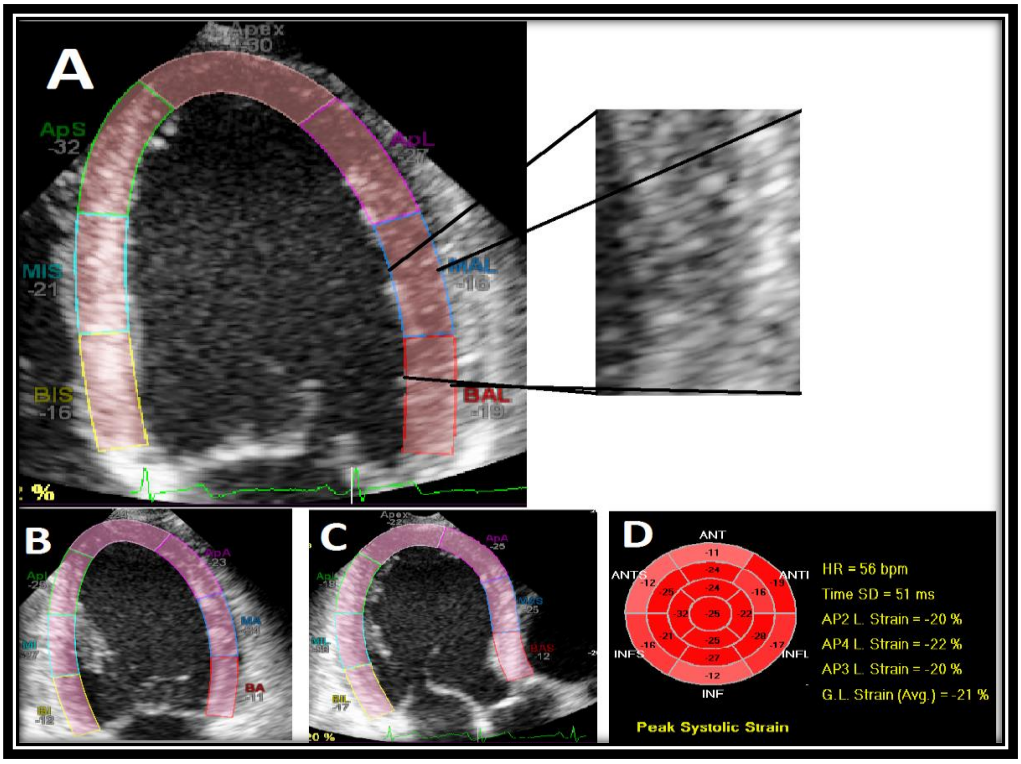

Figure 5. Speckle tracking analysis. The myocardial tissue has naturally stable speckles. They originate from myocardial fibres with different orientation. On the right upper corner, a part of the left ventricle's lateral wall is zoomed to illustrate the myocardial speckles. Speckle tracking analysis follows these speckles from frame to frame and calculates myocardial deformation in different directions. On A, B and C the left ventricle in four-chamber, two-chamber and three-chamber views has been analysed with speckle tracking software. The regional and global longitudinal results are displayed in D.

2.5.2.1 Global longitudinal strain

GLS is an averaged value of longitudinal strain values in three apical views of the LV. The GLS is automatically calculated from the four-, three- and two-chamber views by the soft-ware program. The longitudinal strain is considered to present the endocardial function of the LV (232). As the endocardium seems to be the most vulnerable part of the LV, the earliest signs of LV dysfunction can be detected in parameters describing the longitudinal function, such as GLS (232). In patients with hypertension, diabetes,

obesity, sarcoidosis, rheumatoid disease and ischemic heart disease, changes in GLS can be detected even in the absence of other changes in conventional systolic dysfunction (239-246). In heart failure patients requiring heart transplantation, GLS was strongly associated with LV fibrosis (247).

GLS can be used also in clinical *diagnostics* and in the determination of patient's prognosis. There are several clinical scenarios where conventional echocardiography and measurement of the LVEF are not sufficient for clinical diagnostics. For example, differentiating cardiomyopathy from atheltes' heart is often challenging. Acute and prolonged exercise have been reported to induce a transient decline in cardiac function detectable with GLS (248-250), where exercise related tachycardia, increase in ventricular wall stress and changes in loading conditions probably are participating factors. Compared to the normal population, athletes have mildly lower GLS values due to physiological cardiac adaptation that persist for years after the active training period (251, 252), though, other report showed better strain values in athletes (253). However, clinical issue consists of differentiating athletes from cardiomyopathy with a lookalike phenotype – a differentiation with a huge impact on athlete's carriare. Atheletes have significantly better GLS than patients with cardiomyopathy with a cut-off value of -14% (254, 255). In the screening of cardiomyopathy gene-carriers, GLS seems to be useful in dilating cardiomyopathy (256, 257). Declined values have also been reported in gene-carriers of hypertrophic cardiomyopathy, while some reports have indicated that the initial alterations are changes in twist and regional function (237, 258, 259).

GLS has been proven to be a strong *predictor* in several clinical scenarios. GLS can predict the later deterioration of LV function after chemotherapy treatment (260-264), after valve operations (265-268) and in myocardial infarction patients (269, 270). It has been associated with adverse remodeling in patients with myocardial infarction, dilated cardiomyopathy or diabetes (271-273). Patients with aortic stenosis with and without reduced LVEF as well as patients with heart failure and with chronic ischemic cardiomyopathy, with amyloidosis or chronic kidney disease show increased mortality associated to lower GLS (274-279). In fact, a low GLS is an independent predictor of many major cardiac adverse events, such as cardiac and overall mortality, stroke, hospitalisation for cardiac reasons and for arrhythmias in patients with pre-existing cardiac disease and in other patient populations and even in unselected population (239, 280-287).

GLS has not yet been videly adopted in the follow-up recommendations, or for guiding patient management, even though it can be an early indicator of myocardial involvement, it can help to differentiate pathological and normal conditions, and it has a strong prognostic value. In the Cardio-oncology position paper released by European Society of Cardiology in 2016, it was recommended that chemotherapy patients should be measured for GLS during the surveillance of the cardiotoxicity (8), with an abnormal response defined as a 10- 15% change from the original value (8, 288, 289). The absence of GLS in the guidelines is probably due to its novelty and therefore shortage of wide-scale research qualifying it to the recommendations rather than its inability to be a useful method in this sense.

2.5.2.2 Other measurements in speckle tracking echocardiography

SR describes the speed by which strain changes (192, 290). Compared to strain measurements, it is less affected by heart rate and changes in cardiac preload and afterload (291, 292). SR, however, is undermined by technical limitations and has not been adopted to clinical practice (231).

Circumferential strain can be measured in the parasternal short axis views of the LV (Figure 6). Circumferential strain measures the transverse (tangential) contraction of the LV (233). The transverse fibres of the LV dominate the outer and apical layers of the LV (232). Circumferential strain better represents epicardial function than GLS. In most of the common heart diseases, the more vulnerable endocardial portion of the LV is the first to be affected, and circumferential contraction gets afflicted in more advanced stages of the disease or in local transmural diseases. In patients with acute heart failure with low LVEF and GLS, global circumferential strain (GCS) independently predicted adverse events (293). On the other hand, in conditions that affect primary epicardial layers, such as constriction or myocarditis, the primary phenomenon can be circumferential strain depression without a significant decline in GLS (232, 238, 294).

Radial strain measures myocardial systolic thickening (233). It is measured in the parasternal short axis views. It shows compensatory increase in response to longitudinal strain decline in diabetic patients (240, 242). It seems to detect different myocardial pathologies, but it has been seriously undermined by its poor repeatability (295).

In addition, LV rotation can be measured from the parasternal views and is measured in degrees (°). Seen from the apex, basal rotation is usually counterclockwise and apical rotation is clockwise (232). The difference between apical and basal rotation is expressed as twist (°), and when the exact distance between the basal and apical segments can be measured, it can be expressed as torision (°/cm) (232). The twisting motion of the LV improves the mechanical efficacy of the LV in systole, and stores kinetic energy, which is released like a spring during early diastole (232). In the early stage of myocardial dysfunction, the endocardial layers are most often affected. The balance between the endocardial and epicardial fibers is thereby shifted, and in the apical segments, the stronger effect of epicardial layers produces stronger, and delayed, clockwise rotation (296). Such effects have been seen in ischaemia, diabetes, hypertension and even with ageing (296). Enhanced rotation delayes early diastolic function, and it has been postulated that further deterioration gradually leads to changes in longitudinal systolic function and finally to a reduction in all directions, thus leading to changes in global systolic function (296). In extreme cases, the reversal of apical rotation can be seen in patients with advanced dilated cardiomyopathy (297).

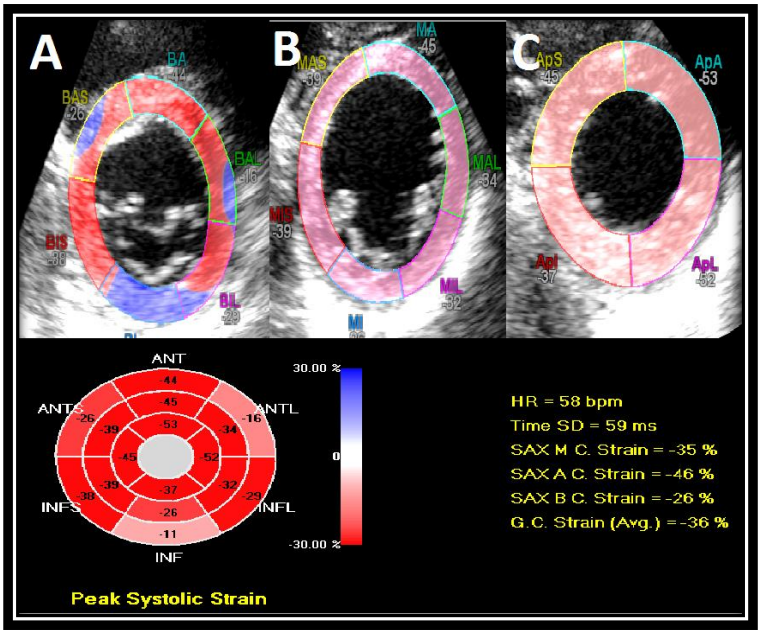

Figure 6. Circumferential speckle tracking analysis. The top figures from A to C illustrate the parasternal short axis clips from the mitral valve, the papillary muscle and from the apical levels, respectively. The global and regional results are displayed on the bottom.

The versatility of the STE technique has produced several other measurements that, so far, have been used only in reseach. Mechanical dyssyncrony has been evaluated by the differences in the regional time-delay in the different LV regions. It is used to predict responders for cardiac resyncronising therapy (*i.e.*, biventricular pacing), however, its role is unclear (298, 299). Mechanical dispersion has been detected in patients with long QT syndrome (300). Delayed regional systolic contraction (*i.e.*, post-systolic strain) has been associated with ischaemic segments and viability, but it can also be observed in scarred tissue (231, 301, 302).

The novel techniques are 3D strain measurements and layer specific strain evaluation. There are three major advandages regarding 3D strain measurements. First, the false apex -problem and second, out-of-plane movement of the speckles, can virtually be eliminated. Third, all views are measured simultaneously, and thus, the differences by shorter or longer cycles will be eliminated. Also, from 3D strain measurements, area strain was introduced (303). However, with current technology, spatial and temporal resolution are poor, and the reproducibility of the 3D strain is not sufficient enough to qualify it for clinical use (231). There are a few validation studies regarding layer specific strain. The longitudinal strain's intra and interobserver variability measured with correlation coefficients were 0.94-0.97 and 0.80-0.83, respectively (304). However, its clinical significance has so far not been impressive – layer specific strain did not exhibit improved diagnostic value over conventional GLS in ischaemic patients (305).

2.5.2.3 Validation, strengths and weaknesses of the STE measurements

To be a valid tool, a new method needs to be validated, the variability and normal values need to be defined and its strengths and weaknesses need to be addressed.

At the beginning of the 21st century, STE validation against sonomicrometry and CMR was performed (302, 306-310). The issue of intervendor differences has been actively addressed by a EACVI-ASE-Industry Task Force (12, 233). Even so, the intervendor differences still exist, and the values derived from different vendors are not fully interchangeable, although small reports indicate that intervendor variability is as low as 5% (12, 311, 312). However, the GLS results from vendor to vendor differ, and there seems to be a discrepancy of the influence of patients' age between the vendors (12). The normal GLS values are now well defined, for Philips and for 50-70 years old ladies (as in our study), it is approximately -13% to -17% (12, 313). The variability of the STE measurements have been extensively explored. The intraobserver variability for GLS has been good, 3-5% (relative), 1.1% (absolute) or ICC 0.84-0.95 and the interobserver variability 6-8% (relative), 1.1-1.5% (absolute) or ICC 0.71-0.91 (12, 273, 311, 314). The validation values for circumferential and radial strain, and for SR and for rotational measurements have been worse (231).

The STE method has several other strengths. Direct measurement of myocardial function by STE can be considered to be a more precise method than sole LVEF measurement. For example, in small hypertrophied LV, the calculated LVEF can be normal or even supranormal despite functional abnormalities, which misassumption can be avoided with direct myocardial measurements by using the GLS measurement. In addition, both global and local function can be estimated with STE technique. Compared to TDI, the major advandage of the STE technique is that it is less angle dependent (192). The block of speckles can be followed-up in 2D images in any direction, but due to poorer lateral resolution in echocardiography in general, the axial movements are more accurately followed (192, 231). However, deviations from direct the axial angle do not significantly undermine the results.

There are some pitfals one must be aware of while using the STE measurements. Like in the measurement of Simpson's LVEF, true apex and loading conditions have major effects on the GLS measurement. A forshortened apex leads to overestimation of the contractility, and thus, the consideration of the apex must actively be incorporated in the

evaluation of th image quality (192, 231). Likewise, the GLS measurement is sensitive to loading conditions. Blood pressure and valvular abnormalities should be taken into account while evaluating the GLS measurements (231, 295, 313). Furthermore, the frame rate of the images should be between 40 and 80 frames/second, since lower and higher frame rates lead to a loss of information in the calculation process. Some of the events, especially systolic and diastolic SR measurements, are faster than that and would optimally require frame rates over 100 frames/second (231, 233). With lower frame rates, some information can be lost, and peak velocities can be missed (232). In 2D imaging, the twisting movement and respiration derived displacement of the heart can cause the speckles to move out of the plane, and thereby cause inadequate tracking (192). In addition, with serial image acquisition, instread of simultaneous, the loops can have varying lengths, which in theory can influence the global values. Finally, doubt has been cast over the reproducibility of the GLS measurement outside the academic enviroment, even though small studies show that the level of expertise has less influence on the GLS results than on the measurements of the LVEF (315).

3. AIMS OF THE STUDY

The aims of this study were to explore whether modern conformal RT for early-stage breast cancer induces any echocardiographically detectable global or local changes in cardiac structures or function in the early phase after the treatment and whether they are

- associated with the RT doses and fields
- accompanied by abnormalities in ECG and biomarkers
- potentially useful in the screening of patients who would benefit from well-organised long-term follow-up

4. METHODS

4.1 Patients

4.1.1 Recruitment of patients

The study population was recruited at the Department of Oncology, Tampere University Hospital, Finland from July 2011 to November 2013 and the cardiological examinations were performed at the Heart Center, Tampere University Hospital, Finland. The study population consisted of eligible breast cancer patients treated with adjuvant RT after breast cancer resection or ablation. A total of 119 patients were included (Figure 4.1). The studies presented here focused on the patients receiving adjuvant RT only to exclude confounding effects of the chemotherapy treatment. A total of sixty patients with left-sided and twenty patients with right-sided breast cancer were included in the analysis. The exclusion criteria were age under 18 years or over 80 years, other malignancy, pregnancy or breast feeding, acute myocardial infarction within 6 months, symptomatic heart failure (NYHA 3-4), dialysis, permanent anticoagulation therapy and severe psychiatric disorders. Patients with atrial fibrillation, left bundle branch block, permanent cardiac pacemaker and severe lung disease were also excluded in order to improve the quality of the echocardgiographic imaging.

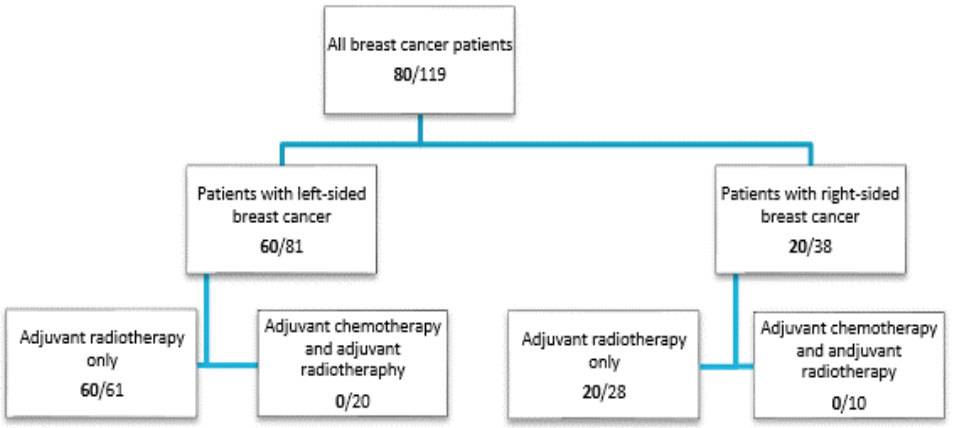

Figure 7. Flow chart showing the subgroups of the recruited patients. Bolded numbers show patients analysed in this dissertation.

4.1.2 Study protocol

The recruited patients were examined 6±8 days prior to RT and again at 1±1 days after the completion of RT. The time interval between the studies was 19 to 91 days. In addition to the comprehensive echocardiography examination, each study visit included measurement of blood pressure, a 12-lead ECG and 24-hours Holter recording. Blood samples were collected prior to RT, once during the treatment course and at the last visit. Data from each visit were analysed, and a patient record was created in the Tampere University Hospital clinical electronic patient database (Miranda).

4.1.3 Ethical aspects

The study protocol was approved by the Ethics Committee of Tampere University Hospital. The protocol complies with the Declaration of Helsinki. Written informed consent was obtained from all study participants.

4.2. Radiotherapy

Treatment planning was done using 3D CT imaging (Philips Big Bore City, Philips Medical Systems, Wisconsin, USA) with an Eclipse v.10 System (Varian Medical Systems, Palo Alto, CA, USA) by the same radiation oncologist (Figure 8). Radiation doses were calculated using the anisotropic analytical algorithm, and dose-volume histograms were generated for different cardiac structures in each patient (Table 2). The treatment doses complied with local clinical guidelines, the standard treatment doses were 50 Gy in 2 Gy fractions, and the hypofractionated doses were 42.56 Gy in 2.66 Gy fractions. An additional boost of 16 Gy in 2 Gy fractions to the tumour bed was administered when clinically indicated.

Table 2. Radiation doses to the different cardiac structures in Grays

	Left-sided breast cancer n=60		Right-sided breast cancer n=20	
	Median	Range [min, max]	Median	Range [min, max]
Whole heart				
Mean	3.1	[0.7, 6.8]	0.6	[0.3, 4.8]
Peak	47.0	[5.8, 64.2]	4.5	[2.5, 19.1]
Left ventricle				
Mean	4.4	[0.8, 12.3]	0.1	[0.0, 3.3]
Peak	45.8	[4.5, 63.8]	0.4	[0.2, 5.2]
LAD-region				
Mean	19.2	[2.0, 41.4]	0.1	[0.0, 1.4]
Peak	45.3	[4.4, 77.0]	0.4	[0.2, 5.2]
Right ventricle				
Mean	2.4	[0.9, 9.2]	0.4	[0.2, 4.5]
Peak	38.8	[2.9, 50.6]	1.6	[0.7, 8.1]

LAD, the region of the heart perfused by the left anterior descending artery.

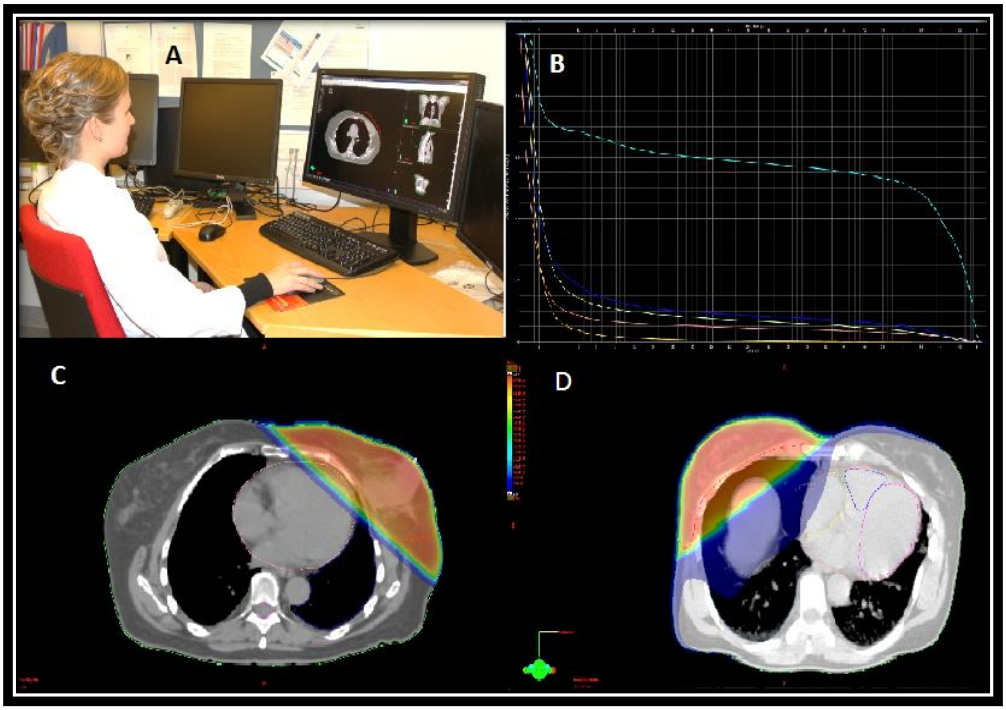

Figure 8. Radiotherapy planning. On the left upper corner (A), radiation oncologist is contouring treatment doses on her workstation. The right upper corner (B) shows dose-volume histograms for different cardiac structures derived from 3D treatment planning. The bottom figures show 3D CT treatment planning in one plane for a patient with left-sided (C) and for a patient with right-sided (D) breast cancer. The different colors in the CT images indicate different radiation doses, blue coloring indicating lower doses and increasing doses from yellow to red. The treatment doses are shown with 5 Gy for red color in patients with left-sided breast cancer (C) and 1 Gy in patients with right-sided breast cancer (D).

4.3 Echocardiographic examinations

A predefined protocol included structured acquisition of on-line measurements and optimised clips for further off-line analysis. The same cardiologist created the protocol and performed all of the studies (SST). All echocardiographic examinations were performed with a cardiac ultrasound machine (Philips ie33 ultrasound system, Bothell, Washington, USA) equipped with a 1-5 MHz matrix-array X5-1 transducer.

All of the acquisitions were performed at rest, and the Doppler recordings were acquired at end-expiration. Subcostal imaging was performed with patients in the supine position, and other imaging was performed when the patient was lying in the left lateral decubitus position. A simultaneous superimposed ECG was displayed throughout the echocardiography and care was taken to assure optimal signal for the off-line analysis for speckle tracking and to enable the differentiation of the cardiac phases in Doppler recordings. The image quality was graded from 1 to 4 (1 being very poor image quality making reliable measurements difficult in over 20% of the on-line measurements, and 4 being optimal image quality). The mean image quality in the baseline study was 2.80±0.88 (mean±SD) and in post-RT study was 2.86±0.88. At baseline examination image quality was excellent (class 4) in 17 (21.3%) and very poor (class 1) in 7 (8.8%) patients. The corresponding numbers at the control examinations were 20 (25.0%) and (7.5%), respectively.

The raw data were stored in an external hard drive, and the off-line analyses were performed using spesific software (Philips Qlab, Bothell, Washington, USA; version 8.1.2 for IBS and 3D LV analysis and 9.0 for all STE analysis). All measurements were performed according to contemporary international recommendations for echocardiographic examinations (192, 316-320). When clinically significant cardiac abnormality was detected, additional measurements and other examinations were performed according to normal clinical practise. All imaging was stored in the Tampere University Hospital clinical database (Excelera, Philips).

4.3.1 Conventional echocardiography

4.3.1.1 Conventional two-dimensional echocardiography

Optimisation of 2D imaging was performed by several means as predefined in the protocol. The images were shortened and the sector was narrowed to show only the focused issues with the highest possible frame rate. Lower transducer frequencies and harmonic imaging were applied when needed. Optimal gain was tuned and additional optimising with time- and lateral gain was performed when necessary.

Right ventricle (RV) basal dimensions were measured from the apical four-chamber view at end-diastole while ensuring that the true apex and the crux of the atrioventricular valves were visualised. The aortic root, conventional left atrial diameter, LV dimensions and wall thicknesses were measured from the parasternal long axis view as orthogonal as possible. The left atrial volume was measured by tracing from the apical two- and four-chamber views at the maximal atrial diastole and it was indexed to body surface area.

4.3.1.2 M-mode analysis

M-mode was used to measure wall thickness and dimensions as well as left atrial and aortic root diameters. Tricuspid annular plane systolic excursion (TAPSE) was measured in the apical four-chamber view by placing the measurement line in the lateral tricuspid annulus while minimising the angle error between the measurement line and the longitudinal contraction of the RV free wall. The absolute angle error was 6.1±5.5 ° in the baseline study and 7.6±4.3 ° in the control study. The mean difference between the studies was 3.0±2.3 °, and the maximal angle difference from the baseline to the control study was 9.7° (Figure 9). The parasternal measurements were performed as perpendicular as possible.

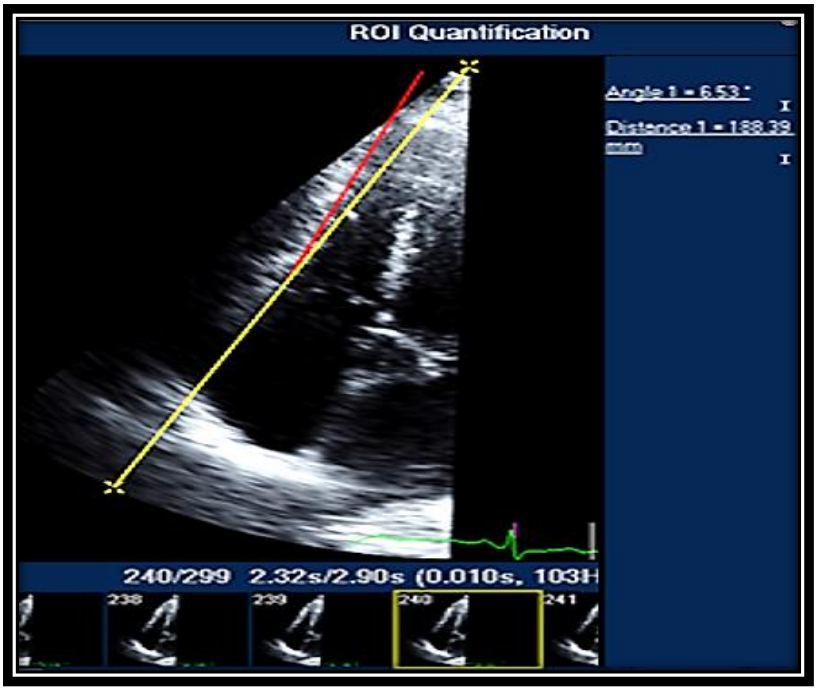

Figure 9. Measurement of the angel error. The clip is freezed at maximal contraction. The yellow line is the cursor line. The red line follows the proximal RV free wall with starting point at lateral tricuspid annulus. The measured angle at 6.53 ° is the angel between these lines.

4.3.1.3 Doppler echocardiography

All Doppler recordings were performed during quiet breathing at end-expiration. Care was taken to minimise the angle error in all Doppler recordings. The mitral and tricuspid inflow was measured by placing the measurement point of the pulsed Doppler at the tips of the valve. The LV and RV outflow recordings were performed at the level where the closing signal but not the opening signal could be detected. Continuous Doppler was used to record tricuspid regurgitation gradients and to record aortic and pulmonic valve flow velocities. Additional measurements were taken as needed in valvular pathologies.

4.3.1.4 Pulsed tissue Doppler echocardiography

Pulsed tissue Doppler analyses were performed at the RV lateral annulus and at the septal, lateral, anterior and posterior mitral annulus. In all recordings, the angle error was minimised and the image was narrowed. The measurement point was placed approximately 0.5-1 cm apically from the annulus in the middle of the myocardium. In addition, visual inspection was used to assure that the measurement point stayed within the myocardium throughout the whole cardiac cycle prior to recording.

4.3.1.5 Three dimensional echocardiographic analysis

3D echocardiography was performed from the apical views as full-volume four-cycle acquisitions. Due to low image quality, 3D echocardiography analysis could not be performed in 11 (14%) of the patients in the baseline study and in 13 (16%) of the patients in the control study.

4.3.2 Advanced echocardiography

4.3.2.1 Integrated backscatter

IBS was measured off-line from the parasternal long-axis clip and from the parasternal short-axis clip at the papillary muscle level. Prior to the clip acquisition, the time and lateral gains were set to the neutral position. Gain was increased to a level where the cavity colouring was slightly grey instead of black. An acquisition contained at least three cycles. The parasternal clip was as perpendicular as possible, and the short-axis clip was as round as possible.

4.3.2.1.1 Calibrated integrated backscatter

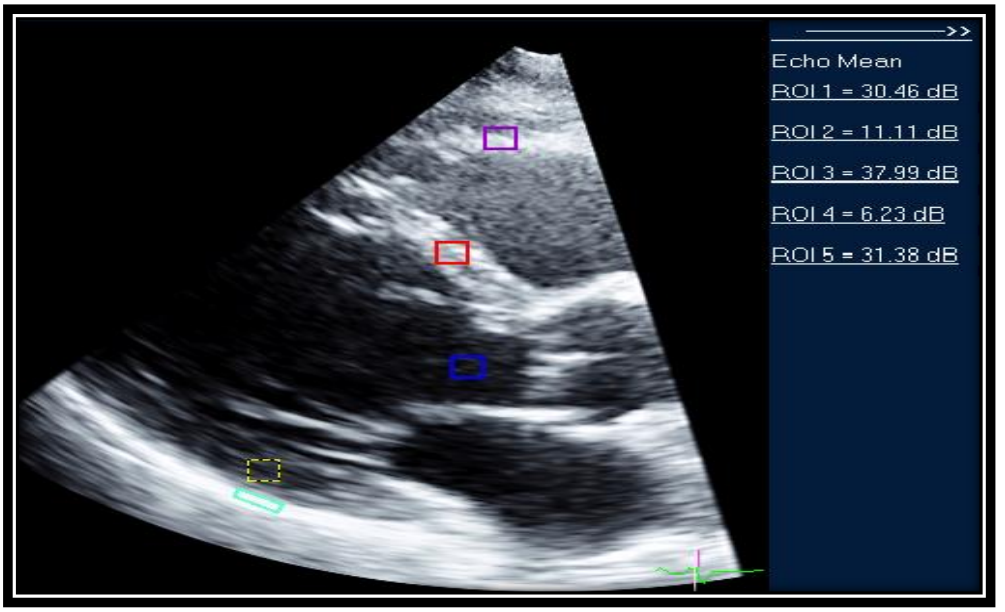

Figure 10. Measurement of the calibrated integrated backscatter. The clip is scrolled to the end-diastole. The septal square is red and the corresponding value is presented on the left margin as ROI 1. The yellow posterior square is ROI 2, the turquise pericardial rectangle is ROI 3, the blue outflow tract square is ROI 4 and the purple right ventricular free wall square is ROI 5.

A parasternal long-axis clip was analysed with the region of interest (ROI) program in the Philips Qlab software (version 8.1). The clip was scrolled to first frame where the mitral valve was closed. A square of five millimetres was placed in the basal interventricular septum, carefully avoiding the endocardial bright borders as well as very bright or dark areas within the myocardium. A second square was placed in the posterior wall, and a third square was placed in the LV outflow tract and fourth in the RV free wall. A rectangle was placed in the posterior pericardium (Figure 10). After the first values were recorded, the clip was then scrolled to the next end-diastolic frame, and new measurements were made. The measurement area was repositioned if necessary. The average of three measurements was used for the calculations. The myocardial values were calibrated by subtracting the cavity or the pericardial value from the myocardial value (191). Analysis of the cIBS was possible in 72 (90%) patients in the baseline study and in 78 (98%) in the control study.

4.3.2.1.2 Cyclic variation of the integrated backscatter

Measurements of the CVIBS were performed in Philips Qlab (version 8.1). A five millimetre square was placed in the anterior part of the interventricular septum and a second square was placed in the posterior wall (Figure 11). The clip was inspected throughout the cycles and repositioning was made if necessary. The highest and the lowest values were recorded, and the CVIBS was calculated as the difference between these two values. The septal and posterior CVIBS was analysable in 71 (89%) and 70 (88%) in the baseline and in 76 (95%) and 77 (96%) in the control studies, respectively.

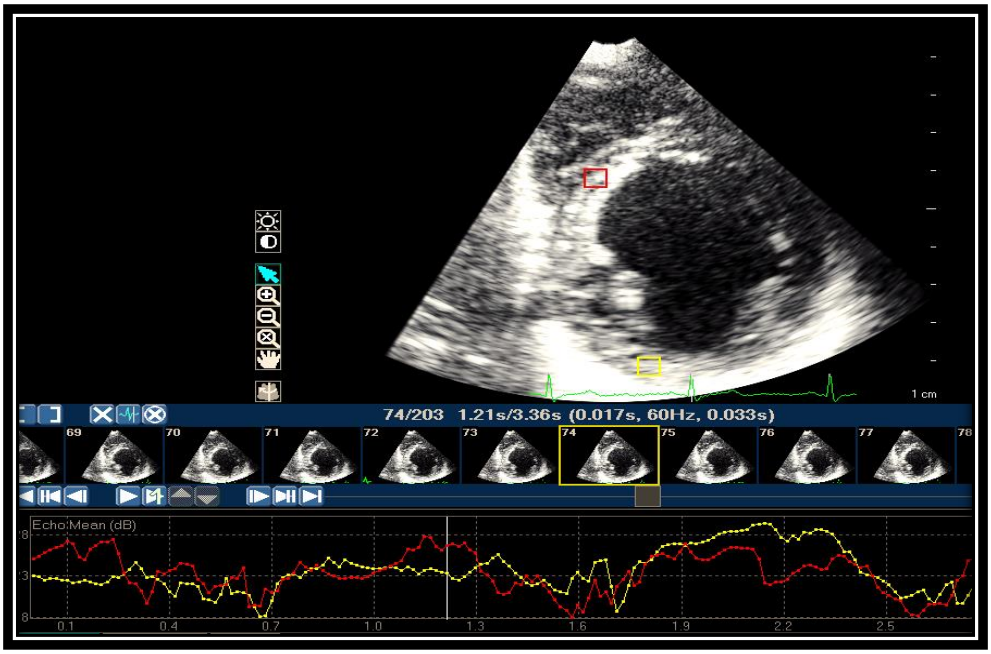

Figure 11. Measurement of the CVIBS. A parasternal short axis view at the level of papillary muscles is acquired for further analysis. The regions of interest were placed in the anterior septum (yellow box and line) and in the posterior wall (red box and line). After visual inspection of adequate tracking, the highest and lowest values were collected. The CVIBS was calculated as the difference between these values.

4.3.2.2 Speckle tracking echocardiography

Three apical and three parasternal clips of the LV over three cardiac cycles were acquired for off-line STE analysis. The apical clips were apical four-chamber, apical two-chamber and apical three-chamber clips. The three parasternal short-axis clips were recorded at the mitral valve level, at the level of papillary muscles and at the apex level. In addition to the general image optimising, further optimising was performed in order to ensure the best possible tracking. The most important step in the additional optimisation processes was to exclude bright shadowing and other image artefacts from and near the measurement fields. Also, the gain was manipulated to visualise the natural speckles of the myocardium in the best possible way over the whole area of interest. Furthermore, attention was payed to the ECG quality.

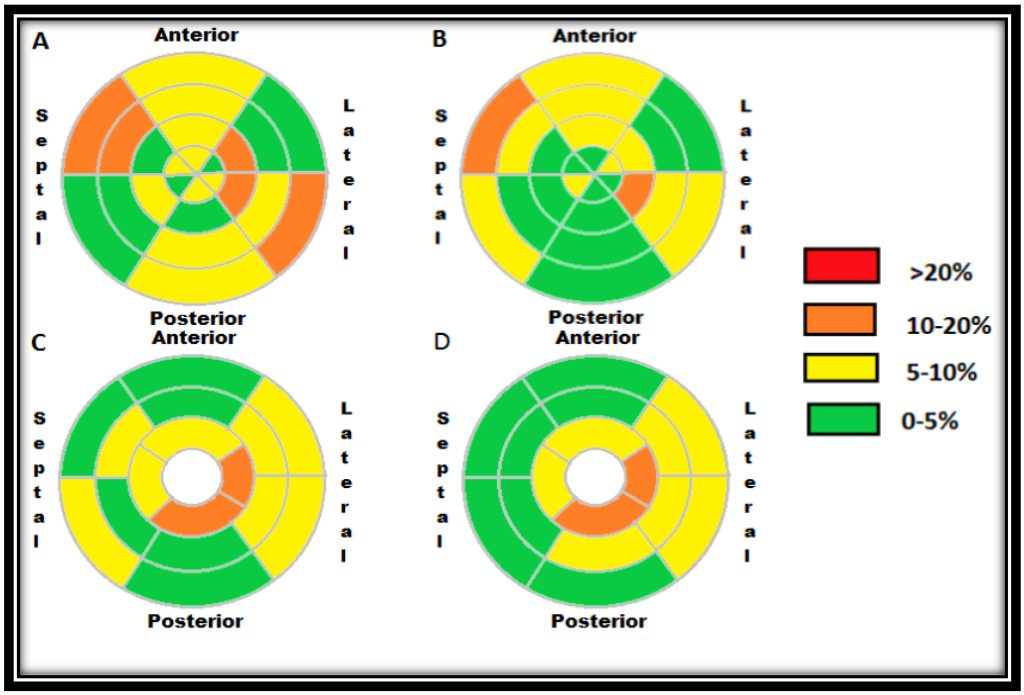

Figure 12. Measurability of the segments in speckle tracking analysis. The upper row shows longitudinal measurements (A and B), and the lower row presents the circumferential measurements (C and D). The baseline studies are on the left (A and C), and the control studies are on the right (B and D). The colouring shows the percentage of the excluded segments, with the green colour showing the best measurability and the red the worse. The number of green segments rose from seven to ten in the longitudinal strain measurements from baseline to the control study, and from six to seven in the circumferential measurements.

4.3.2.2.1 Strain analysis in speckle tracking echocardiography

STE strain analyses were performed off-line with Philips Qlab version 9.0 with a semiautomatic software program. End-systole was defined either by aortic valve closure, by visual estimation based on LV contraction or by the end of the T-wave in ECG. Adequate tracking was controlled by visual inspection, and correction with reanalysis was performed when necessary. Segments with repeated inadequate tracing were excluded from the final analysis. In apical recordings the highest segmental exclusion rate was 15% and 12% (basal anterior septum) in the baseline and control studies, respectively and 10% and 5% (apical posterior segment) for the respective parasternal short-axis clips. Global and segmental values were recorded and regional values were calculated as an average of the segments involved. When two or more segments were missing, regional calculations were not made.

4.3.2.2.2 Strain rate analysis in speckle tracking echocardiography

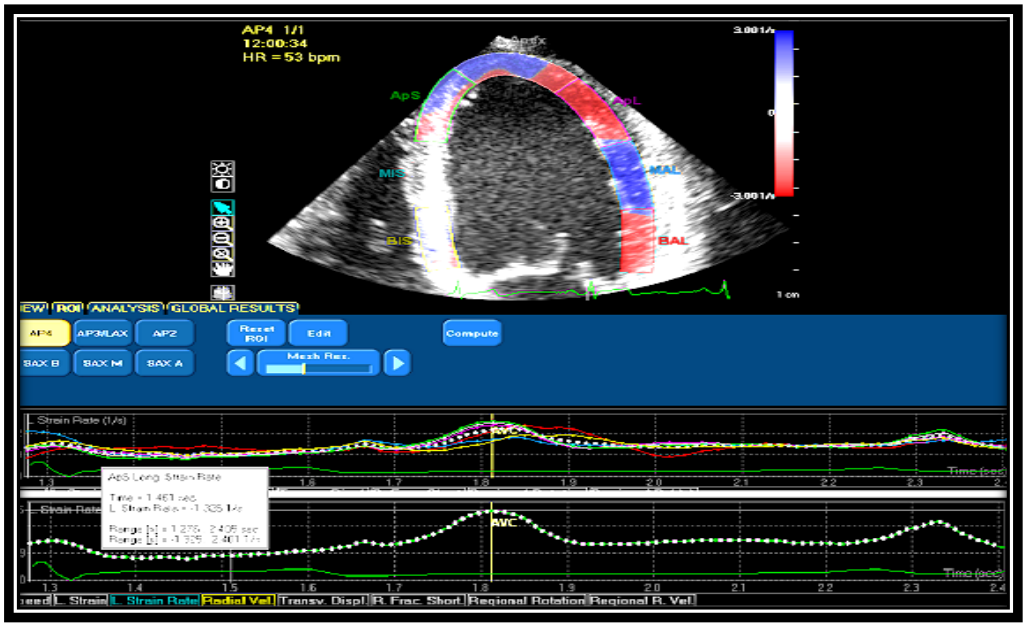

Figure 13. Measurement of the systolic longitudinal strain rate in STE. The upper part of the figure shows measurements of several segments in the apical four-chamber view with a cluster of strain rate lines in the panel underneath. The bottom of the figure shows an individual line from the apical septal segment after other segments were removed. From this line, the deepest systolic strain rate is -1.325/s.

The systolic strain rate in the STE analysis was defined as the peak negative velocity during the systole in each segmental slope (Figure 13). The regional and global values were calculated as an average of the segments involved.

4.3.2.2.3 Rotation and twist in speckle tracking echocardiography

STE analysis for the parasternal short-axis clips was used to define basal and apical rotation. The maximal values and their timing were recorded. The timing was adjusted to the pulse at the time of the recording. Twist was calculated as the difference between basal and apical rotation.

4.4 ECG

A 12-lead ECG was obtained at each visit. The ECG was taken with a 50 mm per second speed with a voltage calibration of 10 mm=1 mV. Heart rate, QRS morphology and T-wave inversions and their locations were recorded.

4.5 Cardiac biomarkers

A blood sample for high-sensitivity troponin T (hsTnt) and proBNP analyses were collected at the baseline visit, once during the treatment period and at the control visit. The analysis was performed in the hospital laboratory using routine clinical analysis. A value of 4 ng/l was used in the analysis if hsTnt was lower than the detection threshold of 5 ng/l.

4.6 Statistical methods

Categorical data are presented as absolute numbers and percentages. Continuous variables are described by the mean and standard deviation in normally distributed data and by medians with ranges for variables with skewed distribution. Normality of the distribution was assessed after visual inspection of the histogram and bar-plot appearance, by the Kolmogorov-Smirnov test, by taking into account of the skewness, kurtosis, and by comparing the similarity of means and medians. Comparisons between non-related groups were performed with independent samples t-test, with the independent samples Mann-Whitney U test and with the Chi-Square or Fishers exact test for variables with normal, skewed distribution and categorical variables, respectively. The differences between baseline and post RT values were tested with paired t-tests for normally distributed variables and with Wilcoxon signed-rank test for variables with a skewed distribution. Categorical variables were tested with Chi-Square or Fishers exact test. Associations between normally distributed variables were tested with Pearson correlation, and with Spearman correlation when non-normally distributed variables were tested. Binary logistic or linear regression analyses were employed to conduct univariate and multivariable analyses. Reproducibility was tested with inter class correlation and Blant Altmant plots. All tests were two-sided and P-values <0.05 were considered statistically significant. Statistical analysis was carried out with IBM SPSS statistics for Windows, versions 19, 20, 22 and 23 (**I**, **II**, **III**, **IV**).

5. RESULTS

5.1 Characteristics of the study population

The characteristics of the study population and their distribution in publications I-IV are presented in Table 3. One patient withdrew her involvement in the study between the baseline and the control examination and she was excluded from the final analysis. The follow-up success was 99%.

None of the patients had any cardiac symptoms in the study period, except for palpitations in two patients. One patient had undergone CABG 20 years previously and another patient had a biological aortic valve replacement operation four years prior to the breast cancer treatment. Both had moderate aortic stenosis at the baseline study. Two patients had moderate aortic regurgitation, and two others had a bicuspid, but well-functioning aortic valve with a mildly dilated ascending aorta. One patient had a mild ebstanoid dysplastic tricuspid valve anomaly. Two patients had mild sick sinus syndrome and two patients were put on beta blocker medication due to an excess amount of ventricular extrasystolies on the Holter recording. Finally, a dual-chamber cardiac pacemaker was installed for one patient for a Morbitz type-2 atrio-ventricular block that was discovered on the Holter recording.

In summary, abnormal findings in the baseline examination led either to clinical follow-up or to a change in the patient treatment in ten patients (13%). However, the findings and treatment between the baseline and the control studies were unchanged and did not influence our results. After the study period, the patient with previous CABG underwent through a TAVI procedure, and the patient with aortic valve prosthesis has been treated conservatively so far.

Table 3. Baseline characteristics of the study population

	The whole group n=80		Left-sided breast cancer n=60		Right-sided breast cancer n=20		
	n	(%)	n	(%)	n	(%)	p
Included in study I	49	(61.3)	49	(81.7)	0	(0.0)	
Included in study II	78	(97.5)	58	(96.7)	20	(100.0)	
Included in study III	73	(91.3)	53	(88.3)	20	(100.0)	
Included in study IV	80	(100.0)	60	(100.0)	20	(100.0)	
Age(years) *	63	6	63.6	6.8	62.9	4.7	0.657
BMI (kg/m^2) †	26.4	(24.3, 30.0)	26.3	(24.1, 29.9)	26.6	(24.7, 30.0)	0.567
Breast cancer ablation	1	(1.3)	1	(1.7)	0	(0.0)	1.000
Adjuvant aromatase inhibitor	30	(37.5)	22	(36.7)	8	(40.0)	0.790
Adjuvant tamoxifen	6	(7.5)	2	(3.3)	4	(20.0)	**0.032**
Smoking							
Current	10	(12.5)	8	(15.3)	2	(10.0)	0.722
Previous	9	(11.3)	7	(11.7)	2	(10.0)	1.000
Concurrent diagnosis of							
Hypertension	35	(43.8)	22	(36.7)	13	(65.0)	**0.027**
Diabetes mellitus	7	(8.8)	4	(6.7)	3	(15.0)	0.358
High cholesterol	18	(22.5)	14	(23.3)	4	(20.0)	1.000
Coronary artery disease	1	(1.3)	1	(1.7)	0	(0.0)	1.000
Significant valvular abnormality	5	(6.3)	3	(5.0)	2	(10.0)	0.594
Hypothyreosis	10	(12.5)	7	(11.7)	3	(15.0)	0.705
Otherwise healthy	33	(41.3)	28	(46.8)	5	(25.0)	0.088
Regurlar medication of							
Betablocker	12	(15.0)	7	(11.7)	5	(25.0)	0.163
Calsium channel blocker	8	(10.0)	4	(6.7)	4	(20.0)	0.102
ACE/ATRB	25	(31.3)	15	(25.0)	10	(50.0)	**0.037**
Statin	16	(20.0)	12	(20.0)	4	(20.0)	1.000
Diuretics	15	(18.8)	8	(13.3)	7	(35.0)	**0.047**

BMI, body mass index; ACE, angiotensin inhibiting enzyme; ATRB, angiotensin reseptor blocker. * mean and standard deviation. † median and (Q_1, Q_3). The p-value marks the difference between left-sided and right-sided breast cancer patients.

5.2 Changes in RV function after RT

The changes in RV function are presented in Study **I**. RT induced a decline in TAPSE from 24.5±4.0 mm to 22.4±3.9 mm ($p<0.001$) in patients with left-sided breast cancer. There were no other significant changes in the RV functional parameters, including pulsed tissue Doppler parameters; isovolumetric velocity (IVV), acceleration of the isovolumetric velocity (IVA) and the systolic velocity of the pulsed tissue Doppler derived from the lateral tricuspid annulus were 13.0±4.8 cm/s and 12.6±3.8 cm/s ($p=0.828$), 2.8±1.0 cm/s and 2.7±0.9 cm/s ($p=0.439$), 12.7±3.1 cm/s^2 and 12.2±3.9 cm/s^2 ($p=0.114$) at baseline and after RT, respectively. Patients using levothyroxine ($p=0.030$) diuretics ($p=0.030$) and ACE/ARBs ($p=0.060$) had a smaller reduction of TAPSE after RT the in univariate analyses.

5.3 Changes in cIBS after RT

The impact of RT-induced changes on the cIBS measurements was evaluated in Study **II**. Patients with left-sided breast cancer showed increased tissue density after RT in the RV free wall and in the interventricular septum but not in the LV posterior wall. The RV values with pericardial calibration changed from -15.0±7.3 dB to -13.7±7.9 dB ($p=0.079$) and with cavity calibration from 20.4±5.9 dB to 22.1±5.6 dB ($p=0.046$). The values in the interventricular septum with pericardial and cavity calibration changed from -18.2±5.1 dB to -16.0±6.4 dB ($p=0.002$) and from 17.3±5.2 dB to 19.8±5.5 dB ($p<0.001$), respectively. The patients with right-sided breast cancer were spared from these changes.

In the multivariable analyses the septal cIBS values were independently associated with the percentage of LV that was exposed to 20 Gy radiation (OR 3.22 [95% CI 1.05-9.88]) and with the mean lung dose (OR 1.69 [95% CI 1.01-2.84]). Changes in the RV were associated with the changes in TAPSE ($p=0.045$), mitral inflow dt ($p=0.022$) and diabetes ($p=0.015$).

5.4 Changes in CVIBS after RT

The changes in CVIBS after RT were examined in Study **III**. The patient group was divided based on the mean heart radiation dose, into those who received less than a 2 Gy mean heart dose and to those who received more than a 2 Gy mean heart dose. The septal CVIBS values decreased from 12.0±3.4 dB to 9.6±2.5 dB ($p<0.001$) and posterior

values declined from 12.8±2.7 dB to 11.3±2.4 dB (p=0.007) in patients with more than a 2 Gy mean heart dose. Patients who received under a 2 Gy mean heart dose did not have significant changes in the CVIBS measurements.

In the multivariable analyses, AI (β=2.986, p=0.001) and body mass index (BMI) (β=-0.241, p=0.014) were independently associated with the septal CVIBS reduction, whereas the mean lung dose (β=-0.485, p=0.018) and non-smoking status (β=2.411, p=0.009) were independently associated with declining posterior CVIBS values.

5.5 Systolic changes in speckle tracking analysis after RT

5.5.1 Global changes

In Study **IV**, the RT-induced changes in STE measurements were analysed with special attention devoted to the detection of differences between patients with left-sided versus right-sided breast cancer. In the whole study population there was a reduction in global systolic function as the GLS declined from -17.9±3.3% to -17.2±3.1% (p=0.028). The GLS was reduced from -18.3±3.1% to -17.2±3.3% (p=0.003) in patients with left-sided breast cancer, and a decrease of over 10% from the baseline was experienced by 17 patients (28%). In patients with right-sided breast cancer, there were no statistically significant differences between the baseline values -16.9±3.8% and values after RT -17.2±2.8% (p=0.577). In circumferential strain and circumferential and longitudinal SR measurements there were no significant changes between the baseline and the control examinations.

In the multivariable analyses the use of AI (β=-2.002, p=0.001) and the decline in LV diastolic volume (β=-0.070, p=0.025) were independently associated with the GLS change.

5.5.2 Local changes in patients with left-sided vs. right-sided breast cancer

In patients with left-sided breast cancer, regional apical strain declined and basal values increased. Apex strain decreased from -18.3±5.1% to -16.5±4.8% (p=0.003) and apical values decreased from -18.6±5.3% to -16.7±4.9% (p=0.002). Prolonged apical rotation time (β=0.012, p=0.011) and increasing LV myocardial mass (β=-0.076, p=0.024) were independently associated with the apical changes in patients with left-sided breast cancer. Basal values increased from -21.6±5.0% to -23.3±4.9% (p=0.024) and increased reflectivity, cIBS, had an independent association with it (β=0.293, p=0.045).

Patients with right-sided breast cancer displayed a local decline in the basal anterior segment. Longitudinal strain in this segment was reduced from -26.2±7.8% to -17.9±8.2% (p<0.001), and anterior basal velocity in pulsed tissue Doppler from (7.1 [6.1, 7.7] cm/s to 5.6 [5.3, 6.5] cm/s (p<0.001). Delayed basal rotation time (β=-0.035, p=0.020) was independently associated with decline in strain, and hypertension (β=1.272, p=0.009) and change in LV end-diastolic diameter (β=0.042, p=0.024) with pulsed tissue Doppler measurement.

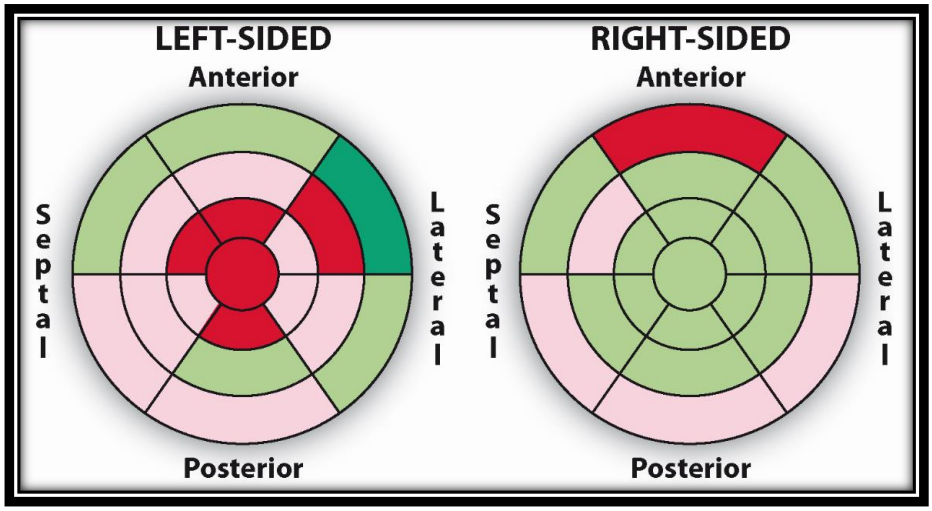

Figure 14. Segmental changes in longitudinal strain after radiotherapy. The areas with green colour show increasing function, areas with red colour indicate declining function. The darker coloring show segments with statistically significant change ($p<0.05$). Patients with left-sided breast cancer are shown on the left side and patients with right-sided breast cancer on the right side.

5.6 Other changes in echocardiography after RT

The summary of the changes in the conventional echocardiographic parameters is displayed in Table 4. In general, the LV walls got thicker and LV mass increased after RT. The changes were accompanied with minor changes in diastology, and were more frequent in patients with left-sided breast cancer.

Table 4. General changes in conventional echocardiography

	The whole group n=80					Change after RT in patients with left-sided breast cancer n=60			Change after RT in patients with right-sided breast cancer n=20		
	Baseline		After RT								
	Mean	SD	Mean	SD	p_1	Mean	SD	p_1	Mean	SD	p_1
Left ventricle											
Structures											
LVEDD (mm)	44.8	4.2	44.5	3.9	0.213	-0.5	2.7	0.157	0.1	2.2	0.920
LVEDS (mm)	30.2	3.4	29.8	3.5	0.325	-0.3	3.3	0.455	-0.4	2.1	0.428
IVS (mm) *	10.0	[9.0, 11.0]	10.2	[9.1, 11.5]	**0.001**	0.1	[-0.1, 1.0]	**0.009**	0.6	[0.0, 1.6]	**0.018**
PW (mm) *	10.0	[9.0, 10.9]	10.3	[9.8, 11.0]	**0.001**	0.4	[0.0, 1.1]	**0.003**	0.2	[-0.7, 1.6]	0.251
RWT (%) *	0.43	[0.40, 0.49]	0.46	[0.43, 0.51]	**0.002**	0.03	[-0.01, 0.07]	**0.003**	0.01	[-0.04, 0.08]	0.411
LVEDV (ml) *	97	[84, 110]	94	[82, 107]	*0.061*	-5	[-11, 3]	**0.037**	-1	[-5, 6]	0.981
LVESV (ml) *	39	[34, 45]	37	[33, 47]	0.947	-1	[-6, 3]	0.240	3	[-3, 7]	*0.068*
LVEDM (g) *	105	[91, 120]	106	[92, 123]	**0.012**	1	[-3, 6]	**0.013**	-3	[-3, 7]	0.467
Diastolic function											
Mitral E (cm/s) *	73	[64, 83]	67	[59, 79]	**0.005**	-3	[-8, 4]	**0.031**	-6	[-18, 4]	*0.067*
Mitral dt (ms) *	226	[193, 253]	239	[204, 271]	**0.018**	5	[-18, 32]	0.214	22	[-8, 64]	**0.015**
Mitral a (cm/s) *	77	[63, 91]	77	[63, 87]	0.151	-3	[-9, 7]	*0.092*	1	[-13, 9]	0.968
Mitral Ee'-ratio *	9.3	[7.3, 11.4]	9.0	[7.3, 10.3]	0.250	-0.2	[-1.4, 0.8]	0.183	0.2	[-1.5, 1.1]	0.970
IVRT (ms) *	106	[90, 124]	109	[99, 123]	0.312	4	[-8, 20]	0.204	0	[-14, 9]	0.711
LAVI (ml/m^2)	32.2	8.6	31.8	8.2	0.565	-0.7	6.5	0.432	0.4	5.8	0.784
Systolic function											
LVEF (%)	64	8	65	7	0.637	0	10	0.810	1	10	0.616
LVOT VTI (cm)	22.7	4.1	22.3	4.0	0.281	-0.4	3.0	0.341	-0.4	3.5	0.620

Right ventricle											
RV (mm) *	34.2	[30.9, 38.6]	33.6	[30.5, 36.4]	0.470	-0.5	[-2.8, 2.5]	0.523	-0.6	[-4.1, 2.2]	0.765
TAPSE (mm)	24.1	4.3	22.3	4.3	**<0.001**	-2.0	3.1	**<0.001**	-1.5	4.3	0.141
IVC (mm)	15.7	4.0	15.1	3.4	0.115	-0.9	4.1	0.116	-0.2	2.8	0.767
vIVC (%)	61	16	60	15	0.901	-2	17	0.312	-8	21	0.112
TR gr (mmHg)	22	6	21	5	0.174	0	[-3, 3]*	0.695	-3	[-5, 1]*	**0.048**
RV s' (cm/s) *	12.4	[10.4, 13.8]	12.1	[10.2, 13.7]	0.127	-0.4	[-1.4, 0.7]	0.099	-0.2	[-1.7, 1.7]	0.681
P at (ms)	148	32	145	34	0.492	-3	35	0.567	-4	43	0.714
RVOT VTI (cm)	16.5	3.2	15.9	2.6	**0.027**	-0.7	2.6	**0.038**	-0.4	2.3	0.442

LVEDD and LVEDS, left ventricle's end-diastolic and end-systolic diameters; IVS and PW, interventricular and posterior end-diastolic wall thickness; RWT, relative wall thickness of the left ventricle; LVEDV, LVESV and LVEDM, left ventricular end-diastolic and end-systolic volumes and end-diastolic mass derived from the three-dimensional acquisition; Mitral E, dt, and a, mitral inflow E (early)-wave velocity, early wave's declaration time and a (late) wave diastolic velocity; Mitral Ee'-ratio, the ratio between mitral inflow E-wave and averaged pulsed tissue Doppler e' velocities derived septal, lateral, anterior and posterior walls; IVRT, isovolumetric relaxation time of the left ventricle; LAVI, left atrial volume derived from apical four chamber and two chamber views and indexed to patients body surface area calculated by Mosteller's model; LVEF, left ventricular ejection fraction; LVOT and RVOT VTI, velocity time integral derived from pulsed Doppler measurement from left and right ventricular out-flow tracts; RV, right ventricular basal measurement from apical four chamber acquisition in end-diastole; TAPSE, tricuspid annular plane systolic excursion; IVC and vIVC, inferior vena cava maximal diameter and its variability by sniffing; TR gr, maximal gradient derived from tricuspid regurgitation flow with continues Doppler measurements; RV s', the peak systolic velocity of the right ventricular basal free wall in pulsed tissue Doppler measurement; P at, the acceleration time of the pulmonary flow measurement with pulsed Doppler. * median with [Q_1, Q_3].

5.7 Validation of the advanced echocardiography measurements

Validation measurements were performed for the cIBS, the CVIBS and the STE analysis. Twenty volunteers were recruited and recordings for intra- and interobserver variability and test-retest reproducibility were collected. All validation measurements were blinded. The intraobserver measurements were repeated with more than a month interval. For retest analyses, a second clip was acquired and analysed. Intraclass correlation was used to validate the cIBS and STE, while Blant-Altman plots were performed for the CVIBS measurements.

Table 6. The principles of ICC value intepretation (kappa)

Value of ICC	Strenght of Agreement
≤0.20	Poor
0.21-0.40	Fair
0.40-0.60	Moderate
0.61-0.80	Good
0.81-1.00	Very good

ICC, intraclass correlation

Table 5. Reproducibility data of the speckle tracking analysis in healthy volunteers

	Intraobserver variability		Interobserver variability		Test-retest variability	
	ICC	(CI 95%)	ICC	(CI 95%)	ICC	(CI 95%)
Longitudinal strain						
GLS	0.914	(0.796-0.965)	0.714	(0.406-0.876)	0.634	(0.277-0.837)
Regional values	0.799	(0.743-0.844)	0.402	(0.279-0.513)	0.516	(0.406-0.611)
Segmental	0.747	(0.701-0.768)	0.521	(0.477-0.588)	0.402	(0.318-0.480)
Longitudinal strain rate						
Global value	0.478	(0.056-0.754)	0.252	(0.000-0.617)	0.426	(0.000-0.725)
Regional values	0.454	(0.366-0.558)	0.255	(0.120-0.380)	0.273	(0.140-0.397)
Segmental	0.456	(0.377-0.529)	0.466	(0.366-0.520)	0.251	(0.159-0.339)
Circumferentiell strain						
GCS	0.840	(0.639-0.933)	0.641	(0.289-0.841)	0.711	(0.402-0.875)
Regional values	0.789	(0.727-0.839)	0.627	(0.530-0.708)	0.731	(0.655-0.792)
Segmental	0.711	(0.652-0.761)	0.709	(0.650-0.760)	0.621	(0.548-0.684)
Circumferentiell strain rate						
Global value	0.913	(0.793-0.965)	0.028	(0.000-0.456)	0.759	(0.458-0.897)
Regional values	0.702	(0.620-0.769)	0.265	(0.124-0.396)	0.638	(0.543-0.717)
Segmental	0.563	(0.483-0.633)	0.561	(0.480-0.631)	0.515	(0.429-0.591)
Rotation measurements						
Basal	0.750	(0.470-0.893)	0.593	(0.216-0.817)	0.178	(0.000-0.567)
Apical	0.622	(0.321-0.851)	0.405	(0.000-0.734)	0.490	(0.072-0.761)
Twist	0.734	(0.441-0.885)	0.000	(0.000-0.388)	0.522	(0.116-0.779)
ABRT	0.713	(0.405-0.876)	0.666	(0.315-0.856)	0.484	(0.065-0.758)
AART	0.678	(0.515-0.928)	0.481	(0.060-0.756)	0.578	(0.193-0.808)

ICC, intraclass correlation; CI, confidence interval; GLS, global longitudinal strain; GCS, global circumferential strain; Twist, calculated as difference between basal and apical rotation; ABRT and AART, time of maximal rotation in the basal and apical segments adjusted to the heart rate.

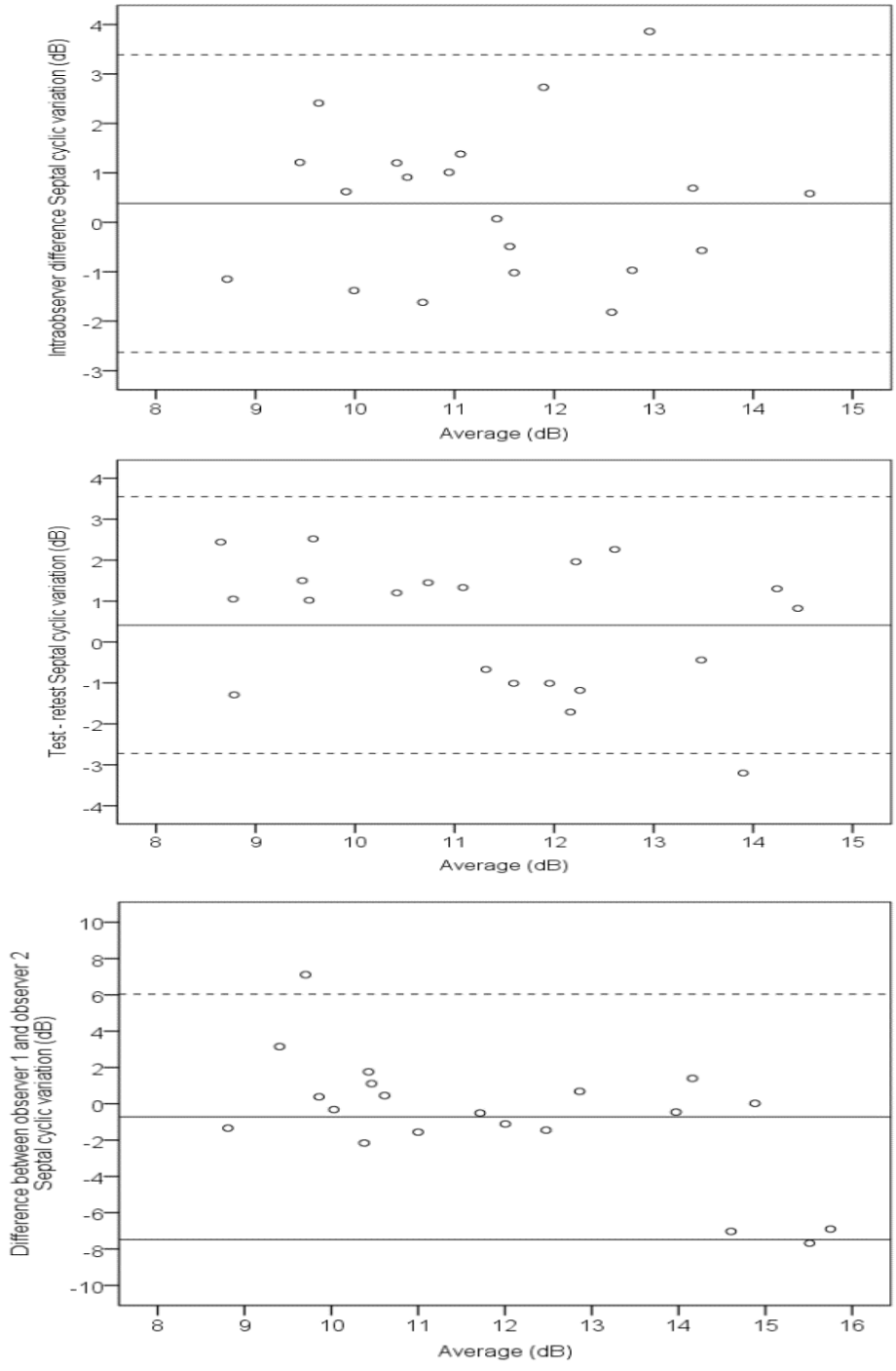

Figure 15. Bland Altman plots for the cyclic variation of the integrated back scatter. Figures in page 74 present septal and in page 75 posterior measurements.

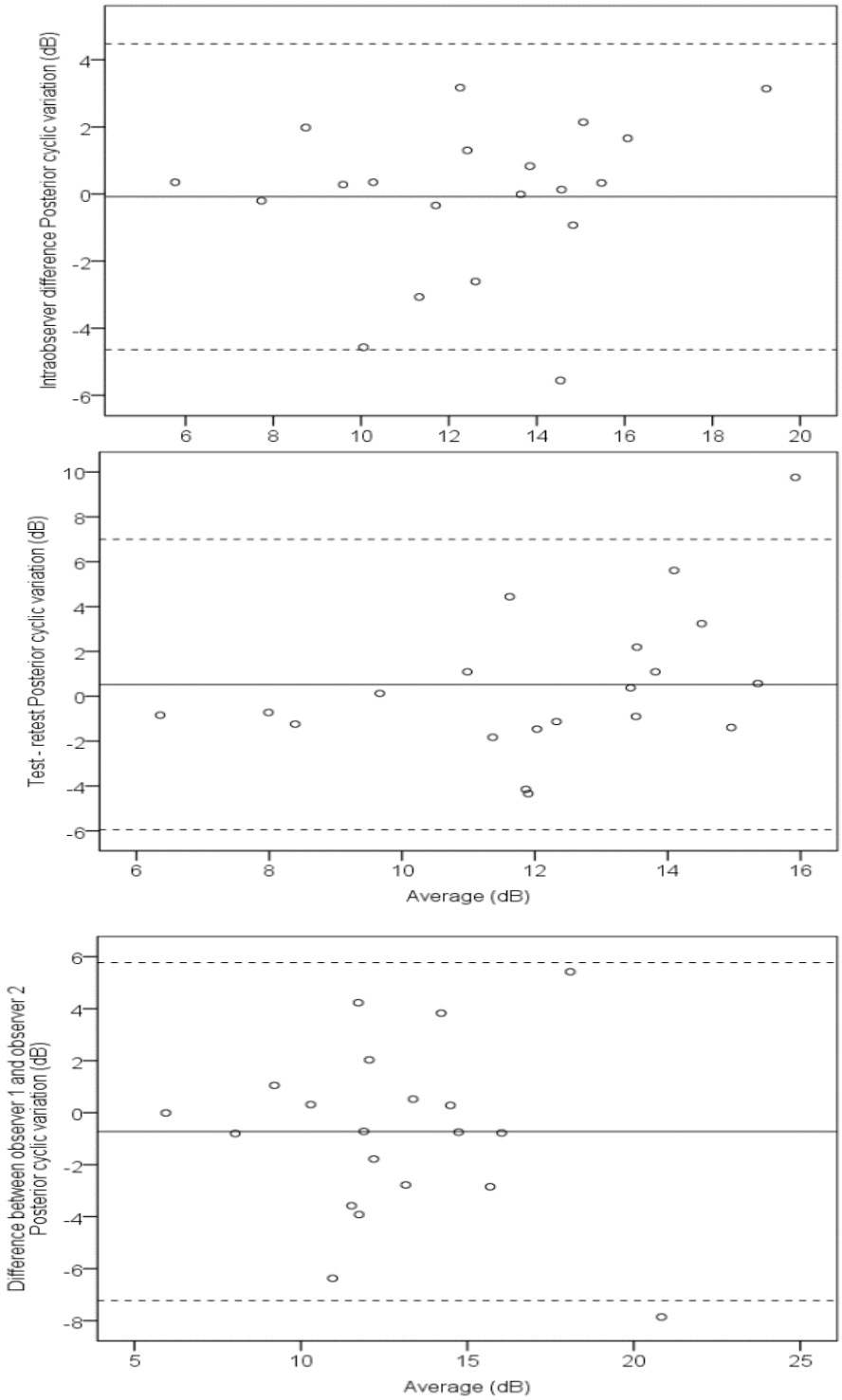

The upper rows show intraobserver variability, the middle rows show test-retest results, and the lowest rows show interobserver variability.

5.8 Changes in ECG and cardiac biomarkers after RT

Typical RT-induced ECG-changes are shown in Figure 16. T-wave flattening or inversions in the precordial leads V1-4 and in the standard leads aVL and I were the most common ECG findings. T-wave inversions were more prevalent in patients with left-sided breast cancer (39 patients) than in patients with right-sided breast cancer (5 patients) (p=0.003). The distribution of the changes in T-waves is shown in Figure 17.

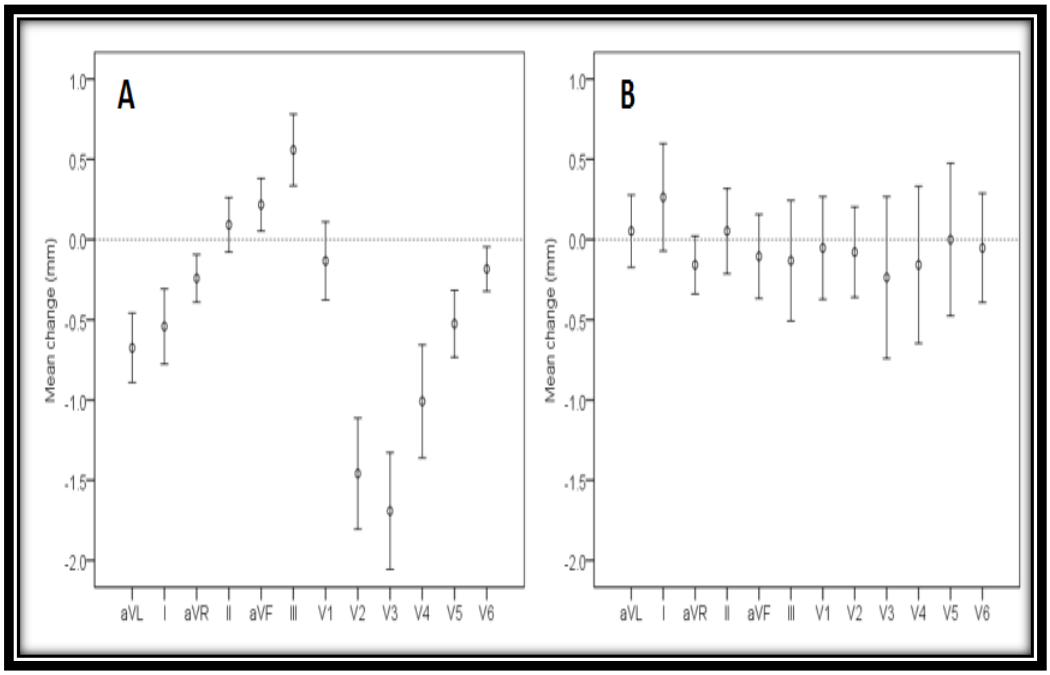

Figure 17. Distribution of the T-wave changes after RT. Figure A illustrates T-wave changes in patients with left-sided breast cancer with largest changes in precordial leads V2-V4. Figure B presents patients with right-sided breast cancer with no significant T-wave changes in the ECG. Courtesy from Heini Huhtala and Konsta Keski-Pukkila

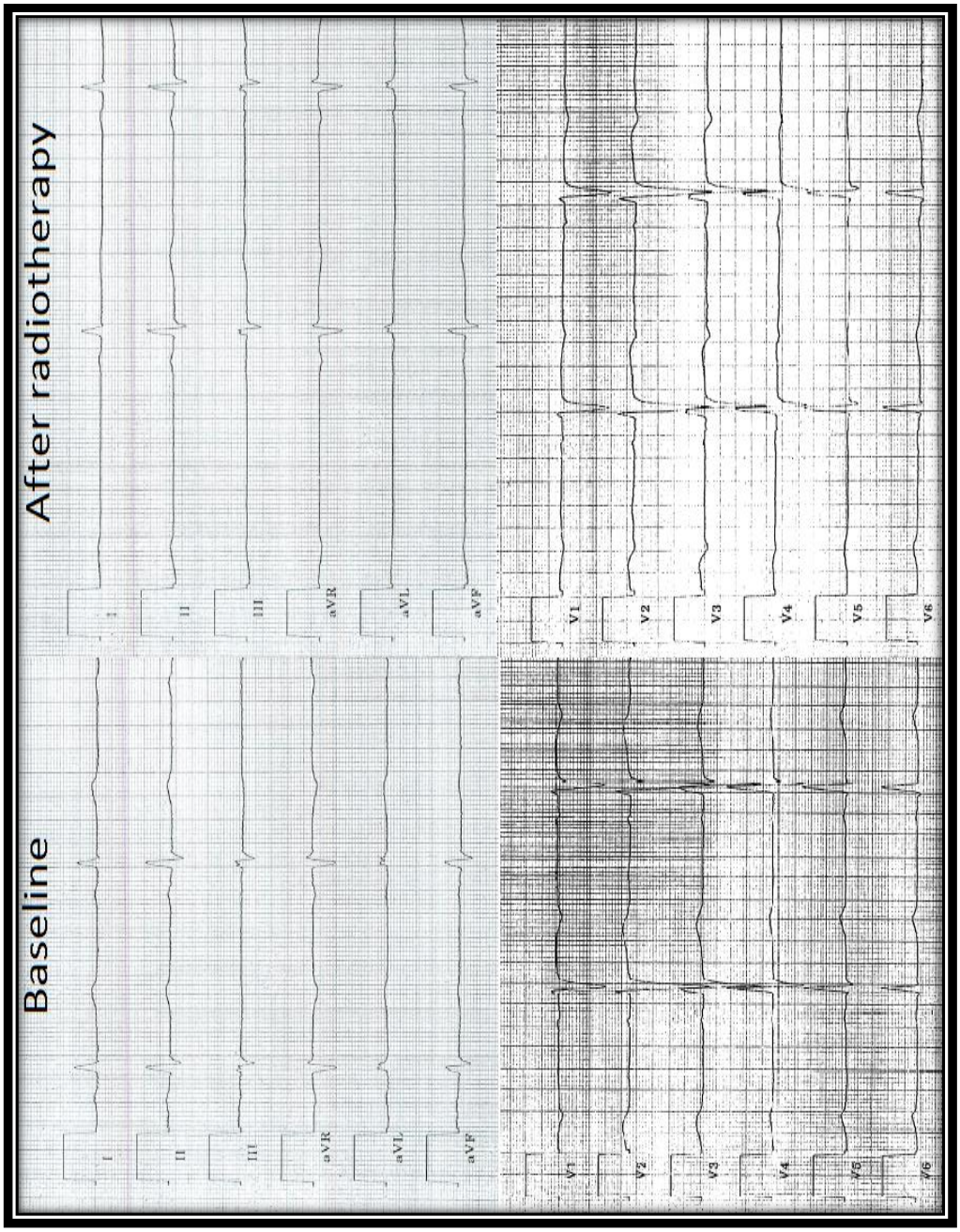

Figure 16. RT induced ECG changes in a study patient. The baseline recording is shown on the left side, the control on the right side. Subtle flattening of the T-wave can be observed in I and aVL leads, new T-wave inversions in V2-4 leads.

RT-induced changes in cardiac biomarkers are displayed in Table 7. The levels of hsTnt were below clinical significance in most of the patients. The highest baseline value and the highest value after RT were 33 ng/l and 20 ng/l, respectively. A greater than 30% rise from the baseline value was observed in fourteen (23%) patients with left-sided breast cancer and in one (5%) patient with right-sided breast cancer ($p<0.001$). The level of proBNP was above the reference value in three (7%) patients with left-sided breast cancer and in one (5%) patient with right-sided breast cancer ($p=0.325$). A more than 30% increase from the baseline value was observed in 32 (53%) patients with left-sided breast cancer and in 4 (20%) patients with right-sided breast cancer ($p=0.014$).

Table 7. Cardiac biomarkers at baseline and after RT

	Left-sided breast cancer N=60					Right-sided breast cancer N=20				
	Baseline		After RT		p	Baseline		After RT		p
	Md	[Q_1, Q_3]	Md	[Q_1, Q_3]		Md	[Q_1, Q_3]	Md	[Q_1, Q_3]	
hsTnt (ng/l)	4	[4, 15]	5	[4, 15]	**0.006**	4	[4, 33]	5	[4, 20]	0.287
proBNP (ng/l)	59	[38, 125]	88	[50, 161]	**<0.001**	95	[63, 130]	88	[52, 129]	0.809

Md, median; hsTnt, high sensitivity troponin T; proBNP, pro-B type natriuretic protein.

6. DISCUSSION

RT caused early changes in echocardiography, cardiac biomarkers and ECG in most of the eighty patients with early-stage breast cancer included in our study. There was a close association of the distribution and magnitude of these changes with the total heart dose and localisation of the RT fields.

6.1 Cardiac changes after RT

6.1.1 Structural changes in echocardiography after RT

RT induced multiple changes in the LV including increased myocardial mass, thickening of LV septal and posterior walls with a simultaneous decline in LV cavity diameters in 2D acquisition (**I**, **II, III, IV**). Consistent with these changes the myocardial mass increased and the LV volume was reduced also in the 3D images (**II, III, IV**). As the control study was executed within a few days after the last RT, it is possible that part of the changes was caused by the RT-induced early inflammatory process. An inflammatory process with extravasation and tissue swelling could explain the increase in LV wall thickness, the decrease in LV volumes and the increase in myocardial mass.

Tissue reflectivity increased in the patients with left-sided breast cancer after RT (**II**). Increased myocardial reflectivity is traditionally considered to reflect increased tissue fibrosis, especially collagen content (200, 201, 203, 226). Even though the fibrotic process seems to be launched at the very early phase with complex cascades involved, it is uncertain whether the changes in tissue reflectivity among our patients can be explained at any extend by the actual increase in tissue fibrosis. The results of the studies on patients with hypertrophic cardiomyopathy and iron or copper accumulation indicate that the increase in myocardial reflectivity may also be caused factors other than collagen, such as fibre disarray (195, 207, 215, 216). In addition, there are studies showing that cIBS values can increase acutely or be reversed (194, 214, 225, 227-229), which imply that *f. ex.* inflammatory tissue responses might contribute to tissue reflectivity. The exact mechanism causing the increase in the cIBS values of the patients with left-sided breast cancer remains to be established since endomyocardial biopsies were not acquired due to ethical issues. Considering transient reflectivity changes in other patient populations, an early inflammatory RT-induced process is a potential explanation to the changes seen in tissue reflectivity after RT among our patient population. Concomitant changes in LV morphology, which suggest the presence of tissue swelling, support this theory.

6.1.2 Functional changes in echocardiography after RT

RT caused changes both in LV diastolic and systolic function. There were several changes in the conventional diastology. The mitral E-wave declined, and IVRT and mitral dt were prolonged (**II, III, IV**). The mitral inflow a-wave, Ea-ratio or Ee'-ratio were unchanged indicating that atrial function and the left-sided filling pressure were unchanged (**II, III, IV**). The changes in mitral E-wave, dt and IVRT indicate prolonged relaxation and would be a logical consequence of the changes seen in the LV walls. A swollen myocardium would be stiffer, and could explain changes in relaxation with sparing of the atrial component.

Although the conventional LV systolic parameters remained unchanged after RT, there were significant changes in the GLS and the CVIBS (studies **III** and **IV**). GLS has shown to be a sensitive predictor of early cardiotoxicity and myocardial remodeling, with important prognostic value over a wide range of clinical scenarios (239, 260, 261, 271-287). Hence, it is tempting to speculate that the changes in GLS in our patient population could be clinically significant early signs of RT-induced cardiac injury. Furthermore, the septal and posterior CVIBS declined in patients who received more than a 2 Gy mean heart radiation dose. Although the use of the CVIBS as a clinical tool is controversial, it seems to be a sensitive marker of early systolic change in cardiac ischaemia, reperfusion, myocardial viability and hibernation (197, 198, 212, 218, 230). It may also be useful in detecting preclinical myocardial changes and predicting adverse events in several diseases (191, 204, 205, 215, 219, 220, 222, 223). In concordance with previous studies, we demonstrated that the RT-induced subclinical changes can be detected by advanced echocardiographic techniques such as GLS and CVIBS analysis, even in patients without changes in LVEF (204, 215, 219, 220, 239-242).

In addition to the changes in LV function, there were also changes in the right side of the heart. The average decline in TAPSE was approximately 2 mm after RT and a ≥4 mm decline was detected in 39% of the patients with left-sided breast cancer (**I**). Other RV parameters remained unchanged. However, in many pathologies influencing RV longitudinal function, such as RV pressure overload or ageing, circumferential contraction increases (321-323). Such compensation was not observed in our patients, and it could be speculated that this combination of reduced TAPSE without a simultaneous increase in circumferential function could imply more serious damages than that judged by a TAPSE decline alone. Furthermore, in study **II**, the changes in RV tissue reflectivity seemed to be associated with the decline in TAPSE. The association

of simultaneous structural and functional changes is a stronger implication of RT-induced changes than a single sporadic finding.

6.1.3 Influence of breast cancer laterality, RT dose and fields on cardiac changes

The heart radiation doses are higher in patients with left-sided than those with right-sided breast cancer as the heart is located on the left side of the thorax. In cohort studies, patients with left-sided breast cancer have a 1.3-1.6-fold relative risk for cardiovascular complications 10 years after RT compared to patients with right-sided breast cancer (58, 59, 113, 114). Hence, breast cancer laterality has a major influence on cardiac radiation exposure. In our studies, patients with left-sided breast cancer had a higher prevalence of ECG changes, cardiac biomarker increase and alterations in echocardiography. The prevalence of T-wave changes was significantly higher in patients with left-sided versus right-sided breast cancer (**II**, **IV**). In addition, there was a small but statistically significant increase in cardiac biomarker levels in patients with left-sided but not those with right-sided breast cancer (**II**, **IV**).

GLS declined in patients with left-sided breast cancer while patients with right-sided breast cancer did not show significant deterioration in the GLS (**IV**). The analysis of the CVIBS showed that a mean heart dose over 2 Gy produced a significantly higher deterioration in the CVIBS in the septum than in patients receiving under 2 Gy (**III**). TAPSE declined significantly in patients with left-sided breast cancer while in patients with right-sided breast cancer the changes were not statistically significant (**IV**). Furthermore, the changes in diastology and the changes in LV morphology were generally more prevalent in patients with left-sided breast cancer (**II**, **IV**).

In addition to the global changes, there were regional differences in ECG, in the CVIBS, the cIBS and in the STE analysis. T-wave inversions on the ECGs were most prevalent in the precordial anterior leads. The changes in CVIBS and cIBS were more pronounced in the anterior fields (RV and septum for cIBS and septum over the posterior wall in the CVIBS) which is logical considering the RT fields (**II, III**). In regional STE analysis, RT caused changes in the apical area in patients with left-sided breast cancer and in the antero-basal segments in patients with right-sided breast cancer as expected by the differences in the localisation of the RT fields (**IV**). The apical decline in patients with left-sided breast cancer was associated with delayed apical rotation and the basal changes in patients with right-sided breast cancer were associated with prolonged basal rotation.

A reduction in regional function seemed to be reflected in the corresponding rotational movement.

Overall, RT induced several changes in echocardiography, cardiac biomarkers and in ECG corresponding to the RT doses and the field used. Our findings in ECG and in myocardial deformation imaging (IBS and STE) imply an association of the RT doses and fields with myocardial injury.

6.1.4 External factors influencing cardiac changes after RT

In the multivariable analyses the concurrent use of AI (**III, IV**), BMI (**III**) and smoking status (**III**) were independently associated with the echocardiographic changes. Correlation analysis also showed an association between the patients' medication (**I**) and the cardiac changes after RT.

One-third of our patients used AI as an adjuvant therapy. Patients using AI had lower baseline septal CVIBS values and an augmented CVIBS decline after RT when the mean cardiac dose exceeded 2 Gy (**III**). Also, the concurrent use of AI had an independent association with the decline of the GLS (**IV**). Aromatase-enzyme regulates the final pathway of the oestrogen metabolism. When this pathway is blocked by AI, the tissue levels of oestrogen declines, and oestrogen-induced growth stimulation in the cancer tissue is reduced. However, oestrogen seems to have a positive effect on cardiac function and recovery (324, 325). The use of AI during RT sensitises the heart to the effects of RT (326, 327). Our study was not designed nor powered to explore the effects of different medical treatments, but the negative influence of AI on several parameters and plausible mechanisms explaining the association could imply a clinically significant phenomenon that should be studied in the future.

BMI, smoking status and the patients' medication also had an association with the changes in echocardiography parameters. Each unit of BMI was associated with a 0.24 dB decrease in the septal CVIBS after RT (**III**). It has been speculated that obesity causes more frequent deep setup errors and thereby higher cardiac radiation doses (328). Whether this was the case in our patients is unclear, but such a mechanism would be a logical explanation for the association between higher BMI and the larger decrease in the septal CVIBS. Surprisingly, non-smokers had a stronger deterioration of the posterior CVIBS (**III**). It has been shown that lower tissue oxygen levels reduce the effect of radiation (40, 329, 330), and may also alleviate the adverse effects in healthy

tissue. Furthermore, the use of levothyroxine for hypothyreosis, the use of ACE/ARBs and the use of diuretics protected patients from a decline in TAPSE (**I**). Thyroid function plays an important role in the tissue effects of radiation. Lower levels of triiodothyronine were associated with more severe and prolonged enteritis after pelvic RT (331). On the other hand, several rodent studies have shown that thyroid hormone supplementation in diabetics or after acute myocardial infarction has had a positive effect on cardiac function (332-334). In our study, hypothyreosis was defined as a previously diagnosed disease with levothyroxine substitution. Therefore, a similar mechanism could have explained the connection between the seemingly protective effect of hypothyreosis and the lesser decline in TAPSE.

The results of the experimental studies show that the adverse effects of radiation can be alleviated in the heart, lungs, bowel, kidneys, skin and neurological tissue by the use of ACE/ARBs (138, 139, 141-147, 149-151, 335). There are no randomised controlled studies on the protective effect of ACE/ARBs in humans receiving RT. Still, our finding of ACE/ARBs seemingly protective effect against RT-induced TAPSE decline (**I**) is interesting considering the strong evidence from the animal studies. The association of the use of diuretics and the smaller reduction in TAPSE (**I**) could be explained by less severe inflammatory tissue swelling due to the use of diuretics, but this is merely speculative and is without any solid support from clinical studies.

6.2 Clinical implication

RIHD develops late, years to decades after radiation exposure. The fibrotic process launched at the initial phase after RT seems to produce progressive tissue changes, (4, 11, 17, 59, 63, 65, 83, 85, 86, 91, 98, 105, 110-114), and clinically significant CAD, valvular lesions, constriction, diastolic dysfunction and restrictive heart failure along with conduction and rhythm disturbances and even constriction after several years of latency (4, 8-11, 59, 65, 68, 70, 72-81, 83, 85-87). Advances in RT techniques have reduced the cardiac exposure (17), but due to relatively short follow-up time the full benefit cannot be estimated yet and mandate further analysis with time (4). Bovelli stated that the 'detection of cardiac injury is crucial since it may facilitate early therapeutic measures' (9) and Cuomo complied that 'the cardiac morbidity and mortality associated with RT can be reduced if treated early, which justifies the need for screening and early detection of RIHD' (10). Therefore, the follow-up and early detection of adverse cardiac changes are important. Early subclinical changes, such as those observed in our study, indicate that RT has a cardiac impact, and may subsequently increase the risk for late sequelae.

TAPSE, GLS and hsTnt all have strong prognostic importance over a wide variety of diseases and even in general population (183-186, 239, 260, 261, 265-287, 336-344). TAPSE is an independent predictor of death, heart transplantation, prolonged hospitalisation and adverse events in patients with heart failure, constriction, acute and chronic states of pulmonary hypertension and in patients with valvular interventions with a range from 14 to 18 mm as a threshold for poorer prognosis (337-344). In a meta-analysis of pulmonary hypertension patients, a 5 mm drop of TAPSE was associated with a 1.72 hazard ratio for mortality or cardiac transplantation (342). Forfia *et al* determined, that each 1 mm decrease in TAPSE in pulmonary hypertension patients increase mortality by 17% (344). A greater than 4 mm decline in TAPSE was observed in 19 (39%) patients with left-sided breast cancer after RT (**I**), which may have prognostic significance.

Reduced GLS is a predictor of adverse remodelling and post-operative outcome (260, 261, 265-273), and it has been associated with increased mortality and overall major adverse cardiac events (239, 274-287). Furthermore, a reduction in GLS after chemotherapy was a strong predictor of a subsequent decline in LVEF and cardiotoxicity (260, 262-264).

Elevated troponin levels have been associated with poor prognosis in patients with cardiac and non-cardiac diseases, and even in community based screening (183-186, 336). The combination of GLS and elevated troponins have even stronger predictive power in patients receiving cardiotoxic chemotherapy (12). In our study, GLS significantly declined in patients with left-sided breast cancer, and almost one-third of them had a decline over 10% accompanied by a statistically significant increase in hsTnt.

In conclusion, the fact, that our patients displayed changes in all of these important prognostic measurements, could be considered clinically significant although a long-term follow-up is needed to confirm this hypothesis.

6.3 Future considerations

6.3.1 Patient screening and RT treatment protocols

Awareness of the adverse effects of RT has pursued to continuous evolution towards safer treatment protocols. With 3D computed treatment planning, the healthy tissue burden has been significantly reduced without compromising the treatment effects. DIHB and IMRT techniques and different patient positioning have been used to reduce heart radiation exposure during RT in the chest. Whether the contemporary lower heart radiation doses are safe without late increase of RIHD, is uncertain. Even a small exposure seems to increase the risk for RIHD, and there is currently no known safe threshold (60). To continue to improve the safety of the treatment protocols, the long latency of RIHD is problematic. Therefore, the early subclinical changes induced by RT could be used as surrogate markers for the RT impact. The results of our study and those of others could be used to guide the further improvements of the RT protocols.

On the other hand, the individual risk for late cardiac sequelae varies. It has been estimated that only 20% can be explained by the radiation exposure and known risk factors alone (6). The pre-existence of cardiac diseases and risk factors for it, roughly double the patients' vulnerability to RT (10). Genetic syndromes affecting DNA repair make individuals affected extremely vulnerable to RT, and even small doses have been lethal (42). It has been speculated, that a genetic variation in other genes could explain some of the differences in RT effects between individuals (6). Such differences cannot currently be predefined by testing, and therefore, the adverse cardiac effects of chest RT remain unpredictable to some extent on an individual level. The extent and severity of the early subclinical changes could identify individuals with stronger RT impact. This could be used in the future to guide follow-up and perhaps cardioprotective procedures. A follow-up protocol of a large patient population, as currently suggested (8, 11), would be more cost-efficient if it could be targeted to individuals with increased risk.

Currently, cardioprotection consists of measures of the RT, but several other alleviating methods are being investigated (10, 57). In addition to the RT protocols, concurrent treatment with cardiotoxic chemotherapy increases the cumulative cardiac risk. So far, the evidence of the early subclinical cardiac changes after RT have no place in guiding patient treatment, but potential for such guidelines could exist in case of easily usable and reliable markers of cardiac involvement. Several of our results could fulfil the criteria for such. TAPSE is a well-validated, easily acquired measurement used in daily clinical

practice and with prognostic importance over wide variety of diseases (337-344). GLS is a novel measurement, but with increasing evidence of being an early, sensitive measurement with acceptable variability and good prognostic importance (12, 233, 260, 261, 265-287, 302, 304-314). These measurements together with the changes in troponins could be suitable in the clinical use in this context in the future.

6.3.2 Long-term follow-up

The awareness of the RT-induced late sequelae has led to recommendations of follow-up protocol for the patients with RT in the chest region (8, 11). In 2013, it was suggested that these patients should be followed-up with non-invasive testing for CAD ten years after the treatment, or earlier if the patient has multiple risk factors. Other examinations are indicated when the patients show symptoms or signs suggesting adverse RT-induced changes (11). In the Cardio-oncology position paper by the European Society of Cardiology in 2016, careful follow-up was recommended only to patients who had received mediastinal RT starting five years post-RT (8). Our contribution to this body of knowledge was to elucidate some of the early cardiac changes and their localisation. The current knowledge of the late cardiac effects mostly orginates from large cohort studies that used now out-dated protocols, and the more detailed knowledge of the actual nature and localisation of the initial changes might help to predict the mid-term and late changes. In theory, our findings could help identify patients with more pronounced initial changes, and help guide in the search for mid-term subclinical sequelea. In addition, our study points-out new parameters that might be practical in the follow-up of this patient population.

6.3.3 Other research methods to study RT-induced changes

Studies with other methods would deepen and widen the knowledge regarding the early RT-induced changes in the heart. A myocardial biopsy would shed light on the exact mechanism of the tissue changes, but as it carries a risk of serious complications in otherwise healthy patients, it will not be ethically justifiable. CMR is excellent at differentiating tissue properties. The high cost and poor availability limit its use in the clinical scenario in this patient population. In addition, its ability to detect diffuse fibrosis, such as fibrosis after RT, has been limited. However, there are new techniques that may overcome this limitation and a comparison between our current findings with CMR would be a valuable asset (345-347). Finally, there are several types of biomarkers that reflect different phases in the fibrosis formation and in the cascades leading to it

(348, 349). The analysis of such biomarkers would provide additional perspectives into the process initiated by tissue radiation. The follow-up of this patient population is currently ongoing, and the use of these complementary methods is under consideration.

6.4 Strengths and limitations of the study

There are clear limitations of this study. The study population was rather small and there was an unequal distribution of left-sided and right-sided breast cancer patients. However, the very short-term follow-up was the biggest limitation of this study - the end-points were surrogate changes in echocardiography, biomarkers and ECG. Whether they have any clinical significance will be revealed in the planned 12-year follow-up of this patient population. In addition, the IBS technique lacks its validation in the clinical setting even though it seems to be a relatively easily usable tool with prognostic significance in studies on different cardiac diseases. Due to its status as an exclusive scientific tool, there are no normal values available, nor is there robust data of what can be considered to be an abnormal response. In addition, even though TAPSE is a central parameter of the RV function, the information derived from it conserning RV function is limited and shall be supplemented with more sophisticated methods later on. Finally, the high variability and poor repeatability reduced the clinical value of some of the measurements, *e.g.* the SR values in the STE analysis.

There were also clear strengths in this study. All of the echocardiography acquisitions were performed by a single person with a long experience in echocardiography and with a 'Certification for Adult Transthoracic Echocardiography' awarded by the European Association of Echocardiography/ European Society of Cardiology. Furthermore, the equipment used was always the same. These facts ensured unique standardised conditions and excluded the intervendor and interperson variation, which increased the reliability of the results. Even though the results were surrogate end-points in echocardiography, ECG and in cardiac biomarkers, the changes found were not sporadic changes here and there, but clusters of changes in parameters illustrating changes in similar things or functions. These clusters matched with each other and were logical considering the RT fields and doses. Finally, the exclusion criteria were not too strict to limit the patient population to individuals with exceptionally good echocardiography acquisition properties. Rather, the study population closely resembled patients we see in the daily clinical practice – ladies in their sixties, in general little chubby and some with severe obesity, and some with limited windows. Such an appearance of real life data can

be considered as a strength, but of course keeping in mind the exclusion criteria otherwise when interpolating these results.

7. SUMMARY AND CONCLUSIONS

The results of our study demonstrated that modern conformal RT for early-stage breast cancer induced echocardiographically detectable structural and functional changes in most of the patients.

- These changes were associated with the radiation dose and fields, and they were more obvious in patients with left-sided versus right-sided breast cancer
- The novel finding was that RT induced negative changes in TAPSE, cIBS, CVIBS measurements and that it induced regional differences in the STE measurements in left-sided versus right-sided breast cancer patients
- The changes in echocardiography were accompanied by abnormalities in the ECG and cardiac biomarkers
- TAPSE, GLS and hsTnt might be feasible tools for the screening of RT-induced adverse cardiac changes

8. ACKNOWLEDGEMENTS

This study was conducted at the Department of Cardiology, Heart Hospital, Tampere University Hospital and School of Medicine, Tampere University in collaboration with the Department of Oncology, Tampere University Hospital.

This thesis is a result of consecutive major contributors during my professional life, that one by one have led to this exciting pathway culminating in this thesis. First I would like to thank Johnny Vegsundvåg. I consider myself very fortunate to have been able to work with him in Ålesund, Norway from 2001 to 2006. It was like magic watching him do echoes, and with his natural teaching skills he managed to pass on some of his knowledge to me, too. I shall always be grateful to him and remember the years in Norway with warm feelings.

Secondly, Pekka Raatikainen, my supervisor, is the reason why I was converted from pure blooded clinician into a researcher. Pekka must have seen a potential in me when he hooked me up with this project. Through these years, he provided a perfect combination of trust and support, all in the right places. I consider myself privilidged to have Pekka as my supervisor, colleague, and a friend and I'm looking forward to continue to work with him in the years to come.

The third, and at least as important part in this process, are our research group oncologists Tanja Skyttä and Pirkko-Liisa Kellokumpu-Lehtinen. I admire Tanja for the elegance in everything she does. There are numerous situations where things smoothly glided into right direction by the smallest things she did. Also Pirkko has a special place in my heart. She has always been encouraging and her believe in this project and in me has been invaluable. Our regular meetings were always warm and frictionless, the responses immediate and it has been easy to be involved in the active research environment created by Tanja and Pirkko. Honestly, I think that every researcher should have these kind of people in their group and this kind of environment to be nourished to be a researcher. I'm glad that our journey continues far beyond this dissertation and we will have many meetings together in the years to come.

However, the cornerstone in all my activities in this project and in other professional activities, have been the research nurses in the Heart Hospital, Virpi Palomäki, Hanna-Leena Näppilä and Kati Helleharju. Nothing has ever been a problem or impossible to get through with the help of You. You have carried out the logistics of this study, lightened the burden of reseach byrocracy for me and taken care that I'm in the right place at the right time. But Your value to me goes far beyond the practicalities – to know You and to work with You makes life better and I'm frankly proud to say that I know You.

I would like to thank Vesa Virtanen and Heart Center Co for believing in this process, and for affording me the facilities and opportunities for free to start this study in 2011 to 2012. Without this contribution and support this study, and this dissertation, would never have seen the light.

I would like to express my gratitude to all the personel in the cardiological deparment, both in the out-patient clinic and in the wards, for the flexibility and patience that all the extra nuicance my project must have caused. I also thank all the people that have participated as validation objects in our study, and Marko Virtanen and Tuija Poutanen for carrying out the validation measurements. Furthermore, I would like to offer my special thanks to Kjell Nikus and Saila Vikman, the members of the Heart Hospital's reseach team, for their important role in this project. We have had many flourishing discussions of this and many other projects and reseach in general with Kjell, and his guidance and help have been invaluable to me. Saila, the leader of the research team, though not directly involved with this study, has had a major contribution for its continuation further on. I'm imdephted to her for this, and also for having being a good colleague whom I value and look up to. Furthermore, I'm grateful for all the co-authors and the statisticians, Tiina Luukkaala and Heini Huhtala, who have helped me in prosessing all the data derived from this study, and in making me see the light in the world of statistics.

I'm also indephted to all the women participating in this study.

I owe my gratitude also to Helena Hänninen, Jyri Lommi and all the others in Meilahti Hospital, not only for the friendly welcoming, but also for understanding the almost endless need for free from work to finalise this thesis and to carry on with family life.

My sincerest thanks are due to the official reviewers of the dissertation, docent Marja Hedman and docent Tiina Ojala for taking time to help to improve this thesis by their careful evaluation and constructive comments of the manuscript. My warmest thanks goes to Antti Saraste, opponent of this thesis. I'm very honored to have Antti as my opponent knowing his many excuisite skills in imanging, cardiology and science.

A thesis like this is an end-product of massive amount of labour, long hours throughout the years and dedication even in times of tiredness and disbelief. In addition to encouragement and support from within the study group, and from friends and relatives, it has been of utmost important to have financial support from several non-profit communities to be able to take free from job to finalise the analysis and to finish the papers. Therefore, my sincerest thanks goes to Paavo and Eila Salonen legacy, to The Finnish Medical Foundation, to Ida Montin Fund, to The Finnish Cultural Foundation, Pirkanmaa Regional Fund, to The Finnish Foundation for Cardiovascular Research, to Finnish Society for Oncology, to Finnish-Norwegian Medical Foundation, to Pirkanmaa Cancer Society and to Aarne and Aili Turunen Foundation. In addition, Vesa Laiho from Philips has been a precious support in the technical aspects for the off-line analysis.

Next I want to pay tribute to my friends, relatives and family. Thank you for bringing joy and support in my life, for dragging me out of the world of science and work and for giving prespective in things. Of course, my parents, Hilkka and Seppo created the foundation for all of this. Their encouragement for studying and their support guided this pathway and had eased my way. I owe my thanks to my brother Kari, and my babybrother Tuomas and his spouse Jenna, who have managed to bring new sunshine into our lives, Antton. I would like to thank also my mother in law, Ritva, for all the support she has provided during these years. She has taken care of our children and rabbits whenever needed, without this would many things have been difficult.

My deepest and sincerest thanks goes to my husband, Timo Julkunen. Your unconditional loyalty, love, and support has covered all parts of my life now through more than half of our lives. You have couraged me in everything, enabled all my dreams and needs, and standed by me even when I'm impossible. We have started to get wrinkled together, and I couldn't imagine a better life. This thesis is a tribute to You, too, since everything we have, we share. Finally, and most importantly, I would like to declare (behind computer desk – which our children propably now think, is an ingrown part of me) the utmost meaning of Laura and Joonas to me. Your existence gives meaning to everything and I love You with all my heart.

Tampere, 9th April 2017

Immu (alias Suvi Tuohinen)

9. REFERENCES

1. Ferlay J, Shin H, Bray F, Forman D, Mathers C, Parkin D. GLOBOCAN 2008 v1.2. Cancer Incidence and Mortality Worldwide: IARC CancerBase No. 10 (Internet). 2010.

2. Senkus E, Kyriakides S, Ohno S, Penault-Llorca F, Poortmans P, Rutgers E, et al. Primary breast cancer: ESMO Clinical Practice Guidelines for diagnosis, treatment and follow-up. Ann Oncol 2015;26 Suppl 5:v8-30.

3. http://www.cancer.fi/syoparekisteri/tilastot/.

4. Jaworski C, Mariani JA, Wheeler G, Kaye DM. Cardiac complications of thoracic irradiation. J Am Coll Cardiol 2013;61:2319-2328.

5. Giordano SB, Gradishar W. Breast cancer: updates and advances in 2016. Curr Opin Obstet Gynecol 2017;29:12-17.

6. Barnett GC, West CM, Dunning AM, Elliott RM, Coles CE, Pharoah PD, et al. Normal tissue reactions to radiotherapy: towards tailoring treatment dose by genotype. Nat Rev Cancer 2009;9:134-142.

7. Ringborg U, Bergqvist D, Brorsson B, Cavallin-Stahl E, Ceberg J, Einhorn N, et al. The Swedish Council on Technology Assessment in Health Care (SBU) systematic overview of radiotherapy for cancer including a prospective survey of radiotherapy practice in Sweden 2001--summary and conclusions. Acta Oncol 2003;42:357-365.

8. Zamorano J. An ESC position paper on cardio-oncology. Eur Heart J 2016;37:2739-2740.

9. Bovelli D, Plataniotis G, Roila F, ESMO Guidelines Working Group. Cardiotoxicity of chemotherapeutic agents and radiotherapy-related heart disease: ESMO Clinical Practice Guidelines. Ann Oncol 2010;21 Suppl 5:v277-82.

10. Cuomo JR, Sharma GK, Conger PD, Weintraub NL. Novel concepts in radiation-induced cardiovascular disease. World J Cardiol 2016;8:504-519.

11. Lancellotti P, Nkomo VT, Badano LP, Bergler J, Bogaert J, Davin L, et al. Expert consensus for multi-modality imaging evaluation of cardiovascular complications of radiotherapy in adults: a report from the European Association of Cardiovascular Imaging and the American Society of Echocardiography. Eur Heart J Cardiovasc Imaging 2013;14:721-740.

12. Plana JC, Galderisi M, Barac A, Ewer MS, Ky B, Scherrer-Crosbie M, et al. Expert consensus for multimodality imaging evaluation of adult patients during and after cancer

therapy: a report from the American Society of Echocardiography and the European Association of Cardiovascular Imaging. Eur Heart J Cardiovasc Imaging 2014;15:1063-1093.

13. Armenian SH, Lacchetti C, Barac A, Carver J, Constine LS, Denduluri N, et al. Prevention and Monitoring of Cardiac Dysfunction in Survivors of Adult Cancers: American Society of Clinical Oncology Clinical Practice Guideline. J Clin Oncol 2016:JCO2016705400.

14. Eschenhagen T, Force T, Ewer MS, de Keulenaer GW, Suter TM, Anker SD, et al. Cardiovascular side effects of cancer therapies: a position statement from the Heart Failure Association of the European Society of Cardiology. Eur J Heart Fail 2011;13:1-10.

15. Mandala M, Falanga A, Roila F, ESMO Guidelines Working Group. Management of venous thromboembolism (VTE) in cancer patients: ESMO Clinical Practice Guidelines. Ann Oncol 2011;22 Suppl 6:vi85-92.

16. Curigliano G, Cardinale D, Suter T, Plataniotis G, de Azambuja E, Sandri MT, et al. Cardiovascular toxicity induced by chemotherapy, targeted agents and radiotherapy: ESMO Clinical Practice Guidelines. Ann Oncol 2012;23 Suppl 7:vii155-66.

17. Giordano SH, Kuo YF, Freeman JL, Buchholz TA, Hortobagyi GN, Goodwin JS. Risk of cardiac death after adjuvant radiotherapy for breast cancer. J Natl Cancer Inst 2005;97:419-424.

18. Li T, Mello-Thoms C, Brennan PC. Descriptive epidemiology of breast cancer in China: incidence, mortality, survival and prevalence. Breast Cancer Res Treat 2016;159:395-406.

19. Joensuu H, Huovinen R, Leidenius M, Suominen S. Luku 33 rintasyöpä. In: Joensuu H, Roberst P, Kellokumpu-Lehtinen P, Jyrkkiö S, Kouri M, Teppo L, editors. Syöpätaudit. 5th ed. Saarijärvi: Kustannus Oy Duodecim; 2013. p. 591-620.

20. Prat A, Pineda E, Adamo B, Galvan P, Fernandez A, Gaba L, et al. Clinical implications of the intrinsic molecular subtypes of breast cancer. Breast 2015;24 Suppl 2:S26-35.

21. Gnant M, Thomssen C, Harbeck N. St. Gallen/Vienna 2015: A Brief Summary of the Consensus Discussion. Breast Care (Basel) 2015;10:124-130.

22. Bleicher RJ, Ruth K, Sigurdson ER, Daly JM, Boraas M, Anderson PR, et al. Breast conservation versus mastectomy for patients with T3 primary tumors (>5 cm): A review of 5685 medicare patients. Cancer 2016;122:42-49.

23. Zumsteg ZS, Morrow M, Arnold B, Zheng J, Zhang Z, Robson M, et al. Breast-conserving therapy achieves locoregional outcomes comparable to mastectomy in women with T1-2N0 triple-negative breast cancer. Ann Surg Oncol 2013;20:3469-3476.

24. Lynch SP, Lei X, Hsu L, Meric-Bernstam F, Buchholz TA, Zhang H, et al. Breast cancer multifocality and multicentricity and locoregional recurrence. Oncologist 2013;18:1167-1173.

25. Nijenhuis MV, Rutgers EJ. Who should not undergo breast conservation? Breast 2013;22 Suppl 2:S110-4.

26. van Nijnatten TJ, Schipper RJ, Lobbes MB, Nelemans PJ, Beets-Tan RG, Smidt ML. The diagnostic performance of sentinel lymph node biopsy in pathologically confirmed node positive breast cancer patients after neoadjuvant systemic therapy: A systematic review and meta-analysis. Eur J Surg Oncol 2015;41:1278-1287.

27. Lyman GH, Temin S, Edge SB, Newman LA, Turner RR, Weaver DL, et al. Sentinel lymph node biopsy for patients with early-stage breast cancer: American Society of Clinical Oncology clinical practice guideline update. J Clin Oncol 2014;32:1365-1383.

28. Cortazar P, Geyer CE,Jr. Pathological complete response in neoadjuvant treatment of breast cancer. Ann Surg Oncol 2015;22:1441-1446.

29. Gianni L, Pienkowski T, Im YH, Roman L, Tseng LM, Liu MC, et al. Efficacy and safety of neoadjuvant pertuzumab and trastuzumab in women with locally advanced, inflammatory, or early HER2-positive breast cancer (NeoSphere): a randomised multicentre, open-label, phase 2 trial. Lancet Oncol 2012;13:25-32.

30. Walker RA, Cove DH, Howell A. Histological detection of oestrogen receptor in human breast carcinomas. Lancet 1980;1:171-173.

31. Turner N, Biganzoli L, Di Leo A. Continued value of adjuvant anthracyclines as treatment for early breast cancer. Lancet Oncol 2015;16:e362-9.

32. Molina R, Ciocca DR, Tandon AK, Allred DC, Clark GM, Chamness GC, et al. Expression of HER-2/neu oncoprotein in human breast cancer: a comparison of immunohistochemical and western blot techniques. Anticancer Res 1992;12:1965-1971.

33. Tetu B, Brisson J. Prognostic significance of HER-2/neu oncoprotein expression in node-positive breast cancer. The influence of the pattern of immunostaining and adjuvant therapy. Cancer 1994;73:2359-2365.

34. Moja L, Tagliabue L, Balduzzi S, Parmelli E, Pistotti V, Guarneri V, et al. Trastuzumab containing regimens for early breast cancer. Cochrane Database Syst Rev 2012;(4):CD006243. doi:CD006243.

35. Joensuu H, Bono P, Kataja V, Alanko T, Kokko R, Asola R, et al. Fluorouracil, epirubicin, and cyclophosphamide with either docetaxel or vinorelbine, with or without trastuzumab, as adjuvant treatments of breast cancer: final results of the FinHer Trial. J Clin Oncol 2009;27:5685-5692.

36. Balduzzi S, Mantarro S, Guarneri V, Tagliabue L, Pistotti V, Moja L, et al. Trastuzumab-containing regimens for metastatic breast cancer. Cochrane Database Syst Rev 2014;(6):CD006242. doi:CD006242.

37. Early Breast Cancer Trialists' Collaborative Group (EBCTCG), Darby S, McGale P, Correa C, Taylor C, Arriagada R, et al. Effect of radiotherapy after breast-conserving surgery on 10-year recurrence and 15-year breast cancer death: meta-analysis of individual patient data for 10,801 women in 17 randomised trials. Lancet 2011;378:1707-1716.

38. Cosset JM. The dawn of radiotherapy, between strokes of genius, dramas and controversies. Cancer Radiother 2016;20:595-600.

39. Foray N. Victor Despeignes (1866-1937): how a hygienist became the first radiation oncologist. Cancer Radiother 2013;17:244-254.

40. Connell PP, Hellman S. Advances in radiotherapy and implications for the next century: a historical perspective. Cancer Res 2009;69:383-392.

41. Bernier J, Hall EJ, Giaccia A. Radiation oncology: a century of achievements. Nat Rev Cancer 2004;4:737-747.

42. Pollard JM, Gatti RA. Clinical radiation sensitivity with DNA repair disorders: an overview. Int J Radiat Oncol Biol Phys 2009;74:1323-1331.

43. MORRISON R, NEWBERY GR, DEELEY TJ. Preliminary report on the clinical use of the medical research council 8 MeV linear accelerator. Br J Radiol 1956;29:177-186.

44. Ash DV, Andrews B, Stubbs B. A method for integrating computed tomography into radiotherapy planning and treatment. Clin Radiol 1983;34:99-101.

45. Kouri M, Tenhunen M. Sädehoito. In: Syöpätaudit. 5th ed. Helsinki: Kustannus Oy Duodecim; 2013. p. 147-72.

46. Formenti SC, DeWyngaert JK, Jozsef G, Goldberg JD. Prone vs supine positioning for breast cancer radiotherapy. JAMA 2012;308:861-863.

47. Smyth LM, Knight KA, Aarons YK, Wasiak J. The cardiac dose-sparing benefits of deep inspiration breath-hold in left breast irradiation: a systematic review. J Med Radiat Sci 2015;62:66-73.

48. Minniti G, Osti MF, Niyazi M. Target delineation and optimal radiosurgical dose for pituitary tumors. Radiat Oncol 2016;11:135.

49. Badiyan SN, Regine WF, Mehta M. Stereotactic Radiosurgery for Treatment of Brain Metastases. J Oncol Pract 2016;12:703-712.

50. Mirzaei HR, Sahebkar A, Salehi R, Nahand JS, Karimi E, Jaafari MR, et al. Boron neutron capture therapy: Moving toward targeted cancer therapy. J Cancer Res Ther 2016;12:520-525.

51. England CG, Rui L, Cai W. Lymphoma: current status of clinical and preclinical imaging with radiolabeled antibodies. Eur J Nucl Med Mol Imaging 2016.

52. Cabanillas ME, McFadden DG, Durante C. Thyroid cancer. Lancet 2016;388:2783-2795.

53. Stewart A, Parashar B, Patel M, O'Farrell D, Biagioli M, Devlin P, et al. American Brachytherapy Society consensus guidelines for thoracic brachytherapy for lung cancer. Brachytherapy 2016;15:1-11.

54. www.stuk.fi.

55. Yarnold J, Brotons MC. Pathogenetic mechanisms in radiation fibrosis. Radiother Oncol 2010;97:149-161.

56. Fajardo LF, Stewart JR. Pathogenesis of radiation-induced myocardial fibrosis. Lab Invest 1973;29:244-257.

57. Westbury CB, Yarnold JR. Radiation fibrosis--current clinical and therapeutic perspectives. Clin Oncol (R Coll Radiol) 2012;24:657-672.

58. Sardaro A, Petruzzelli MF, D'Errico MP, Grimaldi L, Pili G, Portaluri M. Radiation-induced cardiac damage in early left breast cancer patients: Risk factors, biological mechanisms, radiobiology, and dosimetric constraints. Radiother Oncol 2012;103:133-142.

59. Darby SC, Ewertz M, McGale P, Bennet AM, Blom-Goldman U, Bronnum D, et al. Risk of ischemic heart disease in women after radiotherapy for breast cancer. N Engl J Med 2013;368:987-998.

60. Shimizu Y, Kodama K, Nishi N, Kasagi F, Suyama A, Soda M, et al. Radiation exposure and circulatory disease risk: Hiroshima and Nagasaki atomic bomb survivor data, 1950-2003. BMJ 2010;340:b5349.

61. Frandsen J, Boothe D, Gaffney DK, Wilson BD, Lloyd S. Increased risk of death due to heart disease after radiotherapy for esophageal cancer. J Gastrointest Oncol 2015;6:516-523.

62. Nolan MT, Russell DJ, Marwick TH. Long-term Risk of Heart Failure and Myocardial Dysfunction After Thoracic Radiotherapy: A Systematic Review. Can J Cardiol 2016;32:908-920.

63. Hooning MJ, Botma A, Aleman BM, Baaijens MH, Bartelink H, Klijn JG, et al. Long-term risk of cardiovascular disease in 10-year survivors of breast cancer. J Natl Cancer Inst 2007;99:365-375.

64. Gagliardi G, Constine LS, Moiseenko V, Correa C, Pierce LJ, Allen AM, et al. Radiation dose-volume effects in the heart. Int J Radiat Oncol Biol Phys 2010;76:S77-85.

65. Mulrooney DA, Yeazel MW, Kawashima T, Mertens AC, Mitby P, Stovall M, et al. Cardiac outcomes in a cohort of adult survivors of childhood and adolescent cancer: retrospective analysis of the Childhood Cancer Survivor Study cohort. BMJ 2009;339:b4606.

66. Filopei J, Frishman W. Radiation-induced heart disease. Cardiol Rev 2012;20:184-188.

67. Slama MS, Le Guludec D, Sebag C, Leenhardt AR, Davy JM, Pellerin DE, et al. Complete atrioventricular block following mediastinal irradiation: a report of six cases. Pacing Clin Electrophysiol 1991;14:1112-1118.

68. Orzan F, Brusca A, Gaita F, Giustetto C, Figliomeni MC, Libero L. Associated cardiac lesions in patients with radiation-induced complete heart block. Int J Cardiol 1993;39:151-156.

69. Authors/Task Force Members, Adler Y, Charron P, Imazio M, Badano L, Baron-Esquivias G, et al. 2015 ESC Guidelines for the diagnosis and management of pericardial diseases: The Task Force for the Diagnosis and Management of Pericardial Diseases of

the European Society of Cardiology (ESC)Endorsed by: The European Association for Cardio-Thoracic Surgery (EACTS). Eur Heart J 2015.

70. van Leeuwen-Segarceanu EM, Bos WJ, Dorresteijn LD, Rensing BJ, der Heyden JA, Vogels OJ, et al. Screening Hodgkin lymphoma survivors for radiotherapy induced cardiovascular disease. Cancer Treat Rev 2011;37:391-403.

71. Nilsson G, Witt Nystrom P, Isacsson U, Garmo H, Duvernoy O, Sjogren I, et al. Radiation dose distribution in coronary arteries in breast cancer radiotherapy. Acta Oncol 2016;55:959-963.

72. Orzan F, Brusca A, Conte MR, Presbitero P, Figliomeni MC. Severe coronary artery disease after radiation therapy of the chest and mediastinum: clinical presentation and treatment. Br Heart J 1993;69:496-500.

73. Schomig K, Ndrepepa G, Mehilli J, Pache J, Kastrati A, Schomig A. Thoracic radiotherapy in patients with lymphoma and restenosis after coronary stent placement. Catheter Cardiovasc Interv 2007;70:359-365.

74. Liang JJ, Sio TT, Slusser JP, Lennon RJ, Miller RC, Sandhu G, et al. Outcomes after percutaneous coronary intervention with stents in patients treated with thoracic external beam radiation for cancer. JACC Cardiovasc Interv 2014;7:1412-1420.

75. Crestanello JA, McGregor CG, Danielson GK, Daly RC, Dearani JA, Orszulak TA, et al. Mitral and tricuspid valve repair in patients with previous mediastinal radiation therapy. Ann Thorac Surg 2004;78:826-31; discussion 826-31.

76. Chang AS, Smedira NG, Chang CL, Benavides MM, Myhre U, Feng J, et al. Cardiac surgery after mediastinal radiation: extent of exposure influences outcome. J Thorac Cardiovasc Surg 2007;133:404-413.

77. Handa N, McGregor CG, Danielson GK, Orszulak TA, Mullany CJ, Daly RC, et al. Coronary artery bypass grafting in patients with previous mediastinal radiation therapy. J Thorac Cardiovasc Surg 1999;117:1136-1142.

78. Cella L, Liuzzi R, Conson M, Torre G, Caterino M, De Rosa N, et al. Dosimetric predictors of asymptomatic heart valvular dysfunction following mediastinal irradiation for Hodgkin's lymphoma. Radiother Oncol 2011;101:316-321.

79. Machann W, Beer M, Breunig M, Stork S, Angermann C, Seufert I, et al. Cardiac magnetic resonance imaging findings in 20-year survivors of mediastinal radiotherapy for Hodgkin's disease. Int J Radiat Oncol Biol Phys 2011;79:1117-1123.

80. Christiansen JR, Hamre H, Massey R, Dalen H, Beitnes JO, Fossa SD, et al. Left ventricular function in long-term survivors of childhood lymphoma. Am J Cardiol 2014;114:483-490.

81. Lund MB, Ihlen H, Voss BM, Abrahamsen AF, Nome O, Kongerud J, et al. Increased risk of heart valve regurgitation after mediastinal radiation for Hodgkin's disease: an echocardiographic study. Heart 1996;75:591-595.

82. Adams MJ, Lipsitz SR, Colan SD, Tarbell NJ, Treves ST, Diller L, et al. Cardiovascular status in long-term survivors of Hodgkin's disease treated with chest radiotherapy. J Clin Oncol 2004;22:3139-3148.

83. Cutter DJ, Schaapveld M, Darby SC, Hauptmann M, van Nimwegen FA, Krol AD, et al. Risk of valvular heart disease after treatment for Hodgkin lymphoma. J Natl Cancer Inst 2015;107:10.1093/jnci/djv008. Print 2015 Apr.

84. van der Pal HJ, van Dijk IW, Geskus RB, Kok WE, Koolen M, Sieswerda E, et al. Valvular abnormalities detected by echocardiography in 5-year survivors of childhood cancer: a long-term follow-up study. Int J Radiat Oncol Biol Phys 2015;91:213-222.

85. Bijl JM, Roos MM, van Leeuwen-Segarceanu EM, Vos JM, Bos WJ, Biesma DH, et al. Assessment of Valvular Disorders in Survivors of Hodgkin's Lymphoma Treated by Mediastinal Radiotherapy +/- Chemotherapy. Am J Cardiol 2016;117:691-696.

86. Carlson RG, Mayfield WR, Normann S, Alexander JA. Radiation-associated valvular disease. Chest 1991;99:538-545.

87. Galper SL, Yu JB, Mauch PM, Strasser JF, Silver B, Lacasce A, et al. Clinically significant cardiac disease in patients with Hodgkin lymphoma treated with mediastinal irradiation. Blood 2011;117:412-418.

88. Beohar N, Kirtane AJ, Blackstone E, Waksman R, Holmes D,Jr, Minha S, et al. Trends in Complications and Outcomes of Patients Undergoing Transfemoral Transcatheter Aortic Valve Replacement: Experience From the PARTNER Continued Access Registry. JACC Cardiovasc Interv 2016;9:355-363.

89. Aleman BM, van den Belt-Dusebout AW, De Bruin ML, van 't Veer MB, Baaijens MH, de Boer JP, et al. Late cardiotoxicity after treatment for Hodgkin lymphoma. Blood 2007;109:1878-1886.

90. Marks LB, Yu X, Prosnitz RG, Zhou SM, Hardenbergh PH, Blazing M, et al. The incidence and functional consequences of RT-associated cardiac perfusion defects. Int J Radiat Oncol Biol Phys 2005;63:214-223.

91. Prosnitz RG, Hubbs JL, Evans ES, Zhou SM, Yu X, Blazing MA, et al. Prospective assessment of radiotherapy-associated cardiac toxicity in breast cancer patients: analysis of data 3 to 6 years after treatment. Cancer 2007;110:1840-1850.

92. Hardenbergh PH, Munley MT, Bentel GC, Kedem R, Borges-Neto S, Hollis D, et al. Cardiac perfusion changes in patients treated for breast cancer with radiation therapy and doxorubicin: preliminary results. Int J Radiat Oncol Biol Phys 2001;49:1023-1028.

93. Eftekhari M, Anbiaei R, Zamani H, Fallahi B, Beiki D, Ameri A, et al. Radiation-induced myocardial perfusion abnormalities in breast cancer patients following external beam radiation therapy. Asia Ocean J Nucl Med Biol 2015;3:3-9.

94. Lind PA, Pagnanelli R, Marks LB, Borges-Neto S, Hu C, Zhou SM, et al. Myocardial perfusion changes in patients irradiated for left-sided breast cancer and correlation with coronary artery distribution. Int J Radiat Oncol Biol Phys 2003;55:914-920.

95. Gyenes G, Fornander T, Carlens P, Glas U, Rutqvist LE. Detection of radiation-induced myocardial damage by technetium-99m sestamibi scintigraphy. Eur J Nucl Med 1997;24:286-292.

96. DePasquale EC, Nasir K, Jacoby DL. Outcomes of adults with restrictive cardiomyopathy after heart transplantation. J Heart Lung Transplant 2012;31:1269-1275.

97. Saxena P, Joyce LD, Daly RC, Kushwaha SS, Schirger JA, Rosedahl J, et al. Cardiac transplantation for radiation-induced cardiomyopathy: the Mayo Clinic experience. Ann Thorac Surg 2014;98:2115-2121.

98. Groarke JD, Tanguturi VK, Hainer J, Klein J, Moslehi JJ, Ng A, et al. Abnormal exercise response in long-term survivors of hodgkin lymphoma treated with thoracic irradiation: evidence of cardiac autonomic dysfunction and impact on outcomes. J Am Coll Cardiol 2015;65:573-583.

99. Pohjola-Sintonen S, Totterman KJ, Salmo M, Siltanen P. Late cardiac effects of mediastinal radiotherapy in patients with Hodgkin's disease. Cancer 1987;60:31-37.

100. Gottdiener JS, Katin MJ, Borer JS, Bacharach SL, Green MV. Late cardiac effects of therapeutic mediastinal irradiation. Assessment by echocardiography and radionuclide angiography. N Engl J Med 1983;308:569-572.

101. Marks LB, Yu X, Vujaskovic Z, Small W,Jr, Folz R, Anscher MS. Radiation-induced lung injury. Semin Radiat Oncol 2003;13:333-345.

102. Abratt RP, Morgan GW, Silvestri G, Willcox P. Pulmonary complications of radiation therapy. Clin Chest Med 2004;25:167-177.

103. Hille-Betz U, Vaske B, Bremer M, Soergel P, Kundu S, Klapdor R, et al. Late radiation side effects, cosmetic outcomes and pain in breast cancer patients after breast-conserving surgery and three-dimensional conformal radiotherapy : Risk-modifying factors. Strahlenther Onkol 2016;192:8-16.

104. Mukesh MB, Harris E, Collette S, Coles CE, Bartelink H, Wilkinson J, et al. Normal tissue complication probability (NTCP) parameters for breast fibrosis: pooled results from two randomised trials. Radiother Oncol 2013;108:293-298.

105. Wethal T, Nedregaard B, Andersen R, Fossa A, Lund MB, Gunther A, et al. Atherosclerotic lesions in lymphoma survivors treated with radiotherapy. Radiother Oncol 2014;110:448-454.

106. Vogelius IR, Bentzen SM, Maraldo MV, Petersen PM, Specht L. Risk factors for radiation-induced hypothyroidism: a literature-based meta-analysis. Cancer 2011;117:5250-5260.

107. Shilkrut M, Belkacemi Y, Kuten A, Association of Radiotherapy and Oncology of the Mediterranean arEa (AROME). Secondary malignancies in survivors of breast cancer: how to overcome the risk. Crit Rev Oncol Hematol 2012;84 Suppl 1:e86-9.

108. Melliere D, Becquemin JP, Berrahal D, Desgranges P, Cavillon A. Management of radiation-induced occlusive arterial disease: a reassessment. J Cardiovasc Surg (Torino) 1997;38:261-269.

109. Wethal T, Lund MB, Edvardsen T, Fossa SD, Pripp AH, Holte H, et al. Valvular dysfunction and left ventricular changes in Hodgkin's lymphoma survivors. A longitudinal study. Br J Cancer 2009;101:575-581.

110. Hooning MJ, Aleman BM, van Rosmalen AJ, Kuenen MA, Klijn JG, van Leeuwen FE. Cause-specific mortality in long-term survivors of breast cancer: A 25-year follow-up study. Int J Radiat Oncol Biol Phys 2006;64:1081-1091.

111. Zinzani PL, Gherlinzoni F, Piovaccari G, Frezza G, Bendandi M, Ferretti RM, et al. Cardiac injury as late toxicity of mediastinal radiation therapy for Hodgkin's disease patients. Haematologica 1996;81:132-137.

112. Harris EE, Correa C, Hwang WT, Liao J, Litt HI, Ferrari VA, et al. Late cardiac mortality and morbidity in early-stage breast cancer patients after breast-conservation treatment. J Clin Oncol 2006;24:4100-4106.

113. Darby SC, McGale P, Taylor CW, Peto R. Long-term mortality from heart disease and lung cancer after radiotherapy for early breast cancer: prospective cohort study of about 300,000 women in US SEER cancer registries. Lancet Oncol 2005;6:557-565.

114. Bouillon K, Haddy N, Delaloge S, Garbay JR, Garsi JP, Brindel P, et al. Long-term cardiovascular mortality after radiotherapy for breast cancer. J Am Coll Cardiol 2011;57:445-452.

115. Wang J, Wu Y, Yuan F, Liu Y, Wang X, Cao F, et al. Chronic intermittent hypobaric hypoxia attenuates radiation induced heart damage in rats. Life Sci 2016;160:57-63.

116. Nilsson K, Henriksson R, Cai YQ, Hellstrom S, Hornqvist Bylunds S, Bjermer L. Effects of tobacco-smoke on radiation-induced pneumonitis in rats. Int J Radiat Biol 1992;62:719-727.

117. Chen MH, Blackington LH, Zhou J, Chu TF, Gauvreau K, Marcus KJ, et al. Blood pressure is associated with occult cardiovascular disease in prospectively studied Hodgkin lymphoma survivors after chest radiation. Leuk Lymphoma 2014;55:2477-2483.

118. Gabriels K, Hoving S, Seemann I, Visser NL, Gijbels MJ, Pol JF, et al. Local heart irradiation of ApoE(-/-) mice induces microvascular and endocardial damage and accelerates coronary atherosclerosis. Radiother Oncol 2012;105:358-364.

119. Stewart FA, Hoving S, Russell NS. Vascular damage as an underlying mechanism of cardiac and cerebral toxicity in irradiated cancer patients. Radiat Res 2010;174:865-869.

120. Jagsi R, Griffith KA, Koelling T, Roberts R, Pierce LJ. Rates of myocardial infarction and coronary artery disease and risk factors in patients treated with radiation therapy for early-stage breast cancer. Cancer 2007;109:650-657.

121. Hilbers FS, Boekel NB, van den Broek AJ, van Hien R, Cornelissen S, Aleman BM, et al. Genetic variants in TGFbeta-1 and PAI-1 as possible risk factors for cardiovascular disease after radiotherapy for breast cancer. Radiother Oncol 2012;102:115-121.

122. Wurschmidt F, Stoltenberg S, Kretschmer M, Petersen C. Incidental dose to coronary arteries is higher in prone than in supine whole breast irradiation. A dosimetric comparison in adjuvant radiotherapy of early stage breast cancer. Strahlenther Onkol 2014;190:563-568.

123. Taylor CW, Wang Z, Macaulay E, Jagsi R, Duane F, Darby SC. Exposure of the Heart in Breast Cancer Radiation Therapy: A Systematic Review of Heart Doses Published During 2003 to 2013. Int J Radiat Oncol Biol Phys 2015;93:845-853.

124. Hampson NB, Holm JR, Wreford-Brown CE, Feldmeier J. Prospective assessment of outcomes in 411 patients treated with hyperbaric oxygen for chronic radiation tissue injury. Cancer 2012;118:3860-3868.

125. Wang J, Albertson CM, Zheng H, Fink LM, Herbert JM, Hauer-Jensen M. Short-term inhibition of ADP-induced platelet aggregation by clopidogrel ameliorates radiation-induced toxicity in rat small intestine. Thromb Haemost 2002;87:122-128.

126. Mennie AT, Dalley VM, Dinneen LC, Collier HO. Treatment of radiation-induced gastrointestinal distress with acetylsalicylate. Lancet 1975;2:942-943.

127. Verheij M, Stewart FA, Oussoren Y, Weening JJ, Dewit L. Amelioration of radiation nephropathy by acetylsalicylic acid. Int J Radiat Biol 1995;67:587-596.

128. Delanian S, Porcher R, Rudant J, Lefaix JL. Kinetics of response to long-term treatment combining pentoxifylline and tocopherol in patients with superficial radiation-induced fibrosis. J Clin Oncol 2005;23:8570-8579.

129. Gothard L, Cornes P, Earl J, Hall E, MacLaren J, Mortimer P, et al. Double-blind placebo-controlled randomised trial of vitamin E and pentoxifylline in patients with chronic arm lymphoedema and fibrosis after surgery and radiotherapy for breast cancer. Radiother Oncol 2004;73:133-139.

130. Jeong BK, Song JH, Jeong H, Choi HS, Jung JH, Hahm JR, et al. Effect of alpha-lipoic acid on radiation-induced small intestine injury in mice. Oncotarget 2016;7:15105-15117.

131. Jang SS, Kim HG, Lee JS, Han JM, Park HJ, Huh GJ, et al. Melatonin reduces X-ray radiation-induced lung injury in mice by modulating oxidative stress and cytokine expression. Int J Radiat Biol 2013;89:97-105.

132. Sieber F, Muir SA, Cohen EP, Fish BL, Mader M, Schock AM, et al. Dietary selenium for the mitigation of radiation injury: effects of selenium dose escalation and timing of supplementation. Radiat Res 2011;176:366-374.

133. Haydont V, Bourgier C, Pocard M, Lusinchi A, Aigueperse J, Mathe D, et al. Pravastatin Inhibits the Rho/CCN2/extracellular matrix cascade in human fibrosis explants and improves radiation-induced intestinal fibrosis in rats. Clin Cancer Res 2007;13:5331-5340.

134. Nubel T, Damrot J, Roos WP, Kaina B, Fritz G. Lovastatin protects human endothelial cells from killing by ionizing radiation without impairing induction and repair of DNA double-strand breaks. Clin Cancer Res 2006;12:933-939.

135. Ostrau C, Hulsenbeck J, Herzog M, Schad A, Torzewski M, Lackner KJ, et al. Lovastatin attenuates ionizing radiation-induced normal tissue damage in vivo. Radiother Oncol 2009;92:492-499.

136. Ran XZ, Ran X, Zong ZW, Liu DQ, Xiang GM, Su YP, et al. Protective effect of atorvastatin on radiation-induced vascular endothelial cell injury in vitro. J Radiat Res 2010;51:527-533.

137. Zhang K, He X, Zhou Y, Gao L, Qi Z, Chen J, et al. Atorvastatin Ameliorates Radiation-Induced Cardiac Fibrosis in Rats. Radiat Res 2015;184:611-620.

138. Ghosh SN, Zhang R, Fish BL, Semenenko VA, Li XA, Moulder JE, et al. Renin-Angiotensin system suppression mitigates experimental radiation pneumonitis. Int J Radiat Oncol Biol Phys 2009;75:1528-1536.

139. Molteni A, Moulder JE, Cohen EF, Ward WF, Fish BL, Taylor JM, et al. Control of radiation-induced pneumopathy and lung fibrosis by angiotensin-converting enzyme inhibitors and an angiotensin II type 1 receptor blocker. Int J Radiat Biol 2000;76:523-532.

140. Medhora M, Gao F, Wu Q, Molthen RC, Jacobs ER, Moulder JE, et al. Model development and use of ACE inhibitors for preclinical mitigation of radiation-induced injury to multiple organs. Radiat Res 2014;182:545-555.

141. Ryu S, Kolozsvary A, Jenrow KA, Brown SL, Kim JH. Mitigation of radiation-induced optic neuropathy in rats by ACE inhibitor ramipril: importance of ramipril dose and treatment time. J Neurooncol 2007;82:119-124.

142. Nguyen L, Ward WF, Ts'ao CH, Molteni A. Captopril inhibits proliferation of human lung fibroblasts in culture: a potential antifibrotic mechanism. Proc Soc Exp Biol Med 1994;205:80-84.

143. Ward WF, Molteni A, Ts'ao CH, Hinz JM. Captopril reduces collagen and mast cell accumulation in irradiated rat lung. Int J Radiat Oncol Biol Phys 1990;19:1405-1409.

144. Kma L, Gao F, Fish BL, Moulder JE, Jacobs ER, Medhora M. Angiotensin converting enzyme inhibitors mitigate collagen synthesis induced by a single dose of radiation to the whole thorax. J Radiat Res (Tokyo) 2012;53:10-17.

145. Yoon SC, Park JM, Jang HS, Shinn KS, Bahk YW. Radioprotective effect of captopril on the mouse jejunal mucosa. Int J Radiat Oncol Biol Phys 1994;30:873-878.

146. Cohen EP, Molteni A, Hill P, Fish BL, Ward WF, Moulder JE, et al. Captopril preserves function and ultrastructure in experimental radiation nephropathy. Lab Invest 1996;75:349-360.

147. Moulder JE, Cohen EP, Fish BL. Captopril and losartan for mitigation of renal injury caused by single-dose total-body irradiation. Radiat Res 2011;175:29-36.

148. Robbins ME, Zhao W, Garcia-Espinosa MA, Diz DI. Renin-angiotensin system blockers and modulation of radiation-induced brain injury. Curr Drug Targets 2010;11:1413-1422.

149. Ward WF, Molteni A, Ts'ao C, Hinz JM. The effect of Captopril on benign and malignant reactions in irradiated rat skin. Br J Radiol 1990;63:349-354.

150. van der Veen SJ, Ghobadi G, de Boer RA, Faber H, Cannon MV, Nagle PW, et al. ACE inhibition attenuates radiation-induced cardiopulmonary damage. Radiother Oncol 2015;114:96-103.

151. Yarom R, Harper IS, Wynchank S, van Schalkwyk D, Madhoo J, Williams K, et al. Effect of captopril on changes in rats' hearts induced by long-term irradiation. Radiat Res 1993;133:187-197.

152. Molthen RC, Wu Q, Fish BL, Moulder JE, Jacobs ER, Medhora MM. Mitigation of radiation induced pulmonary vascular injury by delayed treatment with captopril. Respirology 2012;17:1261-1268.

153. Yu AF, Raikhelkar J, Zabor EC, Tonorezos ES, Moskowitz CS, Adsuar R, et al. Two-Dimensional Speckle Tracking Echocardiography Detects Subclinical Left Ventricular Systolic Dysfunction among Adult Survivors of Childhood, Adolescent, and Young Adult Cancer. Biomed Res Int 2016;2016:9363951.

154. Armstrong GT, Joshi VM, Ness KK, Marwick TH, Zhang N, Srivastava D, et al. Comprehensive Echocardiographic Detection of Treatment-Related Cardiac Dysfunction in Adult Survivors of Childhood Cancer: Results From the St. Jude Lifetime Cohort Study. J Am Coll Cardiol 2015;65:2511-2522.

155. Heidenreich PA, Hancock SL, Vagelos RH, Lee BK, Schnittger I. Diastolic dysfunction after mediastinal irradiation. Am Heart J 2005;150:977-982.

156. Dogan SM, Bilici HM, Bakkal H, Aydin M, Karabag T, Sayin MR, et al. The effect of radiotherapy on cardiac function. Coron Artery Dis 2012;23:146-154.

157. Cao L, Cai G, Chang C, Miao AY, Yu XL, Yang ZZ, et al. Diastolic Dysfunction Occurs Early in HER2-Positive Breast Cancer Patients Treated Concurrently With Radiation Therapy and Trastuzumab. Oncologist 2015;20:605-614.

158. Erven K, Jurcut R, Weltens C, Giusca S, Ector J, Wildiers H, et al. Acute radiation effects on cardiac function detected by strain rate imaging in breast cancer patients. Int J Radiat Oncol Biol Phys 2011;79:1444-1451.

159. Erven K, Florian A, Slagmolen P, Sweldens C, Jurcut R, Wildiers H, et al. Subclinical cardiotoxicity detected by strain rate imaging up to 14 months after breast radiation therapy. Int J Radiat Oncol Biol Phys 2013;85:1172-1178.

160. Lo Q, Hee L, Batumalai V, Allman C, MacDonald P, Delaney GP, et al. Subclinical cardiac dysfunction detected by strain imaging during breast irradiation with persistent changes 6 weeks after treatment. Int J Radiat Oncol Biol Phys 2015;92:268-276.

161. Heggemann F, Grotz H, Welzel G, Dosch C, Hansmann J, Kraus-Tiefenbacher U, et al. Cardiac Function After Multimodal Breast Cancer Therapy Assessed With Functional Magnetic Resonance Imaging and Echocardiography Imaging. Int J Radiat Oncol Biol Phys 2015;93:836-844.

162. Tsai HR, Gjesdal O, Wethal T, Haugaa KH, Fossa A, Fossa SD, et al. Left ventricular function assessed by two-dimensional speckle tracking echocardiography in long-term survivors of Hodgkin's lymphoma treated by mediastinal radiotherapy with or without anthracycline therapy. Am J Cardiol 2011;107:472-477.

163. Sioka C, Exarchopoulos T, Tasiou I, Tzima E, Fotou N, Capizzello A, et al. Myocardial perfusion imaging with (99 m)Tc-tetrofosmin SPECT in breast cancer patients that received postoperative radiotherapy: a case-control study. Radiat Oncol 2011;6:151-717X-6-151.

164. Seddon B, Cook A, Gothard L, Salmon E, Latus K, Underwood SR, et al. Detection of defects in myocardial perfusion imaging in patients with early breast cancer treated with radiotherapy. Radiother Oncol 2002;64:53-63.

165. Yu X, Prosnitz RR, Zhou S, Hardenberg PH, Tisch A, Blazing MA, et al. Symptomatic cardiac events following radiation therapy for left-sided breast cancer: possible association with radiation therapy-induced changes in regional perfusion. Clin Breast Cancer 2003;4:193-197.

166. Chung E, Corbett JR, Moran JM, Griffith KA, Marsh RB, Feng M, et al. Is there a dose-response relationship for heart disease with low-dose radiation therapy? Int J Radiat Oncol Biol Phys 2013;85:959-964.

167. Zhang P, Hu X, Yue J, Meng X, Han D, Sun X, et al. Early detection of radiation-induced heart disease using (99m)Tc-MIBI SPECT gated myocardial perfusion imaging in patients with oesophageal cancer during radiotherapy. Radiother Oncol 2015;115:171-178.

168. Ylanen K, Poutanen T, Savikurki-Heikkila P, Rinta-Kiikka I, Eerola A, Vettenranta K. Cardiac magnetic resonance imaging in the evaluation of the late effects of

anthracyclines among long-term survivors of childhood cancer. J Am Coll Cardiol 2013;61:1539-1547.

169. Umezawa R, Ota H, Takanami K. MRI findings of radiation-induced myocardial damage in patients with oesophageal cancer. 2014;69:1273-1279.

170. Jingu K, Kaneta T, Nemoto K, Ichinose A, Oikawa M, Takai Y, et al. The utility of 18F-fluorodeoxyglucose positron emission tomography for early diagnosis of radiation-induced myocardial damage. Int J Radiat Oncol Biol Phys 2006;66:845-851.

171. Yan R, Song J, Wu Z, Guo M, Liu J, Li J, et al. Detection of Myocardial Metabolic Abnormalities by 18F-FDG PET/CT and Corresponding Pathological Changes in Beagles with Local Heart Irradiation. Korean J Radiol 2015;16:919-928.

172. Elme A, Saarto T, Totterman KJ, Utrianen M, Kautiainen H, Jarvenpaa S, et al. Electrocardiography changes during adjuvant breast cancer therapy: incidence and risk factors. Anticancer Res 2013;33:4933-4939.

173. Lindahl J, Strender LE, Larsson LE, Unsgaard A. Electrocardiographic changes after radiation therapy for carcinoma of the breast. Incidence and functional significance. Acta Radiol Oncol 1983;22:433-440.

174. Strender LE, Lindahl J, Larsson LE. Incidence of heart disease and functional significance of changes in the electrocardiogram 10 years after radiotherapy for breast cancer. Cancer 1986;57:929-934.

175. Gomez DR, Yusuf SW, Munsell MF, Welsh JW, Liao Z, Lin SH, et al. Prospective exploratory analysis of cardiac biomarkers and electrocardiogram abnormalities in patients receiving thoracic radiation therapy with high-dose heart exposure. J Thorac Oncol 2014;9:1554-1560.

176. Adar A, Canyilmaz E, Kiris A, Ilter A, Serdar L, Memis Y, et al. Radiotherapy Induces Development of Fragmented QRS in Patients with Breast Cancer. Breast Care (Basel) 2015;10:277-280.

177. Skytta T, Tuohinen S, Boman E, Virtanen V, Raatikainen P, Kellokumpu-Lehtinen PL. Troponin T-release associates with cardiac radiation doses during adjuvant left-sided breast cancer radiotherapy. Radiat Oncol 2015;10:141-015-0436-2.

178. D'Errico MP, Grimaldi L, Petruzzelli MF, Gianicolo EA, Tramacere F, Monetti A, et al. N-terminal pro-B-type natriuretic peptide plasma levels as a potential biomarker for cardiac damage after radiotherapy in patients with left-sided breast cancer. Int J Radiat Oncol Biol Phys 2012;82:e239-46.

179. Jingu K, Nemoto K, Kaneta T, Oikawa M, Ogawa Y, Ariga H, et al. Temporal change in brain natriuretic Peptide after radiotherapy for thoracic esophageal cancer. Int J Radiat Oncol Biol Phys 2007;69:1417-1423.

180. Nellessen U, Zingel M, Hecker H, Bahnsen J, Borschke D. Effects of radiation therapy on myocardial cell integrity and pump function: which role for cardiac biomarkers? Chemotherapy 2010;56:147-152.

181. Palumbo I, Palumbo B, Fravolini ML, Marcantonini M, Perrucci E, Latini ME, et al. Brain natriuretic peptide as a cardiac marker of transient radiotherapy-related damage in left-sided breast cancer patients: A prospective study. Breast 2016;25:45-50.

182. Oremus M, Raina PS, Santaguida P, Balion CM, McQueen MJ, McKelvie R, et al. A systematic review of BNP as a predictor of prognosis in persons with coronary artery disease. Clin Biochem 2008;41:260-265.

183. Sze J, Mooney J, Barzi F, Hillis GS, Chow CK. Cardiac Troponin and its Relationship to Cardiovascular Outcomes in Community Populations - A Systematic Review and Meta-analysis. Heart Lung Circ 2016;25:217-228.

184. Bessiere F, Khenifer S, Dubourg J, Durieu I, Lega JC. Prognostic value of troponins in sepsis: a meta-analysis. Intensive Care Med 2013;39:1181-1189.

185. Nagarajan V, Hernandez AV, Tang WH. Prognostic value of cardiac troponin in chronic stable heart failure: a systematic review. Heart 2012;98:1778-1786.

186. Tsounis D, Deftereos S, Bouras G, Giannopoulos G, Anatoliotakis N, Raisakis K, et al. High sensitivity troponin in cardiovascular disease. Is there more than a marker of myocardial death? Curr Top Med Chem 2013;13:201-215.

187. Ploegstra MJ, Zijlstra WM, Douwes JM, Hillege HL, Berger RM. Prognostic factors in pediatric pulmonary arterial hypertension: A systematic review and meta-analysis. Int J Cardiol 2015;184:198-207.

188. Savarese G, Musella F, D'Amore C, Vassallo E, Losco T, Gambardella F, et al. Changes of natriuretic peptides predict hospital admissions in patients with chronic heart failure: a meta-analysis. JACC Heart Fail 2014;2:148-158.

189. Rodseth RN, Biccard BM, Le Manach Y, Sessler DI, Lurati Buse GA, Thabane L, et al. The prognostic value of pre-operative and post-operative B-type natriuretic peptides in patients undergoing noncardiac surgery: B-type natriuretic peptide and N-terminal fragment of pro-B-type natriuretic peptide: a systematic review and individual patient data meta-analysis. J Am Coll Cardiol 2014;63:170-180.

190. Perez JE, Miller JG, Barzilai B, Wickline S, Mohr GA, Wear K, et al. Progress in quantitative ultrasonic characterization of myocardium: from the laboratory to the bedside. J Am Soc Echocardiogr 1988;1:294-305.

191. Park SM, Kim YH, Ahn CM, Hong SJ, Lim DS, Shim WJ. Relationship between ultrasonic tissue characterization and myocardial deformation for prediction of left ventricular reverse remodelling in non-ischaemic dilated cardiomyopathy. Eur J Echocardiogr 2011;12:887-894.

192. Mor-Avi V, Lang RM, Badano LP, Belohlavek M, Cardim NM, Derumeaux G, et al. Current and evolving echocardiographic techniques for the quantitative evaluation of cardiac mechanics: ASE/EAE consensus statement on methodology and indications endorsed by the Japanese Society of Echocardiography. Eur J Echocardiogr 2011;12:167-205.

193. Gigli G, Lattanzi F, Lucarini AR, Picano E, Genovesi-Ebert A, Marabotti C, et al. Normal ultrasonic myocardial reflectivity in hypertensive patients. A tissue characterization study. Hypertension 1993;21:329-334.

194. Angermann CE, Nassau K, Stempfle HU, Kruger TM, Drewello R, Junge R, et al. Recognition of acute cardiac allograft rejection from serial integrated backscatter analyses in human orthotopic heart transplant recipients. Comparison with conventional echocardiography. Circulation 1997;95:140-150.

195. Lattanzi F, Bellotti P, Picano E, Chiarella F, Mazzarisi A, Melevendi C, et al. Quantitative ultrasonic analysis of myocardium in patients with thalassemia major and iron overload. Circulation 1993;87:748-754.

196. Barzilai B, Madaras EI, Sobel BE, Miller JG, Perez JE. Effects of myocardial contraction on ultrasonic backscatter before and after ischemia. Am J Physiol 1984;247:H478-83.

197. Komuro K, Yamada S, Mikami T, Yoshinaga K, Noriyasu K, Goto K, et al. Sensitive detection of myocardial viability in chronic coronary artery disease by ultrasonic integrated backscatter analysis. J Am Soc Echocardiogr 2005;18:26-31.

198. Milunski MR, Mohr GA, Wear KA, Sobel BE, Miller JG, Wickline SA. Early identification with ultrasonic integrated backscatter of viable but stunned myocardium in dogs. J Am Coll Cardiol 1989;14:462-471.

199. Mimbs JW, Yuhas DE, Miller JG, Weiss AN, Sobel BE. Detection of myocardial infarction in vitro based on altered attenuation of ultrasound. Circ Res 1977;41:192-198.

200. Hoyt RH, Collins SM, Skorton DJ, Ericksen EE, Conyers D. Assessment of fibrosis in infarcted human hearts by analysis of ultrasonic backscatter. Circulation 1985;71:740-744.

201. Mimbs JW, O'Donnell M, Bauwens D, Miller JW, Sobel BE. The dependence of ultrasonic attenuation and backscatter on collagen content in dog and rabbit hearts. Circ Res 1980;47:49-58.

202. Hoyt RM, Skorton DJ, Collins SM, Melton HE,Jr. Ultrasonic backscatter and collagen in normal ventricular myocardium. Circulation 1984;69:775-782.

203. Picano E, Pelosi G, Marzilli M, Lattanzi F, Benassi A, Landini L, et al. In vivo quantitative ultrasonic evaluation of myocardial fibrosis in humans. Circulation 1990;81:58-64.

204. Lee HH, Hung CS, Wu XM, Wu VC, Liu KL, Wang SM, et al. Myocardial ultrasound tissue characterization of patients with primary aldosteronism. Ultrasound Med Biol 2013;39:54-61.

205. Masuyama T, Valantine HA, Gibbons R, Schnittger I, Popp RL. Serial measurement of integrated ultrasonic backscatter in human cardiac allografts for the recognition of acute rejection. Circulation 1990;81:829-839.

206. Giglio V, Puddu PE, Holland MR, Camastra G, Ansalone G, Ricci E, et al. Ultrasound tissue characterization does not differentiate genotype, but indexes ejection fraction deterioration in becker muscular dystrophy. Ultrasound Med Biol 2014;40:2777-2785.

207. Lattanzi F, Spirito P, Picano E, Mazzarisi A, Landini L, Distante A, et al. Quantitative assessment of ultrasonic myocardial reflectivity in hypertrophic cardiomyopathy. J Am Coll Cardiol 1991;17:1085-1090.

208. Di Bello V, Talarico L, Picano E, Di Muro C, Landini L, Paterni M, et al. Increased echodensity of myocardial wall in the diabetic heart: an ultrasound tissue characterization study. J Am Coll Cardiol 1995;25:1408-1415.

209. Xie L, Wang R, Huang M, Zhang Y, Shen J, Xiao T. Quantitative evaluation of myocardial fibrosis by cardiac integrated backscatter analysis in Kawasaki disease. Cardiovasc Ultrasound 2016;14:3-016-0046-7.

210. Carluccio E, Biagioli P, Zuchi C, Bardelli G, Murrone A, Lauciello R, et al. Fibrosis assessment by integrated backscatter and its relationship with longitudinal deformation and diastolic function in heart failure with preserved ejection fraction. Int J Cardiovasc Imaging 2016;32:1071-1080.

211. Prior DL, Somaratne JB, Jenkins AJ, Yii M, Newcomb AE, Schalkwijk CG, et al. Calibrated integrated backscatter and myocardial fibrosis in patients undergoing cardiac surgery. Open Heart 2015;2:e000278-2015-000278. eCollection 2015.

212. Zuber M, Gerber K, Erne P. Myocardial tissue characterization in heart failure by real-time integrated backscatter. Eur J Ultrasound 1999;9:135-143.

213. Li VW, Cheuk DK, Cheng FW, Yang JY, Yau JP, Ho KK, et al. Myocardial stiffness as assessed by diastolic wall strain in adult survivors of childhood leukaemias with preserved left ventricular ejection fraction. Eur Heart J Cardiovasc Imaging 2016.

214. Romano MM, Maciel LM, Almeida-Filho OC, Pazin-Filho A, Schmidt A, Maciel BC. Myocardial ultrasonic tissue characterization in patients with thyroid dysfunction. Cardiovasc Ultrasound 2010;8:15-7120-8-15.

215. Arat N, Kacar S, Golbasi Z, Akdogan M, Kuran S. Myocardial integrated ultrasonic backscatter for early detection of cardiac involvement in patients with Wilson disease. Turk J Gastroenterol 2014;25:678-684.

216. Naito J, Masuyama T, Tanouchi J, Mano T, Kondo H, Yamamoto K, et al. Analysis of transmural trend of myocardial integrated ultrasound backscatter for differentiation of hypertrophic cardiomyopathy and ventricular hypertrophy due to hypertension. J Am Coll Cardiol 1994;24:517-524.

217. Finch-Johnston AE, Gussak HM, Mobley J, Holland MR, Petrovic O, Perez JE, et al. Cyclic variation of integrated backscatter: dependence of time delay on the echocardiographic view used and the myocardial segment analyzed. J Am Soc Echocardiogr 2000;13:9-17.

218. Barzilai B, Vered Z, Mohr GA, Wear KA, Courtois M, Sobel BE, et al. Myocardial ultrasonic backscatter for characterization of ischemia and reperfusion: relationship to wall motion. Ultrasound Med Biol 1990;16:391-398.

219. Hyodo E, Hozumi T, Takemoto Y, Watanabe H, Muro T, Yamagishi H, et al. Early detection of cardiac involvement in patients with sarcoidosis by a non-invasive method with ultrasonic tissue characterisation. Heart 2004;90:1275-1280.

220. Galetta F, Franzoni F, Mancuso M, Orsucci D, Tocchini L, Papi R, et al. Cardiac involvement in chronic progressive external ophthalmoplegia. J Neurol Sci 2014;345:189-192.

221. Di Bello V, Giorgi D, Talini E, Dell'Omo G, Palagi C, Romano MF, et al. Incremental value of ultrasonic tissue characterization (backscatter) in the evaluation of

left ventricular myocardial structure and mechanics in essential arterial hypertension. Circulation 2003;107:74-80.

222. Koyama J, Ray-Sequin PA, Falk RH. Prognostic significance of ultrasound myocardial tissue characterization in patients with cardiac amyloidosis. Circulation 2002;106:556-561.

223. Ohara Y, Hiasa Y, Hosokawa S, Suzuki N, Takahashi T, Kishi K, et al. Ultrasonic tissue characterization predicts left ventricular remodeling in patients with acute anterior myocardial infarction after primary coronary angioplasty. J Am Soc Echocardiogr 2005;18:638-643.

224. Sagar KB, Pelc LE, Rhyne TL, Wann LS, Waltier DC. Influence of heart rate, preload, afterload, and inotropic state on myocardial ultrasonic backscatter. Circulation 1988;77:478-483.

225. Duygu H, Akman L, Ozerkan F, Akercan F, Zoghi M, Nalbantgil S, et al. Comparison of the effects of new and conventional hormone replacement therapies on left ventricular diastolic function in healthy postmenopausal women: a Doppler and ultrasonic backscatter study. Int J Cardiovasc Imaging 2009;25:387-396.

226. Romano MM, Pazin-Filho A, O'Connel JL, Simoes MV, Schmidt A, Campos EC, et al. Early detection of doxorubicin myocardial injury by ultrasonic tissue characterization in an experimental animal model. Cardiovasc Ultrasound 2012;10:40-7120-10-40.

227. Picano E, Faletra F, Marini C, Paterni M, Danzi GB, Lombardi M, et al. Increased echodensity of transiently asynergic myocardium in humans: a novel echocardiographic sign of myocardial ischemia. J Am Coll Cardiol 1993;21:199-207.

228. Jin X, Rong S, Mei C, Ye C, Chen J, Chen X. Effects of thrice-weekly in-center nocturnal vs. conventional hemodialysis on integrated backscatter of myocardial tissue. Hemodial Int 2011;15:200-210.

229. Wong CY, Byrne NM, O'Moore-Sullivan T, Hills AP, Prins JB, Marwick TH. Effect of weight loss due to lifestyle intervention on subclinical cardiovascular dysfunction in obesity (body mass index >30 kg/m2). Am J Cardiol 2006;98:1593-1598.

230. Glueck RM, Mottley JG, Miller JG, Sobel BE, Perez JE. Effects of coronary artery occlusion and reperfusion on cardiac cycle-dependent variation of myocardial ultrasonic backscatter. Circ Res 1985;56:683-689.

231. Smiseth OA, Torp H, Opdahl A, Haugaa KH, Urheim S. Myocardial strain imaging: how useful is it in clinical decision making? Eur Heart J 2016;37:1196-1207.

232. Geyer H, Caracciolo G, Abe H, Wilansky S, Carerj S, Gentile F, et al. Assessment of myocardial mechanics using speckle tracking echocardiography: fundamentals and clinical applications. J Am Soc Echocardiogr 2010;23:351-69; quiz 453-5.

233. Voigt JU, Pedrizzetti G, Lysyansky P, Marwick TH, Houle H, Baumann R, et al. Definitions for a common standard for 2D speckle tracking echocardiography: consensus document of the EACVI/ASE/Industry Task Force to standardize deformation imaging. Eur Heart J Cardiovasc Imaging 2015;16:1-11.

234. Biering-Sorensen T, Hoffmann S, Mogelvang R, Zeeberg Iversen A, Galatius S, Fritz-Hansen T, et al. Myocardial strain analysis by 2-dimensional speckle tracking echocardiography improves diagnostics of coronary artery stenosis in stable angina pectoris. Circ Cardiovasc Imaging 2014;7:58-65.

235. Norum IB, Ruddox V, Edvardsen T, Otterstad JE. Diagnostic accuracy of left ventricular longitudinal function by speckle tracking echocardiography to predict significant coronary artery stenosis. A systematic review. BMC Med Imaging 2015;15:25-015-0067-y.

236. Schiano-Lomoriello V, Galderisi M, Mele D, Esposito R, Cerciello G, Buonauro A, et al. Longitudinal strain of left ventricular basal segments and E/e' ratio differentiate primary cardiac amyloidosis at presentation from hypertensive hypertrophy: an automated function imaging study. Echocardiography 2016;33:1335-1343.

237. Peyrou J, Reant P, Reynaud A, Cornolle C, Dijos M, Rooryck-Thambo C, et al. Morphological and functional abnormalities pattern in hypertrophy-free HCM mutation carriers detected with echocardiography. Int J Cardiovasc Imaging 2016;32:1379-1389.

238. Kusunose K, Dahiya A, Popovic ZB, Motoki H, Alraies MC, Zurick AO, et al. Biventricular mechanics in constrictive pericarditis comparison with restrictive cardiomyopathy and impact of pericardiectomy. Circ Cardiovasc Imaging 2013;6:399-406.

239. Schouver ED, Moceri P, Doyen D, Tieulie N, Queyrel V, Baudouy D, et al. Early detection of cardiac involvement in sarcoidosis with 2-dimensional speckle-tracking echocardiography. Int J Cardiol 2016.

240. Fang ZY, Leano R, Marwick TH. Relationship between longitudinal and radial contractility in subclinical diabetic heart disease. Clin Sci (Lond) 2004;106:53-60.

241. Ng AC, Delgado V, Bertini M, van der Meer RW, Rijzewijk LJ, Shanks M, et al. Findings from left ventricular strain and strain rate imaging in asymptomatic patients with type 2 diabetes mellitus. Am J Cardiol 2009;104:1398-1401.

242. Vinereanu D, Nicolaides E, Tweddel AC, Madler CF, Holst B, Boden LE, et al. Subclinical left ventricular dysfunction in asymptomatic patients with Type II diabetes mellitus, related to serum lipids and glycated haemoglobin. Clin Sci (Lond) 2003;105:591-599.

243. Ayoub AM, Keddeas VW, Ali YA, El Okl RA. Subclinical LV Dysfunction Detection Using Speckle Tracking Echocardiography in Hypertensive Patients with Preserved LV Ejection Fraction. Clin Med Insights Cardiol 2016;10:85-90.

244. Midtbo H, Semb AG, Matre K, Kvien TK, Gerdts E. Disease activity is associated with reduced left ventricular systolic myocardial function in patients with rheumatoid arthritis. Ann Rheum Dis 2016.

245. Liou K, Negishi K, Ho S, Russell EA, Cranney G, Ooi SY. Detection of Obstructive Coronary Artery Disease Using Peak Systolic Global Longitudinal Strain Derived by Two-Dimensional Speckle-Tracking: A Systematic Review and Meta-Analysis. J Am Soc Echocardiogr 2016;29:724-735.e4.

246. Leung M, Xie M, Durmush E, Leung DY, Wong VW. Weight Loss with Sleeve Gastrectomy in Obese Type 2 Diabetes Mellitus: Impact on Cardiac Function. Obes Surg 2016;26:321-326.

247. Cameli M, Mondillo S, Righini FM, Lisi M, Dokollari A, Lindqvist P, et al. Left Ventricular Deformation and Myocardial Fibrosis in Patients With Advanced Heart Failure Requiring Transplantation. J Card Fail 2016;22:901-907.

248. Stewart GM, Yamada A, Haseler LJ, Kavanagh JJ, Koerbin G, Chan J, et al. Altered ventricular mechanics after 60 min of high-intensity endurance exercise: insights from exercise speckle-tracking echocardiography. Am J Physiol Heart Circ Physiol 2015;308:H875-83.

249. Vitiello D, Cassirame J, Menetrier A, Rupp T, Schuster I, Reboul C, et al. Depressed systolic function after a prolonged and strenuous exercise. Med Sci Sports Exerc 2013;45:2072-2079.

250. Whyte GP, George K, Sharma S, Lumley S, Gates P, Prasad K, et al. Cardiac fatigue following prolonged endurance exercise of differing distances. Med Sci Sports Exerc 2000;32:1067-1072.

251. Caselli S, Montesanti D, Autore C, Di Paolo FM, Pisicchio C, Squeo MR, et al. Patterns of left ventricular longitudinal strain and strain rate in Olympic athletes. J Am Soc Echocardiogr 2015;28:245-253.

252. Demirelli S, Sam CT, Ermis E, Degirmenci H, Sen I, Arisoy A, et al. Long-Term Cardiac Remodeling in Elite Athletes: Assessment by Tissue Doppler and Speckle Tracking Echocardiography. Echocardiography 2015;32:1367-1373.

253. Simsek Z, Hakan Tas M, Degirmenci H, Gokhan Yazici A, Ipek E, Duman H, et al. Speckle tracking echocardiographic analysis of left ventricular systolic and diastolic functions of young elite athletes with eccentric and concentric type of cardiac remodeling. Echocardiography 2013;30:1202-1208.

254. Wasfy MM, Weiner RB. Differentiating the athlete's heart from hypertrophic cardiomyopathy. Curr Opin Cardiol 2015;30:500-505.

255. Afonso L, Kondur A, Simegn M, Niraj A, Hari P, Kaur R, et al. Two-dimensional strain profiles in patients with physiological and pathological hypertrophy and preserved left ventricular systolic function: a comparative analyses. BMJ Open 2012;2:10.1136/bmjopen-2012-001390. Print 2012.

256. Sefa Okten M, Tuluce K, Yakar Tuluce S, Kilic S, Soner Kemal H, Sayin A, et al. Screening first-degree relatives of patients with idiopathic dilated cardiomyopathy. Herz 2016.

257. de Gonzalo-Calvo D, Quezada M, Campuzano O, Perez-Serra A, Broncano J, Ayala R, et al. Familial dilated cardiomyopathy: A multidisciplinary entity, from basic screening to novel circulating biomarkers. Int J Cardiol 2016;228:870-880.

258. Kauer F, van Dalen BM, Michels M, Schinkel AF, Vletter WB, van Slegtenhorst M, et al. Delayed and decreased LV untwist and unstrain rate in mutation carriers for hypertrophic cardiomyopathy. Eur Heart J Cardiovasc Imaging 2016.

259. Authors/Task Force members, Elliott PM, Anastasakis A, Borger MA, Borggrefe M, Cecchi F, et al. 2014 ESC Guidelines on diagnosis and management of hypertrophic cardiomyopathy: the Task Force for the Diagnosis and Management of Hypertrophic Cardiomyopathy of the European Society of Cardiology (ESC). Eur Heart J 2014;35:2733-2779.

260. Guerra F, Marchesini M, Contadini D, Menditto A, Morelli M, Piccolo E, et al. Speckle-tracking global longitudinal strain as an early predictor of cardiotoxicity in breast carcinoma. Support Care Cancer 2016;24:3139-3145.

261. Florescu M, Magda LS, Enescu OA, Jinga D, Vinereanu D. Early detection of epirubicin-induced cardiotoxicity in patients with breast cancer. J Am Soc Echocardiogr 2014;27:83-92.

262. Tang Q, Jiang Y, Xu Y, Xia H. Speckle tracking echocardiography predicts early subclinical anthracycline cardiotoxicity in patients with breast cancer. J Clin Ultrasound 2016.

263. Charbonnel C, Convers-Domart R, Rigaudeau S, Taksin AL, Baron N, Lambert J, et al. Assessment of global longitudinal strain at low-dose anthracycline-based chemotherapy for the prediction of subsequent cardiotoxicity. Ann Cardiol Angeiol (Paris) 2016;65:380.

264. Mousavi N, Tan TC, Ali M, Halpern EF, Wang L, Scherrer-Crosbie M. Echocardiographic parameters of left ventricular size and function as predictors of symptomatic heart failure in patients with a left ventricular ejection fraction of 50-59% treated with anthracyclines. Eur Heart J Cardiovasc Imaging 2015;16:977-984.

265. Lowenthal A, Tacy TA, Behzadian F, Punn R. Echocardiographic predictors of early postsurgical myocardial dysfunction in pediatric patients with aortic valve insufficiency. Pediatr Cardiol 2013;34:1335-1343.

266. Pandis D, Sengupta PP, Castillo JG, Caracciolo G, Fischer GW, Narula J, et al. Assessment of longitudinal myocardial mechanics in patients with degenerative mitral valve regurgitation predicts postoperative worsening of left ventricular systolic function. J Am Soc Echocardiogr 2014;27:627-638.

267. Cho EJ, Park SJ, Yun HR, Jeong DS, Lee SC, Park SW, et al. Predicting Left Ventricular Dysfunction after Surgery in Patients with Chronic Mitral Regurgitation: Assessment of Myocardial Deformation by 2-Dimensional Multilayer Speckle Tracking Echocardiography. Korean Circ J 2016;46:213-221.

268. Witkowski TG, Thomas JD, Debonnaire PJ, Delgado V, Hoke U, Ewe SH, et al. Global longitudinal strain predicts left ventricular dysfunction after mitral valve repair. Eur Heart J Cardiovasc Imaging 2013;14:69-76.

269. Shehata M. Value of two-dimensional strain imaging in prediction of myocardial function recovery after percutaneous revascularization of infarct-related artery. Echocardiography 2015;32:630-637.

270. Woo JS, Kim WS, Yu TK, Ha SJ, Kim SY, Bae JH, et al. Prognostic value of serial global longitudinal strain measured by two-dimensional speckle tracking echocardiography in patients with ST-segment elevation myocardial infarction. Am J Cardiol 2011;108:340-347.

271. Ernande L, Bergerot C, Girerd N, Thibault H, Davidsen ES, Gautier Pignon-Blanc P, et al. Longitudinal myocardial strain alteration is associated with left ventricular

remodeling in asymptomatic patients with type 2 diabetes mellitus. J Am Soc Echocardiogr 2014;27:479-488.

272. Cong T, Sun Y, Shang Z, Wang K, Su D, Zhong L, et al. Prognostic Value of Speckle Tracking Echocardiography in Patients with ST-Elevation Myocardial Infarction Treated with Late Percutaneous Intervention. Echocardiography 2015;32:1384-1391.

273. Chimura M, Onishi T, Tsukishiro Y, Sawada T, Kiuchi K, Shimane A, et al. Longitudinal strain combined with delayed-enhancement magnetic resonance improves risk stratification in patients with dilated cardiomyopathy. Heart 2016.

274. Dahou A, Bartko PE, Capoulade R, Clavel MA, Mundigler G, Grondin SL, et al. Usefulness of global left ventricular longitudinal strain for risk stratification in low ejection fraction, low-gradient aortic stenosis: results from the multicenter True or Pseudo-Severe Aortic Stenosis study. Circ Cardiovasc Imaging 2015;8:e002117.

275. Kusunose K, Goodman A, Parikh R, Barr T, Agarwal S, Popovic ZB, et al. Incremental prognostic value of left ventricular global longitudinal strain in patients with aortic stenosis and preserved ejection fraction. Circ Cardiovasc Imaging 2014;7:938-945.

276. Bertini M, Ng AC, Antoni ML, Nucifora G, Ewe SH, Auger D, et al. Global longitudinal strain predicts long-term survival in patients with chronic ischemic cardiomyopathy. Circ Cardiovasc Imaging 2012;5:383-391.

277. Krishnasamy R, Isbel NM, Hawley CM, Pascoe EM, Burrage M, Leano R, et al. Left Ventricular Global Longitudinal Strain (GLS) Is a Superior Predictor of All-Cause and Cardiovascular Mortality When Compared to Ejection Fraction in Advanced Chronic Kidney Disease. PLoS One 2015;10:e0127044.

278. Sengelov M, Jorgensen PG, Jensen JS, Bruun NE, Olsen FJ, Fritz-Hansen T, et al. Global Longitudinal Strain Is a Superior Predictor of All-Cause Mortality in Heart Failure With Reduced Ejection Fraction. JACC Cardiovasc Imaging 2015;8:1351-1359.

279. Barros-Gomes S, Williams B, Nhola LF, Grogan M, Maalouf JF, Dispenzieri A, et al. Prognosis of Light Chain Amyloidosis With Preserved LVEF: Added Value of 2D Speckle-Tracking Echocardiography to the Current Prognostic Staging System. JACC Cardiovasc Imaging 2016.

280. Kalam K, Otahal P, Marwick TH. Prognostic implications of global LV dysfunction: a systematic review and meta-analysis of global longitudinal strain and ejection fraction. Heart 2014;100:1673-1680.

281. Ersboll M, Valeur N, Mogensen UM, Andersen MJ, Moller JE, Velazquez EJ, et al. Prediction of all-cause mortality and heart failure admissions from global left ventricular longitudinal strain in patients with acute myocardial infarction and preserved left ventricular ejection fraction. J Am Coll Cardiol 2013;61:2365-2373.

282. Mignot A, Donal E, Zaroui A, Reant P, Salem A, Hamon C, et al. Global longitudinal strain as a major predictor of cardiac events in patients with depressed left ventricular function: a multicenter study. J Am Soc Echocardiogr 2010;23:1019-1024.

283. Hartlage GR, Kim JH, Strickland PT, Cheng AC, Ghasemzadeh N, Pernetz MA, et al. The prognostic value of standardized reference values for speckle-tracking global longitudinal strain in hypertrophic cardiomyopathy. Int J Cardiovasc Imaging 2015;31:557-565.

284. Su HM, Lin TH, Hsu PC, Lee WH, Chu CY, Lee CS, et al. Global left ventricular longitudinal systolic strain as a major predictor of cardiovascular events in patients with atrial fibrillation. Heart 2013;99:1588-1596.

285. Sun M, Kang Y, Cheng L, Pan C, Cao X, Yao H, et al. Global longitudinal strain is an independent predictor of cardiovascular events in patients with maintenance hemodialysis: a prospective study using three-dimensional speckle tracking echocardiography. Int J Cardiovasc Imaging 2016;32:757-766.

286. Stanton T, Leano R, Marwick TH. Prediction of all-cause mortality from global longitudinal speckle strain: comparison with ejection fraction and wall motion scoring. Circ Cardiovasc Imaging 2009;2:356-364.

287. Russo C, Jin Z, Elkind MS, Rundek T, Homma S, Sacco RL, et al. Prevalence and prognostic value of subclinical left ventricular systolic dysfunction by global longitudinal strain in a community-based cohort. Eur J Heart Fail 2014;16:1301-1309.

288. Thavendiranathan P, Poulin F, Lim KD, Plana JC, Woo A, Marwick TH. Use of myocardial strain imaging by echocardiography for the early detection of cardiotoxicity in patients during and after cancer chemotherapy: a systematic review. J Am Coll Cardiol 2014;63:2751-2768.

289. Negishi K, Negishi T, Hare JL, Haluska BA, Plana JC, Marwick TH. Independent and incremental value of deformation indices for prediction of trastuzumab-induced cardiotoxicity. J Am Soc Echocardiogr 2013;26:493-498.

290. D'hooge J, Heimdal A, Jamal F, Kukulski T, Bijnens B, Rademakers F, et al. Regional strain and strain rate measurements by cardiac ultrasound: principles, implementation and limitations. Eur J Echocardiogr 2000;1:154-170.

291. Jamal F, Strotmann J, Weidemann F, Kukulski T, D'hooge J, Bijnens B, et al. Noninvasive quantification of the contractile reserve of stunned myocardium by ultrasonic strain rate and strain. Circulation 2001;104:1059-1065.

292. Weidemann F, Jamal F, Sutherland GR, Claus P, Kowalski M, Hatle L, et al. Myocardial function defined by strain rate and strain during alterations in inotropic states and heart rate. Am J Physiol Heart Circ Physiol 2002;283:H792-9.

293. Cho GY, Marwick TH, Kim HS, Kim MK, Hong KS, Oh DJ. Global 2-dimensional strain as a new prognosticator in patients with heart failure. J Am Coll Cardiol 2009;54:618-624.

294. Sengupta PP, Krishnamoorthy VK, Abhayaratna WP, Korinek J, Belohlavek M, Sundt TM,3rd, et al. Disparate patterns of left ventricular mechanics differentiate constrictive pericarditis from restrictive cardiomyopathy. JACC Cardiovasc Imaging 2008;1:29-38.

295. Yingchoncharoen T, Agarwal S, Popovic ZB, Marwick TH. Normal ranges of left ventricular strain: a meta-analysis. J Am Soc Echocardiogr 2013;26:185-191.

296. Borg AN, Ray SG. A unifying framework for understanding heart failure? Response to "Left Ventricular Torsion By Two-Dimensional Speckle Tracking Echocardiography in Patients With Diastolic Dysfunction and Normal Ejection Fraction" by Park SJ et al. J Am Soc Echocardiogr 2009;22:318-20; author reply 321-2.

297. Popescu BA, Beladan CC, Calin A, Muraru D, Deleanu D, Rosca M, et al. Left ventricular remodelling and torsional dynamics in dilated cardiomyopathy: reversed apical rotation as a marker of disease severity. Eur J Heart Fail 2009;11:945-951.

298. European Society of Cardiology (ESC), European Heart Rhythm Association (EHRA), Brignole M, Auricchio A, Baron-Esquivias G, Bordachar P, et al. 2013 ESC guidelines on cardiac pacing and cardiac resynchronization therapy: the task force on cardiac pacing and resynchronization therapy of the European Society of Cardiology (ESC). Developed in collaboration with the European Heart Rhythm Association (EHRA). Europace 2013;15:1070-1118.

299. Chung ES, Leon AR, Tavazzi L, Sun JP, Nihoyannopoulos P, Merlino J, et al. Results of the Predictors of Response to CRT (PROSPECT) trial. Circulation 2008;117:2608-2616.

300. Haugaa KH, Amlie JP, Berge KE, Leren TP, Smiseth OA, Edvardsen T. Transmural differences in myocardial contraction in long-QT syndrome: mechanical consequences of ion channel dysfunction. Circulation 2010;122:1355-1363.

301. Edvardsen T, Aakhus S, Endresen K, Bjomerheim R, Smiseth OA, Ihlen H. Acute regional myocardial ischemia identified by 2-dimensional multiregion tissue Doppler imaging technique. J Am Soc Echocardiogr 2000;13:986-994.

302. Roes SD, Mollema SA, Lamb HJ, van der Wall EE, de Roos A, Bax JJ. Validation of echocardiographic two-dimensional speckle tracking longitudinal strain imaging for viability assessment in patients with chronic ischemic left ventricular dysfunction and comparison with contrast-enhanced magnetic resonance imaging. Am J Cardiol 2009;104:312-317.

303. Shin SH, Suh YJ, Baek YS, Lee MJ, Park SD, Kwon SW, et al. Impact of area strain by 3D speckle tracking on clinical outcome in patients after acute myocardial infarction. Echocardiography 2016;33:1854-1859.

304. Ozawa K, Funabashi N, Kamata T, Kobayashi Y. Inter- and intraobserver consistency in LV myocardial strain measurement using a novel multi-layer technique in patients with severe aortic stenosis and preserved LV ejection fraction. Int J Cardiol 2016;228:687-693.

305. Ejlersen JA, Poulsen SH, Mortensen J, May O. Diagnostic value of layer-specific global longitudinal strain during adenosine stress in patients suspected of coronary artery disease. Int J Cardiovasc Imaging 2016.

306. Amundsen BH, Helle-Valle T, Edvardsen T, Torp H, Crosby J, Lyseggen E, et al. Noninvasive myocardial strain measurement by speckle tracking echocardiography: validation against sonomicrometry and tagged magnetic resonance imaging. J Am Coll Cardiol 2006;47:789-793.

307. Korinek J, Wang J, Sengupta PP, Miyazaki C, Kjaergaard J, McMahon E, et al. Two-dimensional strain--a Doppler-independent ultrasound method for quantitation of regional deformation: validation in vitro and in vivo. J Am Soc Echocardiogr 2005;18:1247-1253.

308. Toyoda T, Baba H, Akasaka T, Akiyama M, Neishi Y, Tomita J, et al. Assessment of regional myocardial strain by a novel automated tracking system from digital image files. J Am Soc Echocardiogr 2004;17:1234-1238.

309. Notomi Y, Lysyansky P, Setser RM, Shiota T, Popovic ZB, Martin-Miklovic MG, et al. Measurement of ventricular torsion by two-dimensional ultrasound speckle tracking imaging. J Am Coll Cardiol 2005;45:2034-2041.

310. Cho GY, Chan J, Leano R, Strudwick M, Marwick TH. Comparison of two-dimensional speckle and tissue velocity based strain and validation with harmonic phase magnetic resonance imaging. Am J Cardiol 2006;97:1661-1666.

311. Costa SP, Beaver TA, Rollor JL, Vanichakarn P, Magnus PC, Palac RT. Quantification of the Variability Associated with Repeat Measurements of Left Ventricular Two-Dimensional Global Longitudinal Strain in a Real-World Setting. J Am Soc Echocardiogr 2013.

312. Sun JP, Lee AP, Wu C, Lam YY, Hung MJ, Chen L, et al. Quantification of left ventricular regional myocardial function using two-dimensional speckle tracking echocardiography in healthy volunteers--a multi-center study. Int J Cardiol 2013;167:495-501.

313. Marwick TH, Leano RL, Brown J, Sun JP, Hoffmann R, Lysyansky P, et al. Myocardial strain measurement with 2-dimensional speckle-tracking echocardiography: definition of normal range. JACC Cardiovasc Imaging 2009;2:80-84.

314. Cheng S, Larson MG, McCabe EL, Osypiuk E, Lehman BT, Stanchev P, et al. Reproducibility of speckle-tracking-based strain measures of left ventricular function in a community-based study. J Am Soc Echocardiogr 2013;26:1258-1266.e2.

315. Negishi T, Negishi K, Thavendiranathan P, Cho GY, Popescu BA, Vinereanu D, et al. Effect of Experience and Training on the Concordance and Precision of Strain Measurements. JACC Cardiovasc Imaging 2016.

316. Nagueh SF, Appleton CP, Gillebert TC, Marino PN, Oh JK, Smiseth OA, et al. Recommendations for the evaluation of left ventricular diastolic function by echocardiography. Eur J Echocardiogr 2009;10:165-193.

317. Rudski LG, Lai WW, Afilalo J, Hua L, Handschumacher MD, Chandrasekaran K, et al. Guidelines for the echocardiographic assessment of the right heart in adults: a report from the American Society of Echocardiography endorsed by the European Association of Echocardiography, a registered branch of the European Society of Cardiology, and the Canadian Society of Echocardiography. J Am Soc Echocardiogr 2010;23:685-713; quiz 786-8.

318. Galderisi M, Henein MY, D'hooge J, Sicari R, Badano LP, Zamorano JL, et al. Recommendations of the European Association of Echocardiography: how to use echo-Doppler in clinical trials: different modalities for different purposes. Eur J Echocardiogr 2011;12:339-353.

319. Lang RM, Badano LP, Mor-Avi V, Afilalo J, Armstrong A, Ernande L, et al. Recommendations for cardiac chamber quantification by echocardiography in adults: an update from the American Society of Echocardiography and the European Association of Cardiovascular Imaging. Eur Heart J Cardiovasc Imaging 2015;16:233-270.

320. Paulus WJ, Tschope C, Sanderson JE, Rusconi C, Flachskampf FA, Rademakers FE, et al. How to diagnose diastolic heart failure: a consensus statement on the diagnosis of heart failure with normal left ventricular ejection fraction by the Heart Failure and Echocardiography Associations of the European Society of Cardiology. Eur Heart J 2007;28:2539-2550.

321. Kind T, Mauritz GJ, Marcus JT, van de Veerdonk M, Westerhof N, Vonk-Noordegraaf A. Right ventricular ejection fraction is better reflected by transverse rather than longitudinal wall motion in pulmonary hypertension. J Cardiovasc Magn Reson 2010;12:35-429X-12-35.

322. Kukulski T, Hubbert L, Arnold M, Wranne B, Hatle L, Sutherland GR. Normal regional right ventricular function and its change with age: a Doppler myocardial imaging study. J Am Soc Echocardiogr 2000;13:194-204.

323. Lindqvist P, Waldenstrom A, Henein M, Morner S, Kazzam E. Regional and global right ventricular function in healthy individuals aged 20-90 years: a pulsed Doppler tissue imaging study: Umea General Population Heart Study. Echocardiography 2005;22:305-314.

324. Jazbutyte V, Stumpner J, Redel A, Lorenzen JM, Roewer N, Thum T, et al. Aromatase inhibition attenuates desflurane-induced preconditioning against acute myocardial infarction in male mouse heart in vivo. PLoS One 2012;7:e42032.

325. Zhao Z, Wang H, Jessup JA, Lindsey SH, Chappell MC, Groban L. Role of estrogen in diastolic dysfunction. Am J Physiol Heart Circ Physiol 2014;306:H628-40.

326. Skytta T, Tuohinen S, Virtanen V, Raatikainen P, Kellokumpu-Lehtinen PL. The concurrent use of aromatase inhibitors and radiotherapy induces echocardiographic changes in patients with breast cancer. Anticancer Res 2015;35:1559-1566.

327. Azria D, Larbouret C, Cunat S, Ozsahin M, Gourgou S, Martineau P, et al. Letrozole sensitizes breast cancer cells to ionizing radiation. Breast Cancer Res 2005;7:R156-63.

328. Evans ES, Prosnitz RG, Yu X, Zhou SM, Hollis DR, Wong TZ, et al. Impact of patient-specific factors, irradiated left ventricular volume, and treatment set-up errors on the development of myocardial perfusion defects after radiation therapy for left-sided breast cancer. Int J Radiat Oncol Biol Phys 2006;66:1125-1134.

329. Hoff CM, Grau C, Overgaard J. Effect of smoking on oxygen delivery and outcome in patients treated with radiotherapy for head and neck squamous cell carcinoma--a prospective study. Radiother Oncol 2012;103:38-44.

330. Overgaard J. Sensitization of hypoxic tumour cells--clinical experience. Int J Radiat Biol 1989;56:801-811.

331. Fan S, Ni X, Wang J, Zhang Y, Tao S, Chen M, et al. Low Triiodothyronine Syndrome in Patients With Radiation Enteritis: Risk Factors and Clinical Outcomes an Observational Study. Medicine (Baltimore) 2016;95:e2640.

332. Weltman NY, Ojamaa K, Schlenker EH, Chen YF, Zucchi R, Saba A, et al. Low-dose T(3) replacement restores depressed cardiac T(3) levels, preserves coronary microvasculature and attenuates cardiac dysfunction in experimental diabetes mellitus. Mol Med 2014;20:302-312.

333. Chen YF, Weltman NY, Li X, Youmans S, Krause D, Gerdes AM. Improvement of left ventricular remodeling after myocardial infarction with eight weeks L-thyroxine treatment in rats. J Transl Med 2013;11:40-5876-11-40.

334. Pantos C, Mourouzis I, Markakis K, Tsagoulis N, Panagiotou M, Cokkinos DV. Long-term thyroid hormone administration reshapes left ventricular chamber and improves cardiac function after myocardial infarction in rats. Basic Res Cardiol 2008;103:308-318.

335. Ward WF, Lin PJ, Wong PS, Behnia R, Jalali N. Radiation pneumonitis in rats and its modification by the angiotensin-converting enzyme inhibitor captopril evaluated by high-resolution computed tomography. Radiat Res 1993;135:81-87.

336. Ahmed AN, Blonde K, Hackam D, Iansavichene A, Mrkobrada M. Prognostic significance of elevated troponin in non-cardiac hospitalized patients: a systematic review and meta-analysis. Ann Med 2014;46:653-663.

337. Ghio S, Guazzi M, Scardovi AB, Klersy C, Clemenza F, Carluccio E, et al. Different correlates but similar prognostic implications for right ventricular dysfunction in heart failure patients with reduced or preserved ejection fraction. Eur J Heart Fail 2016.

338. Ghio S, Recusani F, Klersy C, Sebastiani R, Laudisa ML, Campana C, et al. Prognostic usefulness of the tricuspid annular plane systolic excursion in patients with congestive heart failure secondary to idiopathic or ischemic dilated cardiomyopathy. Am J Cardiol 2000;85:837-842.

339. Bodez D, Ternacle J, Guellich A, Galat A, Lim P, Radu C, et al. Prognostic value of right ventricular systolic function in cardiac amyloidosis. Amyloid 2016;23:158-167.

340. Schwartz LA, Rozenbaum Z, Ghantous E, Kramarz J, Biner S, Ghermezi M, et al. Impact of Right Ventricular Dysfunction and Tricuspid Regurgitation on Outcomes in

Patients Undergoing Transcatheter Aortic Valve Replacement. J Am Soc Echocardiogr 2016.

341. Paczynska M, Sobieraj P, Burzynski L, Kostrubiec M, Wisniewska M, Bienias P, et al. Tricuspid annulus plane systolic excursion (TAPSE) has superior predictive value compared to right ventricular to left ventricular ratio in normotensive patients with acute pulmonary embolism. Arch Med Sci 2016;12:1008-1014.

342. Baggen VJ, Driessen MM, Post MC, van Dijk AP, Roos-Hesselink JW, van den Bosch AE, et al. Echocardiographic findings associated with mortality ortransplant in patients with pulmonary arterial hypertension:A systematic review and meta-analysis. Neth Heart J 2016;24:374-389.

343. Choudhry MW, Homsi M, Mastouri R, Feigenbaum H, Sawada SG. Prevalence and Prognostic Value of Right Ventricular Systolic Dysfunction in Patients With Constrictive Pericarditis Who Underwent Pericardiectomy. Am J Cardiol 2015;116:469-473.

344. Forfia PR, Fisher MR, Mathai SC, Housten-Harris T, Hemnes AR, Borlaug BA, et al. Tricuspid annular displacement predicts survival in pulmonary hypertension. Am J Respir Crit Care Med 2006;174:1034-1041.

345. de Meester de Ravenstein C, Bouzin C, Lazam S, Boulif J, Amzulescu M, Melchior J, et al. Histological Validation of measurement of diffuse interstitial myocardial fibrosis by myocardial extravascular volume fraction from Modified Look-Locker imaging (MOLLI) T1 mapping at 3 T. J Cardiovasc Magn Reson 2015;17:48-015-0150-0.

346. Iles LM, Ellims AH, Llewellyn H, Hare JL, Kaye DM, McLean CA, et al. Histological validation of cardiac magnetic resonance analysis of regional and diffuse interstitial myocardial fibrosis. Eur Heart J Cardiovasc Imaging 2015;16:14-22.

347. Zeng M, Zhang N, He Y, Wen Z, Wang Z, Zhao Y, et al. Histological validation of cardiac magnetic resonance T1 mapping for detecting diffuse myocardial fibrosis in diabetic rabbits. J Magn Reson Imaging 2016.

348. Lepojarvi ES, Piira OP, Paakko E, Lammentausta E, Risteli J, Miettinen JA, et al. Serum PINP, PIIINP, galectin-3, and ST2 as surrogates of myocardial fibrosis and echocardiographic left venticular diastolic filling properties. Front Physiol 2015;6:200.

349. Munch J, Avanesov M, Bannas P, Saring D, Kramer E, Mearini G, et al. Serum Matrix Metalloproteinases as Quantitative Biomarkers for Myocardial Fibrosis and Sudden Cardiac Death Risk Stratification in Patients With Hypertrophic Cardiomyopathy. J Card Fail 2016.

ORIGINAL COMMUNICATIONS

Anticancer Research, 35:2141-2147 © 2015, reprinted with permission from International Institute of Anticancer Research (**I**).

International Journal of Cardiovascular Imaging, 32:767-76 ©2016, reprinted with permission from Springer Science and Business Media (**II**).

Echocardiography, 34:191-198 © 2017, reprinted with permission from Springer Science and Business Media (**III**).

International Journal of Cardiovascular Imaging 33:463-472 © 2016, reprinted with permission from Springer Science and Business Media (**IV**).

Early Effects of Adjuvant Breast Cancer Radiotherapy on Right Ventricular Systolic and Diastolic Function

SUVI SIRKKU TUOHINEN[1*], TANJA SKYTTÄ[2*], VESA VIRTANEN[1], TIINA LUUKKAALA[3], PIRKKO-LIISA KELLOKUMPU-LEHTINEN[2] and PEKKA RAATIKAINEN[4]

[1]*Heart Center Co., Tampere University Hospital and School of Medicine, University of Tampere, Tampere, Finland;*
[2]*Department of Oncology, Tampere University Hospital and School of Medicine, University of Tampere, Tampere, Finland;*
[3]*Science Center Pirkanmaa Hospital District and School of Health Sciences, University of Tampere, Tampere, Finland;*
[4]*Department of Medicine, Central Finland Health Care District and University of Eastern Finland, Jyväskylä, Finland*

Abstract. *Aim: Reduced right ventricular (RV) systolic function correlates with poor prognosis in several heart diseases. The aim of this prospective single-Center study was to investigate whether conformal three-dimensional (3D) breast cancer radiotherapy impairs RV function. Patients and Methods: Forty-nine patients with early-stage left-sided breast cancer underwent comprehensive two-dimensional (2D) echocardiography before and after radiotherapy. RV function was evaluated with tricuspid annular plane systolic excursion (TAPSE), pulsed tissue Doppler peak velocity at the lateral RV wall (S') and RV and venous flow analysis. Results: Radiotherapy reduced TAPSE from 24.5±4.0 mm to 22.4±3.9 mm (p<0.001), S' from 12.7±3.1 m/s to 12.2±2.7 m/s (p=0.11) and pulmonary flow velocity time integral (VTI) from 16.6±3.1 cm to 15.9±2.3 cm (p=0.07), respectively. These changes were unrelated to changes in LV function. Conclusion: Modern radiotherapy reduced RV systolic function. As a readily-available and sensitive measurement, TAPSE is as a practical tool for detection of radiotherapy-induced cardiac changes.*

Breast cancer is the most common cancer in women (1). Improved diagnostics and adjuvant therapies have increased breast cancer survival rates (2). On the other hand, cardiac exposure from adjuvant radiotherapy (RT) has been shown to cause adverse cardiovascular effects. The late sequel includes left ventricular (LV) dysfunction, valvular heart disease and coronary artery disease (3-6). It is important for cardiologists and oncologists to recognize these adverse effects and find means to limit late co-morbidities.

Several investigators have demonstrated that the reduction of right ventricular (RV) systolic performance correlates with poor prognosis across a broad spectrum of diseases (7-9). Despite the important prognostic role of RV function, no prior study has systematically evaluated the effects of breast cancer RT on RV function. The aim of this prospective single-Center study was to investigate whether modern conformal three-dimensional (3D) breast cancer RT impairs RV systolic and diastolic function in the early phase.

Patients and Methods

Patient selection. Forty-nine eligible female patients with an early left-sided breast cancer who received postoperative adjuvant conformal RT without concomitant chemotherapy were included in this single-Center, prospective study. The study was conducted from July 2011 to February 2013. The exclusion criteria were age under 18 years or over 80 years, other malignancy, pregnancy or breast feeding, acute myocardial infarction within 6 months, symptomatic heart failure (NYHA 3-4), dialysis, permanent anti-coagulation and severe psychiatric disorder. To optimize echocardiography image quality, patients with atrial fibrillation, left bundle branch block (LBBB), pacemaker therapy and severe lung disease were excluded. The institutional board of ethics approved the protocol and all participants signed informed consent before enrollment in the study.

Radiotherapy. All patients underwent 3D computer tomography (CT)-based treatment planning (Philips Big Bore CT; Philips Medical Systems, Madison, WI, USA) in a supine position on a

[*]These authors contributed equally to this study.

Correspondence to: Suvi Tuohinen, MD, Heart Hospital, Tampere University Hospital, Finland, PO Box 2000, 33521 Tampere, Finland. Tel: +358 331169580, Fax: +358 331164157, Mob: +358 440353561, e-mail: suvi.tuohinen@sydansairaala.fi

Key Words: Radiotherapy, breast cancer, right ventricle, TAPSE.

Table I. *Radiation doses to the different cardiac structures (N=49)**

	Mean±SD Gy†	Max±SD Gy‡
Whole heart	3.27±1.53	46.17±9.09
Left ventricle	5.41±3.03	44.44±9.52
LAD	20.35±10.63	41.87±13.15
Right ventricle	3.03±2.03	32.06±15.57
Free wall of right ventricle	6.09±4.74	31.91±15.62
Ipsilateral pulmonary dose	8.03±2.01	50.65±5.14

Gy, Grey; LAD, region of the heart perfused by left anterior descending coronary artery; SD, standard deviation. *The radiation doses are derived from three-dimensional (3D) computed tomography (CT) planning pictures by manual tracing. †The average dose to the appointed volume. ‡The maximum point dose to the appointed volume.

breast board with 3 mm thick slices. The breath-hold technique was not used. Treatment planning and contouring were performed with an Eclipse v.10 system (Varian Medical Systems, Palo Alto, CA, USA). Heart contouring was performed by the same oncologist (TS). Treatment doses were either 50 Gy in 2 Gy fractions (standard) or 42.56 Gy in 2.66 Gy fractions (hypofractionated) according to the local guidelines. An additional boost of 16 Gy in 2 Gy fractions to the tumor bed was used if clinically indicated. Doses were calculated using the anisotropic analytical algorithm (AAA) (Figure 1) and dose-volume histograms (DVHs) for different structures were generated for each patient (Table I). The average treatment time was 36±10 days (20-70 days).

Echocardiographic examinations. A comprehensive echocardiography and electrocardiography (ECG) were performed at baseline and at the end of RT (1.0±2.8 days from the last radiation dose). All examinations were performed with the same cardiac ultrasound machine (Philips iE33; Philips, Bothell, WA, USA) and a 1-5 MHz matrix-array X5-1 transducer by the same cardiologist (SST). The interval between the baseline and control studies was 41±11 days. All images were acquired at rest with a simultaneous superimposed ECG. Subcostal imaging was performed in a supine position and other imaging was performed with the patient in the left lateral decubitus position. Doppler recordings were acquired at the end expiration during shallow breathing. Raw data were stored digitally for offline analysis with the Qlab software (Philips). RV systolic performance was measured in an apical four chamber view. Care was taken to identify the true apex and optimize the depth and the sector width of the image. Tricuspid annular plane systolic excursion (TAPSE) was measured with the M-mode cursor placed between the junction of the tricuspid valve and the RV lateral free wall annulus as total displacement of the tricuspid annulus from end-diastole to end-systole. Pulsed tissue Doppler was acquired from a point 1-1.5 cm apical from lateral tricuspid annulus (Figure 2). A 12-lead ECG was recorded at each visit.

Statistical analysis. Means and standard deviations were given for normally-distributed variables and medians and ranges for continuous variables with skewed distributions. Differences between measurements were tested by the paired samples *t*-test or by the Wilcoxon signed-rank test. The Spearman correlation was used to test the linear associations between variables. The associations between TAPSE and other variables were analyzed by the independent samples Mann-Whitney U test (continuous variables) or by the Fisher's exact test (categorical variables). All tests were two-sided and p values <0.05 were considered statistically significant. Statistical analyses were performed using the IBM SPSS (IBM Corp. Released 2010. IBM SPSS Statistics for Windows, Version 19.0. Armonk, NY: IBM Corp.) statistical software package (http://www-01.ibm.com/software/analytics/spss/).

Table II. *Baseline characteristics of the study cohort (N=49).*

Variable	Mean±SD
Age (years)	63±6
Systolic blood pressure (mmHg)*	145±19
Diastolic blood pressure (mmHg)	80±12
Height (cm)	164±6
Weight (kg)	73±13
Body mass index (kg/m^2)	27±4
Body surface area (m^2)	1.80±0.17
	N (%)
Smoking	
Previous	5 (10%)
Current	8 (16%)
Prior diagnosis†	
Hypertonia	17 (35%)
Diabetes mellitus	2 (4%)
Hypercholesterolemia	8 (16%)
Hypothyreosis	5 (10%)
Atherosclerosis	2 (4%)
Significant valvular abnormality	2 (4%)
Medical treatment	
Beta blocker	6 (12%)
Calcium channel blocker	2 (4%)
ACE inhibitors/ARBs	10 (20%)
Diuretics	5 (10%)
Thyroxin	5 (10%)
Nitrates	1 (2%)
Aspirin	3 (6%)
Statin	7 (14%)
Oral diabetes medication	2 (4%)

ACE, Angiotensin-converting enzyme; ARB, angiotensin II blocker. *Measured at first visit. †Defined as medication requiring disease state. The values are presented either as the mean±SD (standard deviation) or the number of cases and percentage in the present study population.

Results

General characteristics. The baseline characteristics of the patients are presented in Table II. The mean age of the population was 63 (range=49–79) years. The most common underlying diseases included hypertension (35%), hypercholesterolemia (16%), hypothyreosis (10%) and diabetes (4%). Twenty-two percent of the patients had no other diseases.

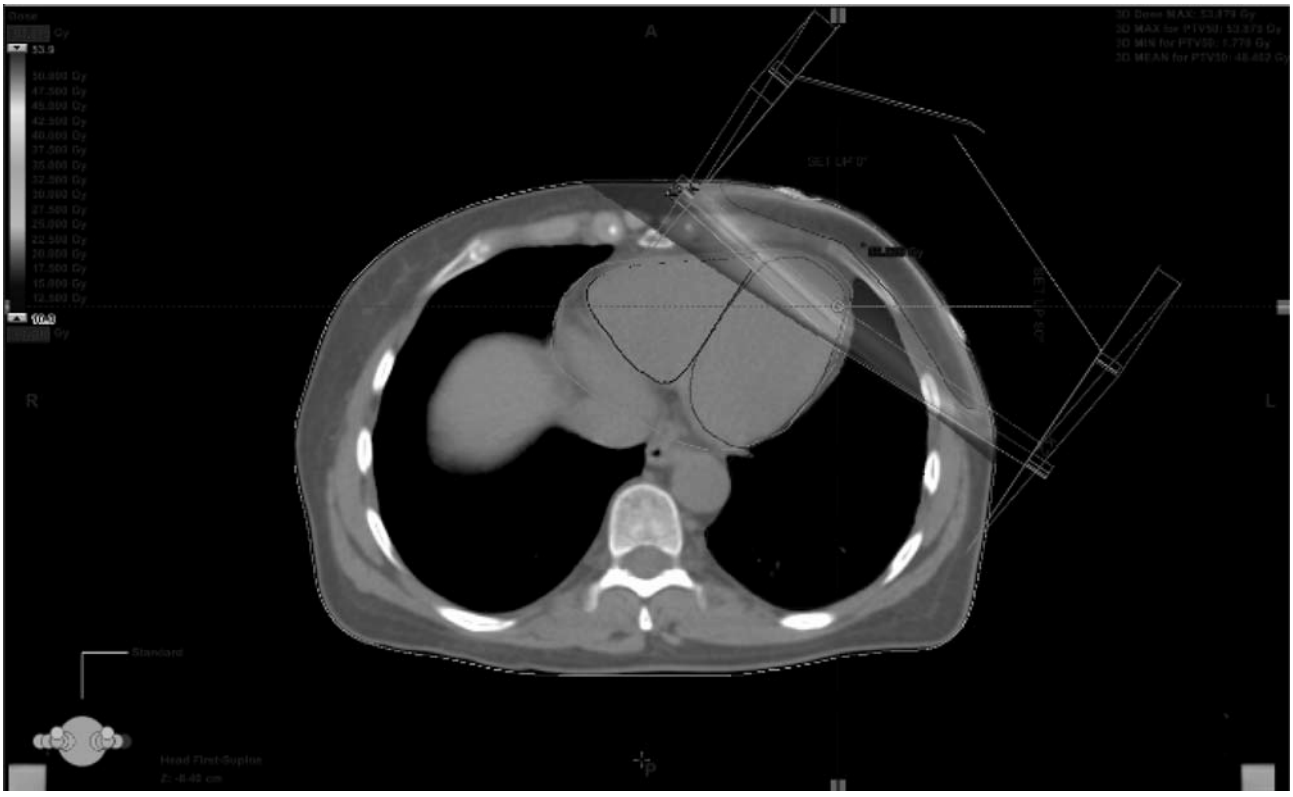

Figure 1. *Three-dimensional (3D) computed tomography (CT) treatment planning. Target volume is planned to cover remaining breast tissue. The dark area shows sites achieving more than 10 Grays with highest dose in the apex. Manually depicted heart contouring is also shown for the whole heart, left ventricle, right ventricle, right ventricle's free wall.*

RV echocardiographic measurements. RT caused significant changes in RV systolic function (Table III). TAPSE declined in 67% of the patients. The average reduction was 2.1±3.2 mm ($p<0.001$). A decrease of 4 mm or more was observed in 39% of the patients. There was no correlation between these changes and the cardiac or pulmonary radiation dose, smoking, ECG changes, body mass index (BMI) or underlying disease, other than hypothyreosis. The use of thyroxin ($p=0.03$) and diuretics ($p=0.03$) were associated with smaller TAPSE reduction. Likewise, the use of angiotensin-converting enzyme inhibitors (ACEIs) or angiotensin II receptor blockers (ARBs) tended to protect against TAPSE decline ($p=0.06$). The reduction in TAPSE was 1.0±4.0 mm and 2.4±3.0 mm ($p=0.22$) among patients using and not using ACEIs/ARBs, respectively.

In keeping with the reduction of TAPSE, the other RV systolic parameters showed a declining tendency, although statistical significance was not reached. S' declined from 12.7±3.1 to 12.2±2.7 ($p=0.11$) and pulmonary flow VTI decreased from 16.6±3.1 to 15.9±2.3 ($p=0.07$). Isovolumetric velocity (IVV) ($p=0.82$) and acceleration of the IVV did not change ($p=0.43$) (Table III). Neither TAPSE nor any other RV systolic parameter was related to LV systolic or diastolic changes.

The changes in the RV diastolic parameters were less obvious than the systolic parameters. The maximal diameter of the inferior *vena cava* was 15.7±4.1 mm at baseline and 14.8±3.5 mm after RT ($p=0.12$). Its respiratory variability remained unchanged. There were no significant changes in the tricuspid Ea and Ee' ratio, whereas the tricuspid inflow E wave showed a slight (48.5±8.5 cm/s *vs*. 45.6±8.4 cm/s) but not statistically significant reduction ($p=0.10$) (Table III).

Minor tricuspid and pulmonary regurgitation were observed in 94% and 69% of the patients, respectively. The regurgitation was hemodynamically insignificant in all patients and no patient had stenosis in the right-sided heart valves. There were no changes in tricuspid or pulmonary valve status between baseline and control examinations.

LV echocardiographic measurements. At baseline, LV dimensions and function were compatible with patient´s age and underlying disease profile in all participants. RT had no significant effect on LV systolic or diastolic function. However, both the interventricular septum (10.0±1.2 mm *vs*. 10.3±1.3 mm, $p=0.02$) and the posterior wall (9.7±1.0 mm *vs*. 10.3±1.2 mm, $p=0.01$) were slightly thicker after RT than at baseline (Table IV).

Table III. *Echocardiographic measurements of the right ventricle (N=49).*

	Baseline		Measurement after radiotherapy		*p*-Value
	Mean±SD	Median (range)	Mean±SD	Median (range)	
RV basal dimension (mm)	33.7±5.5	33.0 (24.0-44.0)	33.3±4.5	33.1 (22.1-44.4)	0.513
TAPSE (mm)	24.5±4.0	24 (16-33)	22.4±3.9	22 (16-33)	<0.001
S' (cm/s)	12.7±3.1	12.1 (8.9-22.2)	12.2±2.7	11.5 (8.9-20.7)	0.114
IVV (cm/s)	13.0±4.8	12.4 (4.9-29.3)	12.6±3.8	12.4 (4.6-21.9)	0.828
IVA (cm/s^2)	2.8±1.0	2.7 (1.0-5.1)	2.7±0.9	2.6 (1.3-5.1)	0.439
Pulmonary peak flow velocity (cm/s)	69.6±14.3	71.0 (46-101)	67.6±11.5	67.4 (47-92)	0.382
Pulmonary flow at (ms)	149.4±33.0	145 (71-239)	147.4±29.3	146 (85-204)	0.668
Pulmonary flow VTI (cm)	16.6±3.1	16.6 (10.9-24.4)	15.9±2.3	15.8 (11.5-22.4)	0.071
Tricuspid gradient (mmHg)*	21.6±5.8	22 (8-34; n=42)	21.2±5.0	22 (8-32; n=39)	0.430
Tricuspid inflow E velocity (cm/s)	48.5±8.7	48.3 (32.6-66.6)	45.6±8.4	45.2 (24.9-68.9)	0.096
Tricuspid inflow a velocity (cm/s)	38.3±8.0	37 (22.7-61.7)	37.5±8.0	37.6 (22.8-61.7)	0.547
Tricuspid inflow dt (ms)	236±73	235 (132-444)	257.5±65,8	252 (140-454)	0.212
Tricuspid Ea ratio	1.30±0.24	1.26 (0.88-1.85)	1.24±0.23	1.26 (0.75-1.81)	0.281
Tricuspid Ee' ratio	4.2±1.1	4.1 (2.5-7.3)	4.3±1.4	4.1 (2.1-8.0)	0.406
IVC maximal diameter (mm)	15.7±4.1	15.9 (1.6-25.9)	14.8±3.5	14.8 (8.8-22.5)	0.119
IVC respiration variability (%)†	62.8±15.2	60.2 (30.6-97.7)	63.8±15.5	62.8 (28.2-92.2)	0.670
Hepatic vein flow SD ratio‡	1.53±0.46	1.55 (0.9-2.8; n=36)	1.62±0.46	1.50 (0.7-3.9; n=35)	0.318

RV, Right ventricle; TAPSE, tricuspid annular plane systolic excursion; S' and IVV, systolic and isovolumetric velocity of pulsed tissue Doppler derived from the lateral basal RV free wall; IVA, acceleration of the IVV; at, acceleration time; VTI, velocity time integral; dt, declaration time; Ee' ratio, ratio between tricuspid inflow E-velocity and pulsed Doppler e' velocity derived from the RV basal free wall; IVC, inferior vena cava; Mean±SD, mean±standard deviation. *Measurable in 83%. †Inferior vena cava respiration variability tested with sniffing. ‡Hepatic vena flow SD ratio calculated as the ratio between the maximal velocities of systolic and diastolic components.

Six patients had moderate valvular abnormalities at the baseline echocardiography examination. Two of them had been diagnosed before (one with stenosis in aortic bioprosthesis and one with moderate mitral regurgitation) and 4 had a new diagnosis (one with moderate aortic stenosis, two with moderate mitral regurgitation and one with mild aortic regurgitation). There were no changes in aortic or mitral valve status between the baseline and control examinations.

ECG. Patients had sinus rhythm, narrow QRS complex and normal PQ and QT time in all ECG recordings. There were no signs of right atrial or ventricular abnormalities in any recordings. RT caused moderate T-wave alterations in 16 patients (33%). These changes did not correlate to the change in TAPSE.

Discussion

We demonstrated that RV systolic function was reduced in the early phase after modern conformal 3D left-sided breast cancer RT, despite a lack of changes in LV function. This novel finding indicates that measurement of RV function is a sensitive indicator of radiation-induced myocardial injury and an attractive tool for the follow-up of patients after RT.

RV function after RT. RV wall is thinner than the LV wall. Therefore, tissue swelling, reduced contractility and diastolic changes can be detected earlier in the RV than in the LV. In the current study, RT did not cause any significant changes in LV systolic or diastolic function, whereas the average decline in TAPSE was 2.1±3.2 mm and declined by 4 mm or more in 39% of the patients. The same tendency was found in the other RV systolic parameters. The changes in RV function were not accompanied by any significant changes in echocardiographic measures of pulmonary function and resistance. Moreover, there was no correlation between TAPSE decline and pulmonary radiation dose.

TAPSE and S' are measurements of RV longitudinal function, whereas IVV and VTI reflect rotational contractility and global RV function, respectively. Longitudinal contractility is the main determinant of RV systolic function (10, 11). The basal circumferential muscle fibers shared by the right and left ventricles initiate systolic contraction and cause rotational contraction (12). In elderly subjects and in diseases that overload the RV, the rotational contractility increases proportionally as the longitudinal contractility is reduced (14) and rotational contractility is increased (12-15). In our patients, the reductions in TAPSE, S' and pulmonary VTI were not accompanied by a compensatory increase in IVV. This indicates that TAPSE-alone may underestimate the RT-induced RV damage.

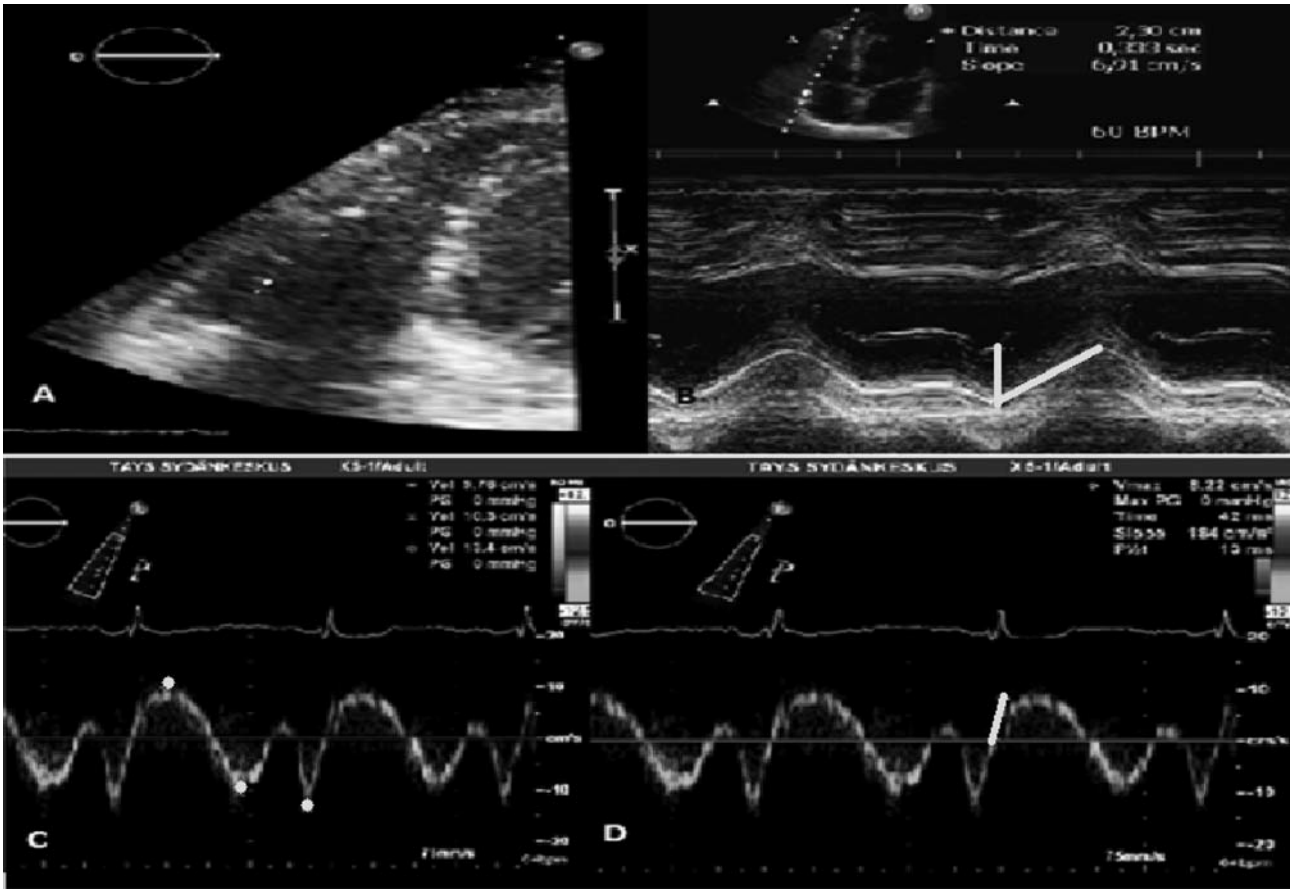

Figure 2. *Measurements of tricuspid annular plane systolic excursion (TAPSE) and pulsed tissue Doppler velocities at the lateral RV wall. A: Focused RV image with cursor placed in the junction of RV lateral wall and tricuspid annulus. B: TAPSE measurement with M-mode. C: Measurements of peak systolic velocity (S'), peak E' velocity and peak A' velocity, respectively. D: Measurements of IVV and IVA.*

Mechanism of the changes in RV function. The inflammatory reaction due to RT begins within hours (16, 17). The second or latent stage of radiation injury is characterized by reduced capillary density (17, 18). The complex fibrotic cascade is initiated as early as 2 weeks after the onset of RT (17, 19) and the earliest evidence of increased myocardial fibrosis has been observed within 40 days after a single radiation dose (16). Since our patients were exposed to RT for 4-5 weeks, all these mechanisms may contribute to the observed changes. Whether thyroxin or ACEI/ATR medication protects the RV from radiation-induced adverse effects remains to be established in larger clinical studies.

Limitations. Our study population was uniform in many ways, which reduced the confounding effects but also made extrapolation of the results to other groups difficult. Due to the small number of patients, a reliable multivariate analysis of related factors was not possible. Time-consuming magnetic resonance imaging and sophisticated 3D echocardiographic measurements were not used because the main idea was to determine whether the change in RV function could be measured with the tools we use in everyday practice.

Clinical implications of RV functional changes. The most important implication of this study was that the modern 3D conformal RT caused prominent changes in RV function in most of our patients. On the basis of the results of previous studies (3, 4), these changes may progress over time and clinically significant cardiac adverse events may emerge during long-term follow-up. These findings support the consensus statement recommending a comprehensive cardiac evaluation and a long-term follow-up of patients after breast cancer RT (20). According to our data, TAPSE is a more sensitive tool for the detection of the radiation-induced early myocardial deterioration than conventional LV measurements.

The result of this and prior studies imply that even small radiation doses may induce myocardial changes (21). In the

Table IV. *Echocardiographic measurements of the left ventricle.*

	Baseline		Measurement after radiotherapy		*p*-Value
	Mean±SD	Median (Range)	Mean±SD	Median (Range)	
LVEDD (mm)	45.4±4.1	45 (34.8-57.1)	44.7±4.1	45.2 (35.0-53.1)	0.084
LVESD (mm)	30.3±3.4	30.6 (18.9-40.0)	30.1±3.8	30.7 (19.0-36.7)	0.983
IVS (mm)	10.0±1.2	10.0 (8.0-12.8)	10.3±1.3	10.0 (8.0-13.0)	0.020
PW (mm)	9.7±1.0	10.0 (7.3-11.3)	10.3±1.2	10.0 (7.3-13.0)	0.011
LVEF (%)	62.2±5.0	62 (52-78)	61.5±5.2	62 (52-73)	0.473
Mitral inflow E (cm/s)	70±12	70 (47-102)	68±13	66 (39-109)	0.138
Mitral inflow a (cm/s)	77±19	74 (38-121)	75±14	77 (46-109)	0.128
Mitral inflow Ea-ratio	0.95±0.26	0.93 (0.56-1.78)	0.94±0.26	0.86 (0.59-1.67)	0.792
IVRT	104±26	103 (58-187)	109±21	106 (77-155)	0.283
Ee' ratio	9.0±2.6	8.7 (5.7-16.7)	8.8±2.1	8.5 (5.7-16.6)	0.554
LAVI (ml/m^2)	32.2±8.8	32.2 (16.7-56.3)	31.9±8.8	31.1 (13.7-53.2)	0.622
Pulmonary vein flow SD ratio	1.3±0.2	1.3 (0.8-1.8)	1.3±0.2	1.3 (0.7-1.8)	0.699

LVEDD, Left ventricular end diastolic diameter; LVESD, left ventricular end systolic diameter; IVS, interventricular septum; PW, posterior wall; LVEF, left ventricular ejection fraction; IVRT, isovolumetric relaxation time; Ee' ratio, ratio between mitral inflow E-velocity, and averaged pulsed Doppler e' velocity derived from septal, lateral, anterior and inferior walls; LAVI, left atrial volume indexed to the patient's body surface area; Pulmonary vein flow SD ratio, ratio between systolic and diastolic peak velocities; Mean±SD, mean±standard deviation.

present study, the RV systolic function was impaired, although the mean dose to the RV free wall in our study group was only 6.09±4.74 Gy. Hence, it is important to use techniques that reduce cardiac radiation exposure, *e.g.* respiratory gating and breath-hold techniques.

Conclusion

Right ventricular systolic function is impaired after breast cancer adjuvant RT. TAPSE is a sensitive and reliable marker of early myocardial injury and can be used as a practical tool to identify patients who would benefit the most from a longterm follow-up.

Acknowledgements

The Authors thank research nurses Virpi Räsänen, Hanna Näppilä and Emmi Vettenranta for their expert assistance during the study. This study was supported by the Pirkanmaa Hospital District, Seppo Nieminen Fund (grant 150613), by Paavo and Eila Salonen Legacy, by Ida Montin Fund and by Finnish Medical Foundation.

References

1 Ferlay J, Shin H, Bray F, Forman D, Mathers C and Parkin D: Cancer Incidence and Mortality Worldwide: IARC CancerBase 2010-last update, GLOBOCAN 2008 v1.2.No. 10 (Internet) [Homepage of International Agency for Research on Cancer], [Online].

2 Early Breast Cancer Trialists' Collaborative Group (EBCTCG), Darby S, McGale P, Correa C, Taylor C, Arriagada R, Clarke M, Cutter D, Davies C, Ewertz M, Godwin J, Gray R, Pierce L, Whelan T, Wang Y and Peto R: Effect of radiotherapy after breast-conserving surgery on 10-year recurrence and 15-year breast cancer death: meta-analysis of individual patient data for 10,801 women in 17 randomised trials. Lancet *378*: 1707-1716, 2011.

3 Wethal T, Lund MB, Edvardsen T, Fossa SD, Pripp AH, Holte H, Kjekshus J and Fossa A: Valvular dysfunction and left ventricular changes in Hodgkin's lymphoma survivors. A longitudinal study. Br J Cancer *101*: 575-581, 2009.

4 Darby SC, Ewerts M, McGale P, Bennet AM, Blom-Goldman U, Brönnum D, Correa C, Cutter D, Gagliardi G, Gigante B, Jensen MB, Nisbet A, Peto R, Rahimi K, Taylor C and Hall P: Risk of ischemic heart disease in women after radiotherapy for breast cancer. N Engl J Med *368*: 987-98, 2013.

5 Adams MJ, Lipsitz SR, Colan SD, Tarbell NJ, Treves ST, Diller L, Greenbaum N, Mauch P and Lipshultz SE: Cardiovascular status in long-term survivors of Hodgkin's disease treated with chest radiotherapy. J Clin Oncol *22*: 3139-48, 2004

6 McGale P, Darby SC, Hall P, Adolfsson J, Bengtsson NO, Bennet AM, Fornander T, Gigante B, Jensen MB, Peto R, Rahimi K, Taylor CW and Ewertz M: Incidence of heart disease in 35,000 women treated with radiotherapy for breast cancer in Denmark and Sweden. Radiother Oncol *100*: 167-175, 2011.

7 Anavekar NS, Skali H, Bourgoun M, Ghali JK, Kober L, Maggioni AP, Mcmurray JJ, Velazquez E, Califf R, Pfeffer MA and Solomon SD: Usefulness of right ventricular fractional area change to predict death, heart failure, and stroke following myocardial infarction (from the VALIANT ECHO Study). Am J Cardiol *101*: 607-612, 2008.

8 Damy T, Kallvikbacka-Bennett A, Goode K, Khaleva O, Lewinter C, Hobkirk J, Nikitin NP, Dubois-Rande JL, Hittinger L, Clark AL and Cleland JG: Prevalence of, associations with, and prognostic value of tricuspid annular plane systolic excursion (TAPSE) among out-patients referred for the evaluation of heart failure. J Card Fail *18*: 216-225, 2012.

9 Forfia PR, Fisher MR, Mathai SC, Housten-Harris T, Hemnes AR, Borlaug BA, Chamera E, Corretti MC, Champion HC, Abraham TP, Girgis RE and Hassoun PM: Tricuspid annular displacement predicts survival in pulmonary hypertension. Am J Respir Crit Care Med *174*: 1034-1041, 2006.
10 Leather HA, Ama R, Missant C, Rex S, Rademakers FE and Wouters PF: Longitudinal but not circumferential deformation reflects global contractile function in the right ventricle with open pericardium. Am J Physiol Heart Circ Physiol *290*: 2369-75, 2006.
11 Rushmer RF, Crystal DK and Wagner C: The functional anatomy of ventricular contraction. Circ Res 1: 162-170, 1953.
12 Buckberg GD, Coghlan HC and Torrent-Guasp F: The structure and function of the helical heart and its buttress wrapping. V. Anatomic and physiologic considerations in the healthy and failing heart. Semin Thorac Cardiovasc Surg *13*: 358-385, 2001.
13 Kind T, Mauritz GJ, Marcus JT, Van De Veerdonk M, Westerhof N and Vonk-Noordegraaf A: Right ventricular ejection fraction is better reflected by transverse rather than longitudinal wall motion in pulmonary hypertension. J Cardiovasc Magn Reson *12*: 35, 429X-12-35, 2010.
14 Kukulski T, Hubbert L, Arnold M, Wranne B, Hatle L and Sutherland GR: Normal regional right ventricular function and its change with age: a Doppler myocardial imaging study. J Am Soc Echocardiogr *13*: 194-204, 2000.
15 Lindqvist P, Waldenstrom A, Henein M, Morner S and Kazzam E: Regional and global right ventricular function in healthy individuals aged 20-90 years: a pulsed Doppler tissue imaging study: Umea General Population Heart Study. Echocardiography *22*: 305-314, 2005.
16 Fajardo Lf and Stewart Jr: Experimental radiation-induced heart disease. I. Light microscopic studies. Am J Pathol *59*: 299-316, 1970.
17 Fajardo LF and Stewart JR: Pathogenesis of radiation-induced myocardial fibrosis. Lab Invest *29*: 244-257, 1973.
18 Yarom R, Harper IS, Wynchank S, Van Schalkwyk D, Madhoo J, Williams K, Salie R, Genade S and Lochner A: Effect of captopril on changes in rats' hearts induced by long-term irradiation. Radiat Res *133*: 187-197, 1993.
19 Yarnold J and Brotons MC: Pathogenetic mechanisms in radiation fibrosis. Radiother Oncol *97*: 149-161, 2010.
20 Lancellotti P, Nkomo VT, Badano LP, Bergler J, Bogaert J, Davin L, Cosyns B, Coucke P, Dulgheru R, Edvardsen T, Gaemperli O, Galderisi M, Griffin B, Heidenreich PA, Nieman K, Plana JC, Port SC, Scherrer-Crosbie M, Schwartz RG, Sebag IA, Voigt JU, Wann S and Yang PC, European Society Of Cardiology Working Groups On Nuclear Cardiology And Cardiac Computed Tomography And Cardiovascular Magnetic Resonance And The American Society Of Nuclear Cardiology, Society For Cardiovascular Magnetic Resonance: Expert consensus for multi-modality imaging evaluation of cardiovascular complications of radiotherapy in adults: a report from the European Association of Cardiovascular Imaging and the American Society of Echocardiography. Eur Heart J Cardiovasc Imaging *14*: 721-740, 2013.
21 Erven K, Jurcut R, Weltens C, Giusca S, Ector J, Wildiers H, Van Den Bogaert W and Voigt JU: Acute radiation effects on cardiac function detected by strain rate imaging in breast cancer patients. Int J Radiat Oncol Biol Phys *79*: 1444-1451, 2011.

Received January 9, 2015
Revised January 24, 2015
Accepted January 26, 2015

Int J Cardiovasc Imaging (2016) 32:767–776
DOI 10.1007/s10554-016-0837-9

ORIGINAL PAPER

Detection of radiotherapy-induced myocardial changes by ultrasound tissue characterisation in patients with breast cancer

Suvi Sirkku Tuohinen[1] · Tanja Skyttä[2] · Vesa Virtanen[1] · Marko Virtanen[1] · Tiina Luukkaala[3] · Pirkko-Liisa Kellokumpu-Lehtinen[2] · Pekka Raatikainen[4]

Received: 9 October 2015 / Accepted: 8 January 2016 / Published online: 12 January 2016
© Springer Science+Business Media Dordrecht 2016

Abstract Radiotherapy (RT) in the thoracic region is associated with an increased risk of late cardiovascular morbidity and mortality. Ultrasonic tissue characterisation (UTC) is a non-invasive method of identifying changes in myocardial tissue, such as increased fibrosis. The aim of this study was to assess whether UTC can detect early RT-induced myocardial alterations. Seventy-eight eligible patients with early stage breast cancer were evaluated before and immediately after RT. Twenty patients had right-sided and 58 left-sided breast cancer. None received chemotherapy. A comprehensive echocardiographic examination included 3D measurements and UTC of the right ventricular (RV) free wall, ventricular septum and left ventricular (LV) posterior wall. Integrated backscatter calibration was done for the pericardium (cpIBS) and LV cavity (ccIBS). RT for left-sided breast cancer was associated with increased echodensity in the UTC analysis. RV free wall and ventricular septum cpIBS increased from -15.0 ± 7.3 to -13.7 ± 7.9 dB ($p = 0.079$) and from -18.2 ± 5.1 to -16.0 ± 6.4 dB ($p = 0.002$), respectively. Likewise, ccIBS in the RV free wall increased from 20.4 ± 5.9 to 22.1 ± 5.6 dB ($p = 0.046$), and in the LV septum from 17.3 ± 5.2 to 19.8 ± 5.5 dB ($p < 0.001$). In 3D echocardiography, LV mass increased from 102 ± 18 to 107 ± 18 g ($p = 0.005$). Patients receiving RT for right-sided breast cancer did not display these changes. Left-sided RT increased myocardial echodensity, particularly in the structures receiving the highest radiation dose. Considering the progressive nature of the RT induced damage, these early changes may help us with individual risk stratification and serve as a tool for screening.

Keywords Ultrasound tissue characterization · Calibrated integrated backscatter · Breast cancer · Radiotherapy

Introduction

Breast cancer is the most common cancer in females [1]. Advances in diagnostics and treatment have reduced cancer mortality rates. Radiotherapy (RT) in the thoracic region is associated with an increased risk of late cardiovascular morbidity and mortality, which may reduce the treatment-related survival benefit [1–3]. Late radiotherapy-induced cardiac changes include coronary artery disease, left-sided valvular stenosis and regurgitation, disturbances in the conduction system and rarely constrictive pericarditis [1, 2, 4–6]. RT-induced myocardial injury results in fibrosis which has been shown to be related to congestive heart failure and arrhythmias [1, 2, 5, 7, 8]. In most cases these injuries become apparent after several years of latency [1, 2, 4–6], and the early detection of RT-induced myocardial changes is challenging.

Myocardial properties can be studied non-invasively by ultrasound tissue characterisation (UTC) [9–12]. When the

✉ Suvi Sirkku Tuohinen
suvi.tuohinen@sydansairaala.fi

[1] Heart Center Co., Tampere University Hospital and School of Medicine, University of Tampere, PO Box 2000, 33521 Tampere, Finland

[2] Department of Oncology, Tampere University Hospital and School of Medicine, University of Tampere, Tampere, Finland

[3] Science Center Pirkanmaa Hospital District and School of Health Sciences, University of Tampere, Tampere, Finland

[4] Department of Medicine, Central Finland Health Care District, University of Eastern Finland, Jyväskylä, Finland

ultrasound beam interacts with tissue components smaller than its wavelength, the signal is scattered and a part of it is directed back toward the probe (backscatter). The intensity of the backscattered signal reflects the acoustic properties of the myocardial tissue, which are related to the collagen content [9, 10, 12, 13]. Our aim was to study whether early myocardial changes after breast cancer RT could be detected by UTC.

Materials and methods

Patient selection

A total of 78 eligible female patients with early breast cancer were included in this single-center, prospective clinical study between July 2011 and November 2013. Fifty-eight of them had left-sided and 20 had right-sided breast cancer. All patients received adjuvant conformal three dimensional (3D) RT after breast cancer resection. None of the patients received cytostatic chemotherapy. The exclusion criteria were: age under 18 years or over 80 years, the presence of other malignancies, pregnancy or breast feeding, recent acute myocardial infarction (in the last 6 months), symptomatic heart failure (NYHA 3–4), dialysis, permanent anticoagulation and severe psychiatric disorders. To optimize echocardiography image quality, patients with atrial fibrillation, left bundle branch block, a permanent pacemaker and severe lung disease were also excluded. The institutional board of ethics approved the protocol and all participants signed informed consent before enrolment in the study.

Radiotherapy

All patients underwent 3D computed tomography (CT; Philips Big Bore City, Philips Medical Systems, Madison, Wisconsin, USA) in a supine position on a breast board with 3 mm-thick slices. Treatment planning and contouring were performed with the Eclipse v.10 system (Varian Medical Systems, Palo Alto, CA, USA). Heart contouring was performed for all patients by the same radiation oncologist (TS; Fig. 1). Treatment doses to the breast cancer region were either 50 Gray (Gy) in 2 Gy fractions (standard) or 42.56 Gy in 2.66 Gy fractions (hypofractionated), according to the local guidelines. An additional boost of 16 Gy in 2 Gy fractions to the tumor bed was used if clinically indicated. The course of treatment took 34 ± 10 days. Doses were calculated using the anisotropic analytical algorithm and dose-volume histograms for different structures were generated for each patient (Table 1).

Electrocardiography (ECG) and biochemical markers

A comprehensive echocardiography and ECG were performed at baseline and at the end of radiotherapy (1 ± 3.9 days from the last radiation dose). High sensitivity troponin T (hsTnt) and pro-B-type natriuretic peptide (proBNP) were measured at each visit.

Echocardiographic examinations

All echocardiographic examinations were performed with a commercially available cardiac ultrasound machine (Philips iE33 ultrasound system, Bothell, Washington, USA) and a 1–5 MHz matrix-array X5-1 transducer by the same cardiologist (SST). The time interval between the baseline and the control study was 39 ± 13 days. All images were acquired at rest with a simultaneous superimposed ECG. Subcostal imaging was performed in a supine position, and other imaging was performed with the patient in the left lateral decubitus position. Doppler recordings were acquired at the end of expiration. A 3D data set was collected as four-cycle full volume imaging.

For two-dimensional UTC analysis, a parasternal long axis view clip was obtained (Fig. 2). No lateral or time gain compensation was used. The raw data was stored in an external hard drive for offline analysis (Qlab Philips, Bothell, Washington, USA). The clip was freezed at the frame of mitral valve closure and all measurements were performed at this time point. A square (5×5 mm) of region of interest (ROI) was positioned strictly perpendicular to the ultrasound beam in the free wall of the right ventricle (RV), the septum, the posterior wall of the left ventricle (LV) and in the left ventricular outflow tract. A rectangular polygon ROI was positioned in the posterior pericardium. Each myocardial measurement area was carefully positioned to avoid areas with bright endocardial or epicardial specular reflections, as well as very bright or hypoechoic regions within the myocardium. The measurements were repeated three times. An average value was used for calculations. The ROIs were controlled at each measurement point and the positioning was adjusted if necessary. The myocardial backscatter values were calibrated to the cavity and to the pericardial value by subtracting. Integrated backscatter calibration to the cavity was marked as ccIBS and to the pericardium as cpIBS.

Reproducibility of the UTC data

Several methodological tests were executed for the UTC data (Table 2). The repeatability of the measurements was tested in 20 healthy volunteers. In each subject, four acquisitions were taken for offline analysis during the same

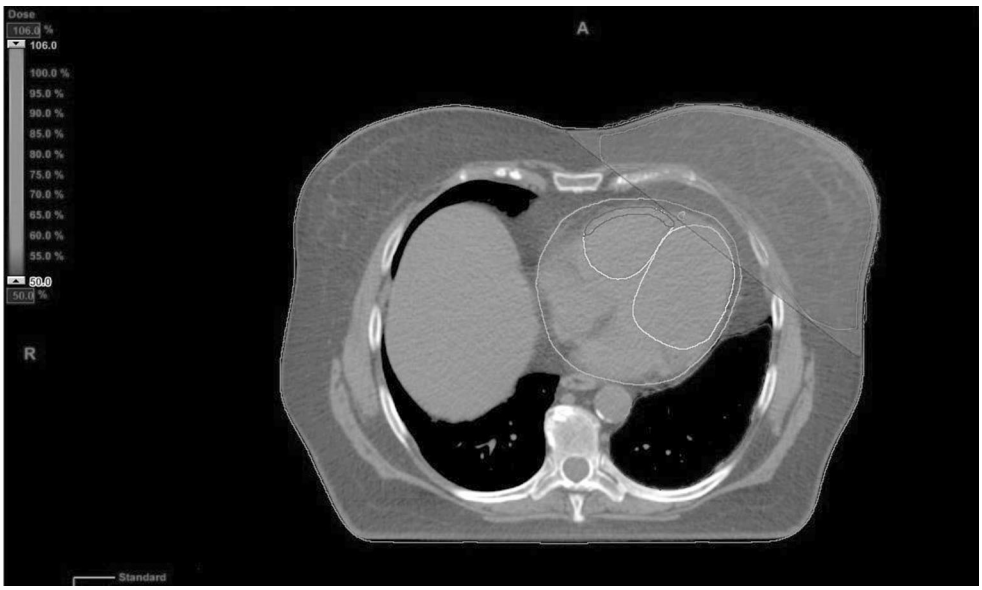

Fig. 1 A horizontal segment of the planning CT. Tangential photon fields are used in the treatment of the left breast. Fifty per cent of the total radiation dose is shown as radiation field. The cardiac structures are also contoured

Table 1 Radiation doses to the different cardiac structures

	Left sided breast cancer (n = 58) Median (range)	Right sided breast cancer (n = 20) Median (range)
Whole heart (Gy)	2.85 (0.68–6.36)	0.57 (0.34–4.83)
Left ventricle (Gy)	4.37 (0.80–12.25)	0.11 (0.05–3.30)
Percentage of the LV with 10 Gy radiation exposure	8.2 % (0–31.7 %)	0 % (0–0 %)
Percentage of the LV with 20 Gy radiation exposure	5.6 % (0–26.1 %)	0 % (0–0 %)
LAD (Gy)	18.77 (1.96–41.38)	0.12 (0.05–1.42)
Right ventricle (Gy)	2.85 (0.68–6.36)	0.45 (0.19–4.46)
Free wall of the right ventricle (Gy)	4.61 (1.20–21.21)	0.51 (0.14–4.03)
Ipsilateral pulmonary dose (Gy)	7.65 (4.57–12.69)	8.41 (5.02–12.4)

The radiation doses are derived from 3D CT planning pictures by manual contouring

Gy Gray, *LAD* left anterior descending coronary artery

day. Intraobserver variability was tested by a blinded reevaluation of the dataset at least 1 month after the initial measurements. An interobserver variability measurement was performed by another cardiologist with echocardiography expertise (MV).

Statistical analysis

Means and standard deviations were given for normally distributed variables, and medians and ranges for continuous variables with skewed distributions. The association between the UTC values and other variables was analysed by independent samples *t* test or by Mann–Whitney U test if variables were continuous. Categorical variables were analysed by the Pearson Chi square test or by Fisher's exact test if expected values were too small. Differences between the baseline and after RT values were tested by the paired samples *t* test or the Wilcoxon signed-rank test. Spearman correlation was used to test the linear associations between the continuous variables. UTC values were also dichotomised into decreased or increased values to describe change from baseline values to after radiotherapy measurements. Increased UTC values were explained by logistic regression analysis, entering all independent variables (age, BMI, mean dose to the heart and left anterior descending coronary artery region, and their percentage of over 45 and 20 Gy radiation exposure, mean RV dose and the exposure, mean dose to the RV free wall and their percentage of the exposures to more than 20 Gy, the mean lung radiation exposure) simultaneously into the multivariate mode. The reproducibility of the data was analysed with related samples using the Friedman's test Two-Way analysis of variance by rank. Intraobserver and interobserver

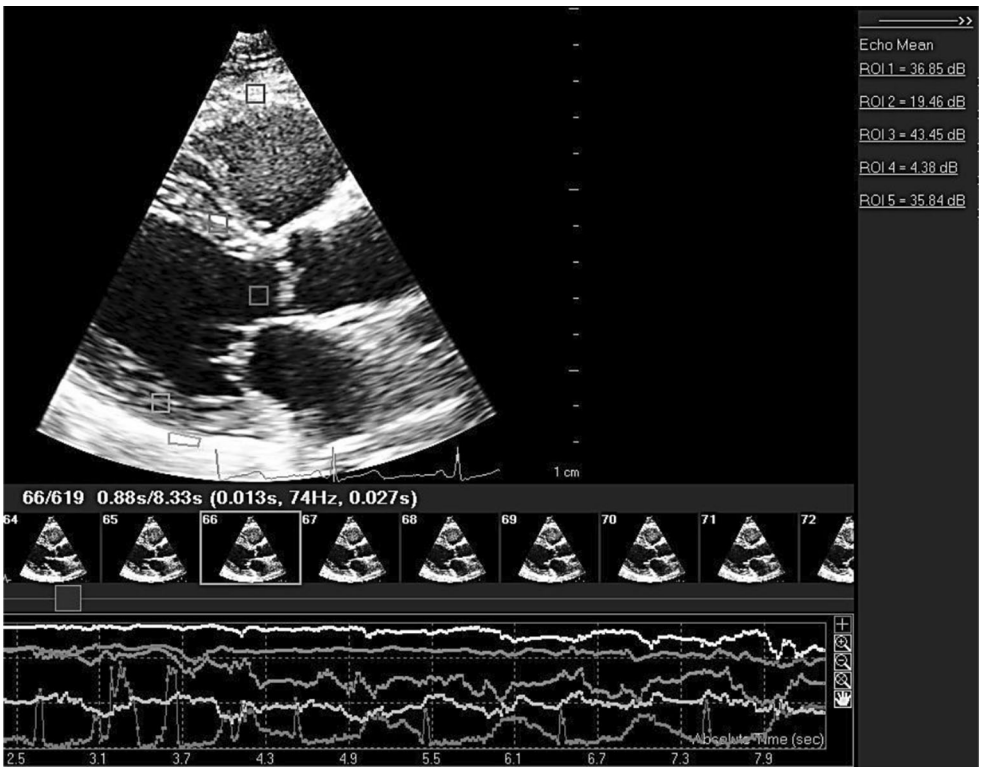

Fig. 2 The parasternal long axis clip is freezed at the end of diastole and scrolled to the frame where mitral valve closes. Region of interests (ROI) are set in septum, posterior wall, pericardium, left ventricular outflow tract and in the right ventricle's free wall. The respective values are on the right panel

Table 2 Validation measurements by intraclass correlation coefficients (ICC) with 95 % confidence intervals (CI)

	Test–retest ICC (95 % CI)	Intraobserver variability ICC (95 % CI)	Interobserver variability ICC (95 % CI)
Calibration for pericardium			
RV free wall	0.52 (0.32–0.75)	0.75 (0.47–0.89)	0.56 (0.17–0.80)
LV septum	0.80 (0.66–0.90)	0.89 (0.75–0.96)	0.88 (0.72–0.95)
LV posterior wall	0.65 (0.45–0.82)	0.94 (0.85–0.97)	0.77 (0.50–0.90)
Calibration for cavity			
RV free wall	0.59 (0.38–0.78)	0.57 (0.19–0.81)	0.52 (0.11–0.78)
LV septum	0.86 (0.76–0.94)	0.91 (0.79–0.97)	0.86 (0.68–0.94)
LV posterior wall	0.70 (0.51–0.85)	0.98 (0.94–0.99)	0.82 (0.60–0.92)

variability were tested by related samples Wilcoxon signed-rank test. All tests were two-sided and p values <0.05 were considered statistically significant. Statistical analyses were carried out with IBM SPSS Statistics for Windows, Version 20.0 Armonk, NY: IBM Corp. Released 2011.

Results

General characteristics

The mean age of the study group was 63 years (49–79 years). Body mass index (BMI) was over 25 cm/m^2 in 62 % of the patients, and 25 % of the patients were active or ex-smokers. The most common underlying diseases were hypertension (44 %), hypercholesterolemia (22 %), and hypothyroidism (13 %). Thirty-three patients (42 %) had no concurrent diseases other than breast cancer. The detailed baseline characteristics of the patients are shown in Table 3.

Ultrasound tissue characterisation

In the patients with left-sided breast cancer, RT increased the echodensity of the RV free wall and the ventricular septum. The pericardially calibrated integrated backscatter

Table 3 Baseline characteristics of the study cohort

Variable	Left sided breast cancer (n = 58)	Right sided breast cancer (n = 20)	*p* value
Age (years), mean ± SD	63 ± 7	63 ± 5	0.723
Systolic blood pressure (mmHg)[a], mean ± SD	145 ± 19	150 ± 20	0.291
Diastolic blood pressure (mmHg), mean ± SD	79 ± 12	79 ± 12	0.945
Height (cm), Md (IQR)	164 (158–167)	162 (158–167)	0.521
Weight (kg), Md (IQR)	69.5 (64–83)	70.5 (65–82)	0.977
Body mass index (kg/m^2), Md (IQR)	26.2 (24.1–30.0)	26.6 (24.7–30.0)	0.533
Smoking, n (%)			1.000
Previous	7 (12 %)	2 (10 %)	
Current	8 (14 %)	2 (10 %)	
Prior diagnosis[b], n (%)			
Hypertension	21 (36 %)	13 (65 %)	0.025
Diabetes mellitus	4 (7 %)	3 (15 %)	0.364
Hypercholesterolemia	13 (22 %)	4 (20 %)	1.000
Hypothyreosis	7 (12 %)	3 (15 %)	0.711
Coronary artery disease	2 (3 %)	1 (5 %)	1.000
Valvular disease	1 (2 %)	1 (5 %)	0.450
Medical treatment, n (%)			
Beta blocker	6 (10 %)	5 (25 %)	0.138
Calcium channel blocker	4 (7 %)	4 (20 %)	0.193
ACE inhibitors/ARBs	14 (24 %)	10 (50 %)	0.031
Diuretics	8 (14 %)	7 (35 %)	0.051
Thyroxin	7 (12 %)	3 (15 %)	0.711
Nitrates	1 (2 %)	0 (0 %)	1.000
Aspirin	6 (11 %)	3 (15 %)	0.689
Statin	11 (19 %)	4 (20 %)	1.000
Oral diabetes medication	4 (7 %)	3 (15 %)	0.364
Aromatase inhibitor	22 (38 %)	8 (40 %)	0.870
Tamoxifen	2 (3 %)	4 (20 %)	0.035

ACE angiotensin-converting enzyme, *ARB* angiotensin II blocker, *Sd* standard deviation, *Md* median, *IQR* interquartile range

[a] Measured at first visit

[b] Defined as medication requiring disease state. The values are presented either as the mean ± SD or the number of cases and percentage in the present study population

(cpIBS) of the RV free wall increased from a baseline value of −15.0 ± 7.3 dB to −13.7 ± 7.9 dB ($p = 0.079$) after RT, and the cavity calibrated IBS (ccIBS) from 20.4 ± 5.9 dB to 22.1 ± 5.6 dB ($p = 0.046$) (Table 4). The septal echodensity with pericardial and cavity calibration increased from −18.2 ± 5.1 dB to −16.0 ± 6.4 dB ($p = 0.002$) and from 17.3 ± 5.2 dB to 19.8 ± 5.5 dB ($p < 0.001$), respectively. RT did not cause any significant changes in the posterior LV echodensity.

A left-sided RT-induced increase in septal cpIBS and ccIBS values correlated with radiation doses to the corresponding cardiac structures. The septal cpIBS value correlated with the mean LAD dose ($\rho = 0.241$, $p = 0.042$), the mean whole heart dose ($\rho = 0.306$, $p = 0.009$), the mean RV dose ($\rho = 0.243$, $p = 0.040$), the mean RV free wall dose ($\rho = 0.246$, $p = 0.037$), and the mean LV dose ($\rho = 0.289$, $p = 0.014$). The septal ccIBS value correlated with the mean LV dose ($\rho = 0.251$, $p = 0.034$). Patient age was weakly associated with an increase in septal cpIBS ($\rho = 0.196$, $p = 0.099$) and ccIBS values ($\rho = 0.238$, $p = 0.044$). Concomitant diseases, ECG changes, hsTnt, proBNP, or medication were not associated with the changes in septal echodensity. A decrease in tricuspid annular plane systolic excursion (TAPSE) correlated with an increase in septal cpIBS ($p = 0.032$). None of the other conventional echocardiographic parameters had an association with changes in the UTC parameters.

A multivariate logistic regression analysis, in which all variables were entered simultaneously into the model, demonstrated an independent relationship between the increased septal cpIBS values and the percentage of the LV exposed to 20 Gy (OR 3.22 [95 % CI 1.05–9.88]). Also,

Table 4 Ultrasound tissue characterization values

Variable	Left-sided breast cancer			Right-sided breast cancer			p_2	p_3
	Baseline	After radiotherapy	p_1	Baseline	After radiotherapy	p_1		
Calibration to the pericardium								
RV free wall (dB)	−15.0 ± 7.3	−13.7 ± 7.9	0.079	−13.9 ± 7.6	−12.4 ± 5.31	0.380	0.562	0.493
LV septum (dB)	−18.2 ± 5.1	−16.0 ± 6.4	0.002	−19.6 ± 5.3	−18.3 ± 5.77	0.313	0.307	0.166
LV posterior wall (dB)	−25.6 ± 4.1	−25.4 ± 4.9	0.414	−25.5 ± 2.7	−25.9 ± 3.96	0.723	0.897	0.699
Calibration to the cavity								
RV free wall (dB)	20.4 ± 5.9	22.1 ± 5.6	0.046	21.1 ± 5.6	22.0 ± 4.0	0.398	0.674	0.910
LV septum (dB)	17.3 ± 5.2	19.8 ± 5.5	<0.001	15.4 ± 4.6	16.2 ± 5.0	0.225	0.157	0.012
LV posterior wall (dB)	9.9 ± 4.7	10.3 ± 4.1	0.487	9.5 ± 4.0	8.4 ± 4.2	0.130	0.700	0.072

Calibration is done by subtracting the myocardial value from pericardial and cavity values. p_1 = difference between baseline and after therapy distributions were tested by paired samples *t* test; p_2 = difference in baseline and p_3 = difference after radiotherapy between left- and right sided breast cancers were tested by independent samples *t* test

the mean lung dose reached statistical significance OR 1.69 (95 % CI 1.01–2.84). Data not shown.

Stable or increased septal ccIBS was independently associated with an increased percentage of the LV exposed to a 20 Gy (Mann–Whitney test $p = 0.017$) and a 10 Gy ($p = 0.009$) radiation dose. Likewise, stable or increasing septal ccIBS values were independently associated with the increased percentage of the LV with exposure to 20 Gy ($p = 0.029$) and 10 Gy ($p = 0.022$) radiation. The increase in the RV free wall cpIBS value was associated with decreasing TAPSE ($p = 0.045$) and with an increase in the mitral inflow declaration time (dt) ($p = 0.022$). In addition, diabetes was associated with a decrease in RV free wall cpIBS ($p = 0.015$). The increase in RV free wall echodensity did not depend on the radiation doses or other parameters.

In contrast to the remarkable changes caused by the adjuvant RT in patients with left-sided breast cancer, it did not cause any significant UCT changes in patients with right-sided breast cancer. Detailed characteristics of the UTC analysis are shown in Table 4.

Conventional echocardiographic measurements

Patients receiving adjuvant RT for left-sided breast cancer experienced minor changes in several conventional echocardiographic parameters (Table 5). The thickness of the septum increased from 10.0 ± 1.4 to 10.3 ± 1.5 mm ($p = 0.030$) and the LV posterior wall from 9.9 ± 1.3 to 10.3 ± 1.9 mm ($p = 0.071$), respectively. In 3D analysis, the LV volume decreased from 98 ± 18 to 94 ± 17 ml ($p = 0.016$) in diastole, and from 40 ± 8 to 38 ± 9 ml ($p = 0.028$) in systole. LV systolic volume decreased in 58 % of patients and diastolic volume in 61 %. LV mass increased from 102 ± 18 to 107 ± 18 g ($p = 0.005$) and an increase in LV mass was observed in 66 % of patients. LV systolic function remained unaffected during the RT. Among the right sided echocardiographic parameters, the only significant RT-induced change was that TAPSE decreased from 24.3 ± 4.0 to 22.3 ± 4.1 mm ($p < 0.001$). No valvular or pericardial changes were observed between the baseline and last echocardiographic examination.

In patients with right-sided breast cancer, most of the RT-induced changes in the conventional echocardiographic parameters were statistically insignificant (Table 5). There was a trend of increased LV wall thickness, but this did not reach statistical significance. However, the declaration time increased from 211 ± 42 to 243 ± 51 ms ($p = 0.015$).

Electrocardiogram

Left-sided RT caused minor ECG changes in 18 patients (31 %). The most typical changes were T-wave inversions in leads V1–4, and in some patients also in leads aVL and I. These changes were not accompanied by any symptoms. Right-sided breast cancer patients did not display RT-induced ECG changes (difference between groups $p = 0.006$).

Biochemical markers

In patients with adjuvant RT for left-sided breast cancer, hsTnt increased from a baseline value of 5.5 ± 2.4 ng/l to a maximum value of 6.1 ± 2.7 ng/l ($p = 0.006$). Twelve patients (17 %) experienced a rise from the basal value of over 30 %, and the highest measured hsTnt value was 15 ng/l. For the baseline, proBNP was 117 ± 143 ng/l and it increased to 149 ± 194 ng/l during RT ($p = 0.002$). The increase from the baseline was over 30 % in 31 patients (53 %).

Adjuvant RT caused no significant changes in biomarkers in patients with right-sided breast cancer. hsTnt was 6.6 ± 6.6 ng/l at the baseline and 6.7 ± 4.1 ng/l ($p = 0.948$) after RT. One patient experienced a rise over

Table 5 Basic echocardiographic measurements

Variable	Left-sided breast cancer (n = 58)			Right-sided breast cancer (n = 20)		
	Baseline	After radiotherapy	*p* value	Baseline	After radiotherapy	*p* value
LVEDD (mm)	45.3 ± 4.0	44.9 ± 3.7	0.188	43.8 ± 0.6	43.8 ± 3.9	0.896
LVEDS (mm)	30.5 ± 3.4	30.1 ± 3.5	0.645	29.7 ± 3.2	29.3 ± 3.4	0.641
IVS (mm)	10.0 ± 1.4	10.3 ± 1.5	**0.023**	10.2 ± 1.7	10.8 ± 1.9	0.018
PW (mm)	9.9 ± 1.3	10.3 ± 1.9	**0.016**	10.1 ± 1.1	10.6 ± 1.6	0.251
LVEDV (ml)	98 ± 18	94 ± 17	**0.018**	99 ± 28	95 ± 27	0.262
LVESV (ml)	40 ± 8	38 ± 9	**0.028**	39 ± 14	41 ± 12	0.246
Stroke volume (ml)	59 ± 12	58 ± 12	0.366	62 ± 21	57 ± 20	0.092
LVED mass (g)	102 ± 18	107 ± 18	**0.005**	104 ± 26	105 ± 26	0.843
LVEF (%)	61.2 ± 5.9	62.2 ± 6.4	0.525	60.6 ± 7.0	59.3 ± 5.6	0.075
Mitral inflow E (cm/s)	73 ± 15	70 ± 15	**0.040**	78 ± 19	72 ± 18	0.067
Mitral inflow a (cm/s)	78 ± 20	75 ± 15	0.114	78 ± 14	78 ± 21	0.968
Mitral inflow Ea-ratio	0.98 ± 0.28	0.97 ± 0.27	0.474	1.02 ± 0.30	0.97 ± 0.29	0.279
Mitral inflow dt[a] (ms)	236 ± 41	243 ± 41	0.291	211 ± 42	243 ± 51	**0.015**
IVRT (ms)	104 ± 22	110 ± 22	0.188	111 ± 22	111 ± 14	0.711
LV Ee' ratio	9.2 ± 2.7	8.9 ± 2.5	0.174	9.9 ± 2.5	10.0 ± 2.8	0.778
LAVI (ml/m^2)	33.2 ± 8.4	32.7 ± 7.8	0.806	32.1 ± 8.4	32.5 ± 4.8	0.733
RV basal dimension (mm)	34.2 ± 5.0	33.6 ± 4.5	0.527	34.3 ± 5.7	33.8 ± 5.8	0.936
TAPSE (mm)	24.3 ± 4.0	22.3 ± 4.1	**<0.001**	23.9 ± 5.4	22.5 ± 5.2	0.133
RV s' (cm/s)	12.2 ± 2.9	11.9 ± 2.6	0.139	12.8 ± 2.7	12.7 ± 2.7	0.421
TR gradient (mmHg)	22.8 ± 4.7	22.1 ± 3.8	0.173	24.5 ± 6.3	21.8 ± 6.3	0.071
RV Ee' ratio	4.2 ± 1.2	4.3 ± 1.3	0.124	4.2 ± 1.6	4.1 ± 1.3	0.356

LVEDD left ventricular end diastolic diameter, *LVESD* left ventricular end systolic diameter, *IVS* interventricular septum, *PW* posterior wall, *LVEDV* left ventricular end diastolic volume, *LVESV* left ventricular end systolic volume, *LVED mass* left ventricular end diastolic mass, *LVEF* left ventricular ejection fraction, *dt* declaration time, *IVRT* isovolumetric relaxation time, *LV Ee' ratio* ratio between mitral inflow E-velocity, and averaged pulsed Doppler e' velocity derived from septal, lateral, anterior and inferior walls, *LAVI* left atrial volume indexed to the patient's body surface area, *TAPSE* tricuspidal annular plane systolic excursion, *RV s'* pulse tissue Doppler systolic velocity derived from the right ventricles free wall, *TR gradient* maximal gradient derived from the tricuspidal regurgitation, *RV Ee' ratio* ratio between tricuspidal inflow E-velocity and the pulsed tissue Doppler e' velocity derived from the RV free wall

[a] There is a significant difference ($p = 0.025$) in baseline values between the groups of left and right sided breast cancer tested by Mann–Whitney U test. Statistical significant p values (<0.05) are bolded

30 % during the RT treatment course. ProBNP baseline and maximal values were 91 ± 42 and 89 ± 43 ng/l ($p = 0.645$). Two patients experienced a rise of over 30 % during the RT treatment course.

Discussion

In this study, we demonstrated for the first time that RT causes significant changes in the ultrasound characteristics of the myocardium. In light of the strong association with increased myocardial echodensity and histopathological changes such as scarring and fibrosis [9, 10, 14], our data indicate that UCT may be a feasible and sensitive non-invasive tool for the detection of cardiac damage early after RT.

Clinical implications

RT increased echodensity in the RV free wall and in the septum in patients with left-sided breast cancer, but there were no changes in the posterior parts of the heart and in patients with right-sided breast cancer. The results of previous UCT studies in patients with prior myocardial infarction, cardiomyopathy, and doxorubicin-induced myocardial alterations indicate that there is a strong association between histological changes (e.g., scarring, collagen content) and increased myocardial backscattering [9–11, 13]. Increased echodensity has also been found in patients with diabetes, thyroid dysfunction, iron overload and acute cardiac allograft rejection, despite no abnormalities in conventional echocardiographic parameters [14–17]. Moreover, RT has been

shown to increase collagen content in myocardial biopsies several years after the treatment course has finished [7].

Hence, our data may have important clinical implications for the detection of RT-induced early myocardial injury. RT is known to initiate a complex fibrotic process. The early phase is characterised by inflammatory tissue changes [2, 5, 8]. The earliest fibrotic tissue manifestations appear 40 days after the start of irradiation [8]. In our study, the control echocardiography was performed 34 ± 11 days after the first RT dose. We demonstrated that RV and septal echodensityincreased in more than 60 % of patients with left-sided breast cancer. Hence, although no myocardial biopsies were taken for histological examination in these otherwise healthy patients, it is possible that in some of them the development of RT-induced fibrosis had already started.

The 2D echocardiographic measurements demonstrated that myocardial wall thickness increased after RT. In 3D analysis, both systolic and diastolic volumes decreased with simultaneous increase of the myocardial mass. All of these changes could be a result of an initial inflammatory process, the early phase of fibrotic manifestations, or both. The concurrent changes in myocardial mass and increased values in UTC in combination are a strong indicator of RT-induced alterations in myocardial structures. Increases in RV and septal echodensity were also associated with a decrease in TAPSE. TAPSE is a reliable and reproducible RV systolic function parameter, which has been shown to be an early indicator of RT-induced myocardial changes [18]. Finally, the distribution of the UTC changes correlated with radiation doses to the different anatomical areas of the heart. Therefore, treatment planning and heart contouring are important for the prevention of late cardiac manifestations.

Radiotherapy-induced heart disease (RIHD) seems to be a slow process that produces clinical adverse sequelae years and decades after RT treatment [1, 2, 4, 5]. A non-invasive tool with a high specificity and sensitivity to identify early structural alterations, fibrosis, and collagen accumulation would be well suited for the risk stratification of patients after breast cancer RT. Our study introduces a new method for the early detection of RT-induced myocardial injury. The primary goal of our study was to show that even modern conformal 3D RT may cause detectable changes in the heart. Our findings thereby support the implementation of careful follow-up programmes for these patients, as recommended in a recent consensus statement [5]. Individual susceptibility to RT-induced injury varies from person to person. Hypertension, heart diseases, smoking, and the radiation volume and dose are known risk factors for RIHD, but there might be also other factors, such as the concurrent use of an aromatase inhibitor [1, 2, 4, 5, 19].

UTC could be a useful tool to identify individuals who are most vulnerable to developing complications after RT and who would benefit the most from a careful follow-up process. However, larger studies are needed to verify our preliminary findings, and a longer follow-up is required to clarify the long-term clinical impact of these findings.

Biochemical markers, ECG, and conventional echocardiographic parameters

Both hsTnt and proBNP increased after RT in patients with left-sided breast cancer, but not in those with right-sided breast cancer. Likewise, there were ECG changes only in patients with left-sided breast cancer. Even though none of these changes caused any immediate cardiac symptoms, the difference between the patients with left-sided and right-sided breast cancer is interesting. It can be speculated that these subtle changes may reflect the same process as the echocardiographic changes and indicate a high risk of late myocardial manifestations.

Technical viewpoints

UTC is unaffected by heart rate, preload, afterload and inotropic state of the heart [20], but ultrasound system settings influence IBS signal intensity [12]. A higher gain setting results in stronger returning signals. Therefore, the received values must be calibrated to measurements derived from an acoustically stable object. Rubber phantom, pericardia and ventricular cavities have been used for this purpose [11, 12]. We used both pericardial and cavity values for calibration. The calibration to the cavity seemed to be more reproducible, whereas interobsever variability was smaller with pericardial calibration. The calibrated values for the septum showed good reproducibility in repeated measurements and reanalysis of the previously acquired clips. The repeatability and interobserver variability of RV measurements with pericardial calibration was worse than with cavity calibration. Due to the attenuation of the ultrasound beam, the returning signal from the deeper parts of the heart, such as from the LV posterior wall, is weaker [14, 16, 21]. This resulted in the poor reproducibility of posterior wall values in our study.

Limitations of our study

The left-sided and right-sided breast cancer patient groups were of uneven size. Both groups were relatively small and further studies are needed to confirm our results. Previous studies have shown a strong correlation between tissue collagen content and integrated backscatter. In our study, a histological confirmation of these findings was not ethically acceptable as the patients had no cardiac symptoms or clinical findings. However, this leaves room for speculation of the fundamental cause of the myocardial changes

detected in our study. Late enhancement MRI studies or fibrosis-dedicated blood samples could be used in future studies and a comparison between the different imaging modalities could enhance our knowledge of this issue. Finally, the control echocardiography study was executed immediately after RT and thereby reflects very short-term consequences. A long-term follow-up is currently underway to reveal the development of late adverse clinical effects.

Conclusion

Ultrasound tissue characterisation revealed an increase in myocardial wall tissue density after breast cancer adjuvant RT, particularly in the areas that received the highest radiation dose, despite no clinical signs of cardiac affliction. As a sensitive marker of myocardial tissue abnormalities, UTC can be used for the screening of early RT-induced changes and as a tool to identify patients who might benefit the most from a long-term follow-up.

Acknowledgments The authors thank research nurses Virpi Räsänen, Hanna Näppilä, and Emmi Vettenranta for their expert assistance during the study. This study was supported by the Pirkanmaa Hospital District, Seppo Nieminen Fund (Grant 150613), Paavo and Eila Salonen Legacy, Ida Montini Fund, the Finnish Foundation for Cardiovascular Research, The Finnish Cultural Foundation, Pirkanmaa Regional Fund and by the Finnish Medical Foundation.

Compliance with ethical standards

This study have received financial support in form of grants from non-commercial foundations. Tanja Skyttä has received grants from the Pirkanmaa Hospital District, Seppo Nieminen Fund (grant 150613) and from the Finnish Foundation for Cardiovascular Research. Suvi Tuohinen has received grants from Paavo and Eila Salonen Legacy, Ida Montini Fund, the Finnish Cultural Foundation, Pirkanmaa Regional Fund and by the Finnish Medical Foundation. This study has been approved by the institutional board of ethics and all participants signed informed consent before enrolment in the study. All procedures performed in studies involving human participants were in accordance with the ethical standards of the institutional and with the 1964 Helsinki declaration and its later amendments or comparable ethical standards. This article does not contain any studies with animals performed by any of the authors.

Conflict of interest None.

References

1. Sardaro A, Petruzzelli MF, D'Errico MP, Grimaldi L, Pili G, Portaluri M (2012) Radiation-induced cardiac damage n early left breast cancer patients: risk factors, biological mechanisms, radiobiology, and dosimetric constraints. Radiother Oncol 103(2):133–142
2. Jaworski C, Mariani JA, Wheeler G, Kaye DM (2013) Cardiac complications of thoracic irradiation. J Am Coll Cardiol 61(23):2319–2328
3. Clarke M, Collins R, Darby S, Davies C, Elphinstone P, Evans E et al (2005) Effects of radiotherapy and of differences in the extent of surgery for early breast cancer on local recurrence and 15-year survival: an overview of the randomised trials. Lancet 366(9503):2087–2106
4. Darby SC, Ewertz M, McGale P, Bennet AM, Blom-Goldman U, Bronnum D et al (2013) Risk of ischemic heart disease in women after radiotherapy for breast cancer. N Engl J Med 368(11):987–998
5. Lancellotti P, Nkomo VT, Badano LP, Bergler J, Bogaert J, Davin L et al (2013) Expert consensus for multi-modality imaging evaluation of cardiovascular complications of radiotherapy in adults: a report from the European Association of Cardiovascular Imaging and the American Society of Echocardiography. Eur Heart J Cardiovasc Imaging 14(8):721–740
6. Wethal T, Lund MB, Edvardsen T, Fossa SD, Pripp AH, Holte H et al (2009) Valvular dysfunction and left ventricular changes in Hodgkin's lymphoma survivors. A longitudinal study. Br J Cancer 101(4):575–581
7. Chello M, Mastroroberto P, Romano R, Zofrea S, Bevacqua I, Marchese AR (1996) Changes in the proportion of types I and III collagen in the left ventricular wall of patients with post-irradiative pericarditis. Cardiovasc Surg 4(2):222–226
8. Fajardo LF, Stewart JR (1970) Experimental radiation-induced heart disease I. Light microscopic studies. Am J Pathol 59(2): 299–316
9. Mimbs JW, O'Donnell M, Bauwens D, Miller JW, Sobel BE (1980) The dependence of ultrasonic attenuation and backscatter on collagen content in dog and rabbit hearts. Circ Res 47(1):49–58
10. Hoyt RH, Collins SM, Skorton DJ, Ericksen EE, Conyers D (1985) Assessment of fibrosis in infarcted human hearts by analysis of ultrasonic backscatter. Circulation 71(4):740–744
11. Romano MM, Pazin-Filho A, O'Connel JL, Simoes MV, Schmidt A, Campos EC et al (2012) Early detection of doxorubicin myocardial injury by ultrasonic tissue characterization in an experimental animal model. Cardiovasc Ultrasound 10:40-7120-10-40
12. Mor-Avi V, Lang RM, Badano LP, Belohlavek M, Cardim NM, Derumeaux G et al (2011) Current and evolving echocardiographic techniques for the quantitative evaluation of cardiac mechanics: ASE/EAE consensus statement on methodology and indications endorsed by the Japanese Society of Echocardiography. Eur J Echocardiogr 12(3):167–205
13. Picano E, Pelosi G, Marzilli M, Lattanzi F, Benassi A, Landini L et al (1990) In vivo quantitative ultrasonic evaluation of myocardial fibrosis in humans. Circulation 81(1):58–64
14. Di Bello V, Talarico L, Picano E, Di Muro C, Landini L, Paterni M et al (1995) Increased echodensity of myocardial wall in the diabetic heart: an ultrasound tissue characterization study. J Am Coll Cardiol 25(6):1408–1415
15. Romano MM, Maciel LM, Almeida-Filho OC, Pazin-Filho A, Schmidt A, Maciel BC (2010) Myocardial ultrasonic tissue characterization in patients with thyroid dysfunction. Cardiovasc Ultrasound 8:15-7120-8-15
16. Lattanzi F, Bellotti P, Picano E, Chiarella F, Mazzarisi A, Melevendi C et al (1993) Quantitative ultrasonic analysis of myocardium in patients with thalassemia major and iron overload. Circulation 87(3):748–754
17. Angermann CE, Nassau K, Stempfle HU, Kruger TM, Drewello R, Junge R et al (1997) Recognition of acute cardiac allograft rejection from serial integrated backscatter analyses in human orthotopic heart transplant recipients. Comparison with conventional echocardiography. Circulation 95(1):140–150
18. Tuohinen SS, Skytta T, Virtanen V, Luukkaala T, Kellokumpu-Lehtinen PL, Raatikainen P (2015) Early effects of adjuvant breast cancer radiotherapy on right ventricular systolic and diastolic function. Anticancer Res 35(4):2141–2147
19. Skytta T, Tuohinen S, Virtanen V, Raatikainen P, Kellokumpu-Lehtinen PL (2015) The concurrent use of aromatase inhibitors

and radiotherapy induces echocardiographic changes in patients with breast cancer. Anticancer Res 35(3):1559–1566
20. Sagar KB, Pelc LE, Rhyne TL, Wann LS, Waltier DC (1988) Influence of heart rate, preload, afterload, and inotropic state on myocardial ultrasonic backscatter. Circulation 77(2):478–483
21. Lattanzi F, Spirito P, Picano E, Mazzarisi A, Landini L, Distante A et al (1991) Quantitative assessment of ultrasonic myocardial reflectivity in hypertrophic cardiomyopathy. J Am Coll Cardiol 17(5):1085–1090

DOI: 10.1111/echo.13433

WILEY Echocardiography

Detection of early radiotherapy-induced changes in intrinsic myocardial contractility by ultrasound tissue characterization in patients with early-stage breast cancer

Suvi Sirkku Tuohinen MD[1] | Tanja Skyttä MD[2] | Heini Huhtala MSc[3] | Vesa Virtanen MD PhD[1] | Marko Virtanen MD[1] | Pirkko-Liisa Kellokumpu-Lehtinen MD PhD[2] | Pekka Raatikainen MD PhD[4]

[1]Heart Center Co., Tampere University Hospital and School of Medicine, University of Tampere, Tampere, Finland

[2]Department of Oncology, Tampere University Hospital and School of Medicine, University of Tampere, Tampere, Finland

[3]School of Health Sciences, University of Tampere, Tampere, Finland

[4]Heart and Lung Center, Helsinki University Hospital, Helsinki, Finland

Correspondence
Suvi Sirkku Tuohinen, Heart Center Co, Tampere University Hospital, Tampere, Finland.
Email: suvi.tuohinen@fimnet.fi

Funding information
Finnish Cultural Foundation, Pirkanmaa Regional Fund; Pirkanmaa Hospital District; Seppo Nieminen Fund, Grant/Award Number: 150613; Paavo and Eila Salonen Legacy; Ida Montin Fund; Finnish Foundation for Cardiovascular Research; Finnish Society for Oncology; Finnish-Norwegian Medical Foundation; Pirkanmaa Cancer Society; Finnish Medical Foundation.

Background: Increased cardiovascular morbidity and mortality are major late complications after radiotherapy (RT) in the thoracic region. Ultrasound tissue characterization (UTC) is a noninvasive method for the identification of myocardial changes. The aim of this prospective clinical trial was to assess whether the analysis of cyclic variation of integrated backscatter (CVIBS) can detect early RT-induced myocardial alterations.

Methods: Seventy-three eligible patients with early-stage breast cancer were evaluated before and immediately after adjuvant RT. Twenty and 53 patients had right-sided and left-sided breast cancer, respectively. None of the patients received chemotherapy. Comprehensive echocardiographic examination included three-dimensional (3D) measurements and UTC analysis of the left ventricular (LV) septum and posterior wall.

Results: RT reduced CVIBS in a dose-dependent manner. The mean heart radiation dose over two gray (Gy) reduced the septal CVIBS from 12.0±3.4 to 9.6±2.5 dB ($P<.001$) and the posterior wall CVIBS from 12.8±2.7 to 11.3±2.4 dB ($P=.007$). The CVIBS remained unchanged when the mean heart RT dose was below 2 Gy. Multivariate analysis showed an independent association with a change in septal CVIBS and the use of aromatase inhibitor ($\beta=2.986$, $P=.001$) and body mass index ($\beta=-0.241$, $P=.014$). The posterior values were worse with higher mean lung dose ($\beta=-.485$, $P=.018$) and with nonsmoking status ($\beta=-2.411$, $P=.009$). Echocardiography parameters showed increased myocardial mass but conventional measurements of the LV systolic function remained unchanged.

Conclusions: Cyclic variation of integrated backscatter analysis seems to be a sensitive method to detect early RT-induced myocardial changes. Hence, it may be useful in screening of patients needing closer follow-up.

KEYWORDS
breast cancer, cyclic variation of integrated backscatter, radiotherapy, ultrasound tissue characterization

 © 2017, Wiley Periodicals, Inc.

1 | INTRODUCTION

Breast cancer is the most common cancer in females in Western countries. Adjuvant radiotherapy (RT) reduces local breast cancer relapses and disease-related mortality.[1,2] However, RT in the thoracic region increases late cardiovascular morbidity and mortality.[3–7] Radiotherapy-induced heart disease (RIHD) includes coronary artery disease, left-sided valvular abnormality, disturbances in the conduction system, myocardial fibrosis, and rarely constrictive pericarditis.[3,5–7] Although RIHD usually becomes clinically apparent after several years of the latency period, detection of early cardiac changes may have an important role in the identification of patients at risk for RIHD.[3,5–7]

The early RT-induced cardiac changes are poorly characterized and detection of subclinical changes is challenging. Ultrasound tissue characterization (UTC) provides convenient means to detect subclinical myocardial changes noninvasively.[8–10] When ultrasound interacts with the myocardial tissue, small components cause scattering of the ultrasound signal. A part of the scattering reflects back to the transducer, that is, backscattered signal. The amount of redirected energy is dependent on the myocardial texture. Myocardial fibrosis, particularly collagen content, is the major component of tissue reflectivity, but fiber architecture, myocyte orientation, and extracellular matrix are also contributing factors.[8–10] The magnitude of reflectivity changes during the cardiac cycle appears to correspond to the regional intrinsic myocardial contractility although the precise basis for cyclic variation of the integrated backscattered (CVIBS) is unknown. CVIBS has been shown to reveal myocardial dysfunction earlier than conventional echocardiographic techniques [11–14] and to have prognostic importance.[14–19] The aim of this study was to evaluate the capability of CVIBS to detect RT-induced myocardial changes in the initial phase after adjuvant RT for early-stage breast cancer.

2 | METHODS

2.1 | Patient selection

A total of 73 eligible female patients with early-stage breast cancer undergoing adjuvant RT were included in this prospective clinical study between July 2011 and November 2013 at Tampere University Hospital. Fifty-three and 20 of the patients had left-sided and right-sided breast cancer, respectively. All patients received adjuvant conformal three-dimensional (3D) RT after breast cancer resection. An adjuvant chemotherapy treatment was not indicated for this early breast cancer population. The exclusion criteria were age under 18 years or over 80 years, other malignancy, pregnancy or breast feeding, acute myocardial infarction within 6 months, symptomatic heart failure (New York Heart Association classification [NYHA]), dialysis, permanent anticoagulation, and severe psychiatric disorders. To optimize the echocardiography image quality, patients with atrial fibrillation, a left bundle branch block, a permanent pacemaker, and a severe lung disease were also excluded. The local institutional board of ethics approved the protocol (R10160), and all participants signed a written informed consent before enrollment.

2.2 | Radiotherapy

RT protocol has been previously described in detail.[20] Briefly, pretreatment 3D computed tomography treatment planning and contouring were performed in all patients by the same radiation oncologist (TS). Treatment doses were either 50 gray (Gy) in 2 Gy fractions (standard) or 42.56 Gy in 2.66 Gy fractions (hypofractionated) according to the local guidelines. An additional boost of 16 Gy in 2 Gy fractions to the tumor bed was used if clinically indicated after breast conserving surgery. Doses were calculated using the anisotropic analytical algorithm, and dose-volume histograms for different structures were generated for each patient (Table 1). The patients were divided into groups according to the mean heart dose on the basis of our previous findings,[21] patients receiving less than 2 Gy mean heart dose (low) and patients receiving over 2 Gy mean heart dose (high).

2.3 | Cardiac examinations

A comprehensive echocardiography and a 12-lead electrocardiogram (ECG) were performed at baseline and at the end of RT (0–6 days from the last radiation dose). The median interval between the first and the second study was 39 days (19–93 days). High sensitivity troponin T (hsTnt) and pro-B-type natriuretic peptide (proBNP) were measured at each visit and during the treatment course.

All echocardiographic examinations were performed using a commercially available cardiac ultrasound machine (Philips iE33 ultrasound

TABLE 1 Radiation doses to the different cardiac structures (Gy)

	Low n=36		High n=37	
	Median	(Range)	Median	(Range)
The whole heart	0.8	(0.3–1.9)	3.6	(2.0–6.4)
Left ventricle	0.5	(0.0–4.3)	5.5	(1.1–12.3)
LAD	1.2	(0.0–14.0)	25.6	(0.7–41.4)
Right ventricle	0.9	(0.2–2.4)	2.9	(1.1–9.2)

LAD, the region of the heart perfused by the left anterior descending coronary artery.

system, Bothell, WA, USA) and a 1–5 MHz matrix-array X5-1 transducer by the same cardiologist (SST). All images were acquired at rest with a simultaneous superimposed ECG. Subcostal imaging was performed in the supine position, and other imaging was performed with the patient in the left lateral decubitus position. Doppler recordings were acquired at the end of expiration.

For two-dimensional UTC analysis, a parasternal short-axis view clip was obtained over several cycles (Figure 1). No lateral or time gain compensation was used. The raw data were stored in an external hard drive for offline analysis (Qlab Philips). A square of 5×5 mm regions of interest (ROI) was carefully positioned in the anterior septum avoiding areas with bright endocardial or epicardial specular reflections, as well as very bright or hypoechoic regions within the myocardium. A second ROI was positioned in the posterior wall. The correct myocardial positioning during the whole clip was controlled by inspection of the ROIs throughout the entire clip, and repositioning was performed if necessary. The maximal and minimal values of the integrated backscatter were recorded. Cyclic variation was calculated as the difference between the maximal and minimal values. All UTC analyses were performed by a single person (SST) and blinded for the cardiac radiation exposure.

The ECG analyses of the baseline and post-RT ECGs were performed manually (SST) according to general clinical practice. Differences between baseline and post-RT recordings were visually judged of the P-waves, QRS-complexes, the T-waves, and the ST-segments. As no other clinically significant changes were found, the T-wave inversions were categorically registered both according to the individual leads and as whether patient had or had not any T-wave inversions. A T-wave inversion was defined either as a change from positive or isoelectric to negative or from negative to positive.

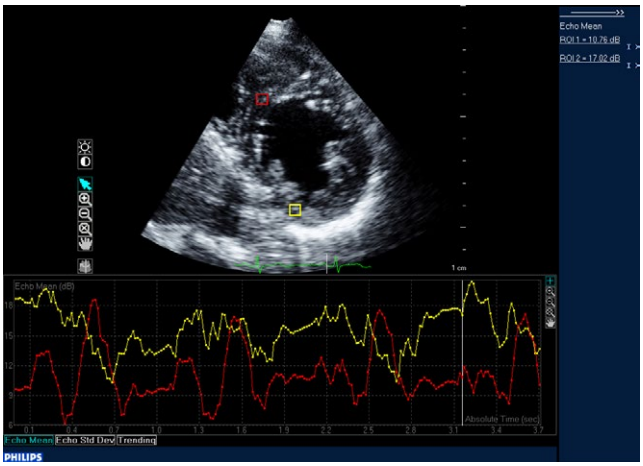

FIGURE 1 Measurement of the cyclic variation. An offline analysis of the parasternal short-axis clip at the papillary muscle level was performed by placing the region of interest (ROI) in the anterior septum (the red box and line) and in the posterior wall (the yellow box and line). The maximum and minimum values were recorded, and the cyclic variation of the integrated backscatter (CVIBS) was calculated as the difference between the two values

2.4 | Statistical analysis

Data are reported as mean and standard deviation for normally distributed variables and as median with range for other continuous variables. Differences between baseline and after RT values were tested using the paired samples *t* test, for variables with skewed distribution after logarithmic transformation. Differences in the baseline characteristics between the groups were tested using Student's *t* test for continuous variables and Fisher's exact test for categorical variables. The association of the variables with the change in CVIBS values was tested using Pearson correlation (rp). Stepwise forward linear multivariate regression analysis was performed to test the independent relationship of the changes in CVIBS values with other parameters (age, diabetes, hypertension, body mass index (BMI), the use of aromatase inhibitor (AI), smoking and the mean heart dose for septal values, and mean lung dose for posterior values). Blinded data from 20 healthy volunteers were used to test the reproducibility of the UTC measurements. The reproducibility and intra- and inter-observer variability were tested using the Bland-Altman plot (Figure 2). All tests were two-sided, and *P*-values <.05 were considered statistically significant. Statistical analyses were performed with IBM SPSS Statistics 22.0 for Windows.

3 | RESULTS

3.1 | General characteristics

The mean age of the study group was 64±6 years. The BMI was over 25 kg/m² in 63% of the patients, and 23% of the patients were current or ex-smokers. Thirty-one patients (43%) had no other concurrent diseases. Detailed baseline characteristics of the patients are shown in Table 2.

3.2 | Ultrasound tissue characterization

Among patients in the high group, the septal CVIBS (sCVIBS) and the posterior CVIBS (pCVIBS) values declined significantly by 2.4±3.0 decibels (dB) (*P*<.001) and 1.5±3.1 dB (*P*=.007) after the RT, respectively. In the low group, the changes were nonsignificant both for sCVIBS 0.2±3.8 dB (*P*=.745) and for pCVIBS 0.2±3.7 dB (*P*=.728). (Table 3).

3.3 | Factors associated with changes in the septal CVIBS

Despite clear tendency, no statistically significant correlations were observed between the sCVIBS change and mean heart radiation dose (rp=−0.211, *P*=.079), mean left ventricle (LV) radiation dose (rp=−0.203, *P*=.091), volume receiving more than 40 Gy in left anterior descending artery (LAD) region (rp=−0.228, *P*=.024), and reduction in LV end-diastolic volume (rp=−0.228, *P*=.075). On the other hand, the reduction in the sCVIBS value was associated with the use of AI (*P*=.013). The mean baseline sCVIBS value in patients using AI was 9.5±2.4 dB and 12.2±3.3 dB among those not using AI (*P*<.001). In patients using AI, the mean sCVIBS value after radiotherapy was 10.3±2.7 dB (*P*=.234)

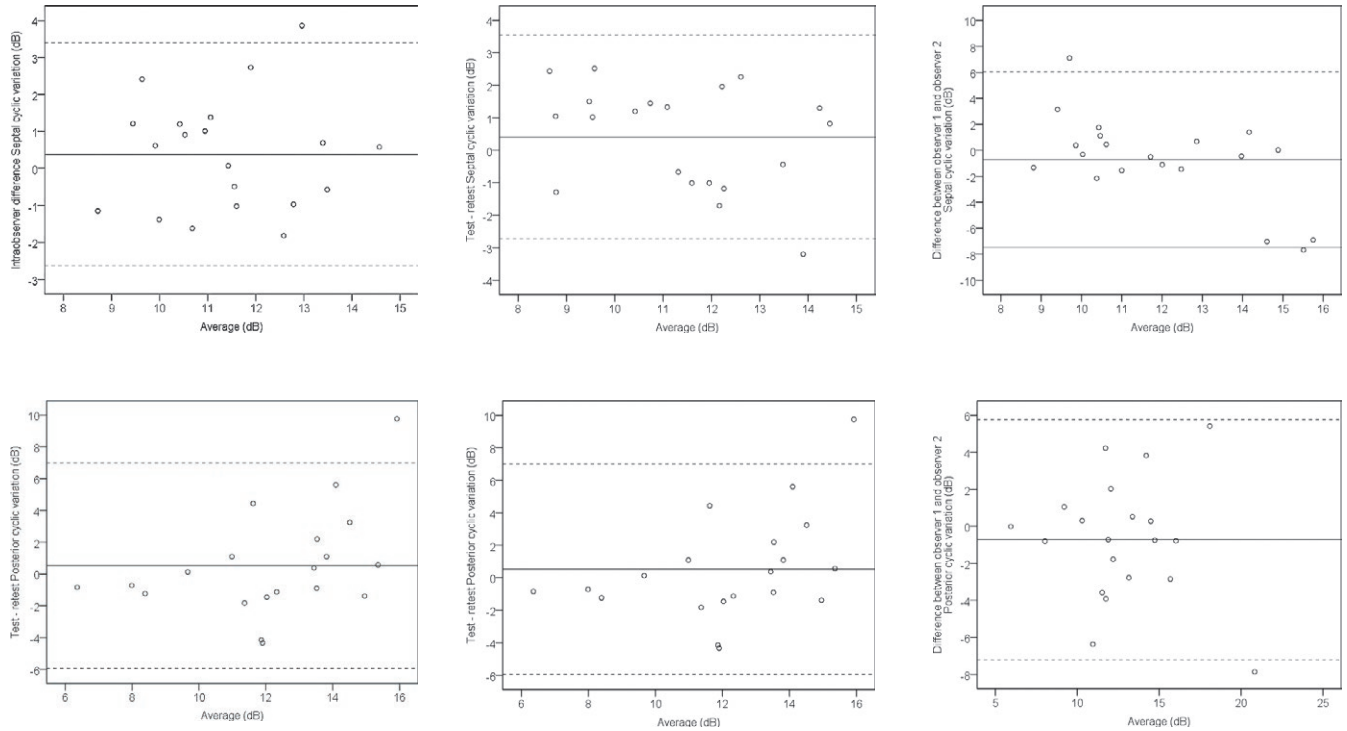

FIGURE 2 Bland-Altman plots for the cyclic variation of the integrated backscatter. The upper row represents the septal wall calculations, and the lower row indicates the posterior wall calculations. The first column indicates the intra-observer Bland-Altman plots, and the second column indicates the test-retest values. The last column indicates the inter-observer Bland-Altman plots

and 8.7±1.8 dB (*P*=.097) in the low and high groups, respectively. The corresponding values for patients not using AI were 9.8±2.6 dB (*P*=.056) in the low group and 10.1±2.8 dB in the high group (*P*<.001). Linear multivariate regression analysis revealed that BMI (β=−0.241, *P*=.014) and the use of AI (β=2.986, *P*=.001) were independently associated with the change of the sCVIBS. An increase in BMI with one unit was associated with a 0.24-dB decrease in sCVIBS after RT.

3.4 | Factors associated with the changes in posterior CVIBS

The pCVIBS change had weak negative correlation with the mean lung radiation dose (rp=−0.272, *P*=.023) and the change in LV end-diastolic volume (rp=−0.232, *P*=.070), and a positive correlation with the LV mass change (rp=0.465, *P*<.001). The reduction in pCVIBS was also associated with the use of tamoxifen (*P*=.050) and nonsmoking status (*P*=.011). Non-smoking (β=−2.411, *P*=.009) and mean lung dose (β=−0.485, *P*=.018) were independently associated with the change in pCVIBS values in linear multivariate regression analysis. Nonsmoking status was associated with a 2.41-dB higher reduction in the pCVIBS. Each increase by one Gy in the mean lung irradiation dose was associated with a pCVIBS decline by 0.49 dB.

3.5 | Conventional echocardiographic measurements

The LV myocardial mass increased from 101±16 g to 105±17 g (*P*=.039) and remained unchanged from 110±24 g to 112±24 g (*P*=.114) in the low and high groups, respectively. The analysis of LV volumes in 3D recordings showed that the end-diastolic volume was unchanged from 96±21 mL to 95±21 mL (*P*=.839) in the low group patients and declined from 102±21 mL to 97±20 mL (*P*=.028) in the high group patients. The ejection fraction of the LV remained essentially unchanged. The other measurements are displayed in Table 4.

3.6 | Electrocardiogram and biochemical markers

RT induced minor asymptomatic ECG changes in 18 patients (25%). The most typical ECG changes were T-wave inversions in leads V_{1-4} and sometimes also in leads aVL and I. ECG changes were more common in the high than the low group (16 vs 2 patients) (*P*<.001).

In the low group, the baseline and highest hsTnt values were 4 (4–8) ng/L and 5 (4–12) ng/L (*P*=.056), respectively. In the high group, the baseline hsTnt was 4 (4–33) ng/L, and the highest value was 5 (4–20) ng/L (*P*=.175). The rise in hsTnt was over 30% in 6% of the patients and 21% of the patients (*P*=.047) in the low and high groups, respectively.

The baseline and highest proBNP values in the low group were 77 (12–305) ng/L and 88 (15-284) ng/L (*P*=.285), respectively. In the high group, the baseline values were 57 (14-824) ng/L and the highest values 84 (20–1101) ng/L (*P*<.001), respectively. The highest proBNP value above reference value was observed in none in the low and in four in the high group patients (*P*=.057).

TABLE 2 Baseline characteristics of the study cohort

	Low n=36	High n=37	
Variable	**Mean±SD**	**Mean±SD**	***P***
Age (y)	63.2±5.4	64.0±7.5	.576
Systolic blood pressure (mm Hg) [a]	145±20	146±20	.862
Diastolic blood pressure (mm Hg) [a]	78±10	79±14	.966
Height (cm)	164±5	163±6	.399
Weight (kg)	70±10	76±14	.054
Body mass index (kg/m^2)	26.1±3.3	28.6±4.8	.184
Smoking	n (%)	n (%)	
Current	3 (8.3%)	5 (13.5%)	.308
Previous	6 (16.7%)	3 (8.1%)	.711
Prior diagnosis[b]			
Hypertension	17 (47.2%)	10 (40.5%)	.640
Diabetes mellitus	2 (5.6%)	5 (13.5%)	.430
Hypercholesterolemia	10 (27.8%)	6 (16.2%)	.269
Hypothyreosis	7 (19.4%)	3 (8.1%)	.190
Coronary artery disease	1 (2.8%)	2 (5.4%)	1.000
Significant valvular abnormality	1 (2.8%)	3 (8.1%)	1.000
Medical treatment			
β-blocker	4 (11.1%)	7 (18.9%)	.515
Calcium channel blocker	3 (8.3%)	5 (13.5%)	.711
ACE inhibitor/ARBs	12 (33.3%)	10 (27.0%)	.616
Diuretics	6 (16.7%)	9 (24.3%)	.564
Thyroxin	7 (19.4%)	3 (8.1%)	.190
Nitrates	0 (0%)	1 (2.7%)	1.000
Aspirin	5 (13.9%)	4 (10.8%)	.732
Statin	8 (22.2%)	6 (16.2%)	.559
Oral diabetes medication	2 (5.6%)	5 (13.5%)	.430
Aromatase inhibitor	14 (38.9%)	13 (35.1%)	.811
Tamoxifen	3 (8.3%)	3 (8.1%)	1.000
	n/n	n/n	
Right-sided / left-sided breast cancer	18/18	2/35	<.001

ACE, angiotensin converting enzyme; ARBs, angiotensin receptor blockers.
[a]measured at the first visit, [b]defined as the medication-requiring state.

4 | DISCUSSION

The results of this study indicate that breast cancer RT-induced early changes in local myocardial function can be detected by UTC analysis but not by conventional systolic LV measurements. In light of the prognostic power of the UTC analysis in other diseases,[14,17–19] these early changes may have an impact on the long-term cardiovascular morbidity and mortality of these patients.

4.1 | Effect of radiotherapy on ultrasound tissue characterization and conventional echocardiographic parameters

As an intrinsic myocardial measurement, ultrasound tissue characterization technique provides a convenient means to detect myocardial fibrosis.[8–10] CVIBS has been shown to be a more sensitive marker of early contractile dysfunction than conventional echocardiographic parameters over a wide range of cardiac diseases. In our study, RT reduced CVIBS values in a dose-dependent manner. RT caused no significant changes in UCT measurements in patients receiving less than 2 Gy mean heart dose, whereas in those with mean heart dose over 2 Gy CVIBS was reduced significantly both in the septum and in the posterior wall. The magnitude of the changes was larger in the septum than in the posterior wall. This is logical considering the position of the RT field, which made the anterior segments of the heart (septum) was more prone to direct radiation, while the posterior segments required a larger general impact to be affected.

4.2 | Mechanism causing RT-induced myocardial changes

The exact mechanism causing the changes detected in our study is speculative. It has been shown that RT induces inflammatory changes in the initial phase with evolution toward fibrotic manifestations as early as 40 days after the initiation of the RT treatment.[22] The endomyocardial biopsy could have verified the histological changes in our patients, but this would have been unethical in otherwise an asymptomatic heart-healthy patient population. However, the RT-induced changes in the UCT were accompanied with changes in several conventional echocardiographic measurements asserting the RT-induced impact. For example, the myocardial mass and LV septal and posterior myocardium thickness increased, mitral inflow parameters showed changes in the direction of relaxation disturbance and tricuspid annular plane systolic excursion (TAPSE) decreased, as shown also in our previous study.[20] However, there were no differences in these changes between the low and the high groups. Hence, CVIBS analysis appeared to be a more sensitive method in detecting RT-induced myocardial changes than the conventional echocardiographic measurements.

4.3 | External factors associated with the changes in ultrasound tissue characterization parameters

In the multivariate analysis, the change in sCVIBS was independently associated with BMI and the use of AIs, and the change in pCVIBS was associated smoking status. In our study, an increase in BMI with one unit was associated with a 0.24-dB decrease in sCVIBS after RT. This was most likely due to the fact that obesity results in higher RT doses by producing more frequently deep setup errors and higher irradiated LV volumes.[23] It is well established that tissue hypoxia caused by smoking is associated with reduced radiation treatment effects.[24,25] This may explain why the reduction in pCVIBS was lower among smokers and ex-smokers than in those who had never smoked.

TABLE 3 Changes in myocardial cyclic variation measurements

	Low n=36			High n=37		
	Baseline	**After RT**	***P***	**Baseline**	**After RT**	***P***
Septal cyclic variation (dB)	10.3±2.9	10.0±2.6	.745	12.0±3.4	9.6±2.5	**<.001**
Posterior cyclic variation (dB)	11.7±3.5	11.5±3.4	.728	12.8±2.7	11.3±2.4	**.007**

dB, decibel; RT, radiotherapy. *P*<.05 are considered as statistically significant (bold).

The effect of AI on the myocardial function was an interesting finding. AIs were prescribed as an adjuvant hormonal treatment prior to RT for one third of the patients. These patients had significantly lower baseline sCVIBS values than those not using AIs. In addition, the harmful effects of radiation were larger among patients receiving high dose RT and adjunct AI therapy. Thus, the use of AI not only had a direct negative effect on LV function but it also augmented the negative effects of RT when the mean heart dose exceeded 2 Gy. These findings are in agreement with prior reports indicating that the use of AI may have adverse cardiac effects.[26,27] In an experimental ischemia/reperfusion study, endogenous estrogen synthesis appeared to have cardioprotective effect, whereas inhibition of estrogen metabolism by AI increased the injury size.[28] In a clinical setting, Duygu et al. recently demonstrated that estrogen replacement therapy in healthy postmenopausal females increased CVIBS values.[29]

4.4 | Clinical implications

Detection of subclinical cardiac changes in the early phase after breast cancer RT is important but challenging. The presence of these changes might indicate increased risk of late manifestations. Common late manifestations of RIHD include diastolic dysfunction, valvular abnormalities, coronary artery stenosis, pericardial constriction, and conduction system disturbances.[3,5–7] According to our data, CVIBS measurement seems to be a more sensitive tool than conventional echocardiographic measurements for detection of the early myocardial changes. As such, it could be used in screening for patients with early changes. As the early subclinical changes precede late, clinically significant cardiac manifestations, a sensitive tool to detect the early changes could be used to guide the development of RT protocols

TABLE 4 Echocardiographic measurements

	Low n=36			High n=37		
	Baseline	**After RT**	***P***	**Baseline**	**After RT**	***P***
LVEDD (mm)	44.1±4.0	44.4±3.4	.600	46.0±4.3	45.4±3.9	.126
LVEDS (mm)	30.3±3.2	30.2±3.1	.739	30.5±3.6	30.0±3.6	.426
IVS (mm)	9.9±1.5	10.3±1.6	*.088*	10.3±1.5	10.6±1.6	**.048**
PW (mm)	9.8±1.2	10.2±1.4	*.073*	10.2±1.4	10.6±2.2	.147
LVEDV (mL)	96±21	95±21	.839	102±21	97±20	**.028**
LVEDS (mL)	39±11	40±11	.319	41±9	40±10	.281
LVED mass (g)	101±16	105±17	**.039**	110±24	112±24	.114
LVEF (%)	59±6	58±6	.230	60±5	60±7	.787
Mitral inflow E (cm/s)	75±19	70±17	**.017**	73±14	70±15	**.047**
Mitral inflow a (cm/s)	77±17	74±14	.222	78±21	75±17	.175
Mitral inflow dt (ms)	224±45	242±48	**.024**	232±40	243±50	.116
LV E/e' ratio[a]	9.8 (7.3–11.8)	9.1 (7.5–10.3)	.231	8.9 (7.0–11.3)	8.3 (7.1-10.5)	.695
RV basal dimension (mm)	33.5±5.6	33.0±4.8	.423	34.2±4.4	34.2±4.7	.991
TAPSE (mm)	24.1±4.6	22.6±4.4	**.030**	23.9±4.1	21.8±4.1	**<.001**
TR gradient (mm Hg)	22.0±6.6	20.4±5.5	**.024**	21.4±5.9	21.4±5.2	.975

LVEDD and LVEDS, left ventricular end-diastolic and end-systolic diameters; IVS and PW, interventricular septum and posterior wall thicknesses at the end diastole; LVEDV, LVESV, and LVED mass, left ventricular end-diastolic and end-systolic volumes and end-diastolic mass derived from the three-dimensional acquisition; dt, declaration time; LV, left ventricular; RV, right ventricle; TAPSE, tricuspidal annular plane systolic excursion; TR gradient, tricuspid regurgitation maximal gradient. *P*<.05 are considered as statistically significant (bold) and *P*-values between .10 and .05 are considered as intermediate significant (italics). [a]median and range.

as well as to point out individuals with increased risk for late RIHD. CVIBS could be considered to be used in this context.

The results of several experimental and clinical studies have proven that fibrosis plays an important role in development of intrinsic myocardial dysfunction.[22,30,31] It has been shown that reduced CVIBS is an early sign of myocardial involvement in doxorubicin-induced cardiotoxicity, sarcoidosis, diabetes and hypertension,[12,13,32] and a sensitive detector of myocardial viability and contractility reserve.[16,33] In experimental studies, CVIBS has been shown to respond faster to ischemia and reperfusion than any conventional contractility measurement.[11] Our results indicate that the negative effects of RT on cardiac function in CVIBS were dose-dependent. Also, elevated hsTnT and proBNP levels have been associated with poor prognosis in various cardiac diseases.[34] Hence, the changes in hsTnT and proBNP in our patient population support the hypothesis that these early echocardiographic changes may later manifest as symptomatic RIHD. These findings pursue the continuing evolution toward safer treatment planning with a special emphasis on healthy tissue-sparing protocols and to targeted treatment for other cardiovascular risk factors such as hypertension, diabetes, dyslipidemia, obesity, smoking, and other lifestyle habits. This may reduce also the risk of secondary malignancies. Also, the potentially harmful effects of AIs should also be taken into account when planning future RT studies for patients with breast cancer.

4.5 | Limitations of our study

The patient population was relatively small and the distribution of the patients with the right- and left-sided breast cancer between the groups was unequal. The main focus on the study was, however, on the mean heart radiation dose, which can be considered to be independent of the RT laterality. Also, all the observed echocardiographic changes were subclinical. Therefore, considering the slow development of RIHD long-term follow-up is needed to verify the prognostic value of these early changes. The long-term follow-up of this patient population is planned. Finally, in our study, the reproducibility was better for intra-observer and test-retest variability than for inter-observer variability.

5 | CONCLUSION

Adjuvant RT in early breast cancer caused dose-dependent changes in cardiac function. These subclinical changes were evident in the UTC analysis but not in the conventional LV systolic echocardiographic examination. Detection of early RT-induced cardiac changes may have an important role in the identification of patients at risk for RIHD.

ACKNOWLEDGMENTS

The authors thank the research nurses, Virpi Räsänen, Hanna Näppilä, and Emmi Vettenranta, for their expert assistance during the study. This study was supported by the Pirkanmaa Hospital District, Seppo Nieminen Fund (grant 150613), Paavo and Eila Salonen Legacy, Ida Montin Fund, the Finnish Foundation for Cardiovascular Research and the Finnish Cultural Foundation, Pirkanmaa Regional Fund, Finnish Society for Oncology, Finnish-Norwegian Medical Foundation, Pirkanmaa Cancer Society, and Finnish Medical Foundation.

CONFLICT OF INTEREST

Suvi Tuohinen, Tanja Skyttä, Heini Huhtala, Vesa Virtanen, Marko Virtanen, Pirkko-Liisa Kellokumpu-Lehtinen, and Pekka Raatikainen declare that they have no conflict of interest.

REFERENCES

1. Clarke M, Collins R, Darby S, et al. Effects of radiotherapy and of differences in the extent of surgery for early breast cancer on local recurrence and 15-year survival: an overview of the randomised trials. *Lancet*. 2005;366:2087–2106.
2. Clark RM, Whelan T, Levine M, et al. Randomized clinical trial of breast irradiation following lumpectomy and axillary dissection for node-negative breast cancer: an update. Ontario Clinical Oncology Group. *J Natl Cancer Inst*. 1996;88:1659–1664.
3. Lancellotti P, Nkomo VT, Badano LP, et al. Expert consensus for multi-modality imaging evaluation of cardiovascular complications of radiotherapy in adults: a report from the European Association of Cardiovascular Imaging and the American Society of Echocardiography. *Eur Heart J Cardiovasc Imaging*. 2013;14:721–740.
4. Aleman BM, van den Belt-Dusebout AW, Klokman WJ, et al. Long-term cause-specific mortality of patients treated for Hodgkin's disease. *J Clin Oncol*. 2003;21:3431–3439.
5. Cutter DJ, Schaapveld M, Darby SC, et al. Risk of valvular heart disease after treatment for Hodgkin lymphoma. *J Natl Cancer Inst* 2015;107:djv008.
6. Darby SC, Ewertz M, McGale P, et al. Risk of ischemic heart disease in women after radiotherapy for breast cancer. *N Engl J Med*. 2013;368:987–998.
7. Jaworski C, Mariani JA, Wheeler G, et al. Cardiac complications of thoracic irradiation. *J Am Coll Cardiol*. 2013;61:2319–2328.
8. Picano E, Pelosi G, Marzilli M, et al. In vivo quantitative ultrasonic evaluation of myocardial fibrosis in humans. *Circulation*. 1990;81:58–64.
9. Hoyt RH, Collins SM, Skorton DJ, et al. Assessment of fibrosis in infarcted human hearts by analysis of ultrasonic backscatter. *Circulation*. 1985;71:740–744.
10. Mimbs JW, O'Donnell M, Bauwens D, et al. The dependence of ultrasonic attenuation and backscatter on collagen content in dog and rabbit hearts. *Circ Res*. 1980;47:49–58.
11. Barzilai B, Vered Z, Mohr GA, et al. Myocardial ultrasonic backscatter for characterization of ischemia and reperfusion: relationship to wall motion. *Ultrasound Med Biol*. 1990;16:391–398.
12. Hyodo E, Hozumi T, Takemoto Y, et al. Early detection of cardiac involvement in patients with sarcoidosis by a non-invasive method with ultrasonic tissue characterisation. *Heart*. 2004;90:1275–1280.
13. Romano MM, Pazin-Filho A, O'Connel JL, et al. Early detection of doxorubicin myocardial injury by ultrasonic tissue characterization in an experimental animal model. *Cardiovasc Ultrasound*. 2012;10:40.
14. Masuyama T, Valantine HA, Gibbons R, et al. Serial measurement of integrated ultrasonic backscatter in human cardiac allografts for the recognition of acute rejection. *Circulation*. 1990;81:829–839.
15. Di Bello V, Giorgi D, Talini E, et al. Incremental value of ultrasonic tissue characterization (backscatter) in the evaluation of left ventricular myocardial structure and mechanics in essential arterial hypertension. *Circulation*. 2003;107:74–80.

16. Muro T, Ota T, Watanabe H, et al. Prediction of contractile reserve by cyclic variation of integrated backscatter of the myocardium in patients with chronic left ventricular dysfunction. *Heart*. 2001;85:165–170.
17. Koyama J, Ray-Sequin PA, Falk RH. Prognostic significance of ultrasound myocardial tissue characterization in patients with cardiac amyloidosis. *Circulation*. 2002;106:556–561.
18. Ohara Y, Hiasa Y, Hosokawa S, et al. Ultrasonic tissue characterization predicts left ventricular remodeling in patients with acute anterior myocardial infarction after primary coronary angioplasty. *J Am Soc Echocardiogr*. 2005;18:638–643.
19. Park SM, Kim YH, Ahn CM, et al. Relationship between ultrasonic tissue characterization and myocardial deformation for prediction of left ventricular reverse remodelling in non-ischaemic dilated cardiomyopathy. *Eur J Echocardiogr*. 2011;12:887–894.
20. Tuohinen SS, Skytta T, Virtanen V, et al. Early effects of adjuvant breast cancer radiotherapy on right ventricular systolic and diastolic function. *Anticancer Res*. 2015;35:2141–2147.
21. Skytta T, Tuohinen S, Boman E, et al. Troponin T-release associates with cardiac radiation doses during adjuvant left-sided breast cancer radiotherapy. *Radiat Oncol*. 2015;10:141.
22. Fajardo LF, Stewart JR. Experimental radiation-induced heart disease. I. Light microscopic studies. *Am J Pathol*. 1970;59:299–316.
23. Evans ES, Prosnitz RG, Yu X, et al. Impact of patient-specific factors, irradiated left ventricular volume, and treatment set-up errors on the development of myocardial perfusion defects after radiation therapy for left-sided breast cancer. *Int J Radiat Oncol Biol Phys*. 2006;66:1125–1134.
24. Hoff CM, Grau C, Overgaard J. Effect of smoking on oxygen delivery and outcome in patients treated with radiotherapy for head and neck squamous cell carcinoma-a prospective study. *Radiother Oncol*. 2012;103:38–44.
25. Overgaard J. Sensitization of hypoxic tumour cells-clinical experience. *Int J Radiat Biol*. 1989;56:801–811.
26. Skytta T, Tuohinen S, Virtanen V, et al. The concurrent use of inhibitors and radiotherapy induces echocardiographic changes in patients with breast cancer. *Anticancer Res*. 2015;35:1559–1566.
27. Seruga B, Zadnik V, Kuhar CG, et al. Association of aromatase inhibitors with coronary heart disease in women with early breast cancer. *Cancer Invest*. 2014;32:99–104.
28. Jazbutyte V, Stumpner J, Redel A, et al. Aromatase inhibition attenuates desflurane-induced preconditioning against acute myocardial infarction in male mouse heart in vivo. *PLoS ONE*. 2012;7:e42032.
29. Duygu H, Akman L, Ozerkan F, et al. Comparison of the effects of new and conventional hormone replacement therapies on left ventricular diastolic function in healthy postmenopausal women: a Doppler and ultrasonic backscatter study. *Int J Cardiovasc Imaging*. 2009;25:387–396.
30. Chello M, Mastroroberto P, Romano R, et al. Changes in the proportion of types I and III collagen in the left ventricular wall of patients with post-irradiative pericarditis. *Cardiovasc Surg*. 1996;4:222–226.
31. Russell NS, Hoving S, Heeneman S, et al. Novel insights into pathological changes in muscular arteries of radiotherapy patients. *Radiother Oncol*. 2009;92:477–483.
32. Maceira AM, Barba J, Beloqui O, Diez J. Ultrasonic backscatter and diastolic function in hypertensive patients. *Hypertension*. 2002;40:239–243.
33. Komuro K, Yamada S, Mikami T, et al. Sensitive detection of myocardial viability in chronic coronary artery disease by ultrasonic integrated backscatter analysis. *J Am Soc Echocardiogr*. 2005;18:26–31.
34. Tsounis D, Deftereos S, Bouras G, et al. High sensitivity troponin in cardiovascular disease. Is there more than a marker of myocardial death? *Curr Top Med Chem*. 2013;13:201–215.

How to cite this article: Tuohinen SS , Skyttä T, Huhtala H , Virtanen V, Virtanen M, Kellokumpu-Lehtinen P-L, and Raatikainen P. Detection of early radiotherapy-induced changes in intrinsic myocardial contractility by ultrasound tissue characterization in patients with early-stage breast cancer. *Echocardiography*. 2017;34:191–198.

Int J Cardiovasc Imaging
DOI 10.1007/s10554-016-1021-y

ORIGINAL PAPER

Radiotherapy-induced global and regional differences in early-stage left-sided versus right-sided breast cancer patients: speckle tracking echocardiography study

Suvi Sirkku Tuohinen[1] · Tanja Skyttä[2] · Tuija Poutanen[3] · Heini Huhtala[4] · Vesa Virtanen[1] · Pirkko-Liisa Kellokumpu-Lehtinen[2] · Pekka Raatikainen[5]

Received: 3 October 2016 / Accepted: 12 November 2016
© Springer Science+Business Media Dordrecht 2016

Abstract Radiotherapy (RT) to the thoracic region increases late cardiovascular morbidity and mortality. The impact of breast cancer laterality on cardiac function is largely unknown. The aim of this prospective study was to compare RT-induced changes in left-sided and right-sided breast cancer patients using speckle tracking echocardiography (STE). Sixty eligible patients with left-sided breast cancer and 20 with right-sided breast cancer without chemotherapy were evaluated prospectively before and early after RT. A comprehensive echocardiographic examination included three dimensional measurements and STE of the left ventricle (LV). The global longitudinal strain (GLS) was reduced from -18.3 ± 3.1 to $-17.2 \pm 3.3\%$ ($p = 0.003$) after RT in patients with left-sided breast cancer. Similarly, regional analysis showed a reduction in the apical strain from -18.7 ± 5.3 to $-16.7 \pm 4.9\%$ ($p = 0.002$) and an increase in basal values from -21.6 ± 5.0 to $-23.3 \pm 4.9\%$ ($p = 0.024$). Patients with right-sided breast cancer showed deterioration in basal anterior strain segments from -26.3 ± 7.6 to $-18.8 \pm 8.9\%$ ($p < 0.001$) and in pulsed tissue Doppler by 0.825 [0.365, 1.710] cm/s ($p < 0.001$). In multivariable analysis, the use of aromatase inhibitor ($\beta = -2.002$, $p = 0.001$) and decreased LV diastolic volume ($\beta = -0.070$, $p = 0.025$) were independently associated with the decrease in GLS. RT caused no changes in conventional LV systolic measurements. RT induced regional changes corresponded to the RT fields. Patients with left-sided breast cancer experienced apical impact and global decline, whereas patients with right-sided breast cancer showed basal changes. The regional differences in cardiac impact warrant different methods in screening and in the follow-up of patients with left-sided versus right-sided breast cancer.

Keywords Speckle tracking · Breast cancer · Radiotherapy · Laterality

Electronic supplementary material The online version of this article (doi:10.1007/s10554-016-1021-y) contains supplementary material, which is available to authorized users.

✉ Suvi Sirkku Tuohinen
suvi.tuohinen@fimnet.fi

[1] Heart Center Co., Heart Hospital, Tampere University Hospital and School of Medicine, University of Tampere, PO Box 2000, 33521 Tampere, Finland

[2] Department of Oncology, Tampere University Hospital and School of Medicine, University of Tampere, Tampere, Finland

[3] Department of Pediatrics, Tampere University Hospital and School of Medicine, University of Tampere, Tampere, Finland

[4] School of Health Sciences, University of Tampere, Tampere, Finland

[5] Heart and Lung Center, Helsinki University Hospital, Helsinki, Finland

Introduction

Breast cancer is the most common cancer in women worldwide [1]. Radiotherapy (RT) reduces local breast cancer relapses and disease-related mortality but doubles late cardiovascular morbidity and mortality [2–4]. Breast cancer laterality has major importance. Patients with left-sided breast cancer have a 1.3 to 1.6-fold relative risk of cardiovascular complications 10 years after RT, compared with right-sided breast cancer patients [1, 4–6]. However, the RT-induced cardiac impact is more associated with the cardiac radiation exposure rather than breast cancer laterality [5], and the increase in coronary events has been estimated to vary from 4 to 7.4% per Gray (Gy) of the mean

heart dose [1, 5]. The average cardiac exposure of patients with right-sided breast cancer has been estimated at 3.3 Gy (0.4–6 Gy) [7, 8], resulting in at least a 1.6–3.0% increase in risk for coronary events. The majority of the studies of RT-induced cardiac changes in breast cancer patients have focused on patients with left-sided breast cancer, and knowledge of the changes among patients with right-sided breast cancer is limited.

Myocardial deformation imaging in echocardiography has major advantages over conventional measurements. It is more sensitive for detecting subtle changes in earlier phases than conventional functional measurements over wide variety of pathologies [9, 10]. Colour strain measurements have detected changes in myocardial deformation in regions receiving radiation doses >3 Gy [11]. In speckle tracking echocardiography (STE) analysis, global longitudinal strain (GLS) decreased after RT in left-sided breast cancer patients [9]. However, the early manifestations after RT in patients with right-sided breast cancer have not been well characterized. The aim of this study was to illuminate the differences induced by RT exposure laterality in the early phase after adjuvant RT in breast cancer patients using the STE method.

Materials and methods

Patient selection

A total of 80 eligible female patients with early-stage breast cancer were included in this single-centre, prospective clinical study between July 2011 and November 2013. Sixty of them had left-sided breast cancer, and 20 had right-sided breast cancer. Following breast cancer surgery, all patients received adjuvant conformal three dimensional (3D) RT. None of these early stage breast cancer patients received chemotherapy. Other exclusion criteria were age under 18 or over 80 years, other malignancies, pregnancy or breast feeding, acute myocardial infarction within 6 months, symptomatic heart failure (NYHA 3–4), dialysis, permanent anticoagulation and severe psychiatric disorders. Patients with atrial fibrillation, left bundle branch block, permanent pacemaker and severe lung disease were also excluded to improve the quality of echocardiographic imaging. The protocol was approved by the local institutional board of ethics (R10160), and all of the participants provided written informed consent before enrolment.

Radiotherapy

The RT protocol used in this study has previously been described in detail [12]. In brief, 3D computed tomography treatment planning and contouring were performed in all of the patients (Fig. 1). The treatment schedule was either 50 Gy in 2 Gy fractions (standard) or 42.56 Gy in 2.66 Gy fractions (hypofractionated). An additional boost of 16 Gy in 2 Gy fractions to the tumour bed was used, if clinically indicated. Doses were calculated using the anisotropic analytical algorithm, and dose-volume histograms for different structures were generated (Table 1).

Cardiac examinations

Patients were examined 6 ± 8 days prior to RT and 1 ± 1 days after RT treatment with median time interval between the studies 38 days (19–93 days). Blood samples for high sensitivity troponin T (hsTnt) and pro-B-type natriuretic peptide (proBNP) were collected at the baseline,

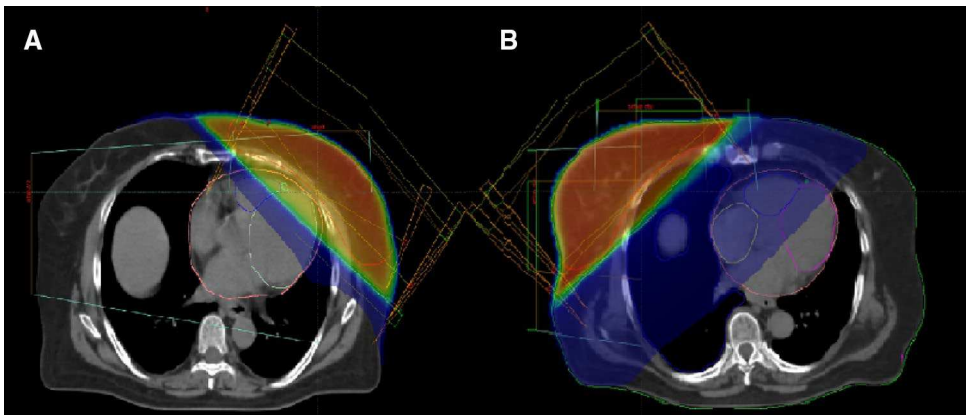

Fig. 1 3D CT radiotherapy treatment planning. On the left side (**a**), treatment fields for left-sided breast cancer are illustrated, with *blue* colouring marking fields receiving a 2 Gy dose and *yellow* to *red* colouring illustrating increasing radiation doses. **b** The typical RT field in patients with right-sided breast cancer, here with the *blue* colouring demonstrating fields receiving 0.5 Gy radiation doses. Manually depicted heart contouring is also shown for the whole heart, for the left ventricle and for the right ventricle

Table 1 Radiation doses to the different cardiac structures in Grays

	Left-sided breast cancer		Right-sided breast cancer	
	n = 60		n = 20	
	Median	[Min, Max]	Median	[Min, Max]
Mean heart	3.1	[0.7, 6.8]	0.6	[0.3, 4.8]
Peak heart	47.0	[5.8, 64.2]	4.5	[2.5, 19.1]
Mean LV	4.4	[0.8, 12.3]	0.1	[0.0, 3.3]
Peak LV	45.8	[4.5, 63.8]	0.4	[0.2, 5.2]

LV left ventricle

once during treatment and at the end of RT treatment. Comprehensive echocardiography was performed, and a 12-lead electrocardiogram (ECG) was obtained at each visit.

All echocardiographic examinations were performed by the same cardiologist (SST) using a commercially available cardiac ultrasound machine (Philips iE33 ultrasound system, Bothell, WA, USA) and a 1–5 MHz matrix-array X5-1 transducer. The imaging was acquired at rest, and Doppler recordings were acquired at end-expiration. The patients were in the left lateral decubitus position. A simultaneous superimposed ECG was used throughout the studies. The images were stored on an external hard drive for off-line analysis (Philips Qlab, Bothell, WA, USA). For STE analysis, three apical clips (four chamber, two chamber and three chamber) and three parasternal clips (short axis clips at the level of the mitral valve, the papillary muscle level and the apex) of the left ventricle (LV) were acquired over three cycles. Care was taken to optimize the visualization of the LV muscle throughout the cycles, aiming at a frame-rate of 60–90 Hz. Adequate tracking was controlled by visual inspection, and reanalysis was performed if necessary. Segments with repeated inadequate tracking were excluded from the final results. Regional results were calculated as average values from the segments located correspondingly.

Statistical analysis

The data are reported as means and standard deviations for normally distributed variables and as medians with ranges for other continuous variables. Differences between the groups in the baseline characteristics were tested with Student's *t*-test for continuous variables and with Fisher's exact test for categorical variables. The change from baseline to after RT was analysed with the paired samples *t*-test for normally distributed variables and with Wilcoxon's signed rank test for variables with skewed distribution. Categorical variables were analysed with the Chi square test/Fisher's exact test. Associations of the variables with the changes in STE values were calculated with Pearson's correlation or with Spearman's correlation for non-normally distributed variables. The differences in GLS changes between patients who smoked or did not smoke and other baseline diagnoses or medications were tested with Student's *t*-test. Binary logistic and linear regression analysis were used to test univariate associations for categorical and continuous variables. Stepwise linear regression analysis was used to test multivariable associations with GLS changes and tested parameters are shown in the corresponding tables. The reproducibility of the STE data was tested in 20 healthy volunteers from blinded data with intraclass correlation. All of the tests were two-sided, and p values <0.05 were considered statistically significant. Statistical analyses were performed using IBM SPSS Statistics software, version 23 for Windows (Armonk, NY, USA).

Results

General characteristics

The mean age of the study group was 63 ± 6 years. Thirty-three patients (41%) had no other concurrent disease. The most common underlying diseases included hypertension (44%), hypercholesterolaemia (23%) and hypothyroidism (13%). Twenty patients (25%) were current or ex-smokers. Fifty patients (63%) had a body mass index (BMI) >25 cm/m^2. Detailed baseline characteristics of the patients in each group are shown in Table 2.

Speckle tracking analysis

Patients with left-sided breast cancer

Patients with left-sided breast cancer displayed changes in global strain of $1.1 \pm 2.7\%$ ($p = 0.003$), and a more than 10% decrease from the baseline GLS value was experienced by 17 patients (28%). Regional analysis showed reductions in apical values of $2.0 \pm 4.5\%$ ($p = 0.002$) and apex values of $1.9 \pm 4.4\%$ ($p = 0.003$) and an increase in basal strain values of $1.7 \pm 5.4\%$ ($p = 0.024$); for details, see Table 3. Circumferential analysis and systolic strain rate analysis (see Supplementary Tables 1, 2) were less sensitive for detecting RT-induced changes in patients with left-sided breast cancer. In multivariable analysis, the changes in the apical segments were independently associated with prolonged apical rotation time ($\beta = 0.012$, $p = 0.011$) and with increasing LV mass ($\beta = -0.076$, $p = 0.024$). In addition, increased myocardia reflectivity (sccIBS) had an independent association with decreasing basal strain values ($\beta = 0.293$, $p = 0.045$).

Table 2 Baseline characteristics of the study population

	Left-sided breast cancer n = 60		Right-sided breast cancer n = 20		p
	Mean	SD	Mean	SD	
Age (years)	63.6	6.8	62.9	4.7	0.657
Systolic blood pressure (mmHg)*	144	19	150	20	0.287
Diastolic blood pressure (mmHg)*	79	12	79	12	0.918
Body mass index (kg/m^2)[a]	26.3	[24.1, 29.9]	26.6	[24.7, 30.0]	0.567
	n	(%)	n	(%)	
Smoking					
Current	9	15	2	10	0.722
Previous	7	12	2	10	1.000
Prior diagnosis[b]					
Hypertension	22	37	13	65	***0.038***
Diabetes mellitus	4	7	3	15	0.358
Hypercholesterolaemia	14	23	4	20	1.000
Hypothyroidism	7	12	3	15	0.705
Coronary artery disease					
Significant valvular abnormality	3	5	2	10	0.594
Medical treatment					
Beta blockers	7	12	5	25	0.163
Calcium channel blockers	4	7	4	20	0.102
ACE inhibitors/ARBs	15	25	10	50	*0.052*
Diuretics	8	13	7	35	***0.047***
Thyroxin	7	12	3	15	0.705
Nitrates	1	2	0	0	1.000
Aspirin	7	12	3	15	0.708
Statins	12	20	4	20	1.000
Oral diabetes medications	4	7	3	15	0.358
Aromatase inhibitors	22	37	8	40	0.796
Tamoxifen	2	3	4	20	***0.032***

Statistically significant p-values ($p < 0.05$) are in bold italics and values with tendency to statistically significance with italics (p-value between 0.05–0.10)

ACE angiotensin-converting enzyme, *ARB* angiotensin receptor blocker

[a]Non-normal distribution, reported as median, [Q_1, Q_3]

[b]Medication-requiring state

*Measured at the first visit

Patients with right-sided breast cancer

No significant change in GLS was observed in patients with right-sided breast cancer. However, segmental analysis revealed a decrease in the basal anterior segment in the strain analysis from -26.2 ± 7.8 to $-17.9 \pm 8.2\%$ ($p < 0.001$) and in the pulsed tissue Doppler analysis from 7.1 [6.1, 7.7] to 5.6 [5.3, 6.5] cm/s ($p < 0.001$) (Fig. 2). In multivariable analysis, delayed basal rotation time ($\beta = -0.035$, $p = 0.020$) was independently associated with changes in strain. Hypertension ($\beta = -1.272$, $p = 0.009$) and change in LV end diastolic diameter ($\beta = 0.042$, $p = 0.024$) had independent associations with the decrease in the anterior pulsed tissue Doppler value.

Multivariate analysis for overall GLS changes

The results of the correlation and multivariable analyses for GLS changes are displayed in Table 4. In multivariable analysis, the use of aromatase inhibitors (AIs) ($\beta = -2.002$, $p = 0.001$) and a decrease in LV diastolic volume had independent associations with a reduction in GLS ($\beta = -0.070$, $p = 0.025$). They explained 23% of the total GLS change after RT.

Table 3 Longitudinal systolic speckle tracking and pulsed tissue Doppler measurements

	Left-sided breast cancer n = 60					Right-sided breast cancer n = 20				
	Baseline		After RT		p	Baseline		After RT		p
Speckle tracing measurements										
Longitudinal strain (%)	Mean	SD	Mean	SD		Mean	SD	Mean	SD	
GLS	−18.3	±3.1	−17.2	±3.3	***0.003***	−16.9	±3.8	−17.2	±2.8	0.577
Basal	−21.6	±5.0	−23.3	±4.9	***0.024***	−21.1	±4.3	−20.3	±4.2	0.576
Mid	−19.4	±4.6	−17.7	±5.9	***0.039***	−17.6	±5.3	−18.5	±5.0	0.489
Apical	−18.7	±5.3	−16.7	±4.9	***0.002***	−16.5	±5.6	−18.0	±4.2	0.159
Apex	−18.3	±5.1	−16.5	±4.8	***0.003***	−16.0	±5.7	−17.1	±4.4	0.334
Anterior	−18.2	±4.3	−17.6	±4.4	0.277	−18.5	±4.4	−16.9	±4.9	*0.089*
Anteroseptal	−19.2	±3.9	−18.5	±4.7	0.281	−17.7	±4.5	−18.7	±5.1	0.374
Inferoseptal	−21.2	±3.7	−20.2	±4.0	0.110	−19.1	±3.8	−20.2	±4.0	0.229
Inferior	−20.3	±4.0	−19.6	±4.8	0.264	−19.8	±4.7	19.6	±2.8	0.854
Inferolateral	−20.2	±4.4	−19.1	±4.5	0.122	−18.6	±4.3	−19.0	±3.4	0.704
Anterolateral	−20.5	±3.6	−20.6	±4.2	0.874	−19.3	±5.0	−20.2	±3.5	0.528
Longitudinal strain rate (1/s)	Median	[Q1, Q3]	Median	[Q1, Q3]		Median	[Q1, Q3]	Median	[Q1, Q3]	
Global	−1.251	[−1.453, −1.107]	−1.296	[−1.450, −1.108]	0.393	−1.324	[−1.531, −1.183]	−1.366	[−1.501, −1.169]	0.823
Basal	−1.455	[−1.752, −1.171]	−1.618	[−1.869, −1.367]	***0.006***	−1.559	[−1.828, −1.380]	−1.521	[−1.859, −1.379]	0.837
Mid	−1.256	[−1.642, −1.095]	−1.381	[−1.602, −1.087]	0.237	−1.471	[−1.698, −1.160]	−1.354	[−1.665, −1.151]	0.794
Apical	−1.093	[−1.295, −0.950]	−1.075	[−1.241, −0.924]	0.201	−1.110	[−1.293, −0.993]	−1.211	[−1.321, −0.963]	0.940
Apex	−1.050	[−1.218, −0.895]	−0.991	[−1.148, −0.870]	0.174	−1.104	[−1.226, −0.940]	−1.159	[−1.369, −0.964]	0.970
Anterior	−1.150	[−1.518, −0.986]	−1.204	[−1.589, −0.999]	0.201	−1.273	[−1.543, −1.137]	−1.261	[−1.467, −1.072]	0.227
Anteroseptal	−1.252	[−1.549,−1.071]	−1.231	[−1.460,−1.092]	0.521	−1.317	[−1.367,−1.009]	−1.312	[−1.637,−1.178]	0.211
Inferoseptal	−1.189	[−1.314, −1.076]	−1.206	[−1.401, −1.101]	0.891	−1.324	[−1.601, −1.178]	−1.363	[−1.543, −1.131]	0.794
Inferior	−1.313	[−1.543, −1.135]	−1.391	[−1.717, 1.157]	0.717	−1.445	[−1.673, −1.258]	−1.434	[−1.717, −1.134]	0.349
Inferolateral	−1.310	[−1.848, −1.063]	−1.366	[−1.613, 1.193]	0.615	−1.498	[−1.713, −1.181]	−1.386	[−1.672, −1.169]	0.981
Anterolateral	−1.313	[-1.801, −1.074]	−1.324	[−1.591, −1.119]	0.402	−1.487	[−1.633, −1.154]	−1.368	[−1.632, −1.223]	0.841
Pulsed tissue Doppler measurements (cm/s)										
Septal	6.6	[6.2–7.4]	6.7	[5.9–7.8]	0.616	6.6	[6.0–7.7]	6.7	[6.0–7.7]	0.498
Lateral	7.2	[6.1–8.4]	7.0	[5.9–8.3]	0.224	7.4	[6.1–8.4]	7.0	[6.2–7.4]	0.227
Posterior	7.8	[7.0–8.6]	7.6	[6.7–8.6]	0.099	7.8	[7.3–8.7]	7.6	[6.7–8.4]	0.355
Anterior	6.2	[5.5–7.5]	5.9	[5.2–7.1]	***0.026***	7.1	[6.1–7.7]	5.6	[5.3–6.5]	***<0.001***

Statistically significant p-values ($p < 0.05$) are in bold italics and values with tendency to statistically significance with italics (p-value between 0.05–0.10)

GLS global longitudinal strain

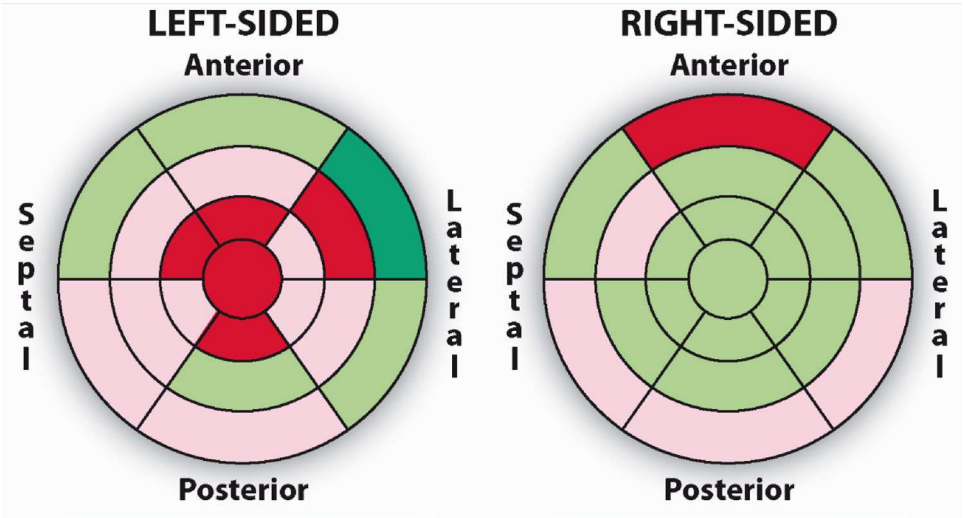

Fig. 2 Segmental changes in longitudinal strain after radiotherapy. The *green* colour shows segments with increasing function and red those with declining function. The *darker green* and *red* colours show segments with statistically significant changes ($p < 0.05$). Patients with left-sided breast cancer are shown on the left side and patients with right-sided breast cancer on the right side

Table 4 Factors associated with GLS changes after radiotherapy

	Correlations					Multivariable analysis[a]		
	r	p				β	SE (β)	p
Age (years)	−0.237	***0.043***						0.549
Mitral E-wave change (cm/s)	−0.300	***0.010****						0.420
LV mass change (3D) (g)	−0.309	***0.012***						0.502
LVDV change (3D) (ml)	−0.292	***0.018***				−0.070	0.025	***0.007***
Ef change (3D) (%)	−0.250	***0.047***						0.457
Mean heart (Gy)	−0.077	0.516						0.790
	GLS change[b]							
	With		Without		p			
	Mean	SD	Mean	SD				
Aromatase inhibitor	−2.0	0.5	0.0	2.7	***0.001***	−2.002	0.579	***0.001***
Smoking	−1.5	2.6	−0.5	2.8	0.173			0.091
Valvular abnormality	−3.2	3.7	−0.5	2.6	***0.037***			0.891
Patient group (left)	−1.1	2.7	0.4	2.8	***0.040***			0.137
Hypertension	−1.0	2.7	−0.5	2.8	0.511			0.910
Diabetes	−1.7	2.6	−0.6	2.8	0.323			0.562

Statistically significant p-values ($p < 0.05$) are in bold italics

GLS global longitudinal strain, *LV* left ventricle, *3D* three-dimensional, *LVDV* LV end-diastolic volume, *Ef* ejection fraction, *Mean heart* mean radiation dose to the whole heart, *Patient group (left)* patients with left-sided breast cancer

*Spearman's correlation; Pearson's correlation for others

[a]The analysis is performed with linear forward stepwise regression analysis

[b]The given number under definition 'with' presents GLS decline with patients using Aromatase inhibitor, patient smoking, with significant valvular lesions, patients with left-sided breast cancer and patients with hypertonia and diabetes, respectively. In the column 'without' the GLS change after RT in patients without these conditions is shown

Conventional echocardiographic measurements

In the whole group, the LV myocardial mass derived from 3D imaging increased from 105 ± 21 to 109 ± 21 g ($p = 0.010$). On two-dimensional imaging, increases were found in relative wall thickness, and in septal and posterior wall thickness: $p = 0.002$, 0.001 and $p = 0.001$, respectively. The changes in diastolic function were found to result in

Table 5 Conventional echocardiography measurements

	Left-sided breast cancer n = 60					Right-sided breast cancer n = 20				
	Baseline		After RT		p	Baseline		After RT		p
	Mean	SD	Mean	SD		Mean	SD	Mean	SD	
LVEDD (mm)	45.1	±4.1	44.7	±3.9	0.157	43.7	±4.6	43.8	±3.9	0.920
LVEDS (mm)	30.3	±3.5	30.0	±3.6	0.455	29.7	±3.2	29.3	±3.4	0.428
IVS (mm)*	10.0	[9.0, 11.0]	10.0	[9.2, 11.0]	***0.009***	10.0	[8.9, 11.3]	10.6	[9.0, 11.9]	***0.018***
PW (mm)*	10.0	[9.0, 10.8]	10.2	[9.7, 11.0]	***0.003***	10.0	[9.1, 11.1]	10.4	[9.9, 11.5]	0.251
RWT*	0.42	[0.40, 0.49]	0.46	[0.43, 0.50]	***0.003***	0.45	[0.41, 0.54]	0.46	[0.43, 0.54]	0.411
LVEDV (ml)	99	±19	95	±18	***0.038***	97	±26	98	±25	0.832
LVEDS (ml)	40	±9	39	±11	0.345	39	±12	41	±11	*0.051*
LVED mass (g)	105	±20	108	±21	***0.012***	106	±23	108	±24	0.483
LV EF (%)	65	±7	65	±7	0.810	64	±10	66	±6	0.616
IVRT (ms)	104	±25	110	±22	*0.082*	111	±22	111	±14	0.981
Mitral inflow E (cm/s)*	71	[64, 83]	67	[58, 79]	***0.031***	76	[63, 89]	67	[61, 80]	*0.067*
Mitral inflow a (cm/s)	78	±20	75	±15	*0.055*	78	±14	78	±21	0.871
Mitral inflow dt (ms)*	230	[203, 260]	239	[207, 271]	0.214	211	[180, 240]	238	[198, 274]	***0.015***
LV E/e' ratio*	8.9	[7.1, 11.1]	9.0	[7.1, 10.0]	0.183	10.1	[7.6, 12.4]	9.3	[7.5, 11.7]	0.970
RV basal dimension (mm)	34.2	±5.0	33.6	±4.5	0.340	34.3	±6.0	33.6	±5.7	0.522
TAPSE (mm)	24.2	±4.0	22.3	±4.0	***<0.001***	23.4	±5.4	22.5	±5.2	0.141
RV s' (cm/s)	11.6	[10.3, 13.2]	11.1	[10.2, 13.2]	0.099	13.4	[10.7, 14.7]	12.2	[10.9, 14.1]	0.681
TR gradient (mmHg)	21.5	±5.6	21.4	±4.7	0.677	23.0	±6.9	20.6	±6.1	***0.025***

Statistically significant p-values ($p < 0.05$) are in bold italics and values with tendency to statistically significance with italics (p-value between 0.05–0.10)

LVEDD and *LVEDS* left ventricular end-diastolic and end-systolic diameters, *IVS* and *PW* interventricular septum and posterior thicknesses at the end-diastole, *RWT* relative wall thickness, *LVEDV, LVESV* and *LVED mass* left ventricular end-diastolic and end-systolic volumes and end-diastolic mass derived from the three dimensional acquisition, *EF* ejection fraction, *IVRT* isovolumetric relaxation time, *dt* declaration time, *E/e' ratio* ratio between mitral inflow E velocity and averaged pulsed Doppler velocity derived from septal, lateral, anterior and posterior walls, *RV* right ventricle, *TAPSE* tricuspidal annular plane systolic excursion, *RV s'* the systolic velocity of pulsed tissue Doppler recording derived from RV lateral basal region, *TR gradient* tricuspid regurgitation maximal gradient

*Median and [Q_1, Q_3]

decreases in mitral inflow E-wave and prolongation of the E-wave's declaration time: p = 0.005 and 0.018, respectively. The changes were more prevalent in left-sided breast cancer patients; Table 5.

Electrocardiogram and biochemical markers

RT induced minor ECG changes in 44 patients (55%). The most typical changes were T-wave inversions or reductions in leads V1-4, aVL and I. ECG changes were more common in patients with left-sided breast cancer than in patients with right-sided breast cancer (39 vs. 5 patients) (p = 0.003).

The baseline and the highest (Q_1, Q_3) hsTnt values were 4 (4, 15) and 5 (4, 15) ng/l (p = 0.006) in patients with left-sided breast cancer and 4 (4, 33) and 5 (4, 20) ng/l (p = 0.287) in patients with right-sided breast cancer, respectively. More than 30% increase in hsTnt was found in 14 patients and one patient among left-sided and right-sided patients, respectively (p < 0.001).

In patients with left-sided breast cancer, the baseline proBNP value was 59 (14, 824) ng/l with an increase to 88 (15, 1101) ng/l (p < 0.001). The respective values were 92 (12, 160) and 86 (24, 261) ng/l (p = 0.809), in patients with right-sided breast cancer. A more than 30% increase in proBNP value was observed in 32 left-sided and four right-sided patients (p = 0.014).

Reproducibility

The longitudinal measurements showed generally higher reproducibility than the circumferential measurements, and

the strain values were higher than the strain rate values. In the regional analysis, the apical regions seemed to be more reproducible than the basal regions in longitudinal measurements, whereas in the circumferential analysis, the anterior regions were more reliable than the posterior regions. For detailed analyses, see Supplementary Table 3.

Discussion

In this prospective study, STE analysis could detect differences in the global and regional changes in myocardial function in the early stage after adjuvant RT in patients with left-sided versus right-sided breast cancer. RT-induced changes in patients with right-sided breast cancer have not been previously reported. Due to different locations of the changes in patients with left-sided and right-sided breast cancer, the late stage complications might differ according to the breast cancer laterality.

RT-induced changes in tissues

Radiation produces sequential, time-dependent changes in tissue. The first phase consists of inflammation with oedema, extravasation and activation of the coagulation cascade [13, 14]. It is generally believed that a complex cascade is launched during the early phase and results in progressive fibrotic changes over years to decades after RT treatment [14]. The inflammatory phase subsides to a latent phase within 2 days after RT exposure [13]. The latent phase is characterized by capillary damage caused by endothelial injury and thrombotic lesions [13, 14]. The first signs of the fibrotic phase have been found 40–70 days after the completion of RT treatment [13]. In the heart, the clinical late sequelae appear 5–15 years after RT treatment and consist of wide variety of changes [3, 15]. The most lethal changes are coronary lesions, typically of a fibrotic nature with ostial and anterior locations [3, 15]. Myocardial changes can produce thickening of the LV walls resulting in filling problems and restrictive cardiomyopathy [3]. Valvular stenosis and regurgitation, arrhythmia and conduction disturbances and pericardial constriction are also well-known complications after thoracic RT treatment [3, 15]. Our patients were re-examined within 3 days after the RT treatment, well within the inflammatory period, though the initial phase of the fibrosis could theoretically have started.

STE changes in patients with left-sided breast cancer

RT induced an apical decline in the LV systolic function in patients with left-sided breast cancer in the present study, which was in concordance with previous studies by Erven and Heggemann [11, 16]. These changes were detectable both in the longitudinal strain and strain rate analyses, as well as at global, regional and segmental levels. The basal regions had a compensatory increase in function. The basal compensation was, however, not sufficient to compensate for the global functional loss, and the patients experienced a decrease in the GLS. Similar findings were reported by Lo [9]. A more than 10% decrease in the GLS is generally considered clinically significant [17], and this change was observed in 28% of our patients with left-sided breast cancer. Other conventional systolic functional LV measurements were not sufficiently sensitive to detect these RT-induced changes.

STE changes in patients with right-sided breast cancer

Patients with right-sided breast cancer received significantly less cardiac radiation. Another main difference was the localization of the RT fields, as shown in Fig. 1. The optimal tangential right-sided RT fields usually do not reach the basis of the LV. However, due to individual anatomy (e.g., large breasts), additional fields were used in some patients to ensure optimal target volume coverage, and a marked variation in LV doses was observed (LV mean 0.0–3.3 Gy). In the LV longitudinal segmental analysis, both strain and pulsed tissue Doppler values decreased in the basal anterior LV myocardium. Because of the small affected area, the global function remained unaffected both in the STE analysis and in the conventional echocardiography measurements. However, in the diastolic parameters, an increase in the declaration time and a tendency towards a decrease in the mitral E-wave were found.

Other RT-induced cardiac changes

Other measurements showed increased thickness in the myocardium on both 2D and 3D echocardiography with a simultaneous decrease in the LV diastolic volume, along with minor changes in diastology, and in TAPSE (tricuspid annular plane systolic excursion). The early inflammatory effect of the RT treatment with extravasation and tissue swelling would be a logic explanation to increased myocardial mass along with the changes in diastology, though the exact mechanism remains speculative in the absence of tissue samples. Furthermore, ECG showed changes in the anterior leads mainly in patients with left-sided breast cancer, corresponding to the anterior location of the RT fields. Moreover, there were slight but statistically significant increases in serum hsTnt and proBNP values in patients with left-sided breast cancer. All of these subtle changes might represent the same subclinical cardiac changes induced by breast cancer adjuvant RT, as observed in the STE analysis.

Clinical implications of the findings in this study

Subclinical cardiac changes precede actual cardiac sequelae, and their presence might indicate greater risk for evolution to radiotherapy-induced heart disease (RIHD). Hence, interest in RT-induced early cardiac changes has emerged, and it is debated whether patients receiving RT in the thoracic regions should be followed up regularly [3]. The early manifestations have not been well characterized, and their detection is considered challenging, even more so for right-sided breast cancer patients. The cardiac radiation dose after left-sided breast cancer RT is higher than that after right-sided breast cancer [7], as also shown in our study. In studies comparing the impact of breast cancer laterality, cardiac mortality and morbidity were higher after left-sided RT [1, 5, 6]. However, the impact of right-sided RT is not negligible. It has been shown that the mean heart radiation dose itself induces an increased cardiac risk, and with a cardiac exposure of 0.3–4.8 Gy, our patients with right-sided breast cancer could face a 2.2–35.5% increased risk of ischaemic heart disease within 5 years [5]. Considering the difference in the location of the RT fields, the cardiac impact after RT and its early lesions might be different in patients with left-sided and right-sided breast cancer. Our study was the first to indicate this decline in systolic function in regions corresponding to the RT fields in patients with right-sided breast cancer, with a clear difference from the changes after left-sided RT in transthoracic echocardiography examination. Considering the screening for early changes, this is a worthwhile fact to notice. Although the GLS has shown promise to be an early and sensitive tool to detect subclinical changes over a wide range of pathologies [10, 17], it might fail to reveal RT-induced cardiac injury in patients with right-sided breast cancer.

The effects of the concurrent endocrine treatment

The impact of the concurrent use of AIs on the GLS decrease after RT was also interesting. Oestrogen has positive effects on cardiac function and recovery [18]. Aromatase is an enzyme regulating the final pathway of oestrogen metabolism. When it is blocked, the tissue level of oestrogen declines. In breast cancer patients, inhibition of this enzyme is used to block oestrogen-induced growth stimulation of cancer tissue. The simultaneous use of AIs during RT has been shown both to sensitize the RT effect and to potentiate RT-induced cardiac functional decline [19, 20]. Similar effects might explain the strong association between the simultaneous use of AIs and a decrease in GLS.

Limitations of our study

The patient population was uniform in many ways, which could limit the application of the results in other patient groups. The echocardiographic studies were performed by a single experienced cardiologist who always used the same equipment, resulting in unique standardized conditions, which might not correspond to general clinical practice. Additionally, the reproducibility was not equally distributed in all of the measured values, which might have influenced the reliability of some of the measurements. Because this study was an observational, non-randomized study with main focus on the group of patients with left-sided breast cancer, the groups with left-sided and right-sided breast cancer were of unequal sizes. Furthermore, the size of the patient population was relatively small, which might limit the clinical implications of the results. Finally, these results showed very short term outcome. Follow-up of this prospectively collected patient population is currently under way to explore the further development of these early cardiac changes.

Conclusion

Our study confirmed the previous findings of global LV functional changes, along with apical impact, after RT in patients with left-sided breast cancer. The basal anterior impact after right-sided RT was a novel finding and indicated that a different approach is needed for the detection of right-sided cancers in screening and follow-up.

Acknowledgements The authors thank research nurses Virpi Räsänen, Hanna Näppilä and Emmi Vettenranta for their expert assistance during the study and Helene Schmidt for the drawings.

Funding This study was supported by the Pirkanmaa Hospital District, Seppo Nieminen Fund (Grant No. 150613), Paavo and Eila Salonen Legacy, the Ida Montin Fund, the Finnish Foundation for Cardiovascular Research, the Competitive State Research Financing of the Expert Responsibility Area of Tampere University Hospital (Grant No. 95021) and the Finnish Cultural Foundation, the Pirkanmaa Regional Fund and the Finnish Medical Foundation.

Compliance with ethical standards

Conflict of interest None of the authors have any conflict of interest to declare, financial or otherwise.

Ethical approval This study has been approved by the local ethics committee and it has been performed in accordance with the ethical standards laid down in the 1964 Declaration of Helsinki and its later amendments.

Informed consent All persons included in this study have given informed consent prior their inclusion in the study.

Research involving animal rights This study does not contain any studies with animals performed by any of the authors.

References

1. Sardaro A, Petruzzelli MF, D'Errico MP, Grimaldi L, Pili G, Portaluri M (2012) Radiation-induced cardiac damage in early left breast cancer patients: risk factors, biological mechanisms, radiobiology, and dosimetric constraints. Radiother Oncol 103:133–142
2. Clarke M, Collins R, Darby S, Davies C, Elphinstone P, Evans E et al (2005) Effects of radiotherapy and of differences in the extent of surgery for early breast cancer on local recurrence and 15-year survival: an overview of the randomised trials. The Lancet 366:2087–2106
3. Lancellotti P, Nkomo VT, Badano LP, Bergler J, Bogaert J, Davin L et al (2013) Expert consensus for multi-modality imaging evaluation of cardiovascular complications of radiotherapy in adults: a report from the European Association of Cardiovascular Imaging and the American Society of Echocardiography. Eur Heart J Cardiovasc Imaging 14:721–740
4. Bouillon K, Haddy N, Delaloge S, Garbay JR, Garsi JP, Brindel P et al (2011) Long-term cardiovascular mortality after radiotherapy for breast cancer. J Am Coll Cardiol 57:445–452
5. Darby SC, Ewertz M, McGale P, Bennet AM, Blom-Goldman U, Bronnum D et al (2013) Risk of ischemic heart disease in women after radiotherapy for breast cancer. N Engl J Med 368:987–998
6. Darby SC, McGale P, Taylor CW, Peto R (2005) Long-term mortality from heart disease and lung cancer after radiotherapy for early breast cancer: prospective cohort study of about 300,000 women in US SEER cancer registries. Lancet Oncol 6:557–565
7. Taylor CW, Nisbet A, McGale P, Darby SC (2007) Cardiac exposures in breast cancer radiotherapy: 1950s–1990s. Int J Radiat Oncol Biol Phys 69:1484–1495
8. Taylor CW, Wang Z, Macaulay E, Jagsi R, Duane F, Darby SC (2015) Exposure of the heart in breast cancer radiation therapy: a systematic review of heart doses published during 2003 to 2013. Int J Radiat Oncol Biol Phys 93:845–853
9. Lo Q, Hee L, Batumalai V, Allman C, MacDonald P, Delaney GP et al (2015) Subclinical cardiac dysfunction detected by strain imaging during breast irradiation with persistent changes 6 weeks after treatment. Int J Radiat Oncol Biol Phys 92:268–276
10. Kalam K, Otahal P, Marwick TH (2014) Prognostic implications of global LV dysfunction: a systematic review and meta-analysis of global longitudinal strain and ejection fraction. Heart 100:1673–1680
11. Erven K, Jurcut R, Weltens C, Giusca S, Ector J, Wildiers H et al (2011) Acute radiation effects on cardiac function detected by strain rate imaging in breast cancer patients. Int J Radiat Oncol Biol Phys 79:1444–1451
12. Tuohinen SS, Skytta T, Virtanen V, Luukkaala T, Kellokumpu-Lehtinen PL, Raatikainen P (2015) Early effects of adjuvant breast cancer radiotherapy on right ventricular systolic and diastolic function. Anticancer Res 35:2141–2147
13. Fajardo LF, Stewart JR (1973) Pathogenesis of radiation-induced myocardial fibrosis. Lab Invest 29:244–257
14. Yarnold J, Brotons MC (2010) Pathogenetic mechanisms in radiation fibrosis. Radiother Oncol 97:149–161
15. Jaworski C, Mariani JA, Wheeler G, Kaye DM (2013) Cardiac complications of thoracic irradiation. J Am Coll Cardiol 61:2319–2328
16. Heggemann F, Grotz H, Welzel G, Dosch C, Hansmann J, Kraus-Tiefenbacher U et al (2015) Cardiac function after multimodal breast cancer therapy assessed with functional magnetic resonance imaging and echocardiography imaging. Int J Radiat Oncol Biol Phys 93:836–844
17. Thavendiranathan P, Poulin F, Lim KD, Plana JC, Woo A, Marwick TH (2014) Use of myocardial strain imaging by echocardiography for the early detection of cardiotoxicity in patients during and after cancer chemotherapy: a systematic review. J Am Coll Cardiol 63:2751–2768
18. Jazbutyte V, Stumpner J, Redel A, Lorenzen JM, Roewer N, Thum T et al (2012) Aromatase inhibition attenuates desflurane-induced preconditioning against acute myocardial infarction in male mouse heart in vivo. PLoS One 7:e42032
19. Skytta T, Tuohinen S, Virtanen V, Raatikainen P, Kellokumpu-Lehtinen PL (2015) The concurrent use of aromatase inhibitors and radiotherapy induces echocardiographic changes in patients with breast cancer. Anticancer Res 35:1559–1566
20. Azria D, Larbouret C, Cunat S, Ozsahin M, Gourgou S, Martineau P et al (2005) Letrozole sensitizes breast cancer cells to ionizing radiation. Breast Cancer Res 7:R156–R163